NUREG/CR-3273
SAND83-1022
R3
Printed May 1984

Combustion of Hydrogen:Air Mixtures in the VGES Cylindrical Tank

William B. Benedick, John C. Cummings,
Peter G. Prassinos

Prepared by
Sandia National Laboratories
Albuquerque, New Mexico 87185 and Livermore, California 94550
for the United States Department of Energy
under Contract DE-AC04-76DP00789

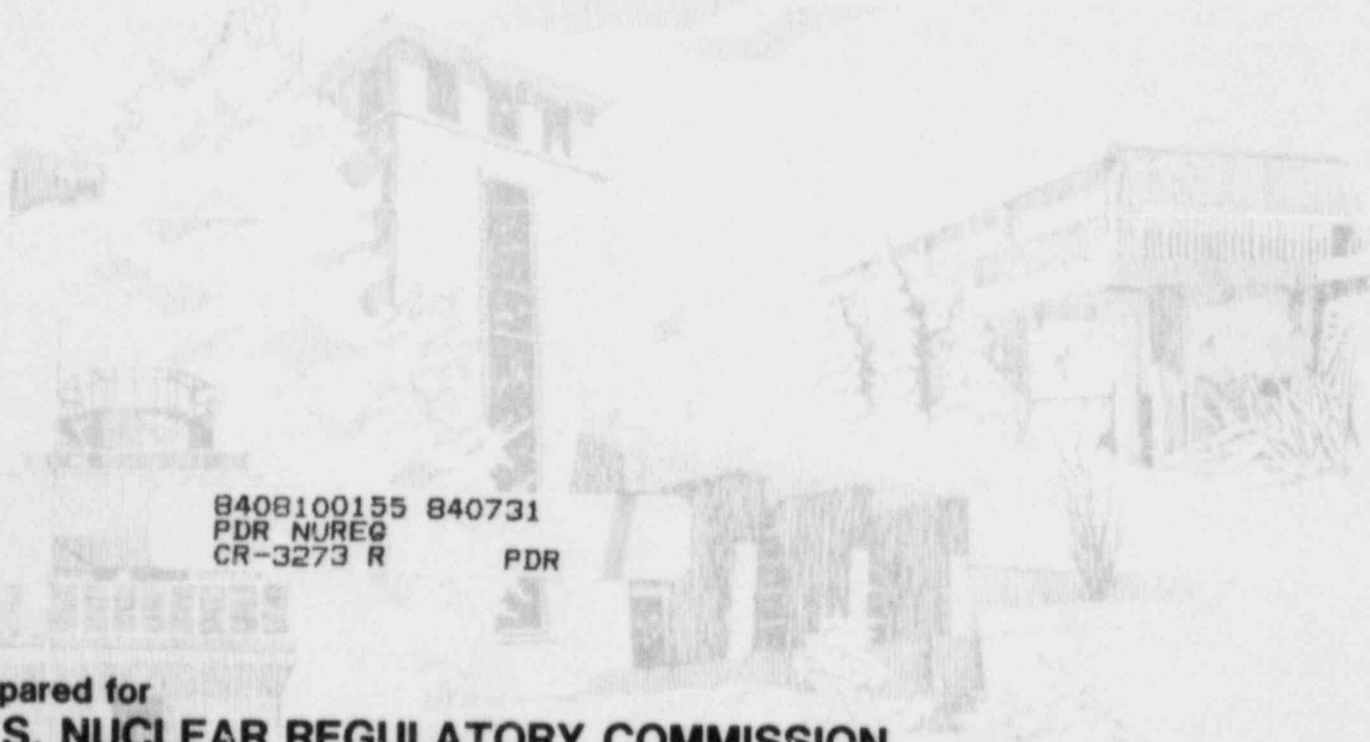

Prepared for
U. S. NUCLEAR REGULATORY COMMISSION

SF2900Q (6-81)

NOTICE

Available from
GPO Sales Program
Division of Technical Information and Document Control
U.S. Nuclear Regulatory Commission
Washington, D.C. 20555

and

National Technical Information Service
Springfield, Virginia 22161

NUREG/CR-3273
SAND83-1022
R3

COMBUSTION OF HYDROGEN:AIR MIXTURES IN THE VGES CYLINDRICAL TANK

William B. Benedick
John C. Cummings
Peter G. Prassinos*

May 1984

Sandia National Laboratories
Albuquerque, New Mexico 87185
Operated by
Sandia Corporation
for the
U.S. Department of Energy

*Technadyne Engineering Consultants, Inc.

Prepared for
Division of Engineering Technology
and
Division of Accident Evaluation
Office of Nuclear Regulatory Research
U.S. Nuclear Regulatory Commission
Washington, DC 20555
Under Memorandum of Understanding DOE 40-550-75
NRC FIN NOs. A1246, A1336

ABSTRACT

Sandia National Laboratories is currently involved in a number of experimental projects to provide data that will help quantify the threat of hydrogen combustion during nuclear plant accidents. Several experimental facilities are part of the Variable Geometry Experimental System (VGES). The purpose of this report is to document the experimental results from the first round of combustion tests performed at one of these facilities: a 5-m^3 cylindrical tank. The data provided by tests at this facility can be used to guide further testing and for the development and assessment of analytical models to predict hydrogen combustion behavior.

CONTENTS

ILLUSTRATIONS

ILLUSTRATIONS (con't)

ILLUSTRATIONS(con't)

TABLES

ACKNOWLEDGMENTS

We would like to thank J. E. Shepherd for his technical involvement during the initial stages of the VGES testing, C. J. Daniel for his assistance in setting up the experimental apparatus and help in conducting the tests, and R. McCurley for initial data reduction. This project was sponsored by the U. S. Nuclear Regulatory Commission under the direction of Dr. J. Larkins and Dr. P. Worthington.

SUMMARY

Sandia National Laboratories is conducting a research and development program for the U.S. Nuclear Regulatory Commission to address issues related to the behavior and control of hydrogen during accidents at nuclear power plants. The program includes analytical, experimental, and engineering tasks. A significant portion of the experimental work has been conducted in a cylindrical pressure vessel (5 m^3 in volume). Since the inception of the program in 1981, over 100 combustion tests, divided into 11 test series, have been carried out in this vessel, and results have been partially documented in bimonthly and semi-annual program reports. The purpose of this report is to complete the documentation and summarize our present interpretation of the results.

Each of the 11 test series has examined the effects on hydrogen:air combustion of varying particular parameters: hydrogen concentration; igniter type; igniter location; pre-combustion gas motion; pre-combustion gas pressure; concentration of additional diluent gas (N_2, CO_2); and the presence of an aqueous foam. One test series was used to investigate the effects of hydrogen:air combustion on equipment and simulated equipment. Principal instrumentation for most experiments consisted of several dynamic-pressure transducers and an array of thermocouples. Gas composition sampling and calorimetry were employed in some of the tests. Thermocouple data were analyzed to produce flame front contour plots, space-time trajectories, and velocities. Pressure transducer data were analyzed to determine peak pressures, pressure rise times, and pressure decay times (heat transfer and condensation rates).

A number of significant conclusions can be drawn from the results of the first 11 test series:

Peak combustion pressures increased rapidly with hydrogen concentration from 5% to 8%. Measured pressures were substantial fractions of the theoretical maximum pressures for hydrogen concentrations above 7%.

Variations in igniter type were found to be unimportant. Igniter location was important only for quiescent mixtures with less than 8% hydrogen--raising the igniter lowered the combustion completeness because the flame propagated only upward.

Pre-combustion gas motion was very important for hydrogen concentrations below 10%. Gas motion caused an increase in combustion completeness and energy release rate--both of which increased the peak pressure.

Pre-combustion gas pressure had little effect on the ratio of peak to final pressure over the range tested.

The addition of diluent gases to the hydrogen:air mixtures had little effect until high concentrations of diluent gas were attained. The increased heat capacity of CO_2, compared to N_2, made it more effective in reducing peak combustion pressure.

A limited number of equipment survivability tests indicated no severe threat due to the thermal environment in the tank. However, extrapolation of these results to full scale indicates that some environments may exceed current LOCA qualification levels.

Aqueous foams were found to be very beneficial at mitigating the combustion environment (pressure and temperature) for hydrogen concentrations below 15%. However, for higher hydrogen concentrations, the foams accelerated the flames and little or no combustion mitigation (of peak pressure) was observed. In fact, for 20% hydrogen, the foam apparently caused dynamic combustion pressures that damaged the foam generator.

I. Introduction

The 5-cubic-meter Burn Tank is one of the several facilities of the Variable Geometry Experimental System (VGES). VGES supports the Hydrogen Program conducted by Sandia National Laboratories and sponsored by the US Nuclear Regulatory Commission (NRC). The overall objectives of the Hydrogen Program are to:

- Assess the threat to nuclear power plants (containment structure, safety equipment, and the primary system) posed by hydrogen combustion, considering several general types of Light Water Reactors and a variety of accident scenarios.
- Assess proposed hydrogen control and disposal methods and develop new concepts.
- Evaluate hydrogen/oxygen detectors and analyzers.
- Disseminate information on hydrogen behavior, detection, control, and disposal.
- Provide technical assistance to the NRC on hydrogen-related matters.

The objective of VGES is to provide data on hydrogen combustion in a short time and at a low cost. In order to meet this objective, the tank was configured to provide data covering a wide range of hydrogen combustion and mitigation phenomena.

Eleven test series and over 100 experiments have been conducted in the tank. A brief description and objectives of each test series (TS) are given below:

TS 1. Perform initial low H_2 concentration burns, obtain base line data, and establish equipment operability utilizing a glowplug igniter. Sixteen burns of 3.8 to 9.2 volume percent (%) H_2.

TS 2. Determine the effects of raising the glowplug igniter to the vertical center of the tank. Eleven burns of 4.8% to 15.3% H_2.

TS 3. Investigate low H_2 concentration burns utilizing a spark igniter. Eight burns of 4.8% to 8.3% H_2.

TS 4. Investigate low H_2 concentration burns with reduced initial pressure. Nine burns of 5.6% to 10.7% H_2.

TS 5. Investigate higher H_2 concentration burns with reduced initial pressure. Six burns of 7.4% to 23.4% H_2.

TS 6. Investigate H_2 burns with greater than atmospheric concentrations of nitrogen (preaccident partial inerting). Twelve burns of 3.9% to 16.7% H_2 and 27.4% to 31.6% added N_2, 71.7% to 82.7% total N_2.

TS 7. Investigate H_2 burns with reduced voltage on the glowplug igniter. Six burns of 5.7% to 10.7% H_2.

TS 8. Investigate higher H_2 concentration burns with both spark and glowplug igniter. Nine burns of 9.9% to 17.4% H_2.

TS 9. Investigate H_2 burns with CO_2 added as an inerting agent and to simulate steam in an unheated vessel. Seven burns of 10% to 20% total H_2 and 27% to 56% total CO_2.

TS 10. Provide data on the behavior of simulated equipment in an H_2 burn environment for the Hydrogen Burn Survivability (HBS) Program. Six burns of 10% to 15% total H_2 and 0% to 10% total CO_2.

TS 11. Investigate H_2 burns in an aqueous foam environment. Fourteen burns with 10% to 20% H_2.

The purpose of this report is to present the data and experimental results from the 11 TS described above. The results of VGES testing provide data that can be used to develop and assess theoretical models of hydrogen combustion behavior.

The overall system and the specific configuration for each test series are given in Section II. The instrumentation and the data acquisition system are discussed in Section III. Test procedure and initial conditions for each test are given in Section IV. Representative raw and calculated data are given in Section V. Experimental results are given in Section VI, and Section VII presents the conclusions. Raw data and calculated values are given in Appendix A.

II. System Description and Configuration

The VGES tank is located in a remote area of Sandia National Laboratories. (See the photographs in Figure 1 and the schematic in Figure 2.) The tank is 4.27 m (14 ft) in length and 1.22 m (4 ft) in diameter. It has a semiellipsoidal bottom end, which is buried in the ground with only the flanged top end exposed. Attached to the top flange is a 0.61-m (2-ft) high, removable, semiellipsoidal cover, which is secured by 48 bolts of 3.16-cm (1 1/4-in.) diameter. The total assembled length of the tank is 4.88 m (16 ft). The tank and cover are made of 1.6-cm (5/8-in.) thick alloy steel and have a maximum pressure rating greater than 5.52 MPa (800 psia).

There are five penetrations in the tank (Figure 2a), located just below the flange. Four of the penetrations are used for instrumentation supports and gas and electrical feedthroughs. The fifth penetration is used to mount a dynamic-pressure transducer. All penetrations are airtight, and the tank cover is sealed with a gasket of RTV material so that the tank is operated as a constant-volume pressure vessel.

Two muffin-type mixing fans are mounted in the upper and lower portions of the tank (Figure 2). The top fan is located just below the top flange, and the bottom fan is located about 51 cm (20 in.) above the tank bottom and offset azimuthally about 25 cm (10 in.) from the upper fan. Each fan is 25.4 cm (10 in.) in diameter and rated at 12.74 m^3/min (450 cfm). Both fans direct the flow downward toward the bottom of the tank. For TS 11, the two fans were removed and a foam generator was installed near the top of the tank. The foam generator (Figure 3) contains a mixing fan and an annular spray header inside a converging-diverging circular metal housing with a perforated metal cover.

The fans are used to mix the contents of the tank before and after hydrogen addition and also before postburn gas sampling. The fan in the foam generator was operated similar by the mixing fans in the tank prior to foam generation.

Three types of igniters were used during VGES tank experimentation. The first type was an exposed 300-W photoflood lamp filament. These igniters were used for the first two tests of TS 1. Following these tests, a standard 14-V glowplug (GM7G) was used for the remainder of TS 1 and TS 2, 6, 7, 8, 9, and 10. This glowplug is identical to the ones that were used in the TVA IDIS system.[1] To obtain a rapid heat-up, approximately 70 V were applied to the glowplug for 1.5 s, then two additional glowplugs (located outside the tank) were switched in series for an additional 3.5 s (voltage ≃ 23 V), then tne voltage was turned off.

Glowplug lifetime was greatly reduced when operated in this manner, and plugs were replaced every five to eight shots.

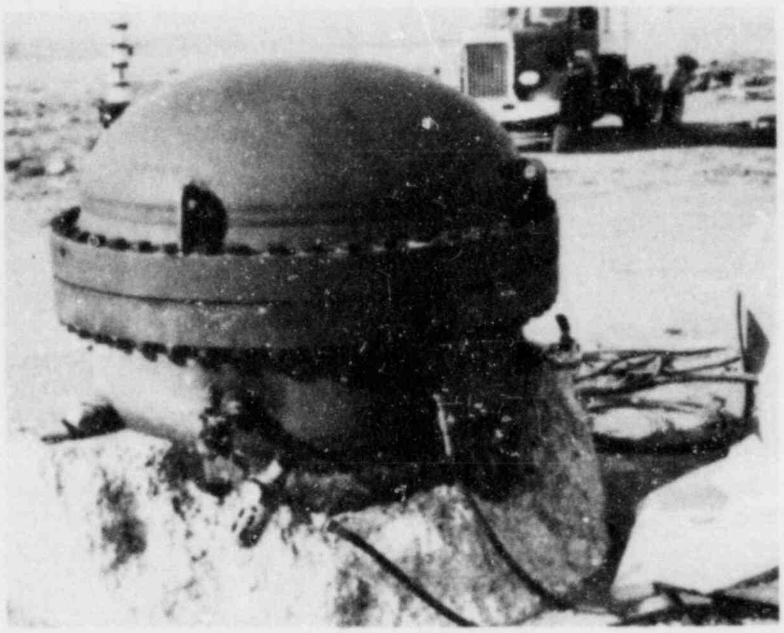

(a)

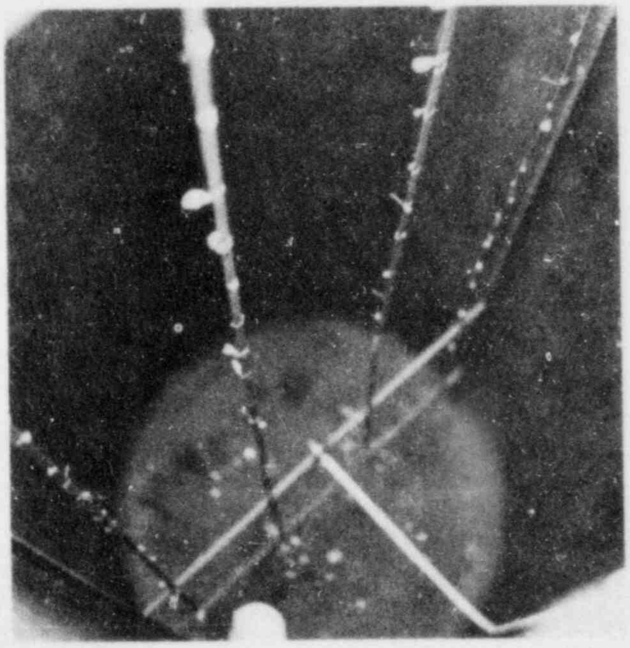

(b)

(c)

Figure 1. (a) Assembled VGES tank showing semiellipsoidal cover. (b) Interior of VGES tank showing thermocouple (TC) array. (c) Modified VGES tank semiellipsoidal cover for foam generation and future test series.

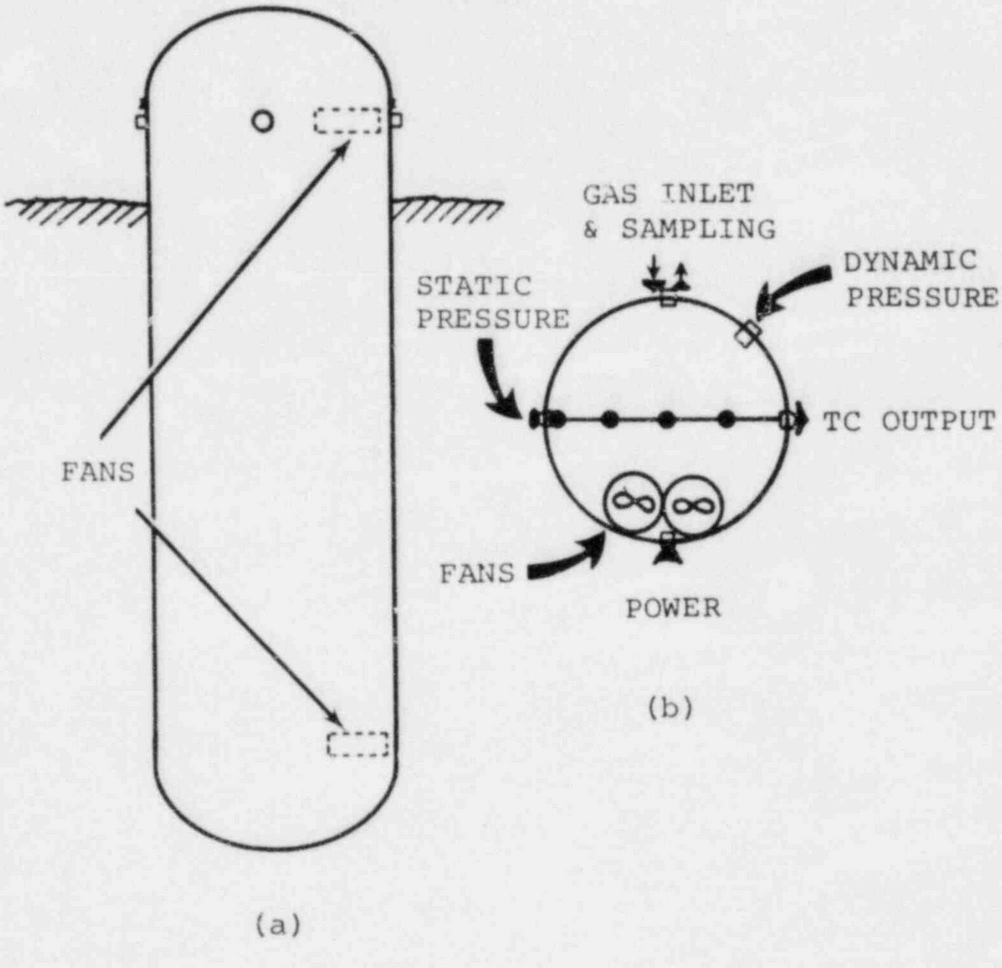

Figure 2. Schematic of the VGES tank, (a) elevation view, and (b) plan view showing access ports.

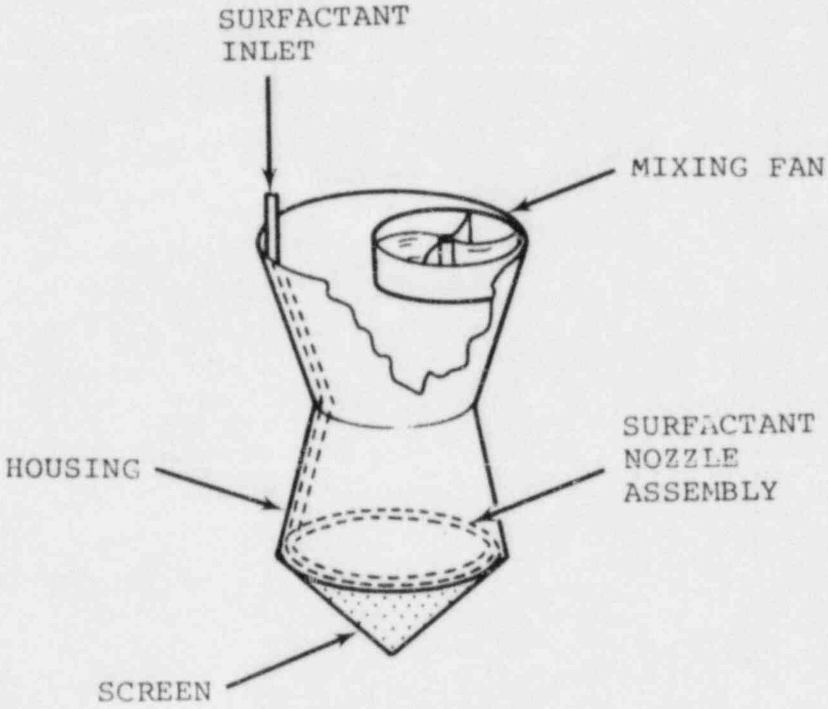

Figure 3. VGES Foam Generator for TS 11

The glowplug igniter was operated in this manner for TS 1, 2, 6, 8, 9, and 10. For TS 7, 14 V was applied to the glowplug for 50 s.

The third type of igniter used during the experiments was a raised spark-gap consisting of two opposed copper wires about 2 mm (0.05 in.) apart. The spark igniter was used for TS 3, 4, 5, 6, 8, and 11. A high-voltage capacitor produced a spark with approximately 30 J of energy. The type of igniter and voltages used for each specific test are indicated in Section VI.

The igniters were located on the tank centerline, 1.22 m (48 in.) from the tank bottom (Figure 4) for all TS except TS 2. For TS 2, the glowplug igniter was located 2.13 m (84 in.) from the tank bottom, on the tank centerline.

Gas samples of the preburn and postburn gas mixture were taken during the experiments. The gas bottles had a volume of 75 cm^3 (4.58 $in.^3$) and were evacuated to less than 5 torr several times prior to sampling. Postburn gas sampling was performed both with and without tank mixing and large differences in the results indicated that mixing was essential to obtain representative samples.

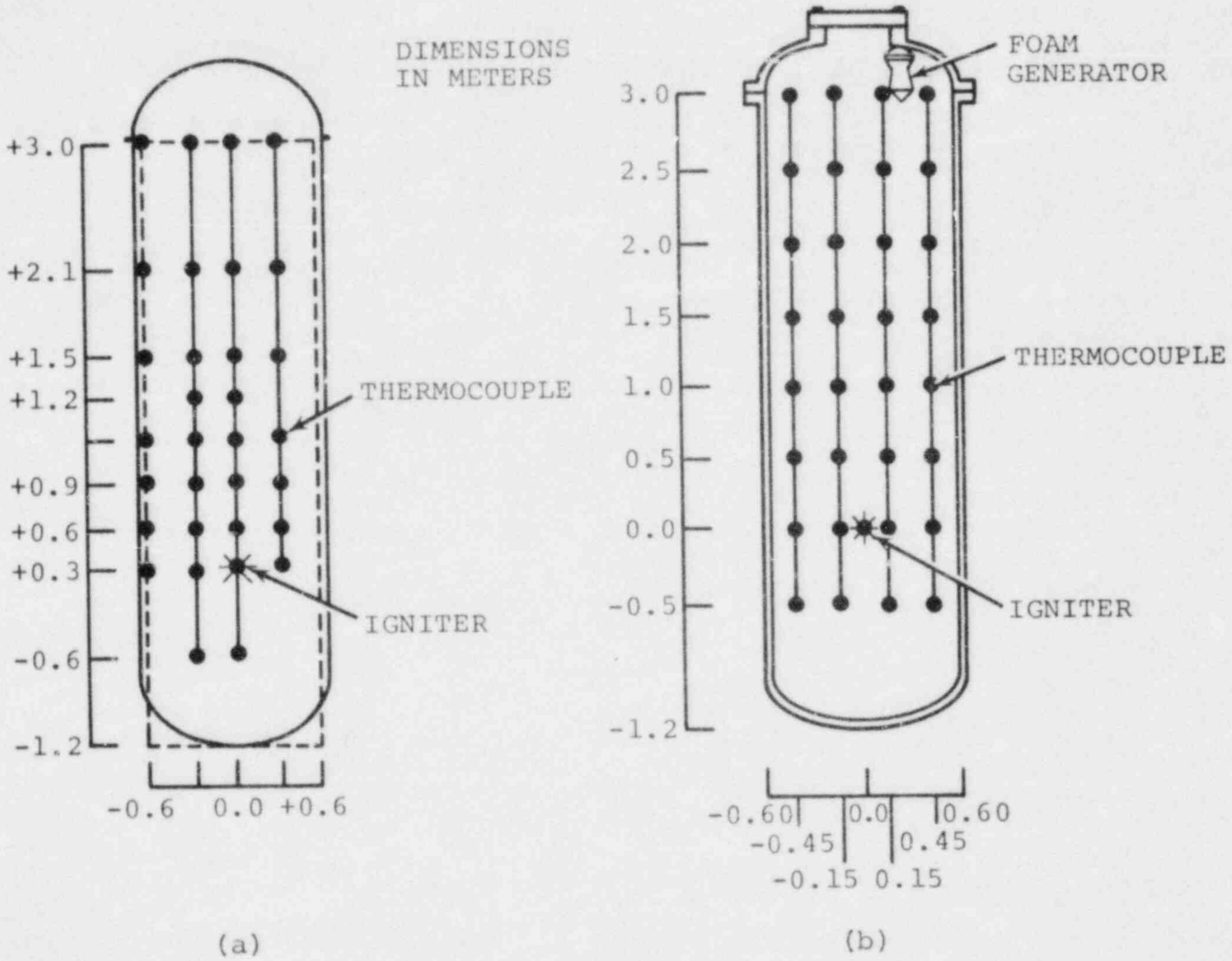

Figure 4. VGES TC arrangement (a) For TS 1-10. (b) For TS 11.

III. Instrumentation and Measurements

The principal instrumentation used during the VGES tank experiments has been an array of 32 thermocouples (TCs) and a dynamic-pressure transducer.

Several types and sizes of TCs were used during the testing. The principal TCs were type K (chromel-alumel), constructed of 0.033-cm (0.013-in.) diameter wire with a 0.079-cm (0.031-in.) diameter bead. Other TCs were used to test their response and survivability in a hydrogen burn environment. These TCs consisted of junction diameters from 0.00254 cm (0.001 in.) to 0.0125 cm (0.005 in.), and 0.0005 cm (0.0002 in.) flat conductors on a Kapton substrate.

The primary use of the TC array was to determine flame arrival times at various locations within the tank. The slow response of the TCs in the array precludes their use as an indicator for peak temperatures.

The TC array consisted of four columns arranged in a plane with one column at the tank centerline, two columns offset by 30 cm (12 in.) from the tank centerline, each in an opposite direction, and one column offset 60 cm (24 in.) from the tank centerline, as shown in Figure 4a. This TC arrangement was constant for TS 1 through 9. For TS 10, some of the TCs were replaced with instrumentation for the HBS Program. The HBS instrumentation consisted of flat plate and cubical calorimeters. The description of this instrumentation is reported elsewhere.[2]

For TS 11, the TC arrangement was changed (Figure 4b). This TC array consisted of four columns arranged in a plane with 30-cm (12-in.) spacing between each column and the array centered between the tank walls. The outer two columns were located 15 cm (6 in.) from the tank walls. The igniter was located vertically 1.8 m (71 in.) from the tank bottom and on the tank centerline. The TCs were equally spaced vertically, 0.5 m (19.7 in.) apart, and an additional TC was located at the igniter position. The 33 TCs for TS 11 consisted of pressure-welded junctions with a diameter of 0.033 cm (0.01 in.). Again, type K TCs were used.

Kulite strain gauge pressure transducers were used to measure dynamic pressure. The sensitive elements of these gauges were isolated from the burn by 1 cm (0.4 in.) of metal felt in all tests and with an additional inflatable rubber membrane in tests with lean mixtures. The intrinsic frequency response of each gauge was ~150 kHz; however, the mounting technique probably limited the actual response to less than 10 kHz. These gauges were located about 30 cm (12 in.) from the top of the flange that accommodates the tank top (Figure 2). Two pressure gauges were used for most of the testing; however, more gauges were added as testing proceeded, with the maximum number being five pressure gauges.

The temperature and pressure signals were recorded by the DAASY multichannel, digital data acquisition system. Each signal was processed by an individual amplifier and an analog-to-digital conversion unit. There were a maximum of 40 channels available for data acquisition. Thirty-two of the channels were used to record the temperature signals and from 2 to 5 channels were used to record the pressure signals. The DAASY system has a capacity of 1024 data points per channel in the time domain, and a digitizer resolution of 10 bits (1024 discrete signal values) in the signal voltage. The data sampling rate varied depending on the length of time data were recorded. The highest sampling rate was 1000 samples per second (sps) and the slowest was 20 sps. The data acquisition system was set to record data for a specific time period for each test.

A permanent record of the data was recorded on floppy discs, one for each test. The data were then transferred to magnetic tapes and transcribed so they were compatible with the CDC 6600 at Sandia National Laboratories, Albuquerque (SNLA). The SNLA computer was used to perform the final data reduction.

IV. Experimental Procedure and Initial Conditions

Test procedure for each test was as follows: after the tank was sealed, the fans were turned on for about 10 min to eliminate any thermal stratification of the air. Monitoring the pressure with a Wallace and Tiernan absolute pressure gauge (accurate to 0.25 torr), nitrogen, carbon dioxide, or hydrogen was admitted to the tank until a predetermined pressure was reached. For the tests with nitrogen and CO_2, these gases were admitted to the tank before the hydrogen. The fans were left on for another 10 min to ensure complete mixing of the tank atmosphere, then the preburn gas sample was taken. For the quiescent burns, the fans were turned off about 10 min prior to ignition. The turbulent, or "fans on," burns were ignited while the fans were still running. Although the fan blades were constructed of black plastic, very little melting or deformation was observed after the quiescent burns, and the same fans were used for all those tests. However, the heat transfer was so greatly enhanced during the turbulent burns that the fan blades were melted after a single shot and the fans had to be replaced after nearly every burn.

For the foam tests, the hydrogen and air concentrations were obtained using the procedure previously discussed. With the fan still running, the surfactant-water mixture contained in a small pressurized tank was added to the foam generator. Foam was generated until a visual inspection of the tank, through the top flanged Lexan window, indicated the tank was full of foam. The fan and foam generator were then turned off prior to ignition.

The initial conditions for each test are given in Table 1. This table indicates the test number, the partial pressures of the gases in the tank, gas volume percent concentration, the igniter type and ignition voltage or energy, the igniter location, and whether the fans were off or on during the ignition. The P_{AIR} values given in Table 1 are the starting pressures of air in the tank prior to any gas addition. The P_{N_2} values are the added partial pressures of nitrogen and do not include the nitrogen contained in the air.

The test number is a four to six digit alphanumeric identifier of each test. The first two to three digits indicate "Burn" and the test number, the next two to three digits indicate hydrogen (H) or foam (F) and the approximate hydrogen:air mixture ratio of the test. For example, B62H10 was the 62nd burn with approximately 10 parts H_2 added to the tank mixture (i.e., 10/100 + 10 = 9.1 volume percent H_2).

Table 1

Initial Conditions for the VGES Testing

TEST	P_{AIR} (mm Hg)	P_{H_2} (mm Hg)	P_{N_2} (mm Hg)	P_{CO_2} (mm Hg)	% AIR	% H_2	% N_2	% CO_2	IGNITER	IGN.LOCAL.	FANS
B1H8	635	50	---	---	92.67	7.33	---	---	300 W Lamp Filament 110 V	C-O*	Off
B2H6	667	37.7			94.35	5.65			300 W Lamp Filament 110 V	C-O	On
B3H4	---	---	---	---	---	---	---	---	--------	---	---
B4H8	628	50.2	---	---	92.6	7.4	---	---	Glowplug 70 V	C-O	Off
B5H6	627	37.6	---	---	94.34	5.66	---	---	Glowplug 70 V	C-O	Off
B6H5	625	31.3	---	---	95.23	4.77	---	---	Glowplug 70 V	C-O	Off
B7H7	630	44	---	---	93.47	6.53	---	---	Glowplug 67 V	C-O	Off
B8H9	629.5	56.7	---	---	91.74	8.26	---	---	Glowplug 68 V	C-O	Off
B9H10	629	63	---	---	90.90	9.10	---	---	Glowplug 68 V	C-O	Off
B10H8	625	50	---	---	92.59	7.41	---	---	Glowplug 70 V	C-O	On
B11H6	630	37.8	---	---	94.34	5.66	---	---	Glowplug 68 V	C-O	On
B12H5	623.5	30.5	---	---	95.34	4.66	---	---	Glowplug 68 V	C-O	On
B13H7	618.5	42.7	---	---	93.53	6.47	---	---	Glowplug 68 V	C-O	On
B14H4	623.5	27.25	---	---	95.81	4.19	---	---	Glowplug 68 V	C-O	On
B15H9	621.3	54.45	---	---	91.94	8.06	---	---	Glowplug 68 V	C-O	On
B16H9	628.5	56.5	---	---	92.75	8.25	---	---	Glowplug 68 V	C-O	On
B17H5	628	31.5	---	---	95.22	4.78	---	---	Glowplug 68 V	C+4**	Off

*C-O = Tank Center Line, 1.22m from tank bottom
**C+4 = Tank Center Line, 2.4m from tank bottom - Vertical Tank Center

Table 1

Initial Conditions for the VGES Testing (continued)

TEST	P_{AIR}	P_{H_2} (mm Hg)	P_{N_2}	P_{CO_2}	% AIR	% H_2	% N_2	% CO_2	IGNITER	IGN. LOCAL.	FANS
B18H5	627	31.25	---	---	95.25	4.75	---	---	Glowplug 68 V	C+4	On
B19H7	630.5	44.5	---	---	93.41	6.59	---	---	Glowplug 68 V	C+4	Off
B20H7	629.25	44.0	---	---	93.46	6.54	---	---	Glowplug 68 V	C+4	On
B21H9	627	56.5	---	---	91.73	8.27	---	---	Glowplug 68 V	C+4	On
B22H9	625.5	56.5	---	---	91.72	8.28	---	---	Glowplug 68 V	C+4	Off
B23H13	627	81.5	---	---	88.5	11.50	---	---	Glowplug 68 V	C+4	Off
B24H13	626.5	81.5	---	---	88.49	11.51	---	---	Glowplug 68 V	C+4	On
B25H18	559.1	99.9	---	---	84.75	15.25	---	---	Glowplug 68 V	C+4	Off
B26H18	627	113	---	---	84.73	15.27	---	---	Glowplug 68 V	C+4	Off
B27H12	623	74.75	---	---	89.29	10.71	---	---	Glowplug 68 V	C+4	Off
B28H9	---	---	---	---	---	---	---	---	-----	---	---
B29H9	623	56	---	---	91.75	8.25	---	---	Spark 5 kV	C-O	Off
B30H7	623	43.75	---	---	93.44	6.56	---	---	Spark 5 kV	C-O	Off
B31H7	622	43.5	---	---	93.46	6.54	---	---	Spark 5 kV	C-O	Off
B32H7	621.75	43.5	---	---	93.46	6.54	---	---	Spark 5 kV	C-O	On
B33H5	625.5	31.25	---	---	95.24	4.76	---	---	Spark 5 kV	C-O	Off
B34H5	625.25	31.25	---	---	95.24	4.76	---	---	Spark 5 kV	C-O	On

Table 1

Initial Conditions for the VGES Testing (continued)

TEST	P_{AIR} (mm Hg)	P_{H_2} (mm Hg)	P_{N_2} (mm Hg)	P_{CO_2} (mm Hg)	% AIR	% H_2	% N_2	TOTAL N_2	% CO_2	IGNITER	IGN.LOCAL.	FANS
B35H9	625	56.25	---	---	91.74	8.26	---		---	Spark 5 kV	C+4	On
B36H8	400	32	---	---	92.59	7.41	---		---	Spark 5 kV	C-O	On
B37H6	398	25	---	---	94.09	5.91	---		---	Spark 5 kV	C-O	On
B38H8	400	32	---	---	92.59	7.41	---		---	Spark 5 kV	C-O	On
B39H8	400	32	---	---	92.59	7.41	---		---	Spark 5 kV	C-O	Off
B40H10	402.5	40	---	---	90.96	9.04	---		---	Spark 5 kV	C-O	On
B41H8	200	16	---	---	92.58	7.41	---		---	Spark 5 kV	C-O	On
B42H18	200	36	---	---	84.75	15.25	---		---	Spark 5 kV	C-O	Off
B43H30	200	61	---	---	76.63	23.37	---		---	Spark 5 kV	C-O	Off
B44H8	100	8	---	---	92.59	7.41	---		---	Spark 5 kV	C-O	On
B45H18	100	18	---	---	84.75	15.25	---		---	-----	C-O	Off
B46H30	100	30	---	---	76.91	23.08	---		---	Spark 5 kV	C-O	Off
B47H6	500	45	250	---	62.89	5.66	31.45	81.13	---	Spark 5 kV	C-O	On
B48H8	400	48	200	---	61.73	7.41	30.86	79.63	---	Spark 5 kV	C-O	Off
B49H10	400	60	200	---	60.61	9.09	30.30	78.18	---	Spark 5 kV	C-O	On
B50H18	400	108	200	---	56.50	15.25	28.25	72.39	---	Spark 5 kV	C-O	Off
B51H8	400	32	200	---	63.29	5.06	31.65	81.66	---	Spark 5 kV	C-O	On

Table 1

Initial Conditions for the VGES Testing (continued)

TEST	P_{AIR}	P_{H_2} (mm Hg)	P_{N_2}	P_{CO_2}	% AIR	% H_2	% N_2	TOTAL N_2	% CO_2	IGNITER	IGN.LOCAL.	FANS
B52H10	400	40	200	---	62.50	6.25	31.25	80.63	---	Spark 5 kV	C-O	On
B53H30	400	120	200	---	55.55	16.67	27.78	71.66	---	Spark 5 kV	C-O	Off
B54H6	629.25	37.75	---	---	94.34	5.66	---		---	Glowplug 14 V	C-O	On
B55H8	629.25	50.25	---	---	92.60	7.40	---		---	Glowplug 14 V	C-O	On
B56H10	628.5	62.75	---	---	90.92	9.08	---		---	Glowplug 14 V	C-O	Off
B57H10	628.5	62.75	---	---	90.92	9.08	---		---	Glowplug 14 V	C-O	On
B58H12	628.5	75.5	---	---	89.28	10.72	---		---	Glowplug 14 V	C-O	Off
B59H12	628.25	75.5	---	---	89.27	10.73	---		---	Glowplug 14 V	C-O	On
B60H12	400	48	---	---	89.29	10.71	---		---	Glowplug 14 V	C-O	Off
B61H12	400	48	---	---	89.29	10.71	---		---	Spark 5 kV	C-O	On
B62H10	400	40	---	---	90.91	9.09	---		---	-----	C-O	Off
B63H10	400	40	---	---	90.91	9.09	---		---	Spark 5 kV	C-O	On
B64H6	400	24	200	---	64.1	3.85	32.05	82.69	---	Spark 5 kV	C-O	On
B65H6	400	24	200	---	64.1	3.85	32.05	82.69	---	Spark 5 kV	C-O	On
B66H7	400	28.27	200	---	63.67	4.50	31.83	82.13	---	Spark 5 kV	C-O	On
B67H7	400	28.5	200	---	63.65	4.53	31.82	82.10	---	Glowplug 60 V	C-O	On
B68H20	400	80	200	---	58.24	11.76	29.41	75.42	---	Glowplug 60 V	C-O	Off

Table 1

Initial Conditions for the VGES Testing (continued)

TEST	P_{AIR} (mm Hg)	P_{H_2} (mm Hg)	P_{N_2} (mm Hg)	P_{CO_2} (mm Hg)	% AIR	% H_2	% N_2	% CO_2	IGNITER	IGN.LOCAL.	FANS
B69H15	627.5	93.5	---	---	87.03	12.97	---	---	Spark 4 kV	C-O	On
B70H15	629.25	94.5	---	---	86.94	13.06	---	---	Spark 4 kV	C-O	Off
B71H18	629.25	113.25	---	---	84.75	15.25	---	---	Spark 4 kV	C-O	Off
B72H18	628.5	113.25	---	---	84.73	15.27	---	---	Spark 4 kV	C-O	On
B73H21	628.0	132.0	---	---	82.63	17.37	---	---	Spark 4 kV	C-O	Off
B74H21	627.25	131.75	---	---	82.64	17.36	---	---	Spark 4 kV	C-O	On
B75H10	630.75	63.1	---	---	90.91	9.09	---	---	Spark 4 kV	C-O	Off
B76H15	630.0	94.5	---	---	86.96	13.04	---	---	Glowplug 60 V	C-O	Off
B77H15	629.0	94.35	---	---	86.96	13.04	---	---	Glowplug 60 V	C-O	On
B78H37	400	150	---	600	34.79	13.04	---	52.17	Glowplug 58 V	C-O	Off
B79H37	400	150.25	---	600	34.78	13.06	---	52.16	Glowplug 58 V	C-O	Off
B80H37	400	150	---	700	32.00	12.00	---	56.00	Glowplug 60 V	C-O	Off
B81H37	400	150	---	650	33.33	12.50	---	54.17	Glowplug 68 V	C-O	Off
B82H37	400	150	---	500	38.10	14.29	---	47.62	Glowplug 60 V	C-O	Off
B83H37	400	150	---	400	42.10	15.79	---	42.11	Glowplug 60 V	C-O	Off
B84H37	400	150	---	200	53.33	20.00	---	26.67	Spark 4.5 kV	C-O	Off
B85H37	400	150	---	300	47.06	17.65	---	35.29	Spark 4 kV	C-O	Off

Table 1

Initial Conditions for the VGES Testing
(continued)

TEST	P_{AIR} (mm Hg)	P_{H_2} (mm Hg)	P_{N_2} (mm Hg)	P_{CO_2} (mm Hg)	% AIR	% H_2	% N_2	% CO_2	IGNITER	IGN.LOCAL.	FANS
B86H18	630	113.5	---	---	84.73	15.27	---	---	Spark 4 kV	C-O	Off
B87H21	630	132.25	---	---	82.65	17.35	---	---	Spark 4 kV	C-O	Off
B88H11	627.25	72.75	---	---	89.61	10.39	---	---	Spark 4 kV	C-O	Off
B89H11	626.25	73.25	---	---	89.53	10.47	---	---	Spark 4 kV	C-O	On
B90H11	628.25	79.0	---	79.00	79.90	10.05	---	10.05	Glowplug 70 V	C-O	Off
B91H11	627	79.0	---	79.00	79.88	10.06	---	10.06	Glowplug 70 V	C-O	On
B92H17	626.0	112.0	---	---	84.82	15.18	---	---	Glowplug 70 V	C-O	Off
B93H17	628.75	111.0	---	---	84.99	15.01	---	---	Spark 4 kV	C-O	On
B94H11	630	70.0	---	---	90.00	10.00	---	---	Spark 3.3 kV	C-O	Off
B95F11	627	70.75	---	---	89.9	10.1	---	---	Spark 3.3 kV	C-O	Off
B96F25	624	156	---	---	80.00	20.00	---	---	Spark kV	C-O	Off
B97F18	630	113	---	---	84.79	15.21	---	---	Spark 3.3 kV	C-O	Off
B98H18	630	113	---	---	84.79	15.21	---	---	Spark 3.3 kV	C-O	Off
B99F25	630	157	---	---	80.05	19.95	----	---	Exploding Bridge Wire	C+10*	Off
B01F25	624.75	156.25	---	---	79.99	20.01	---	---	Spark 3.3 kV	C-O	Off
B02H25	633	158.25	---	---	80.00	20.00	---	---	Spark 3.3 kV	C-O	Off
B03H25	634.25	158.75	---	---	79.98	20.02	---	---	Spark 3.3 kV	C-O	Off

*C+10 - Exploding bridge wire was located at vacuum port, near the top of the tank.

Table 1

Initial Conditions for the VGES Testing (continued)

TEST	P_{AIR} (mm Hg)	P_{H_2} (mm Hg)	P_{N_2} (mm Hg)	P_{CO_2} (mm Hg)	% AIR	% H_2	% N_2	% CO_2	IGNITER	IGN.LOCAL.	FANS
B04H12	630	75.5	---	---	89.3	10.7	---	---	Spark 3.3 kV	C-O	On
B05H25	625	156	--	---	80.03	19.97	---	---	---	C-O	Off

V. Data Presentation

Over 100 experiments have been conducted in the VGES tank. Examples of raw data for temperature and pressure from a few tests are shown in Figure 5. The recorded pressure data for all tests are given in Appendix A.

The TC signals exhibit a slow initial rise due to the thermal inertia and finite heat transfer rates from the flame front and combustion products to the wires and beads. The decaying signal at later times reflects the cooling of the combustion products by radiative and convective heat transfer to the tank wall. A comparison between a TC with a 0.0127-cm (0.005-in.) diameter bead and a 0.079-cm (0.031-in.) diameter bead is shown in Figure 6. These TCs are at the same vertical level (even with the igniter) with the larger TC located 30.5 cm (12 in.) from the igniter and the smaller TC located 61 cm (24 in.) from the igniter. The smaller TC has a faster response to the burn both for the temperature rise and decay, due to its smaller thermal mass. The smaller TC, however, failed in subsequent tests due to the burn environment.

The principal use of the TC data was in determining a cross section of the flame front geometry as a function of time. To do this, the breakaway time, t_b, defined as the time the temperature signal reached 5% of its maximum change, was used as the effective time the flame front arrived at the TC. Both contour plots (showing iso-arrival-time contours) and space-time (x-t) plots of burn front trajectories were constructed using these data. Examples of contour plots comparing "fans on" and "fans off" cases are shown in Figure 7. These plots were obtained by fitting a fifth-degree polynomial to a fine grid interpolated from the array of t_b values. This procedure was implemented in a computer program specifically written for this purpose by P. L. Stanton. However, due to the sparseness of the TC grid and the nature of the data reduction procedure, these contour plots yield only a qualitative indication of the flame geometry and should not be given undue emphasis. Contour plots for all tests are given in Appendix A. Examples of space-time plots are shown in Figures 8 and 9. The three lines shown in Figures 8 and 9 indicate the arrival time of the flame at the TCs located on the three vertical stalks in the tank (one stalk at the tank centerline, one offset 30 cm (11.8 in.) from the centerline and one offset 60 cm (23.6 in.) from the centerline).

The initial rise of the pressure signal is due to the flame propagating outward (and mainly upward) from the igniter. For those tests with the glowplug igniter in very lean mixtures, it is possible to have more than a single flame front or an extended region of combustion within the tank. This makes the analysis of the pressure signal more difficult than

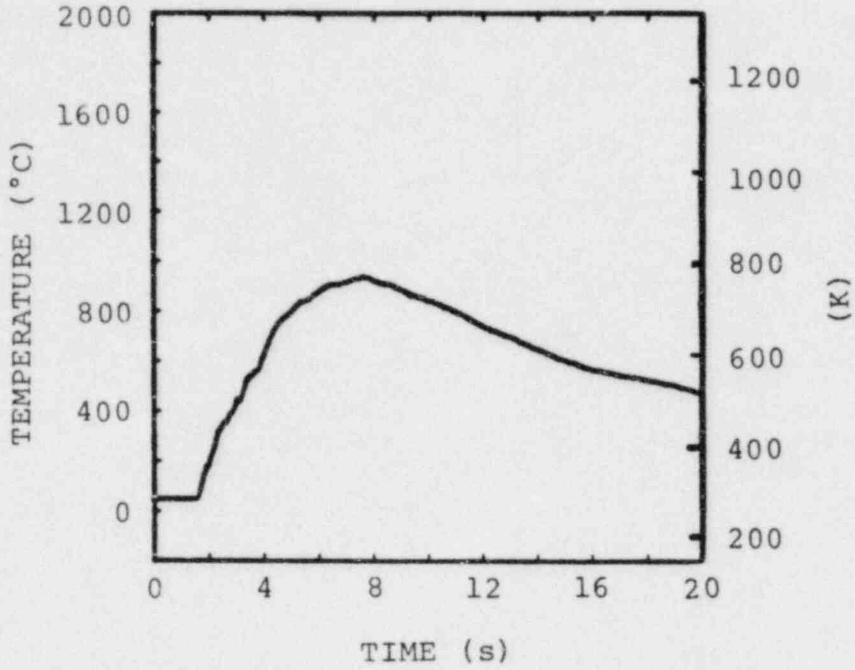

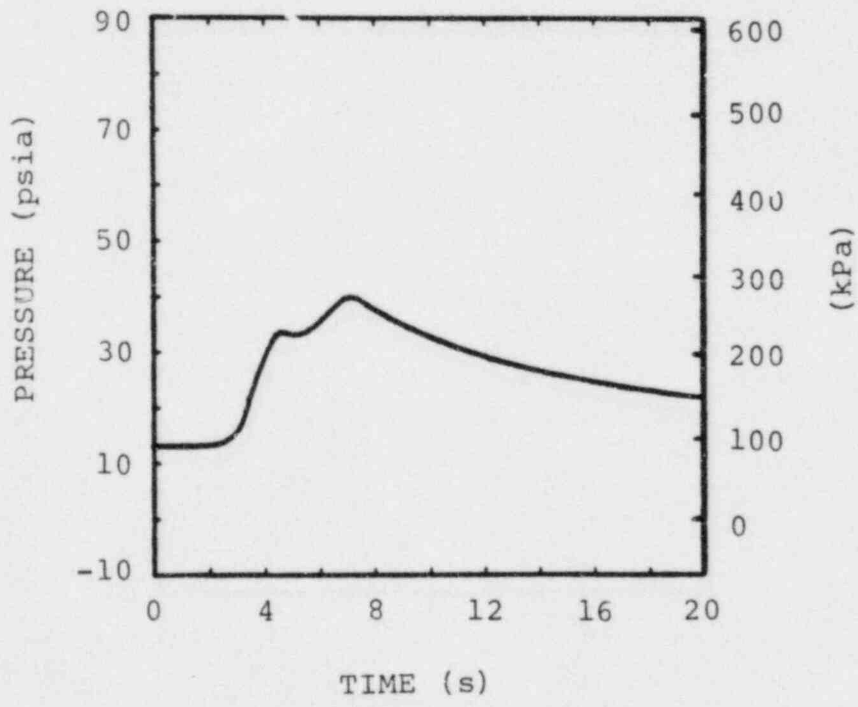

Figure 5. Temperature and Pressure for Test B8H9, 8.26% H_2, Fans Off

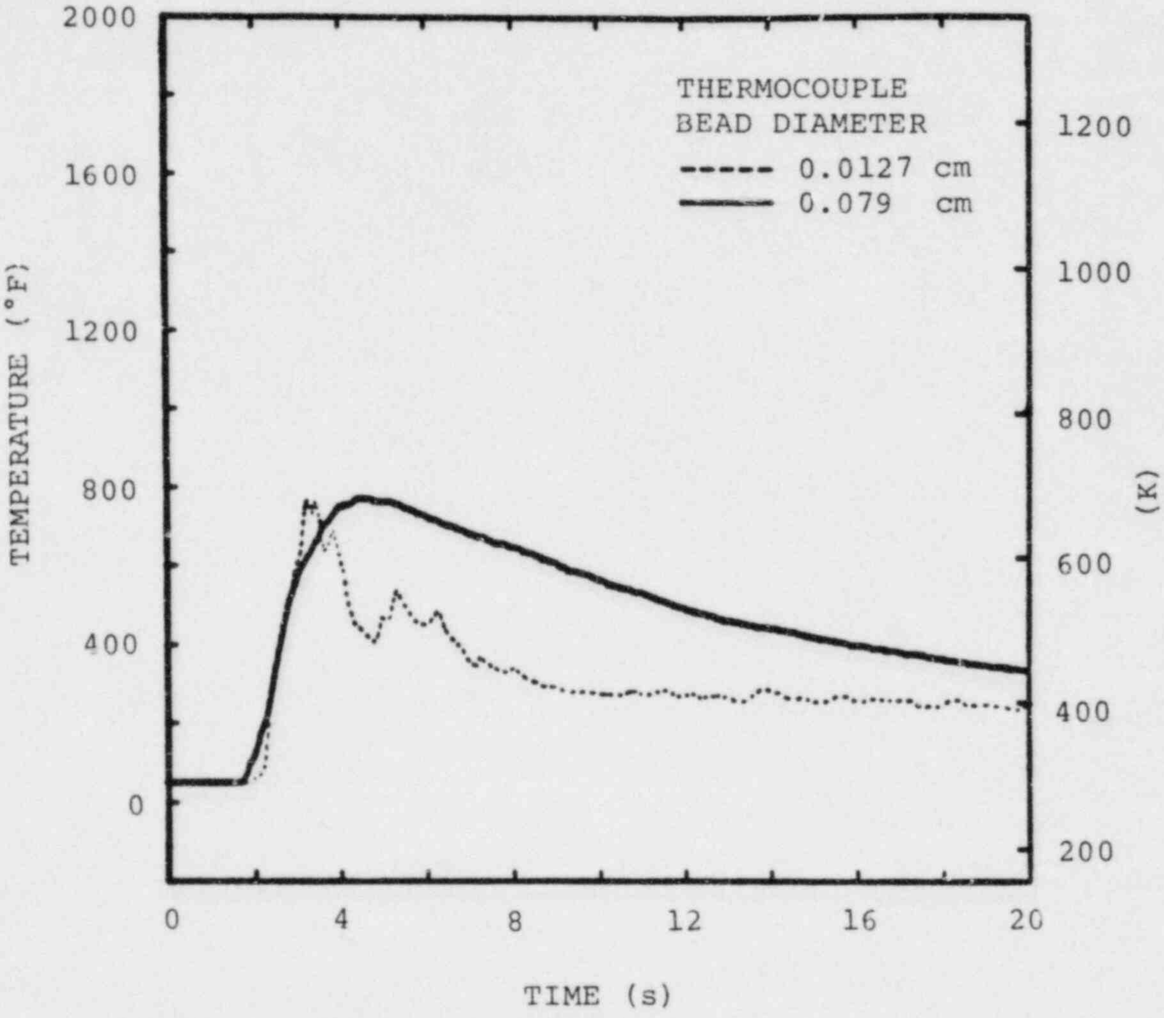

Figure 6. Comparison of the Response of TCs with Different Size Beads

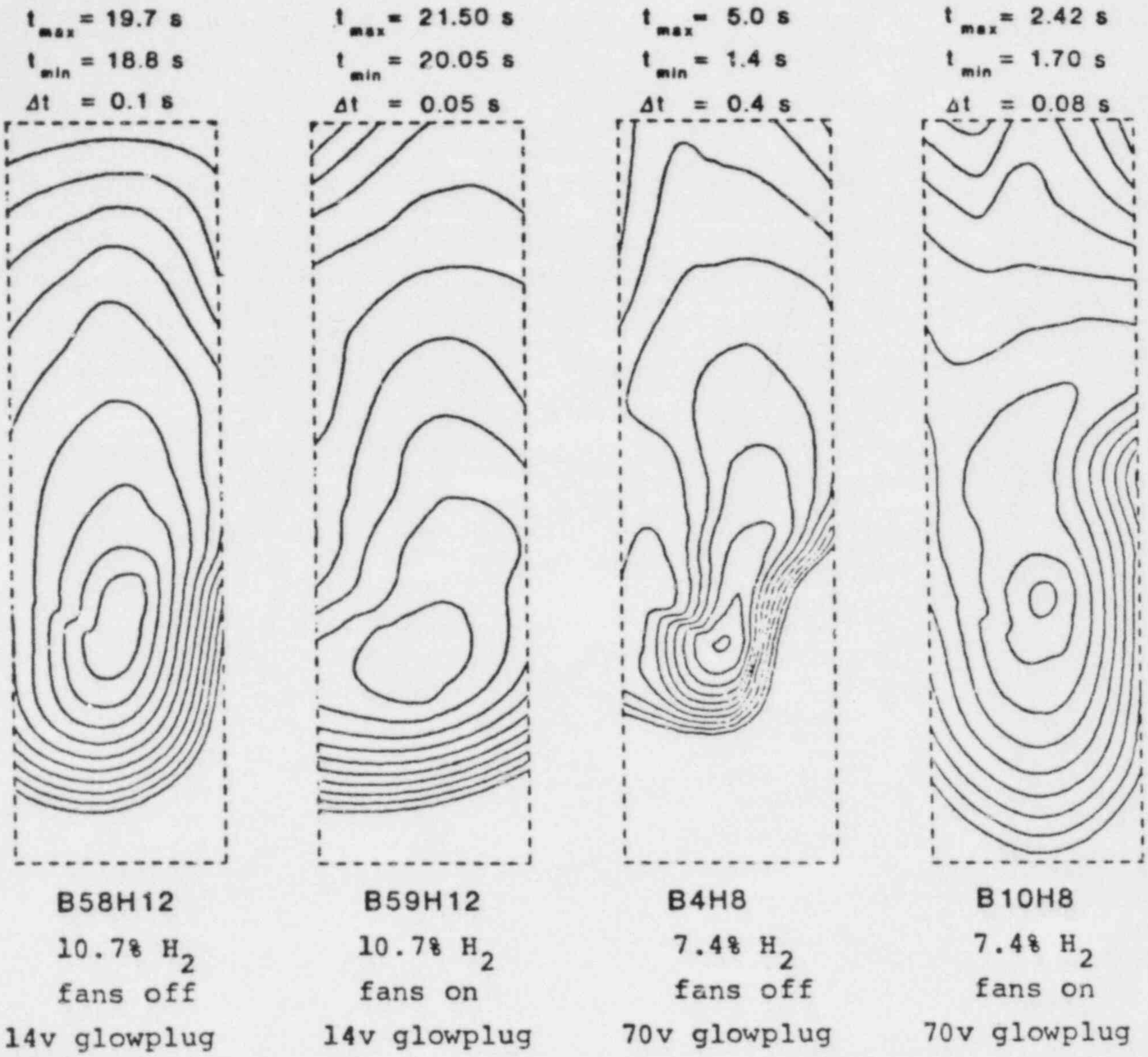

t_{max} = time of last contour

t_{min} = time of first contour

Δt = time between contours

Figure 7. Iso-Arrival-Time Contours for Hydrogen:Air Burns. Dashed lines represent the approximate location of the tank walls. The igniter was located at about 0.3 of the tank height above the bottom.

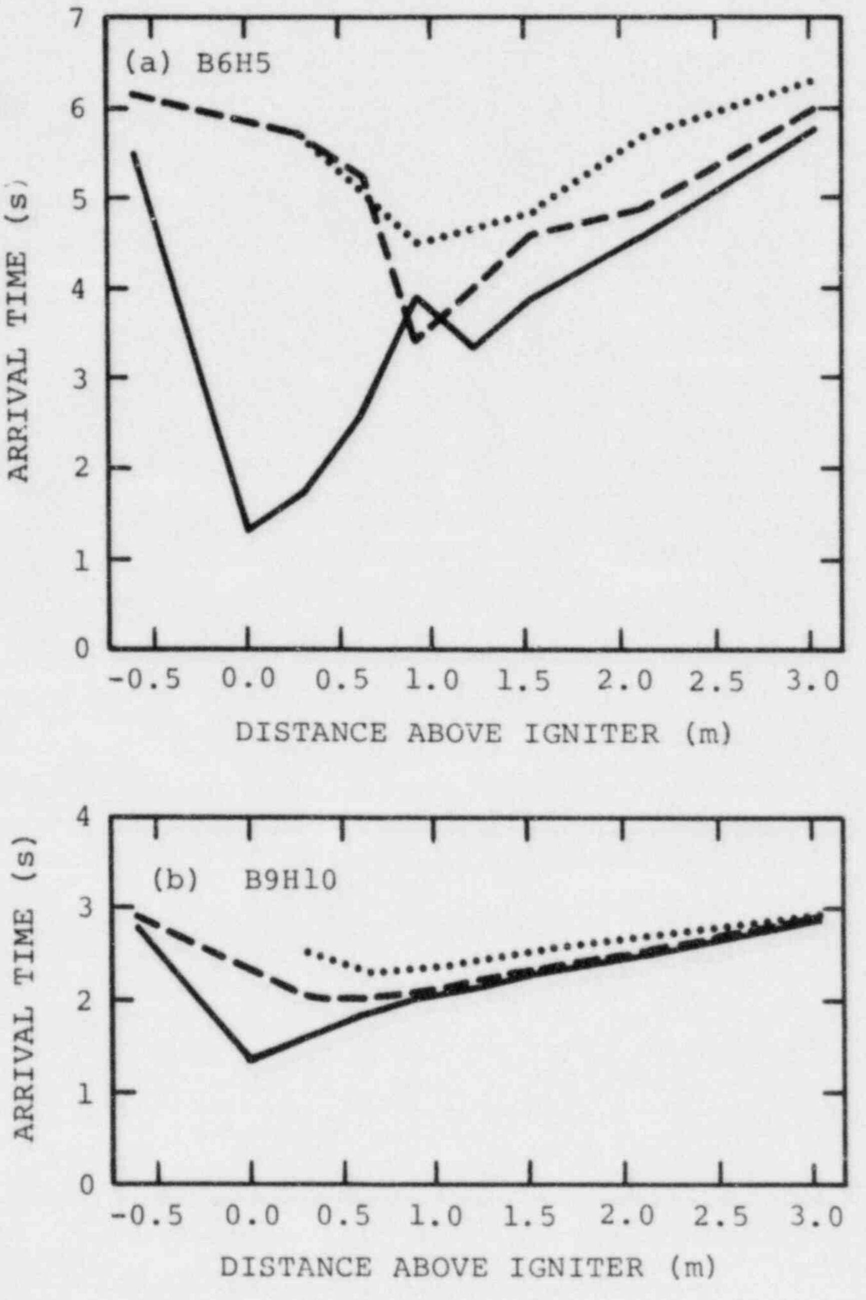

Figure 8. Space-Time (x-t) Plots for Hydrogen:Air Burns
(a) 4.8% H_2, fans off
(b) 9.1% H_2, fans off
. . . . 60 cm from tank centerline
\- - - - 30 cm from tank centerline
_______ tank centerline

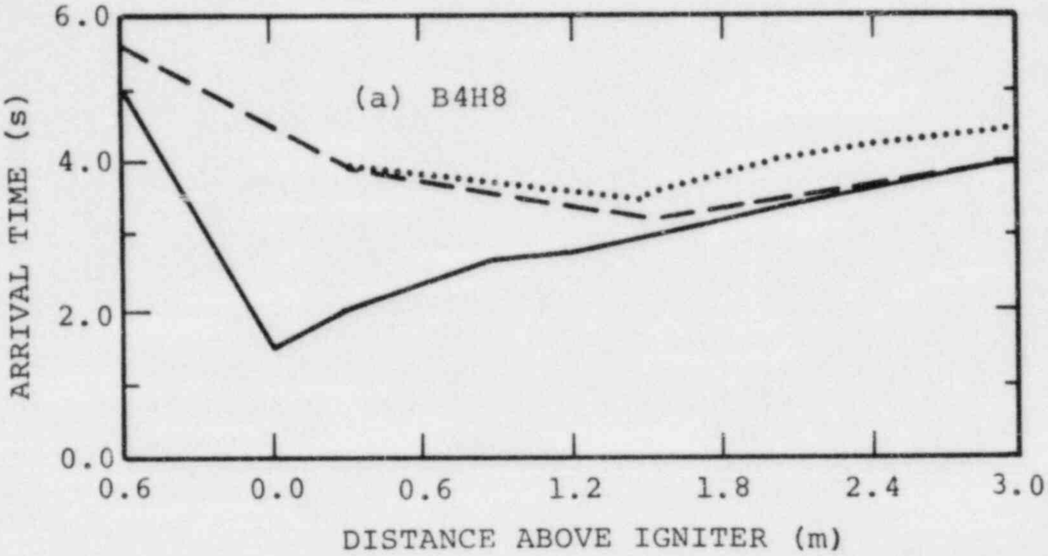

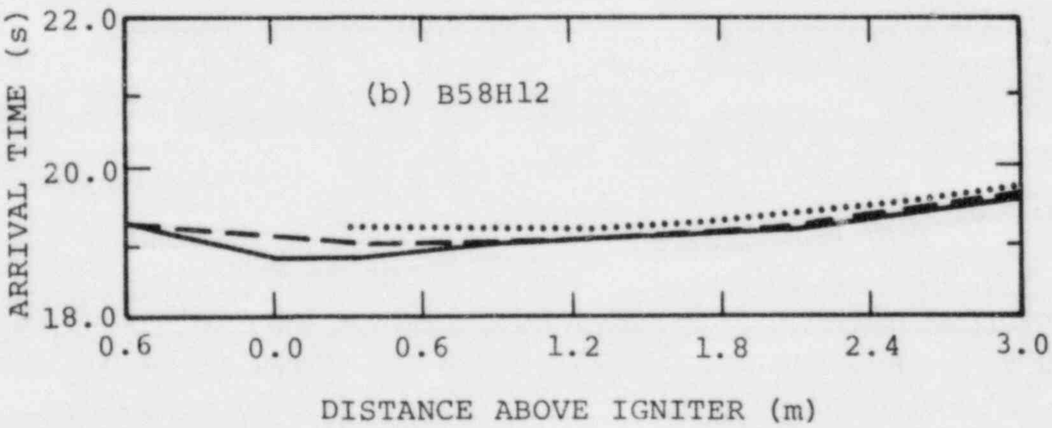

Figure 9. Space-Time (x-t) Plots for Hydrogen:Air Burns
(a) 7.4% H_2, fans off
(b) 10.7% H_2, fans off
. . . . 60 cm from tank centerline
\- - - - 30 cm from tank centerline
________ tank centerline

in the case of spark ignition. The subsequent decay in pressure is due to the gas temperature decay caused by heat transfer from the hot combustion products to the cold tank walls.

Gas samples were taken before and after most burns and were analyzed with a gas chromatograph (GC). Table 2 gives the preburn and postburn results of the GC analysis for all tests in which gas samples were taken. Comparison of preburn GC analysis results with expected compositions computed from pressure measurement revealed a systematic difference of 10% to 15% in total hydrogen content. The uncertainty in the partial pressure method is conservatively estimated to be a factor of 3 less than this. Therefore, we conclude that a large systematic error exists in the GC technique (perhaps due in part to the gas sampling process). Although GC analysis results are reported, the partial pressure measurements were used to establish the preburn hydrogen concentrations. Many tests employed as many as three precision pressure gauges (Wallace and Tiernan, Hiesie) as cross-checks. Variations in partial pressures were usually within 0.1% of each other.

Table 2

Gas Chromatograph Results

TEST NUMBER	BEFORE BURN (VOLUME PERCENT) O_2+Ar	N_2	H_2	CO_2	AFTER BURN (VOLUME PERCENT) O_2+Ar	N_2	H_2	CO_2	PREBURN FROM PARTIAL PRESSURE MEASUREMENTS % H_2
B1H8	---	---	---	---	18.30	81.40	0.34	---	7.3
B2H6	---	---	---	---	19.90	76.60	3.50	---	5.7
B4H8	---	---	---	---	17.91	79.10	0.90	---	7.4
B5H6	19.90	73.72	6.38	---	20.10	75.87	4.03	---	5.7
B6H5	---	---	---	---	20.43	75.51	4.05	---	4.8
B7H7	19.97	72.69	7.34	---	19.54	76.95	3.51	---	6.5
B8H9	19.81	70.93	9.26	---	18.13	81.87	0.01	---	8.3
B10H8	20.10	71.50	8.40	---	18.70	81.30	0.00	---	7.4
B11H6	20.50	73.30	6.20	---	19.90	77.90	2.20	---	5.7
B12H5	20.80	74.00	5.20	---	20.60	75.80	3.60	---	4.7
B13H7	20.20	72.50	7.30	---	19.50	78.40	2.10	---	6.5
B14H4	---	--	--	---	20.70	74.90	4.40	---	4.2
B15H9	20.50	73.00	6.50	---	18.40	81.60	0.00	---	8.1
B16H9	20.14	71.35	8.50	---	18.26	81.74	0.00	---	8.3
B17H5	---	---	---	---	20.62	74.81	4.58	---	4.8
B18H5	20.67	74.07	5.26	---	20.52	75.97	3.52	---	4.8
B19H7	20.45	73.04	6.52	---	19.75	76.06	3.63	---	6.6
B20H7	20.16	73.04	6.80	---	19.41	79.00	1.60	---	6.5
B22H9	19.87	70.82	9.31	---	18.17	81.79	0.06	---	8.3
B23H13	18.23	69.82	11.95	---	16.32	83.68	0.00	---	11.5
B24H13	18.32	70.38	11.30	---	16.34	83.66	0.00	---	11.5
B25H18	18.59	64.09	17.32	---	---	---	--	---	15.3
B26H18	18.67	63.76	17.57	---	---	---	--	---	15.3

Table 2

Gas Chromatograph Results
(continued)

TEST NUMBER	BEFORE BURN (VOLUME PERCENT) O_2+Ar	N_2	H_2	CO_2	AFTER BURN (VOLUME PERCENT) O_2+Ar	N_2	H_2	CO_2	PREBURN FROM PARTIAL PRESSURE MEASUREMENTS % H_2
B27H12	19.58	68.65	11.77	---	16.62	83.38	0.00	---	10.7
B28H9	20.12	70.38	9.50	---	17.98	82.02	0.00	---	8.3
B30H7	20.18	72.40	7.42	---	19.56	77.66	2.97	---	6.6
B31H7	20.38	72.32	7.30	---	19.81	76.89	3.31	---	6.5
B32H7	20.20	72.10	7.70	---	19.93	79.46	0.62	---	6.5
B33H5	20.64	74.85	4.51	---	21.14	73 [illegible]	5.59	---	4.8
B34H5	20.79	73.78	5.43	---	20.64	75.52	3.84	---	4.8
B35H9	19.92	70.60	8.26	---	18.32	81.68	0.00	---	8.3
B36H8	20.51	72.09	7.40	---	19.31	80.42	0.27	---	7.4
B37H6	21.57	72.49	5.94	---	20.58	76.88	2.54	---	5.9
B38H8	21.29	71.39	7.32	---	20.02	79.71	0.27	---	7.4
B39H8	22.26	74.26	3.48	---	20.22	77.67	2.11	---	7.4
B40H10	20.82	70.38	8.80	---	18.73	81.27	0.00	---	9.1
B42H18	19.21	64.90	15.89	---	14.93	85.07	0.00	---	15.3
B43H30	17.53	58.16	24.31	---	4.08	95.92	0.00	---	23.4
B45H18	19.68	63.81	16.51	---	---	---	--	---	15.3
B48H8	13.80	78.13	8.07	---	11.68	88.26	0.06	---	7.4
B49H10	13.51	76.62	9.87	---	10.54	89.46	0.00	---	9.1
B51H8	14.17	80.27	5.56	---	13.93	82.68	3.39	---	5.1
B52H10	14.06	79.17	6.77	---	12.93	85.00	2.07	---	6.3
B53H30	17.68	57.90	24.40	---	5.12	94.88	0.00	---	16.7
B54H6	21.7[illegible]	72.07	6.17	---	20.85	76.49	2.66	---	5.7
B55H8	21.42	70.75	8.23	---	19.30	80.68	0.02	---	7.4

Table 2

Gas Chromatograph Results (continued)

TEST NUMBER	BEFORE BURN (VOLUME PERCENT) O_2+Ar	N_2	H_2	CO_2	AFTER BURN (VOLUME PERCENT) O_2+Ar	N_2	H_2	CO_2	PREBURN FROM PARTIAL PRESSURE MEASURE-MENTS % H_2
B56H10	21.00	69.15	9.85	---	18.49	81.51	0.00	---	9.1
B57H10	21.26	68.74	10.00	---	18.37	82.63	0.00	---	9.1
B58H12	20.51	67.67	11.82	---	16.93	83.07	0.00	---	10.7
B59H12	20.53	67.72	11.75	---	17.40	82.60	0.00	---	10.7
B62H10	21.20	68.80	10.00	---	---	---	--	---	9.1
B63H10	21.02	69.04	9.94	---	---	---	--	---	9.1
B64H6	14.40	81.42	4.18	---	---	---	--	---	3.9
B68H20	13.20	74.55	12.25	---	---	---	--	---	11.8
B69H15	20.13	66.42	13.45	---	--	---	--	---	13.0
B70H15	19.80	65.97	14.23	---	16.10	83.90	0.00	---	13.1
B71H18	19.35	64.17	16.48	---	--	---	--	---	15.3
B72H18	19.14	64.50	16.36	---	14.48	85.52	0.00	---	15.3
B73H21	18.70	62.60	18.70	---	---	---	--	---	17.4
B74H21	18.77	62.52	18.71	---	---	---	--	---	17.4
B75H10	20.78	69.32	9.90	---	---	---	--	---	9.1
B76H15	19.84	66.14	14.02	---	---	---	--	---	13.0
B77H15	19.80	66.20	14.00	---	---	---	--	---	13.0

VI. Experimental Results

The VGES tank testing was designed to provide data on hydrogen combustion in a short time frame. The results of each of the 11 TS completed to date are given below, followed by general results drawn from the overall testing.

VI-1. Test Series 1

TS 1 comprised system checkout tests and initial observations of hydrogen:air combustion. Initial conditions and principal results for TS 1 are given in Table 3. In Table 3 are the initial pressures, temperatures, and H_2 concentrations for each test along with the recorded maximum pressure (P_{max}) and temperature (T_{max}), the calculated pressure rise time (Δt), mean pressure derivative ($\Delta P/\Delta t$), normalized peak pressure (P_{max}/P_o), and the flame propagation speeds for both upward (V_{up}) and downward (V_{down}) propagation. Both the peak pressure rise (ΔP) and the pressure rise time are useful measures of burn strength. The mean pressure derivative can be related to chemical energy release rate and the ratio of peak pressure rise to initial pressure can be related to completeness of combustion.[3] The pressure rise and pressure rise time are shown in Figure 10. The flame propagation speeds were determined from flame arrival times for the TCs located on the tank centerline and their vertical spatial locations. The upward flame speeds were obtained using flame front arrival time data from the TCs located 0.305 and 3.05 m (1 and 10 ft) above the igniter. The downward flame speeds were obtained using data from the TC located at the igniter and the TC located 0.61 m (2 ft) below the igniter. The flame speeds represent average flame velocity within the tank. The pressure rise is defined as $P_{max} - P_o$, and the pressure rise time is the time the pressure attains its maximum value minus the time at which the pressure attains 2% of its maximum rise.

For TS 1, measured peak temperatures ranged from 60% of the calculated adiabatic complete combustion temperatures for 9% H_2 concentration to less than 8% of the adiabatic temperature for the 4% H_2 concentration case. The peak temperatures measured in these experiments are only relative values due to the long time constant of the TC bead.

Contour plots comparing the "fans on" and "fans off" case for 4.8% and 7.4% H_2 are shown in Figure 11.

Inspection of these contour plots and the space-time plots previously presented in Figures 8 and 9 indicate, that the burns were accelerating as the burn front moved up the tank and that downward propagation and/or convection of burned gas occurred in portions of the tank. The flame propagation velocities increased rapidly as the initial hydrogen concentration was increased and, for the same hydrogen concentration, are factors of 4 to 10 higher with "fans on" as compared

Table 3

TS 1: System Checkout and Initial Testing

TEST NUMBER	VOLUME % CO_2	P_o (atm)	P_{max} (atm)	T_o (°C)	T_{max} (°C)	PRESSURE Δt(s)	$\Delta P/\Delta t$ (atm/s)	P_{max}/P_o	V_{up} (m/s)	V_{down} (m/s)
B1H8	----	0.90	----	24.5	300	----	----	----	----	----
B2H6	----	0.93	----	19.8	160	----	----	----	----	----
B3H4	No Data (Data System Fault)									
B4H8	----	0.89	2.35	14.6	457	5.59	0.26	2.66	1.21	0.17
B5H6	----	0.87	1.50	12.1	314	3.69	0.17	1.70	0.85	0.25
B6H5	----	0.86	1.28	15.0	390	5.12	0.08	1.46	0.68	0.15
B7H7	----	0.89	1.69	13.8	340	2.82	0.29	1.91	1.11	0.20
B8H9	----	0.90	2.71	14.4	549	4.70	0.38	3.03	1.42	0.16
B9H10	----	0.91	3.86	16.9	683	1.16	2.54	4.26	1.93	0.41
B10H8-F*	----	0.89	3.11	12.6	488	0.89	2.50	3.57	5.92	3.33
B11H6-F	----	0.88	1.87	15.3	240	1.58	0.62	2.10	3.23	2.62
B12H5-F	----	0.86	1.26	13.9	110	1.74	0.23	1.43	3.50	2.03
B13H7-F	----	0.87	2.34	10.8	617	1.13	1.30	2.76	5.44	3.87
B14H4.5-F	----	0.86	0.96	11.5	42.1	5.12	0.02	1.13	0.80	0.22
B15H9-F	----	0.89	----	4.84	557	----	----	----	4.55	1.47
B16H9-F	----	0.90	3.24	8.82	547	0.84	2.78	3.59	6.40	9.59

*The letter "F" following a test number indicates that the fans were on during the test.

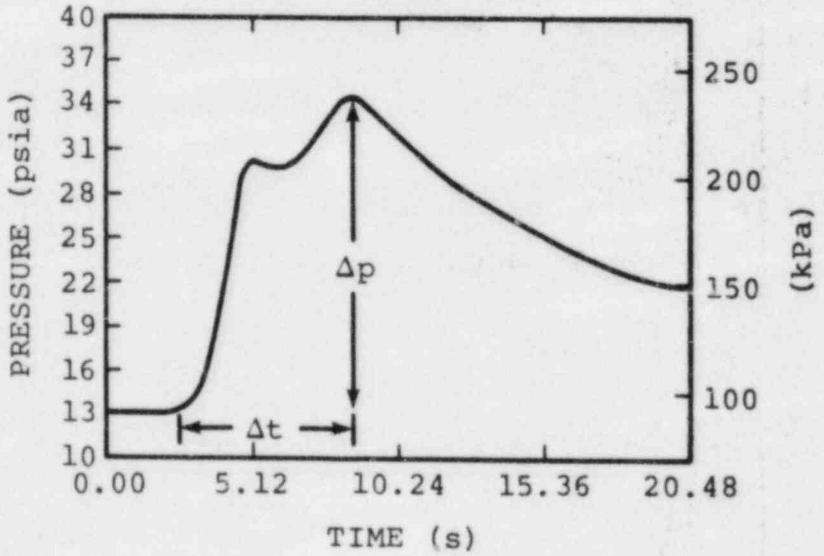

Figure 10. Raw Pressure Data Showing Peak Pressure Rise (ΔP) and Pressure Rise Time (Δt)

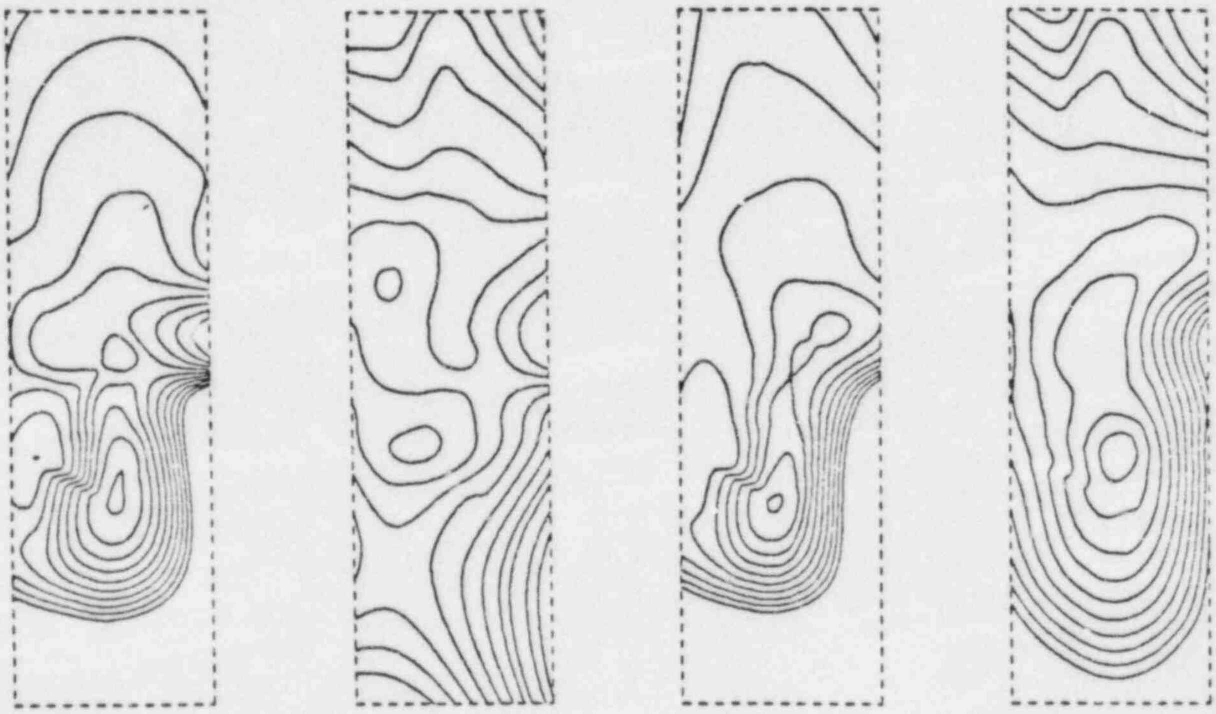

(a) B6H5	(b) B12H5	(c) B4H8	(d) B10H8
t_{min} = 0.75 s	t_{min} = 2.16 s	t_{min} = 1.05 s	t_{min} = 1.74 s
t_{max} = 6.75 s	t_{max} = 3.56 s	t_{max} = 5.55 s	t_{max} = 2.34 s
Δt = 0.6 s	Δt = 0.14 s	Δt = 0.45 s	Δt = 0.06 s

Figure 11. Iso-Arrival-Time Contours for Hydrogen:Air Burns
(a) 4.8% H_2, fans off
(b) 4.8% H_2, fans on
(c) 7.4% H_2, fans off
(d) 7.4% H_2, fans on

Written below each contour plot is the time of the first contour (t_{min}), the time of the final contour (t_{max}), and the time increment between contour lines (Δt). Dashed lines represent the approximate location of the tank walls.

to "fans off" (Table 3). In addition, upward flame speeds are greater than downward flame speeds. This is due primarily to the effects of buoyancy on flame propagation. The difference between the upward and downward flame speeds is largest for low H_2 concentrations with "fans off" and the velocity difference decreases as the H_2 concentration is increased and decreases for burns with the "fans on." Isolated contours seen in Figure 11 suggest the presence of flame globules, which have been observed by other investigators.[4]

The pressure signals from both "fans on" and "fans off" burns are compared in Figure 12 for the 5.7% and 7.4% hydrogen cases. (The double-humped pressure signals, such as that shown in Figure 12 for test B4H8, will be discussed later.) The influence of convection and turbulence caused by the fans is clearly shown; ΔP is larger, Δt is smaller, and the pressure derivatives have increased by factors of 2 to 8.

VI-2. <u>Test Series 2</u>

For TS 2, the glowplug igniter was raised 1.22 m (4 ft) to the vertical tank center. Initial conditions and principal results for TS 2 are given in Table 4. The results indicated in Table 4 are similar to those presented during the discussion of TS 1. Of interest are the tests with higher H_2 concentrations (11.5% and 15.25%). These tests show similar results when comparing the "fans on" and "fans off" cases and further support the observation of increased pressure derivatives and flame propagation speeds with increased H_2 concentrations. At larger H_2 concentrations with the higher quiescent flame speeds, the effects of the fan-generated turbulence are much less significant.

An additional observation is the double-humped pressure signal shown in Figure 13, along with two TC readings taken from test B22H9. The H_2 concentration for this test was 8.28%. The double-humped pressure signal is also present in three other tests, two from TS 1 (B4H8 and B8H9) and one from TS 3 (B29H9). Each of these tests was performed with the fans off. Cases with similar initial conditions but with the fans turned on during combustion did not produce this behavior. Comparing the temperature signals with the pressure signal indicates that the first hump occurs just after the arrival time of the flame at the TC located 1.83 m (6 ft) above the igniter, and the second hump (the peak pressure) occurs just after the arrival time of the flame at the TC located 1.83 m (6 ft) below the igniter.

If the increase in temperature of the lower TC was caused by the convection of hot burn gases from the upper portions of the tank, the pressure signal would not exhibit an increase, but rather a decrease when relatively cold unburned gas equilibrates with the hotter burned gas. This observation is further strengthened by comparing the pressure traces from

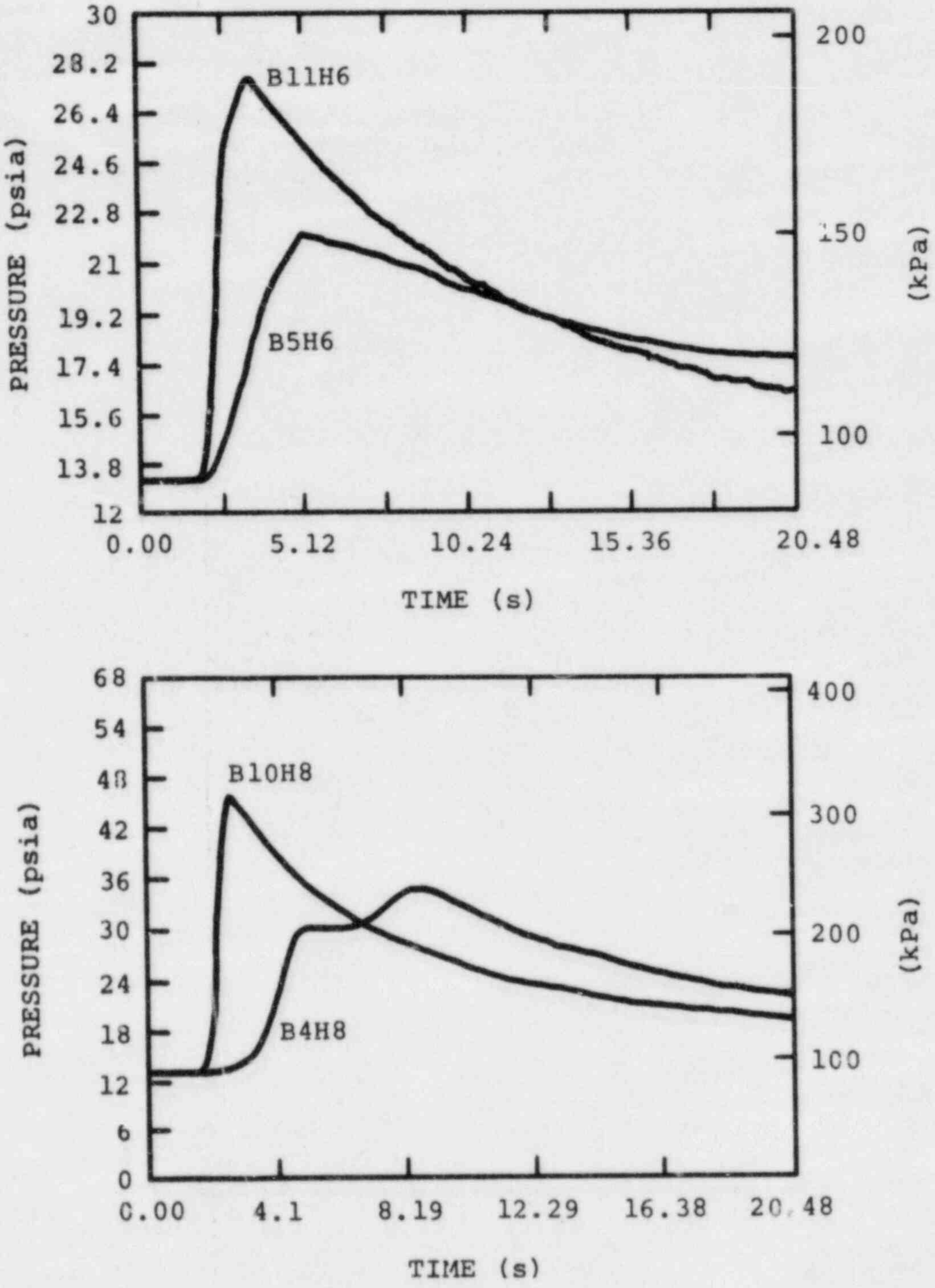

Figure 12. Pressure Histories for Hydrogen:Air Burns
B5H6 - 5.7% H_2, fans off
B11H6 - 5.7% H_2, fans on
B4H8 - 7.4% H_2, fans off
B10H8 - 7.4% H_2, fans on

Table 4

TS 2: Raised Glowplug Igniter

TEST NUMBER	VOLUME % H_2	VOLUME % CO_2	P_o (atm)	P_{max} (atm)	T_o (°C)	T_{max} (°C)	PRESSURE Δt(s)	$\Delta P/\Delta t$ (atm/s)	P_{max}/P_o	V_{up} (m/s)	V_{down} (m/s)
B17H5	4.78	----	0.89	1.03	18.3	161	7.30	0.02	1.18	0.80	---
B18H5-F*	4.75	----	0.87	1.39	15.0	149	2.33	0.23	1.60	1.80	1.40
B19H7	6.59	----	0.89	1.34	20.2	468	2.60	0.17	1.51	1.00	0.50
B20H7-F	6.54	----	0.89	2.48	10.0	362	1.16	1.37	2.79	2.30	2.00
B21H9-F	8.27	----	0.90	3.31	20.3	584	0.90	2.68	3.68	0.40	0.40
B22H9	8.28	----	0.90	2.80	15.8	543	5.75	0.33	3.11	1.30	0.40
B23H13	11.50	----	0.93	4.10	21.7	731	0.95	3.33	4.41	3.10	2.90
B24H13-F	11.51	----	0.93	4.31	20.8	696	0.50	6.76	4.63	6.60	5.90
B25H18	15.25	----	0.87	4.73	25.8	914	0.40	9.66	5.50	14.0	16.0
B26H18	15.25	----	0.98	5.36	26.4	947	0.33	13.3	5.53	16.0	19.0
B27H12	10.71	----	0.92	3.70	26.0	709	1.23	2.26	4.02	2.30	2.00

*The letter "F" following a test number indicates that the fans were on during the test.

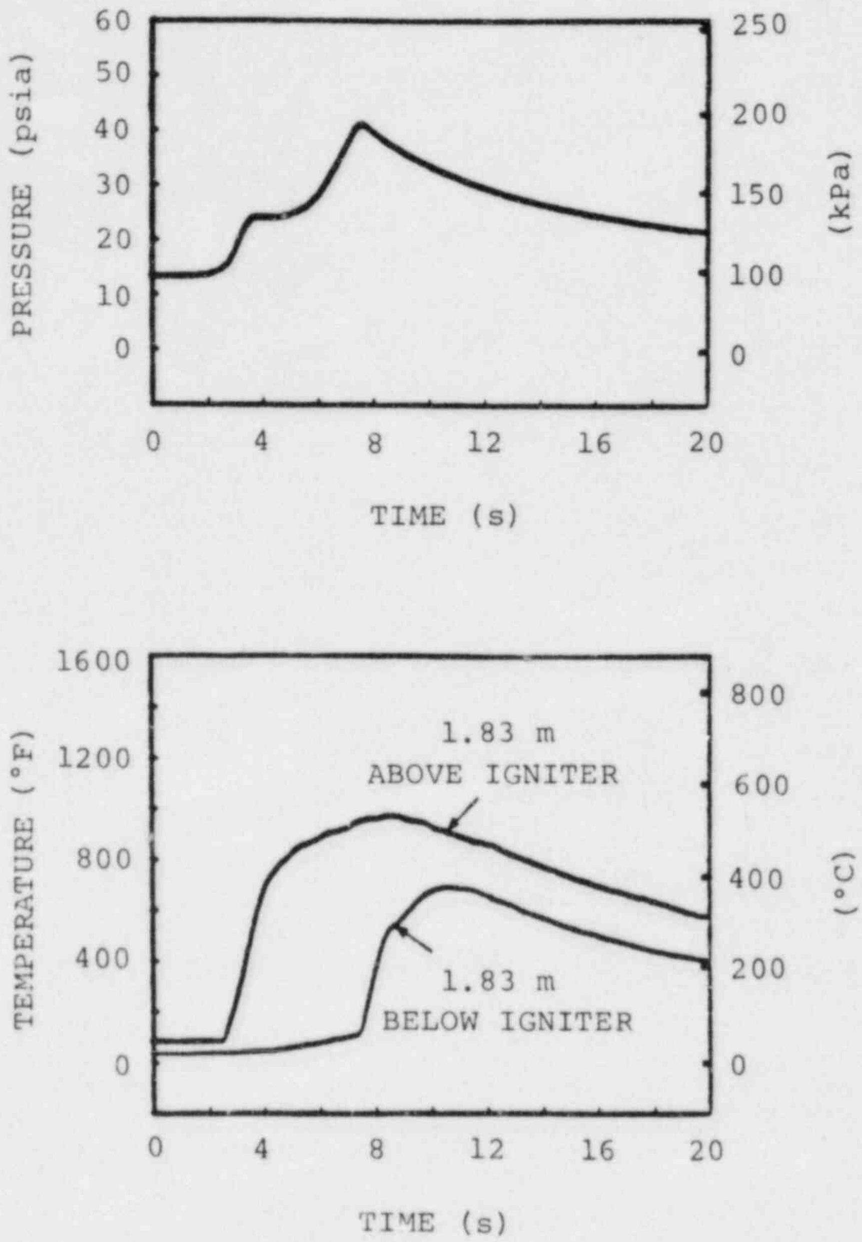

Figure 13. Comparison between pressure and two TC temperatures for test B22H9, 8.28% H_2, fans off. (Both TC beads are 0.079 cm (0.031 in.) O.D.) Note that the igniter was raised to a position 2.4 m (8 ft) above the tank bottom for this test.

B8H9 and B29H9 (Figure 14) to that from B22H9 (Figure 13). All three tests had H_2 concentrations of 8.2% to 8.3%, but B8H9 and B29H9 used igniters located 1.2 m (4 ft) from the tank bottom while B22H9 used an igniter located 2.4 m (8 ft) above the tank bottom. As indicated in Figure 14, the first humps occur later in the transient and have higher values. The timing differences are due to the greater distance the flame has to travel before reaching the tank top with the igniter at the lower position. The magnitude difference is due to relatively more of the total hydrogen:air mixture having been consumed by the time the flame reaches the tank top. A further comparison of pressure signals between B8H9, B29H9, and B22H9 shows that the peak pressures are about the same (~40 psia). The increase in pressure from the first hump to the second is caused by the further liberation of energy within the tank due to the combustion of H_2 and air at the tank bottom.

The observed double-humped pressure rise is really an indication that downward flame propagation has occurred. In these tests, it is clear that the downward flame velocity is very much lower than the upward flame velocity, and the hydrogen: air mixture in the lower portion of the tank is totally consumed only after the portion above the igniter has been totally consumed (indicative of combustion-induced flow). Because tests B8H9, B22H9, and B29H9 had H_2 concentrations of 8.26%, 8.28%, and 8.25%, respectively, and test B4H8 had an H_2 concentration of 7.4%, we did not expect to observe a downward propagating flame.* Other evidence for a propagating downward flame is the time difference between the two pressure humps for test B8H9 (or B4H8, B29H9) and B22H9. The time difference between the two humps for test B22H9 is about twice the time difference for test B8H9 (also B29H9). The distance between the igniter and the tank bottom for test B22H9 is 2.44 m (96 in.) while for the other tests (B4H8, B8H9 and B29H9), this distance is 1.22 m (48 in.).

The double hump in the pressure trace for these tests is due to two nearly discrete burns: the first occurs when the flame propagates upward to the top of the tank, and the second occurs when the flame propagates downward to consume the remaining unburned mixture. The exact nature of the double hump depends on the tank geometry and hydrogen concentration.

VI-3. Test Series 3

TS 3 was performed with a spark igniter located at the lower ignition location. This series was similar to TS 1. Initial conditions and principal results are given in Table 5. A

---

*The generally quoted value for downward flame propagation is 9% H_2. This is strictly valid only in vented tubes of small (~5-cm [2-in.]) diameter.

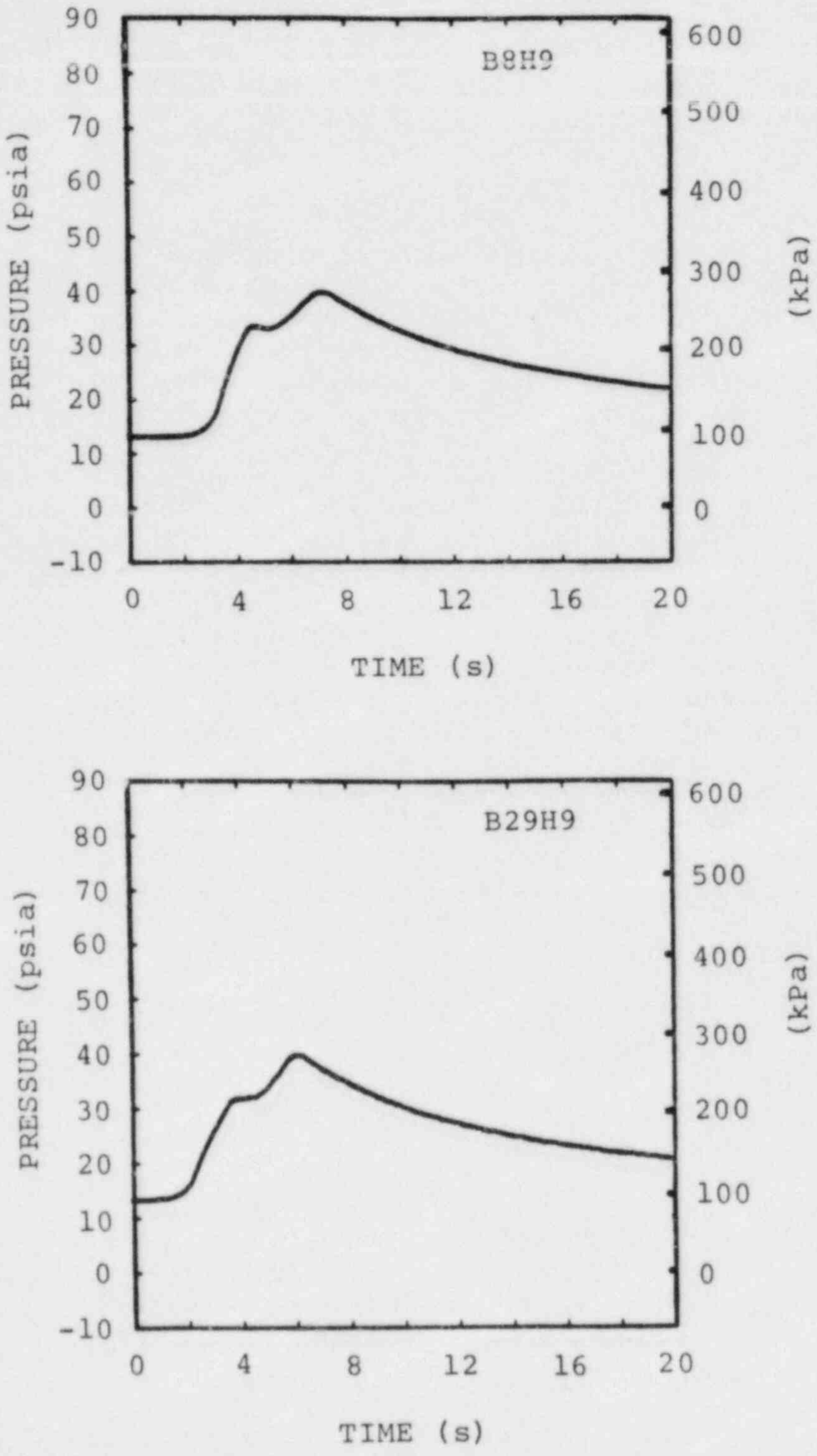

Figure 14. Pressure for tests B8H9 (glowplug igniter) and B29H9 (spark igniter), 8.26% and 8.25% H_2, respectively, fans off.

Table 5

TS 3: Spark Igniter

TEST NUMBER	VOLUME % H_2	VOLUME % CO_2	P_o (atm)	P_{max} (atm)	T_o (°C)	T_{max} (°C)	PRESSURE Δt(s)	$\Delta P/\Delta t$ (atm/s)	P_{max}/P_o	V_{up} (m/s)	V_{down} (m/s)
B28H9-F*	8.27	----	0.90	----	----	---	----	----	----	----	----
B29H9	8.25	----	0.89	2.71	25.0	574	4.70	0.39	3.05	1.20	0.30
B30H7	6.56	----	0.88	1.79	----	371	----	----	2.03	----	----
B31H7	6.54	----	0.88	1.72	25.6	327	2.84	0.30	1.95	1.00	0.40
B32H7-F	6.54	----	0.88	2.50	24.2	407	0.84	1.93	2.84	5.80	4.30
B33H5	4.76	----	0.86	1.13	21.6	124	3.87	0.07	1.31	0.70	0.40
B34H5-F	4.76	----	0.86	1.35	22.1	131	1.78	0.27	1.57	2.80	1.20
B35H9-F	8.26	----	0.90	2.77	22.1	595	0.72	2.60	3.08	6.40	2.10

*The letter "F" following a test number indicates that the fans were on during the test.

review of the temperature and pressure measurement for the tests in this test series did not indicate any significantly different results from those previously discussed. The 5-kV spark caused ignition of the hydrogen:air mixture at the time the spark occurred and deposited sufficient energy to ignite even the 4.76% hydrogen:air mixture. The major differences between glowplug and spark igniters are the rate and duration of energy deposition.

VI-4. Test Series 4

TS 4 was performed with reduced quantities of initial air (53 kPa [400 torr]). Initial conditions and principal results for the series are given in Table 6. The quantity of air (oxygen) available for the reaction with H_2 was sufficient to allow complete combustion. A comparison between tests of TS 4 with those of TS 1, having similar H_2 concentrations and fan operation, indicate generally, lower values of the pressure rise time, the mean pressure derivative, and the ratio of the pressure rise to the initial pressure. This would indicate reductions in the burn strength, chemical release rate, heat transfer rate, and completeness of combustion. This observation may also explain why during test B39H8 there was no double hump of the pressure signal as was observed in B4H8, which had similar initial condition to B39H8 with the exception of the reduced amount of air.

VI-5. Test Series 5

TS 5 was performed with further reductions in the amount of air (27 and 13 kPa [200 and 100 torr]). Initial conditions and principal results for TS 5 are given in Table 7. A comparison between the results of hydrogen:air combustion for ambient and reduced air quantities is given in Table 8 and shown graphically in Figure 15. A comparison of the pressure records for three of the tests given in Table 8 is shown in Figure 16. The H_2 concentration for these tests was 7.4% and the fans were on during the burns.

Figure 15 shows a slight decrease in ΔP, P_{max}/P_O, and $\Delta P/\Delta t$ with a decrease in the amount of air available. Also shown in Figure 15 is a slight increase in the reaction time with decreasing quantities of air. Similar results were obtained during burns of higher H_2 concentrations (Table 9). In this table, the H_2 concentration is ~15.3%, and the fans were off during the burn.

VI-6. Test Series 6

TS 6 was performed with additional nitrogen added to the hydrogen:air mixture. The added N_2 concentrations ranged from 28% to 32%. The total concentrations ranged from 71% to 83%. The initial conditions and principal results for TS 6 are given in Table 10. A comparison between the parameters given in

Table 6

TS 4: 400-torr Air

TEST NUMBER	VOLUME % H_2	VOLUME % CO_2	P_o (atm)	P_{max} (atm)	T_o (°C)	T_{max} (°C)	PRESSURE Δt(s)	$\Delta P/\Delta t$ (atm/s)	P_{max}/P_o	V_{up} (m/s)	V_{down} (m/s)
B36H8-F*	7.41	----	0.59	----	24.8	439	----	----	----	4.59	1.61
B37H6-F	5.91	----	0.56	1.18	26.5	247	1.35	0.46	2.05	2.59	1.38
B38H8-F	7.41	----	0.57	1.68	26.2	471	1.04	1.07	2.79	5.46	2.01
B39H8	7.41	----	0.57	1.17	29.3	413	2.25	0.27	1.97	1.17	0.31
B40H10-F	9.09	----	0.58	1.99	29.7	581	0.80	1.76	3.44	5.59	1.51
B60H12	10.71	----	0.69	2.06	33.3	586	1.23	1.20	3.42	2.75	1.14
B61H12-F	10.71	----	0.60	1.95	31.9	608	0.55	2.49	3.29	9.43	3.38
B62H10	9.09	----	0.58	1.91	29.8	607	1.50	0.88	3.29	1.95	0.38
B63H10-F	9.09	----	0.60	1.92	29.3	594	0.75	1.78	3.40	5.65	1.93

*The letter "F" following a test number indicates that the fans were on during the test.

Table 7

TS 5: 200- and 100-torr Air

TEST NUMBER	VOLUME % H_2	VOLUME % CO_2	P_o (atm)	P_{max} (atm)	T_o (°C)	T_{max} (°C)	PRESSURE Δt(s)	ΔP/Δt (atm/s)	P_{max}/P_o	V_{up} (m/s)	V_{down} (m/s)
B41H8-F*	7.41	----	0.28	0.90	25.6	416	1.12	0.55	3.16	10.3	4.20
B42H18	15.30	----	0.31	1.48	28.0	693	0.39	2.98	4.78	9.14	---
B43H30	23.40	----	0.34	2.23	35.5	1003	0.11	17.46	6.49	40.7	65.8
B44H8-F	7.41	----	0.14	0.43	25.4	351	0.94	0.31	3.04	4.78	2.54
B45H18	15.30	----	0.16	0.74	28.7	518	0.45	1.30	4.78	9.16	4.45
B46H30	23.1	----	0.17	1.07	30.8	673	0.14	6.58	6.23	32.7	22.6

*The letter "F" following a test number indicates that the fans were on during the test.

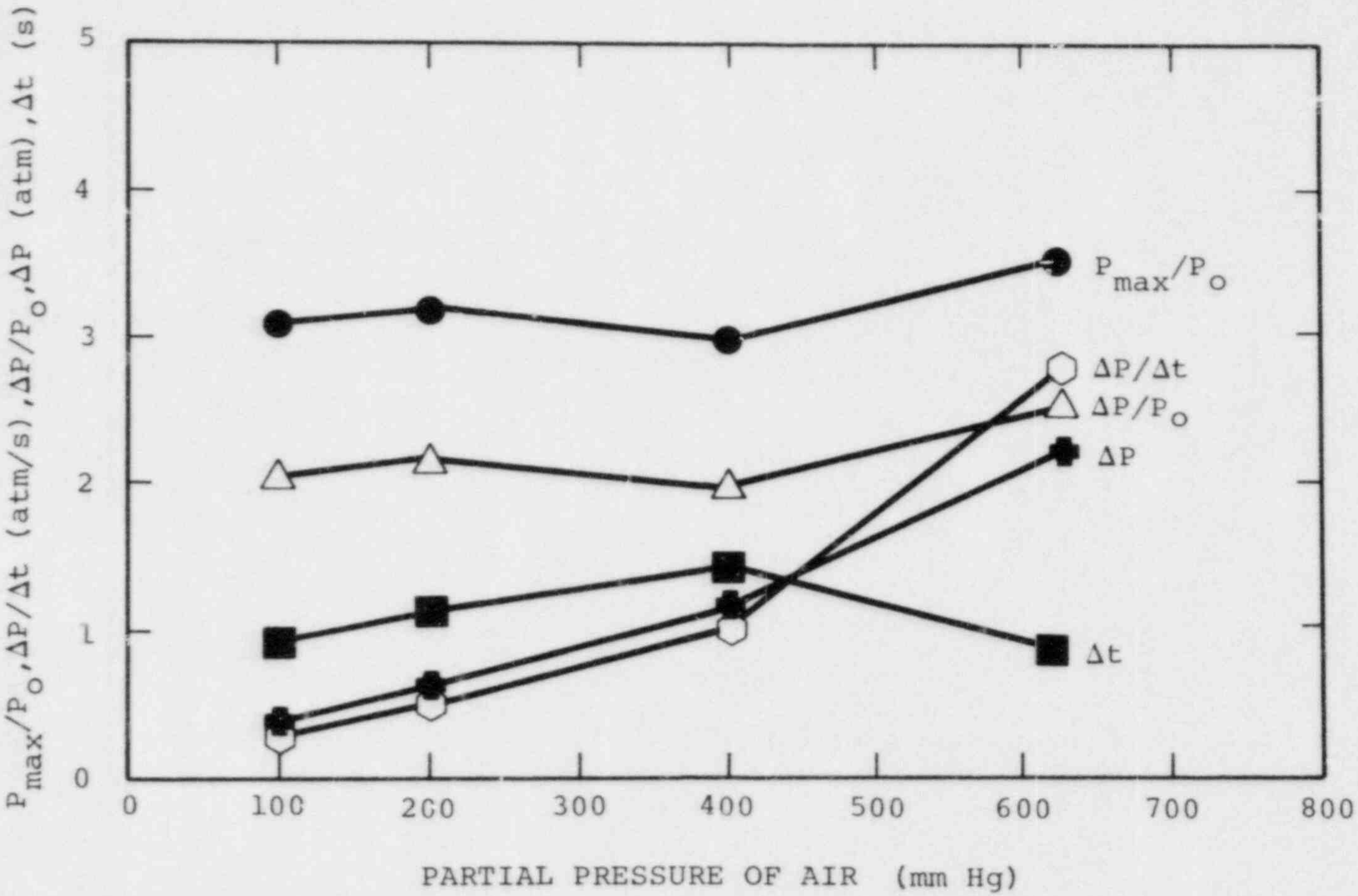

Figure 15. Change in Burn Characteristics with Change in the Initial Amount of Air. 7.4% H_2, Fans On

Table 8

Comparison of Hydrogen:Air Combustion
for Atmospheric and Reduced Air Quantities

TEST NUMBER	PARTIAL PRESSURE (mm Hg) H_2	Air	H_2 (%)	ΔP (atm)	$\Delta P/P_o$	Δt (s)	$\Delta P/\Delta t$ (atm/s)	P_{max}/P_o
B10H8-F*	50	625	7.4	2.22	2.50	0.89	2.50	3.57
B38H8-F	32.0	400.0	7.4	1.11	1.96	1.04	1.07	2.96
B41H8-F	16.0	200.0	7.4	0.61	2.16	1.12	0.55	3.16
B44H8-F	8.0	100.0	7.4	0.29	2.04	0.94	0.31	3.04

*The letter "F" following a test number indicates that the fans were on during the test.

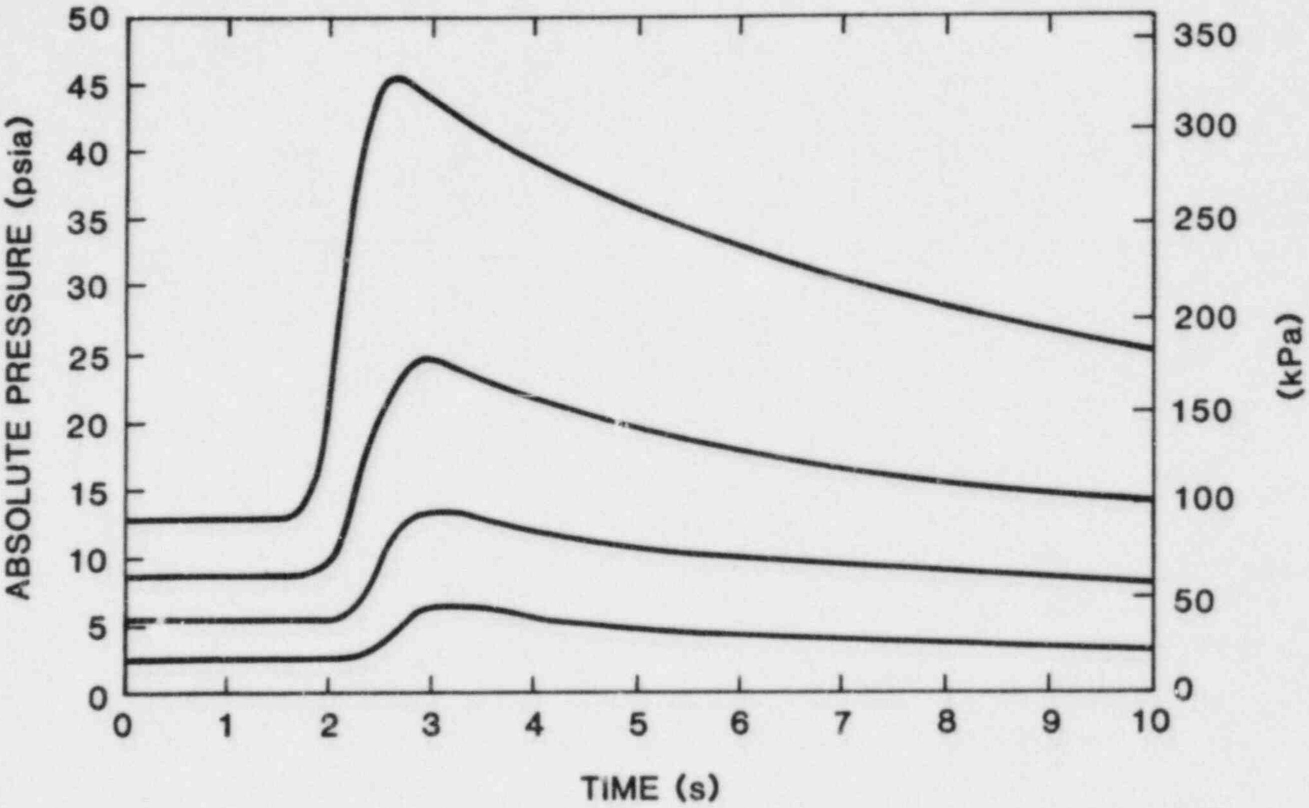

Figure 16. Comparison of Pressure for Atmospheric and Reduced Air Quantities, 7.4% H_2, Fans On

Table 9

Comparison of Hydrogen:Air Combustion
for Atmospheric and Reduced Air Quantities
and Higher Hydrogen Concentrations

TEST NUMBER	PARTIAL PRESSURE (mm Hg)		H_2 (%)	ΔP (atm)	$\Delta P/P_o$	Δt (s)	$\Delta P/\Delta t$ (atm/s)	P_{max}/P_o
	H_2	Air						
B25H18	99.9	559.1	15.25	3.86	4.46	0.40	9.66	5.46
B26H18	113	627	15.25	4.39	4.50	0.33	13.30	5.50
B42H18	36	200	15.30	1.16	3.76	0.39	2.97	4.76
B45H18	18	100	15.30	0.59	3.78	0.45	1.30	4.78

Table 10

TS 6: Additional Nitrogen (Partial Preinerting)

TEST NUMBER	VOLUME % H_2	VOLUME % N_2 ADDED	VOLUME % N_2 TOTAL	P_o (atm)	P_{max} (atm)	T_o (°C)	T_{max} (°C)	PRESSURE Δt(s)	ΔP/Δt (atm/s)	P_{max}/P_o	V_{up} (m/s)	V_{down} (m/s)
B47H6-F*	5.66	31.45	81.13	1.05	2.10	25.4	278	1.35	0.78	2.01	2.90	2.06
B48H8	7.41	30.86	79.63	0.85	2.61	26.9	548	1.04	1.69	3.05	5.12	1.51
B49H10-F	9.09	30.30	78.18	0.87	3.01	30.0	678	0.98	2.18	3.44	4.18	1.12
B50H18	15.30	28.25	72.89	0.93	4.51	30.2	923	0.32	11.22	4.85	16.8	10.3
B51H8-F	5.06	31.65	81.66	0.83	1.32	13.3	182	1.86	0.26	1.61	2.57	4.79
B52H10-F	6.25	31.25	80.63	0.84	1.95	26.6	347	1.27	0.87	2.32	3.52	3.62
B53H30	16.70	27.78	71.66	0.95	4.79	30.0	984	0.34	11.39	5.06	16.0	9.38
B64H6-F	3.85	32.05	82.69	No Burn (Spark Igniter)								
B65H6-F	3.85	32.05	82.69	No Burn (Glowplug Igniter)								
B66H7-F	4.50	31.83	82.13	No Burn (Spark Igniter)								
B67H7-F	4.5	31.82	82.10	0.83	1.08	32.1	110	1.97	1.28	1.30	2.53	0.89
B68H20	11.80	29.41	75.42	0.90	3.43	27.9	750	0.89	2.85	3.84	4.15	1.66

*The letter "F" following a test number indicates that the fans were on during the test.

Table 10 and those for other tests with similar H_2 concentrations and fan operation but without additional nitrogen indicates no significant differences in the burn characteristics. However, the addition of nitrogen to hydrogen:air mixtures will dilute the fraction of H_2 and produce burns indicative of the actual H_2 concentration. This result is illustrated in Figure 17 where the initial and peak combustion pressures are plotted against the initial hydrogen:air molar ratios for tests with and without added nitrogen, and with fans on. As shown in this figure, for the same hydrogen:air ratio, the addition of nitrogen increases the initial pressure prior to ignition and reduces the combustion peak pressure. Obviously, for mixtures diluted with enough nitrogen, the peak pressure can be depressed to the point of inerting the mixture.

VI-7. Test Series 7

TS 7 was performed using 14 volts applied to the GM7G glowplug. The initial conditions and principal results are given in Table 11. A comparison between the tests of TS 7 and tests with similar initial conditions and fan operation (but different igniters) is given in Table 12. Table 12 compares peak pressure, normalized peak pressure, maximum pressure rise, pressure rise time, and the mean pressure derivative for tests with the 14-V glowplug, the 70-V glowplug and the 4-kV spark igniter where applicable. This comparison indicates a consistently smaller value for all the listed parameters except the pressure rise time when the 14-V glowplug was used as the igniter. However, the 14-V glowplug requires 20 s to heat up to the ignition temperature of the hydrogen:air mixtures tested and therefore the data recording system requires a slower sampling rate to record the pressure and temperature rise. The consequences of the low sampling rate (50 ms) is that the peak pressure is represented by an average value during the 50-ms sampling period, and the true peak value may not have been recorded. A comparison between the 4-kV spark and the ~70-V glowplug does not indicate any consistent difference between the recorded or calculated parameters that have been previously presented. These data were recorded with a sampling rate 2 to 25 times faster because of the rapid ignition with these systems.

VI-8. Test Series 8

TS 8 was performed with higher H_2 concentrations, ranging from 9.09% to 17.4% H_2. The initial conditions and principal results for this series are given in Table 13. An inspection of the parameters in Table 13 indicates that as the H_2 concentration is increased so do all the parameters listed except Δt (pressure rise time), which decreases. In addition, there is a small increase in the parameters (except Δt) listed in Table 13 when the fans are operating during the burn as compared to the "fans off" burns, as was previously observed. However, the change in these parameters as a result of fan operation is

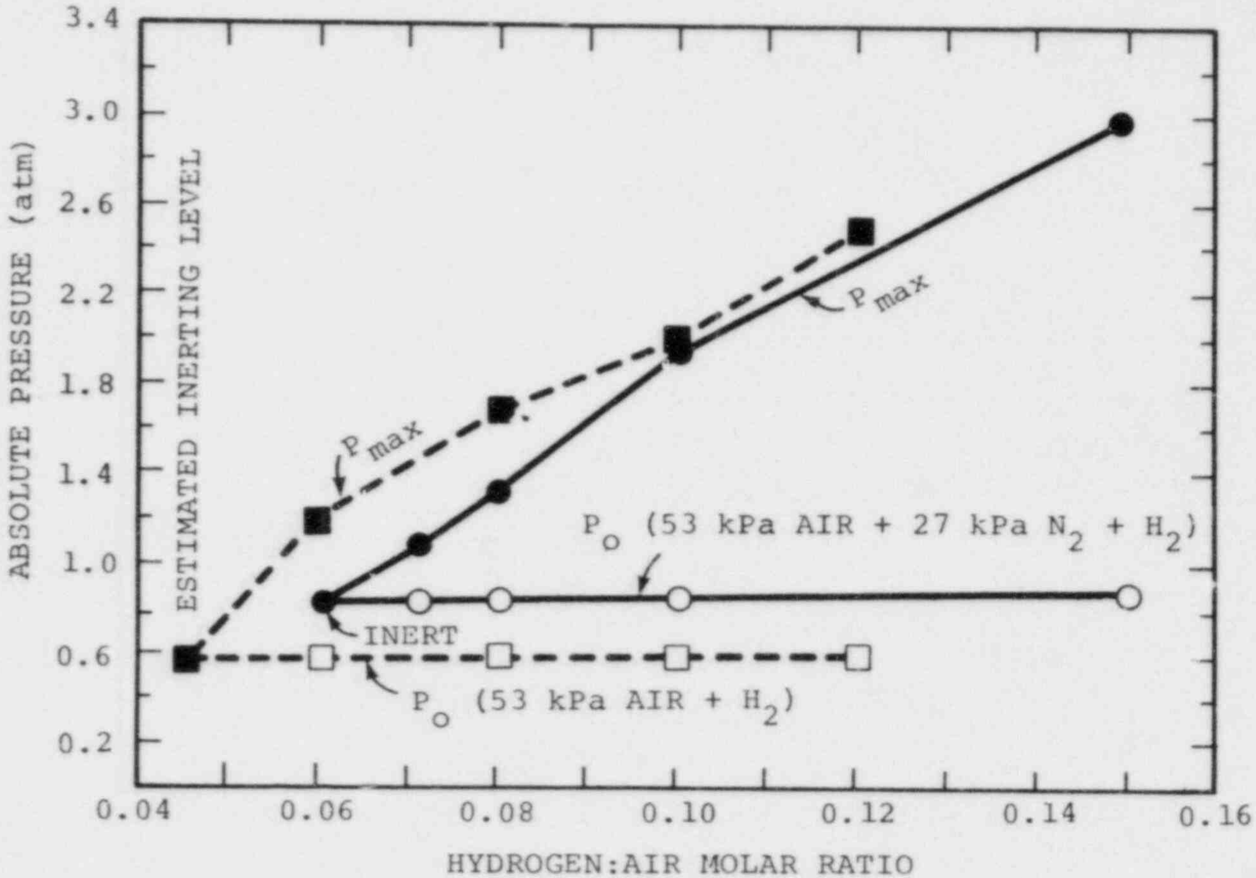

Figure 17. Initial and Combustion Peak Pressures for Tests with Similar Hydrogen:Air Molar Ratios, with and without Added Nitrogen, Fans On

Table 11

TS 7: 14-volt Glowplug

TEST NUMBER	VOLUME % H_2	VOLUME % CO_2	P_o (atm)	P_{max} (atm)	T_o (°C)	T_{max} (°C)	PRESSURE Δt(s)	$\Delta P/\Delta t$ (atm/s)	P_{max}/P_o	V_{up} (m/s)	V_{down} (m/s)
B54H6-F*	5.66	----	0.88	1.72	25.8	254	1.47	0.57	1.97	4.57	1.17
B55H8-F	7.40	----	0.89	2.79	14.0	549	0.95	2.00	3.13	4.52	1.21
B56H10	9.08	----	0.91	3.15	24.4	674	1.48	1.51	3.53	2.05	0.37
B57H10-F	9.08	----	0.91	3.21	27.3	655	0.78	2.95	3.59	8.33	5.60
B58H12	10.70	----	0.93	3.34	17.2	728	1.12	2.16	3.59	3.03	1.93
B59H12-F	10.70	----	0.93	3.61	15.6	729	0.55	4.92	3.95	8.31	2.49

*The letter "F" following a test number indicates that the fans were on during the test.

Table 12

Comparison Between Ignition Sources

TEST NUMBER	IGNITER TYPE	H_2 (%)	P_o (atm)	P_{max}	P_{max}/P_o	ΔP (atm)	Δt (s)	$\Delta P/\Delta t$ (atm/s)
B54H6-F*	14-VOLT GLOWPLUG	5.66	0.88	1.72	1.96	0.84	1.47	0.57
B11H6-F	68-VOLT GLOWPLUG	5.66	0.88	1.87	2.13	0.99	1.58	0.63
B55H8-F	14-VOLT GLOWPLUG	7.40	0.89	2.79	3.12	1.89	0.95	2.00
B10H8-F	70-VOLT GLOWPLUG	7.41	0.89	3.11	3.50	2.22	0.89	2.50
B56H10	14-VOLT GLOWPLUG	9.08	0.91	3.15	3.46	2.24	1.48	1.51
B75H10	4-kV SPARK	9.09	0.91	3.07	3.36	2.16	1.42	1.52
B58H12	14-VOLT GLOWPLUG	10.7	0.93	3.34	3.61	2.41	1.12	2.16
B27H12	68-VOLT GLOWPLUG	10.7	0.92	3.70	4.03	2.78	1.23	2.26
B88H11	4-kV SPARK	10.4	0.92	3.52	3.82	2.60	1.01	2.57
B59H12-F	14-VOLT GLOWPLUG	10.7	0.93	3.61	3.89	2.68	0.55	4.92
B89H11-F	4-kV SPARK	10.5	0.92	3.69	4.01	2.77	0.38	7.29

*The letter "F" following a test number indicates that the fans were on during the test.

Table 13

TS 8: Higher Hydrogen Concentrations

TEST NUMBER	VOLUME % H_2	VOLUME % CO_2	P_o (atm)	P_{max} (atm)	T_o (°C)	T_{max} (°C)	PRESSURE Δt(s)	ΔP/Δt (atm/s)	P_{max}/P_o	V_{up} (m/s)	V_{down} (m/s)
B69H15-F*	13.00	----	0.95	4.01	31.6	817	0.47	6.56	4.20	9.85	7.04
B70H15	13.10	----	0.95	----	28.1	807	----	---	----	6.57	4.25
B71H18	15.30	----	0.98	4.70	31.5	948	0.40	9.40	4.80	14.5	8.21
B72H18-F	15.30	----	0.98	4.81	32.8	928	0.25	15.6	4.93	20.5	12.7
B73H21	17.40	----	1.00	5.35	36.5	1062	0.21	20.9	5.35	28.3	16.8
B74H21-F	17.40	----	1.00	5.37	36.8	1030	0.18	24.5	5.37	33.4	15.8
B75H10	9.09	----	0.91	3.07	29.4	688	1.42	1.52	3.37	1.75	0.35
B76H15	13.00	----	0.95	3.88	31.6	829	0.70	4.18	4.07	6.62	6.82
B77H15-F*	13.00	----	0.95	4.18	32.3	820	0.35	9.24	4.31	13.8	5.92

*The letter "F" following a test number indicates that the fans were on during the test.

somewhat smaller than the changes observed for lower H_2 concentration tests. In order to examine the effects of fan operation on the burn characteristics, the percent change [(fans-on parameter) - (fans-off parameter)]/[fans-off parameter] for P_{max}, Δt, ΔP, and $\Delta P/\Delta t$ is shown in Figures 18 through 21, respectively, as a function of H_2 concentration. The percent change in P_{max}, ΔP, and $\Delta P/\Delta t$, represents the percent increase in these parameters. The percent change in Δt is $((\Delta t_{FANS\ OFF} - \Delta t_{FANS\ ON})/\Delta t_{FANS\ OFF})$ and reflects the percent decrease in Δt. Inspection of Figures 18 through 21, indicates that the largest change in these parameters occurs at H_2 concentrations around ~8% and above ~10% H_2 the changes become relatively small except for Δt, where the influence of the fan-generated turbulence persists to ~15% H_2. The parameter that experiences the largest change with H_2 concentration and fan operation is $\Delta P/\Delta t$, which can be related to chemical energy release rate. The next largest change is seen in ΔP, which can be related to completeness of combustion and heat loss to the walls for low-velocity combustion. The reason for the dramatic increases in these parameters around ~8% H_2 is due primarily to the increase in combustion completeness. At H_2 concentrations below ~10%, incomplete combustion usually occurs. The operation of the fans results in an increase in combustion completeness and a decrease in reaction time. The increase in combustion completeness may be related to the convection of the flame around the tank during fan operation. The arrangement of the fans sets up a large recirculation loop within the tank that tends to "drag" the flame around the tank.

At H_2 concentrations above ~10%, combustion is almost always complete, and the operation of the fans decreases the pressure rise time and increases the chemical energy release rate. The faster the burn, the less time for heat transfer and therefore the higher the values of peak pressure and pressure rise.

The operation of the fans during a burn largely increases the burn parameters for H_2 concentrations below ~10% and is due primarily to an increase in the combustion completeness. For higher H_2 concentrations (above ~10%) the fans increase the P_{max}, ΔP, and $\Delta P/\Delta t$ primarily by decreasing the time for combustion (pressure rise time) and thus decreasing the time for heat transfer from the combustion products. At higher H_2 concentrations, the burning velocities are already high, and fan-generated convective velocities less than the burning velocity may not significantly accelerate the combustion.

VI-9. Test Series 9

TS 9 was conducted to study the ability of CO_2 to inert hydrogen:air mixtures or to mitigate the effects of hydrogen: air combustion and also to determine the degree to which CO_2 will simulate steam in a "cold" test chamber. The initial conditions and principal results for TS 9 are given in Table 14.

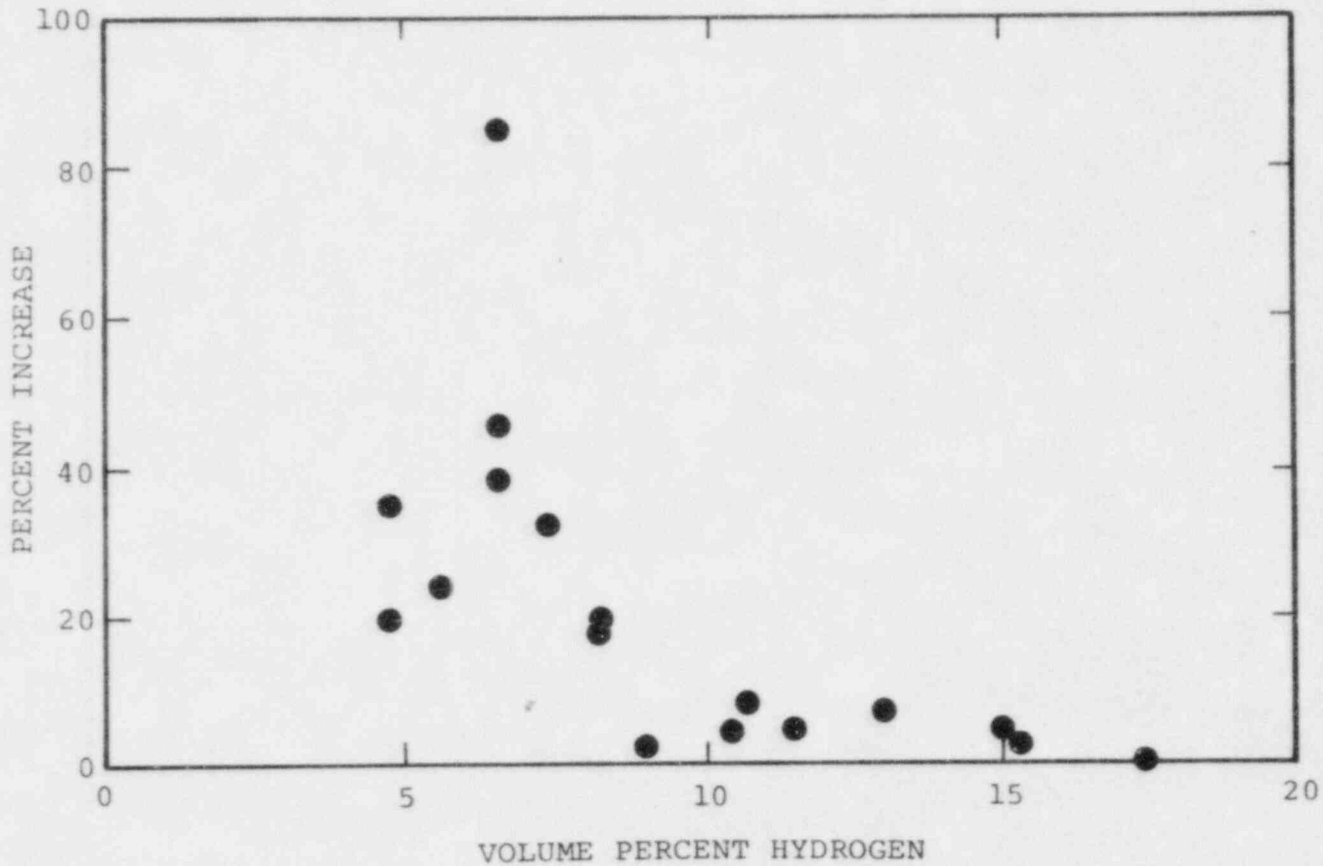

Figure 18. Percent Increase in Peak Pressure (P_{max}) as a Result of Fan Operation

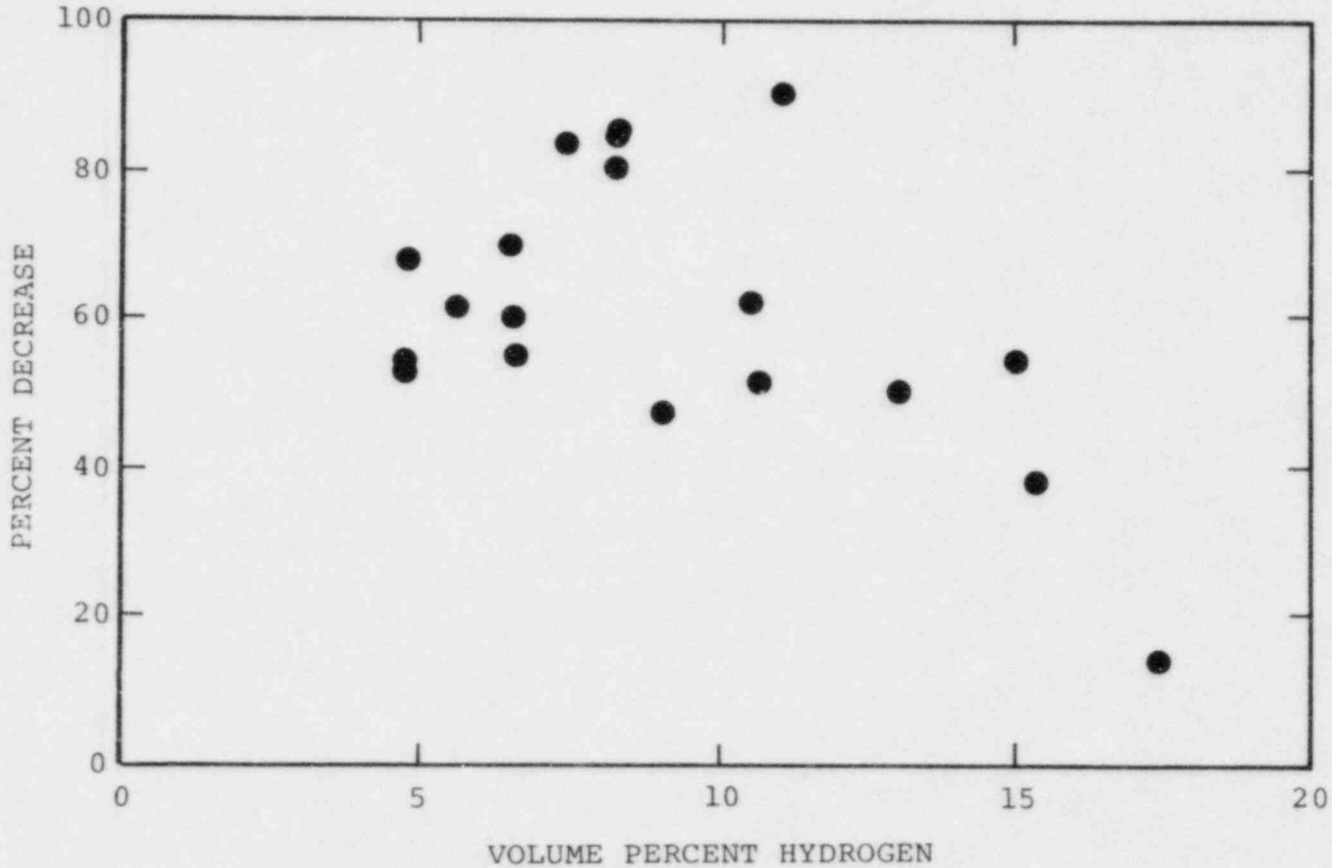

Figure 19. Percent Decrease in Pressure Rise Time (Δt) as a Result of Fan Operation

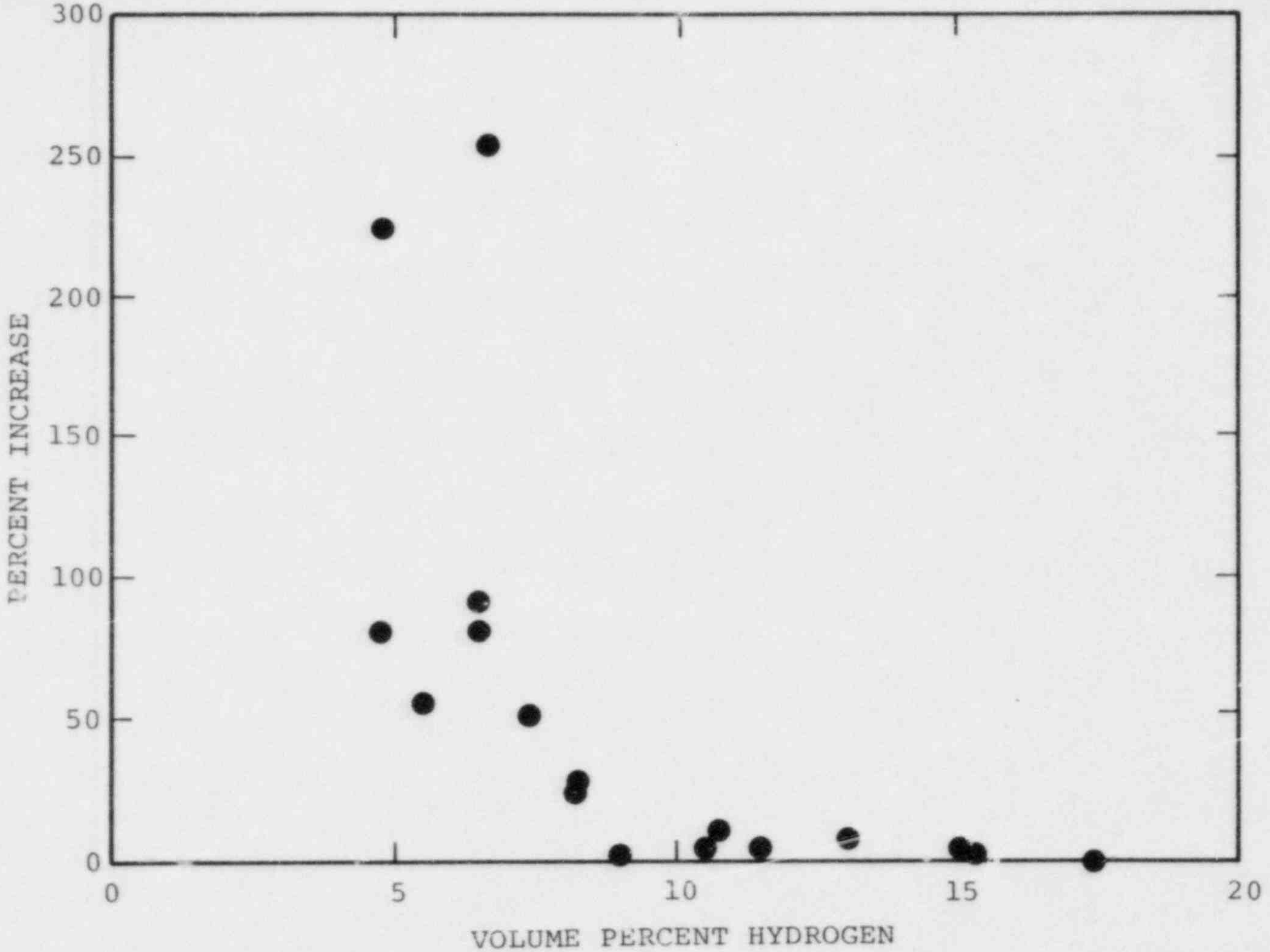

Figure 20. Percent Increase in Pressure Rise (ΔP) as a Result of Fan Operation

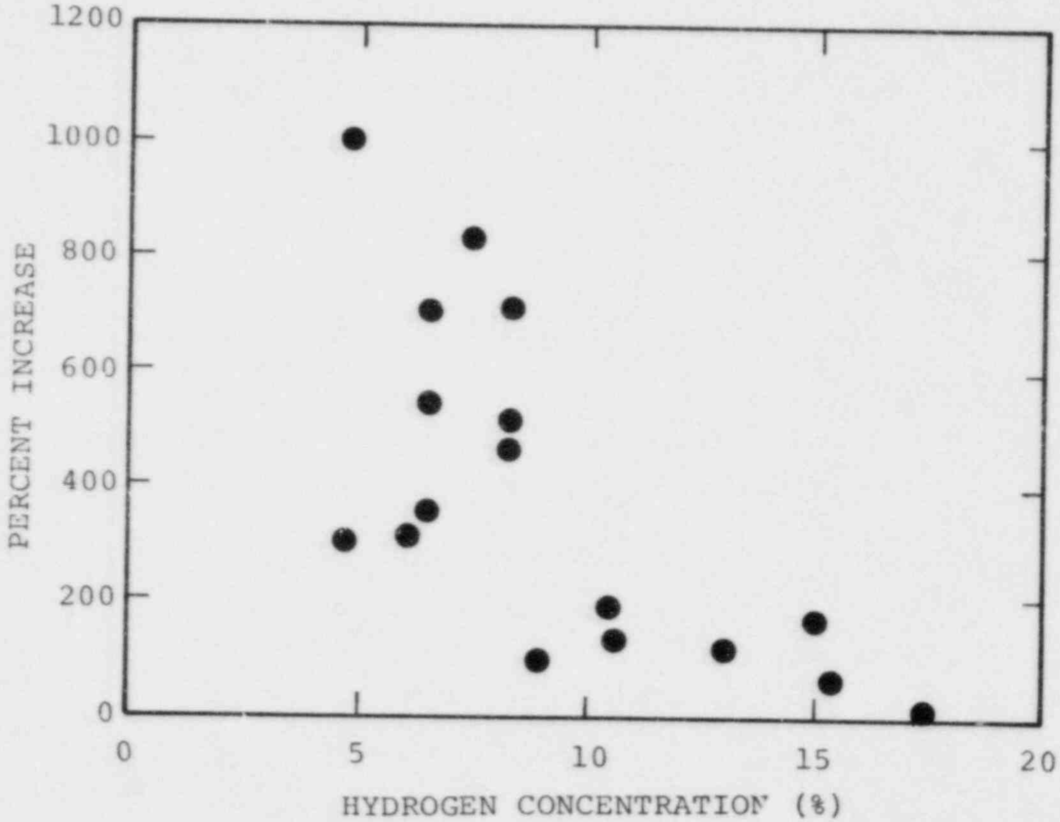

Figure 21. Percent Increase in the Mean Pressure Derivative ($\Delta P/\Delta t$) as a Result of Fan Operation

Table 14

TS 9: CO_2 Addition
(Steam Simulation and Combustion Mitigation/Prevention)

TEST NUMBER	VOLUME % H_2	VOLUME % CO_2	P_o (atm)	P_{max} (atm)	T_o (°C)	T_{max} (°C)	PRESSURE Δt(s)	$\Delta P/\Delta t$ (atm/s)	P_{max}/P_o	V_{up} (m/s)	V_{down} (m/s)
B78H37	13.00	52.20	1.51	----	27.5	----	----	----	----	0.590	0.27
B79H37	13.10	52.60	1.50	3.28	30.0	715	2.25	0.79	2.22	1.24	1.26
B80H37	12.00	56.00	No Burn, Inert (Glowplug Igniter)								
B81H37	12.50	54.20	No Burn, Inert (Glowplug Igniter)								
B82H37	14.29	47.62	1.38	3.70	27.1	767	2.53	0.92	2.68	1.42	0.32
B83H37	15.79	42.11	1.25	4.76	32.5	881	1.27	2.76	3.90	2.34	0.44
B84H37	20.00	26.67	0.99	4.84	27.6	1012	0.430	8.96	5.01	12.7	8.50
B85H37	17.65	35.29	1.12	4.76	19.7	917	0.860	4.23	4.22	4.38	2.33

*The letter "F" following a test number indicates that the fans were on during the test.

The normalized peak pressures (P_{max}/P_O) are plotted in Figure 22. Also plotted in Figure 22 are selected steam data with similar H_2 concentrations in air.[5-7] Inspection of the results of TS 9 indicates that about 54% CO_2 will inert a hydrogen:air mixture, since the two tests, 54.2% and 56.0% CO_2, did not burn, while a test performed just below these CO_2 concentrations (52.6% CO_2) did burn. Furthermore, for the resulting parameters listed in Table 14, an increase in CO_2 concentration caused a decrease in all these parameters except the pressure rise time (Δt), which experienced an increase.

The mitigation effect of CO_2 on hydrogen:air combustion is illustrated in Figure 23. This figure shows the percent decrease in normalized pressure rise ($\Delta P/P_O$) and normalized peak pressure (P_{max}/P_O) as a function of CO_2 concentration. Denoting $\Delta P/P_O$ or P_{max}/P_O by f, the percent decrease in f, $100[f(\text{no } CO_2) - f(CO_2)]/f(\text{no } CO_2)$, was determined by comparing tests with similar <u>total</u> H_2 concentration but with and without CO_2 addition. The values plotted in Figure 23 are the average percent decrease for all the comparisons with the same H_2 concentration

$$P_{H_2}/(P_{H_2} + P_{AIR}) \text{ or } P_{H_2}/(P_{H_2} + P_{CO_2} + P_{AIR}) .$$

These two parameters were the only ones that showed this trend. Figure 23 indicates that about a 50% decrease in the pressure occurs with about 52% CO_2 and the decrease becomes less as the CO_2 concentration is reduced. It is interesting to note that it may be possible to achieve a decrease of ~10% in pressure with as little as 10% CO_2 addition. However, due to the sparseness of the data, these results should not be given undue emphasis. This is an area that will be investigated further.

The degree to which CO_2 will simulate steam cannot be absolutely determined from TS 9. The comparison of normalized pressure rise ($\Delta P/P_O$) for steam and CO_2 addition given in Figure 22 is not conclusive. However, the comparison given in Figure 22 seems to indicate that steam and CO_2 have similar pressure mitigation effects.

VI-10. <u>Test Series 10</u>

TS 10 was conducted to produce data for the Hydrogen Burn Survivability Program. The initial conditions and principal results for TS 10 are given in Table 15. Analysis of the data for this test series is given elsewhere.[2]

VI-11. <u>Test Series 11</u>

TS 11 was conducted to study the effects of H_2 combustion in aqueous foam (620:1 expansion). Several tests with identical mixtures of hydrogen:air with and without foam were performed.

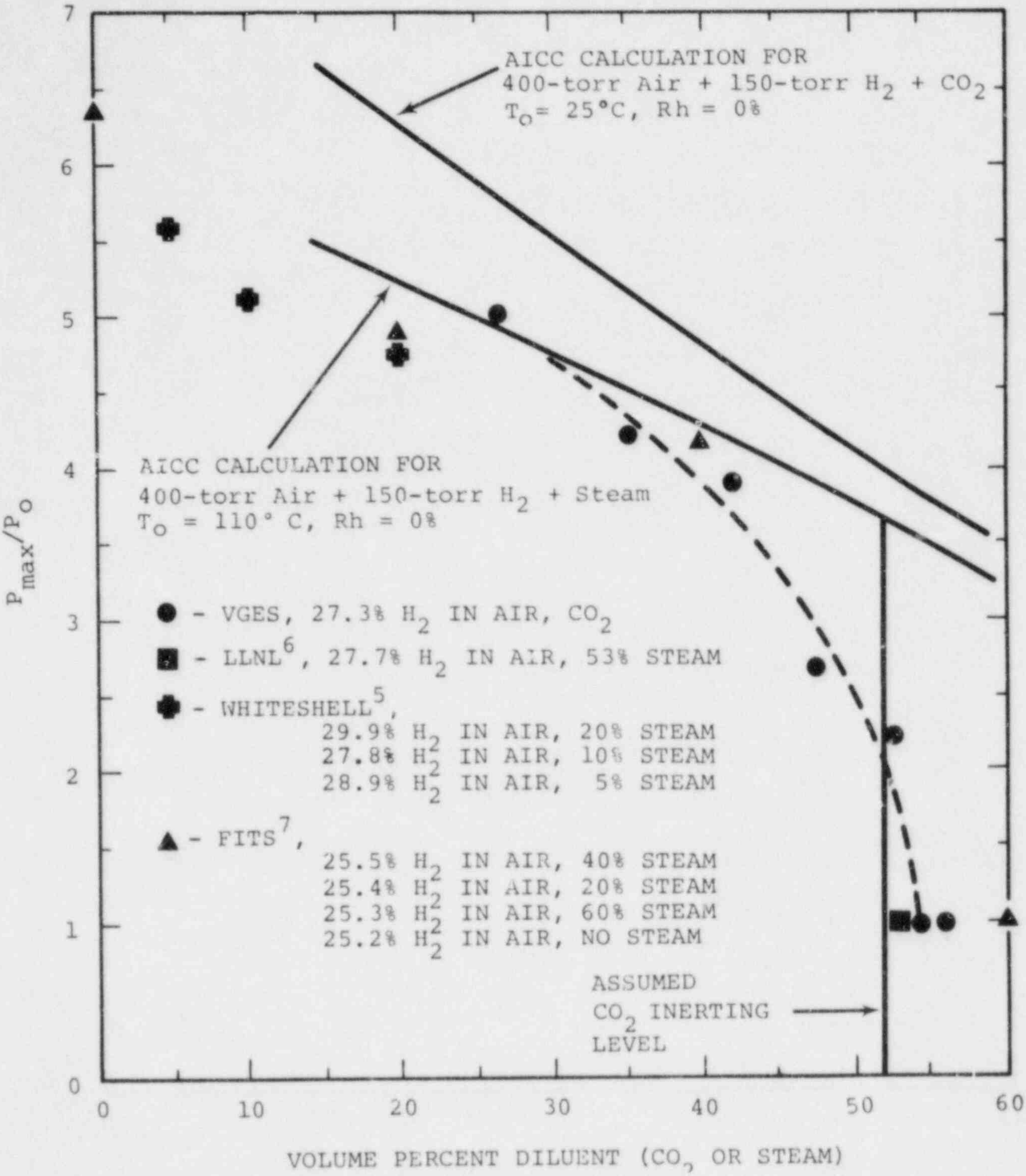

Figure 22. Normalized Peak Pressure (P_{max}/P_o) for Hydrogen: Air:Diluent Mixtures, Comparing CO_2 and Steam (AICC = Adiabatic Isochoric Complete Combustion, Rh = Relative Humidity)

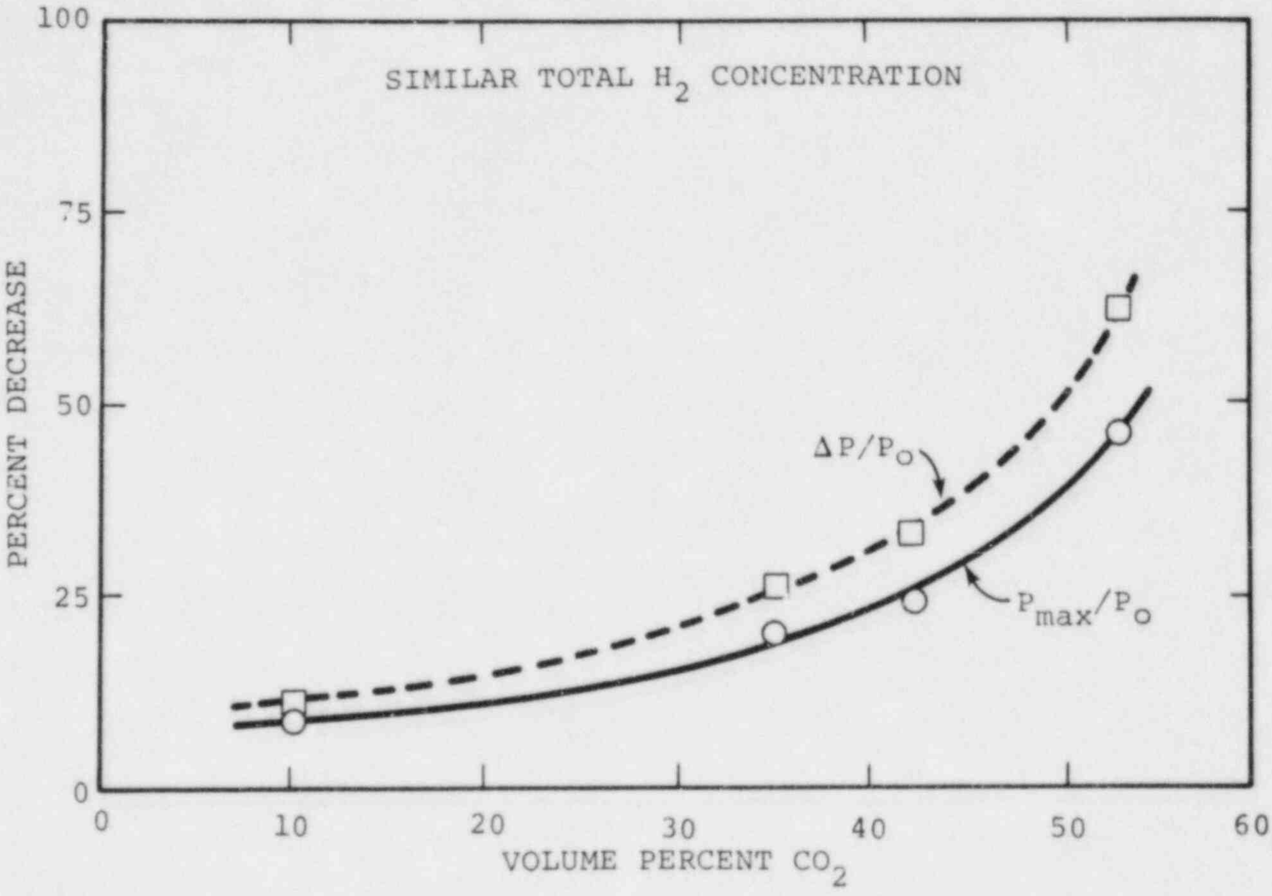

Figure 23. Percent Decrease in Normalized Pressure Rise ($\Delta P/P_O$) and Peak Pressure (P_{max}/P_O) Due to Added CO_2 for the Same Total Hydrogen Concentration

Table 15

TS 10: Equipment Survivability

TEST NUMBER	VOLUME % H_2	VOLUME % CO_2	P_o (atm)	P_{max} (atm)	T_o (°C)	T_{max} (°C)	PRESSURE $\Delta t(s)$	$\Delta P/\Delta t$ (atm/s)	P_{max}/P_o	V_{up} (m/s)	V_{down} (m/s)
B86H18	15.27	---	0.98	----	20.4	958	---	---	----	18.4	11.5
B87H21	17.35	---	1.00	5.48	19.9	1249	0.08	56.0	5.49	34.5	13.9
B88H11	10.42	---	0.92	3.52	21.6	928	1.01	2.57	3.81	2.86	1.53
B89H11-F*	10.50	---	0.92	3.69	19.6	930	0.38	7.66	4.01	12.9	4.04
B90H11	10.12	9.99	1.04	3.61	20.6	862	1.21	2.13	3.44	2.12	0.44
B91H11-F	10.09	10.09	1.03	3.67	21.7	857	0.75	3.52	3.55	5.72	2.46
B92H17	15.17	---	0.97	4.74	23.0	1232	0.37	10.2	4.87	13.6	8.07
B93H17-F	15.01	---	0.97	4.97	20.4	1204	0.17	23.5	5.10	38.6	10.4

*The letter "F" following a test number indicates that the fans were on during the test.

Hydrogen concentrations were 10%, 15%, and 20%. Initial conditions and principal results are given in Table 16. A comparison of the pressure records for tests with and without foam but similar initial H_2 concentrations is shown on Figure 24. This comparison indicates a marked reduction in peak pressure due to the presence of aqueous foam for 10% and 15% H_2. We also noticed a very large decrease in peak temperature recorded by the TC array. A comparison of the pressure rise time (Δt) between the tests with and without foam for the same H_2 concentrations indicated that for mixtures of ~15% and below there was little difference. However, for the 20% H_2 tests, the no-foam test had a Δt of about 70 ms while the foam test had a Δt of about 9 ms. These pressure rise times correspond to average burn velocities of 49 m/s and 380 m/s for the no-foam and foam tests, respectively. The pressure waves and flow generated by the accelerated flames caused severe damage to the foam generator and fan.

VI-12. Overall Results

The overall results drawn from the VGES testing are obtained by considering the hydrogen:air combustion behavior for all the testing conducted to date.

Normalized peak pressure data (P_{max}/P_O) for all the tests in TS 1 through 8 are plotted in Figure 25. Burns with the "fans on" generally produced higher peak pressures for H_2 concentrations below ~8%. This is further illustrated in Figure 26, which shows the peak pressure as a function of H_2 concentration for those tests conducted with ambient air.

Inspection of Figure 25 indicates that the data generally fall away from the adiabatic values above ~10%. The increased burn rate above 10% should tend to decrease the heat transfer from the burn and produce pressures closer to the adiabatic values. There are several reasons for the behavior indicated in Figure 25. Several of the data above ~10% H_2 were obtained from tests conducted with reduced air pressure (53, 27, and 13 kPa). The reduction in the initial amount of air has been shown to cause a slight reduction in peak pressure at lower hydrogen concentrations. Some of the data were produced from tests with additional nitrogen. These tests also started with reduced air quantities (53 kPa). The data produced in TS 8 had initial temperatures higher than the initial temperature used for the AICC calculation (30° to 36°C versus 25°C). An increase in the initial mixture temperature will reduce the combustion peak pressure. It is also of note that the transducers we are using to measure pressure are sensitive to changes in temperature. We used a porous metal cover over the gauge to minimize the temperature change. However, for burns greater than ~10% H_2, the gauge temperature effect may cause slightly lower pressure measurements.

Table 16

TS 11: Aqueous Foam

TEST NUMBER	VOLUME % H_2	VOLUME % CO_2	P_o (atm)	P_{max} (atm)	T_o (°C)	T_{max} (°C)	PRESSURE Δ t(s)	ΔP/Δt (atm/s)	P_{max}/P_o	V_{up} (m/s)	V_{down} (m/s)
B94H11	10.00	---	0.92	3.18	25.9	----	1.44	1.57	3.56	---	---
B95F11	10.10	---	0.92	2.00	22.6	----	1.41	0.77	2.25	---	---
B96F25	20.00	---	1.03	3.95	23.7	319	0.01	243	4.46	---	---
B97F18	15.21	---	0.98	3.69	28.7	189	0.20	13.6	4.13	---	---
B98H18	15.21	---	0.98	4.77	28.7	----	0.19	19.8	5.33	---	---
B99F25	19.95	---	1.04	----	27.0	----	----	---	----	---	---
B01F25	20.01	---	1.03	5.20	10.3	761	0.01	464	5.86	---	---
B02H25	20.00	---	1.04	----	---	----	----	---	----	---	---
B03H25	20.02	---	1.04	6.19	7.60	1210	0.08	67.7	6.88	---	---
B04H12-F*	10.70	---	0.93	4.19	4.80	532	0.69	4.71	4.69	---	---
B05H25	19.97	---	1.03	5.70	---	850	0.06	73.0	6.43	---	---

*The letter "F" following a test number indicates that the fans were on during the test.

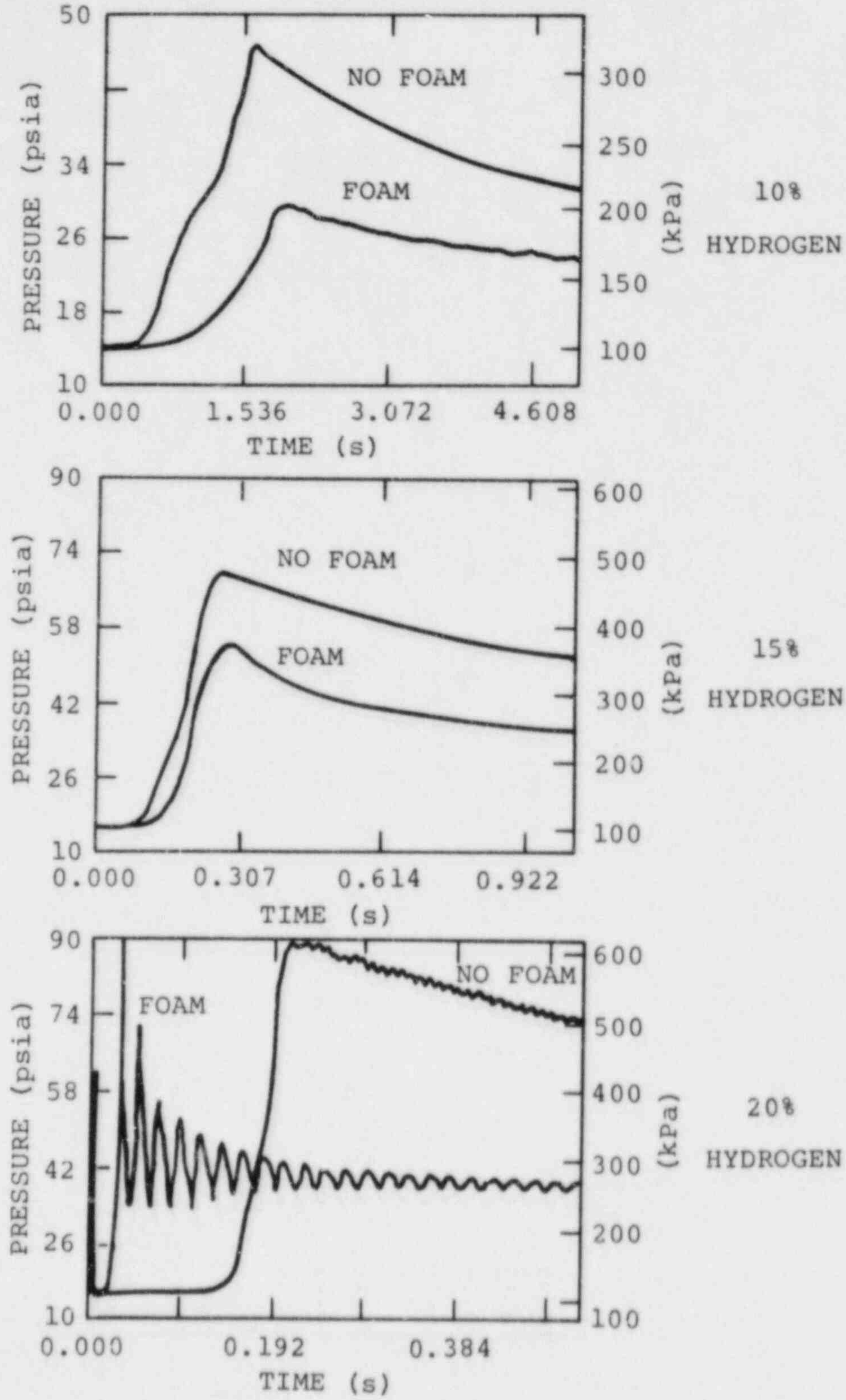

Figure 24. Pressure Histories for Hydrogen Combustion with and without 620:1 Aqueous Foam, 10%, 15% and 20% H_2.

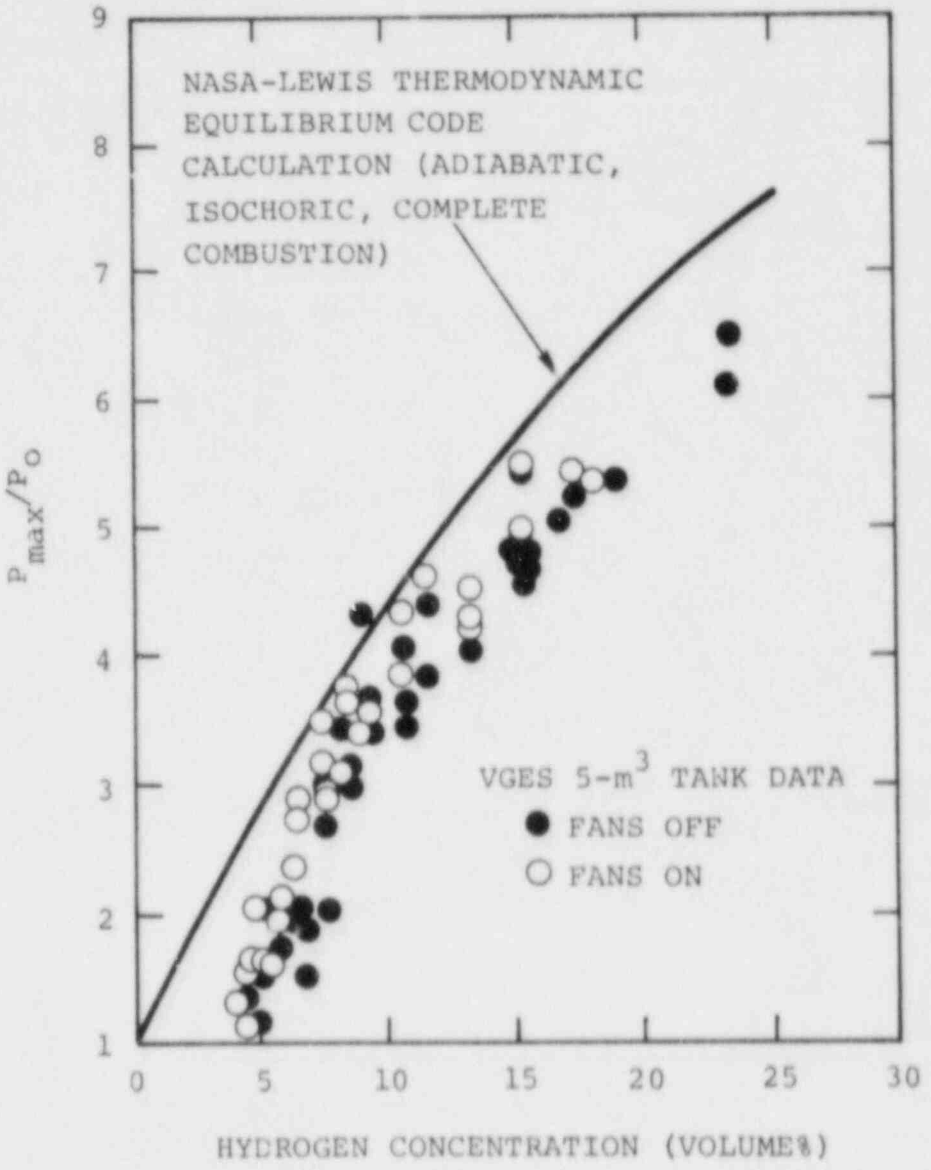

Figure 25. Normalized Peak Pressure (P_{max}/P_o) as a Function of Hydrogen Concentration for VGES TS 1 through 8

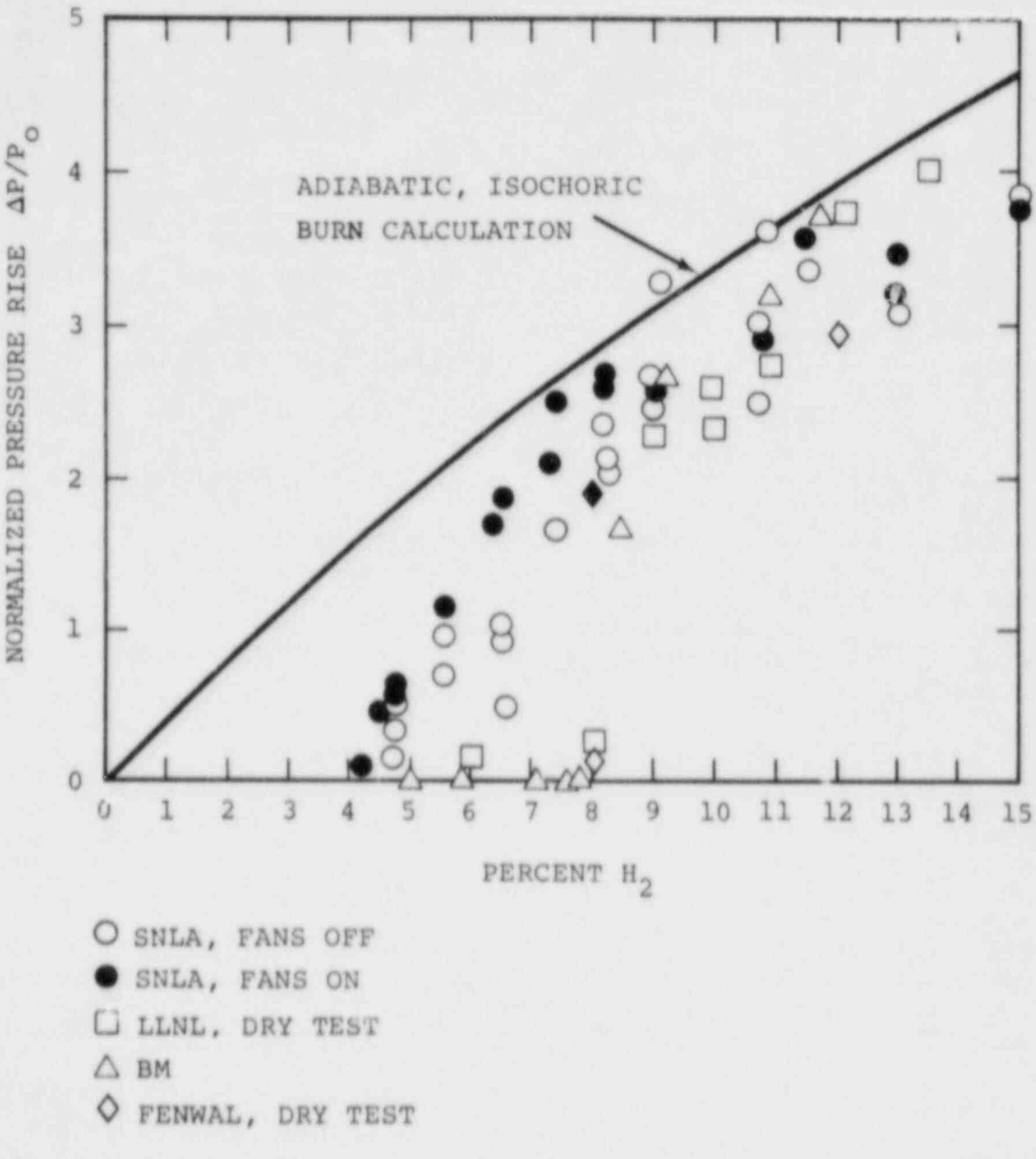

Figure 26. Peak Pressure Rise vs Initial H_2 Concentration. Sandia National Laboratories-Albuquerque (SNLA), Lawrence Livermore National Laboratory (LLNL), [6] Bureau of Mines (BM), [4] and Fenwal [10] Data

The normalized pressure rise ($\Delta P/P_0$) results for tests conducted at four different facilities together with the calculated adiabatic, isochoric complete combustion normalized pressure rise are shown in Figure 26.[8-10] The VGES data were taken from those tests of H_2 and ambient air only. The other data points were computed from the information given in the original references. Theoretical calculations of $\Delta P/P_0$ indicate that this quantity depends mainly on the initial H_2 concentration and is relatively independent of starting pressure. Therefore, these dry hydrogen:air experiments, which were all performed at different initial conditions, can be compared on a single graph, such as in Figure 26. It should be noted, however, that the peak pressure is sensitive to the mixture preburn temperature. The comparison shown in Figure 27 indicates a larger pressure rise during the VGES testing than observed in previous experiments at H_2 concentrations less than ~8%. The VGES results, however, are similar to those obtained by Hertzberg in a 7.57-liter vessel using a pyrotechnic igniter.[8]

The peak temperatures from all the VGES tests with hydrogen: ambient-air are shown in Figure 28 for both the "fans on" and "fans off" burns, along with the calculated AICC temperature. Below ~10% H_2, the recorded temperatures tend to converge on the AICC curve as the H_2 concentration increases. Above ~10% H_2, the recorded temperatures appear to diverge from the AICC curve. Some temperature recordings show larger peaks than do others. The reason for this behavior is the size of the TCs used during the testing. At lower H_2 concentrations, the burn time is long enough to allow the thermocouples to respond and record temperatures close to the maximum. As the H_2 concentration increases, the burn time decreases, and the TCs do not respond fast enough to record the peak temperatures. The few recorded peak temperatures higher than the general trend were recorded with very small diameter junction TCs, which could respond fast enough to record temperatures close to the maximum.

The flame speeds obtained from TC arrival-time data, for both the "fans on" and "fans off" burns, are shown in Figures 29 and 30. The upward flame speeds are shown in Figure 29, and the downward flame speeds are shown in Figure 30. In Figures 29 and 30, the curves shown are a least squares fit to the data. These figures illustrate that burns with the fans on produce higher flame speeds, especially below ~10% H_2 concentration, and that upward flame propagation is faster than downward propagation. This observation is further backed by the behavior of the pressure rise time as a function H_2 concentration (Figure 31). The pressure rise time can be thought of as measure of the a global burn speed or burnout time.* Figure 31 indicates that the time to burn the mixture in the VGES vessel decreases with increased H_2 concentration and is smaller for

*For slow burns (lean mixtures), it is known that the peak in pressure can occur before the end of combustion.

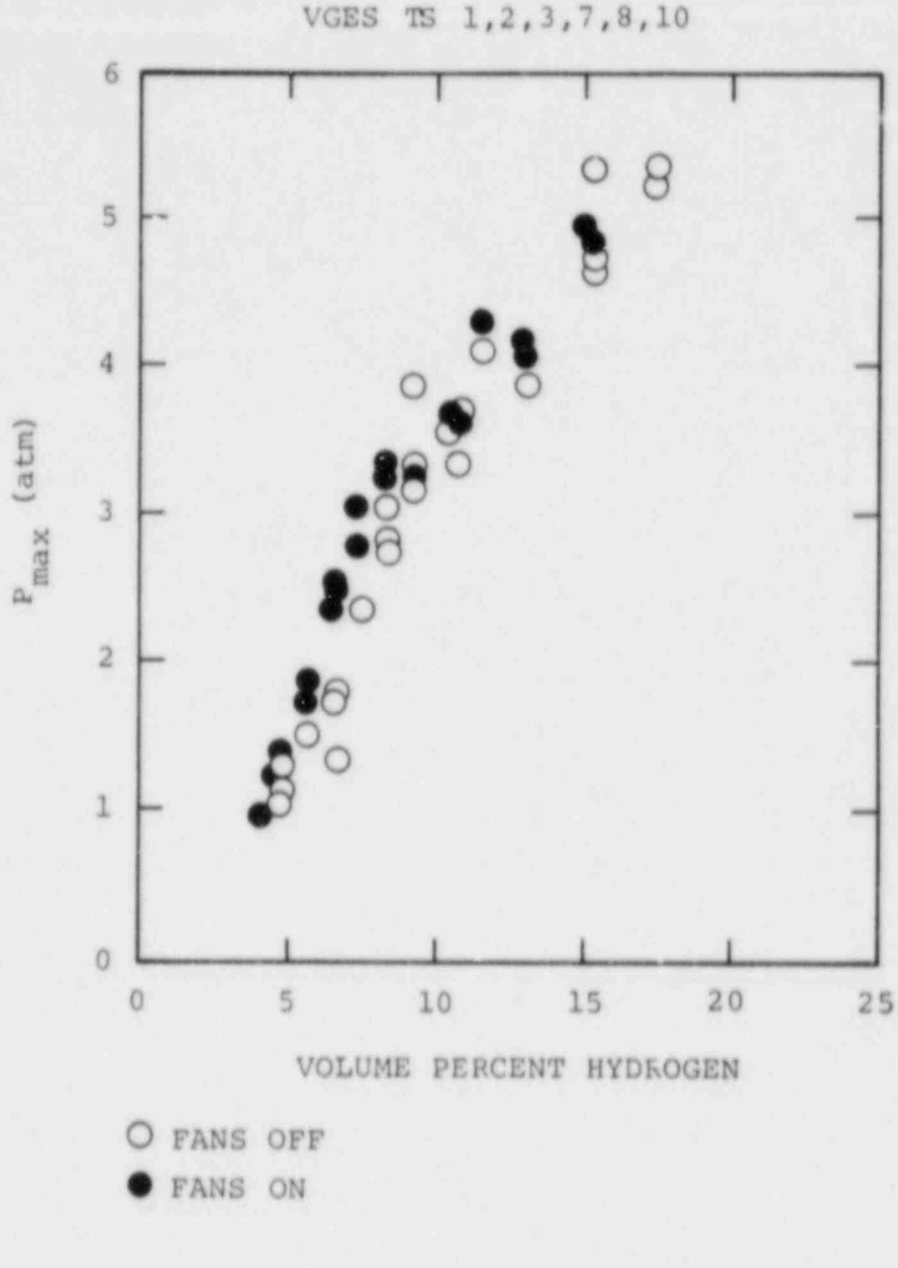

Figure 27. Peak Pressure as a Function of H_2 Concentration

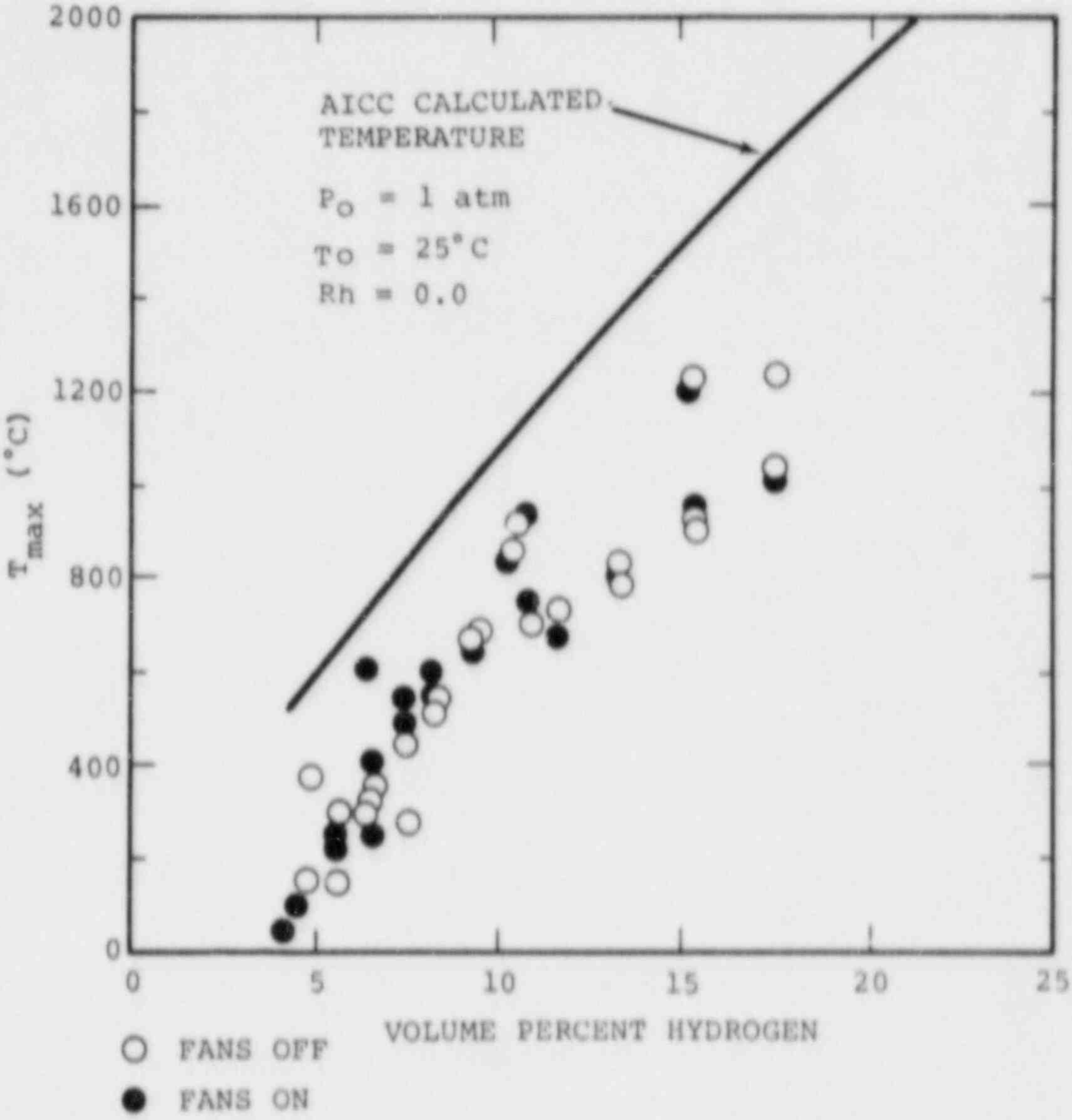

Figure 28. Peak Temperature as a Function of H_2 Concentration for Hydrogen:Ambient-Air

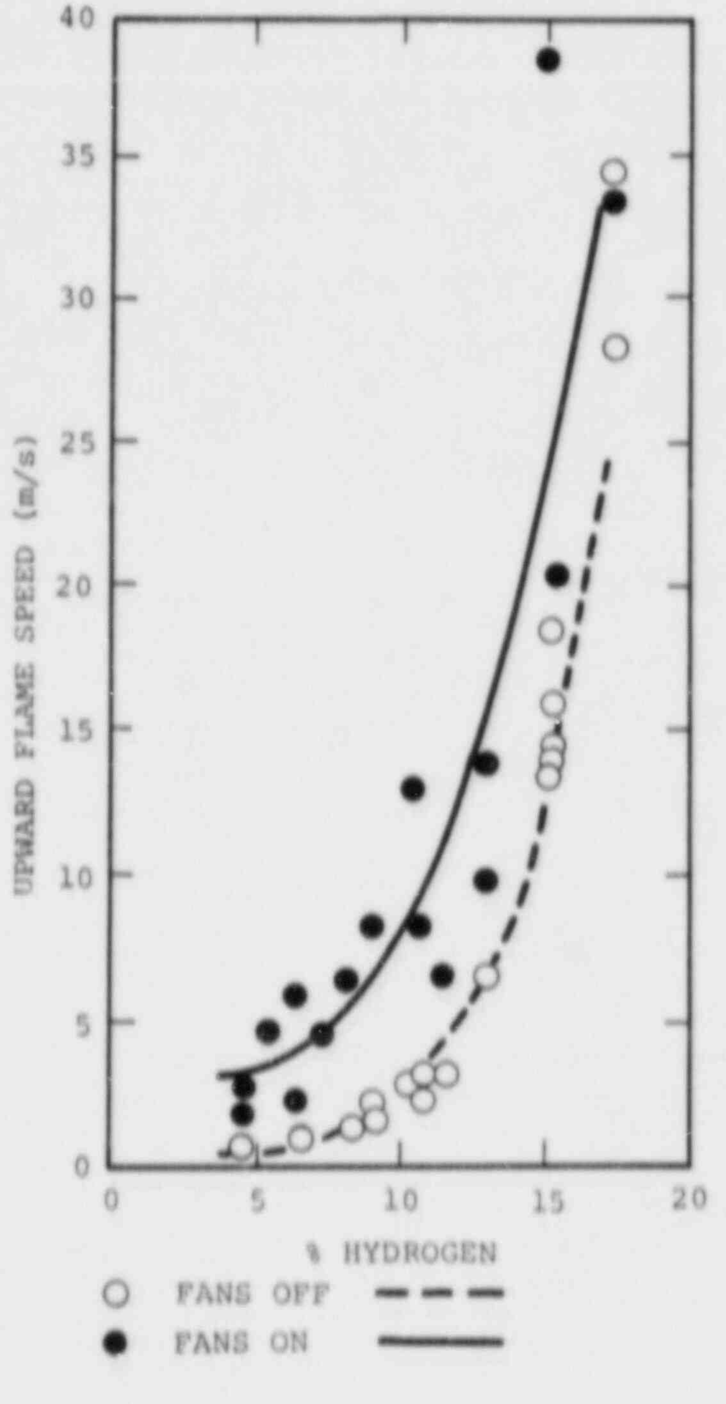

Figure 29. Upward Flame Speed (V_{up}), Fans Off and Fans On

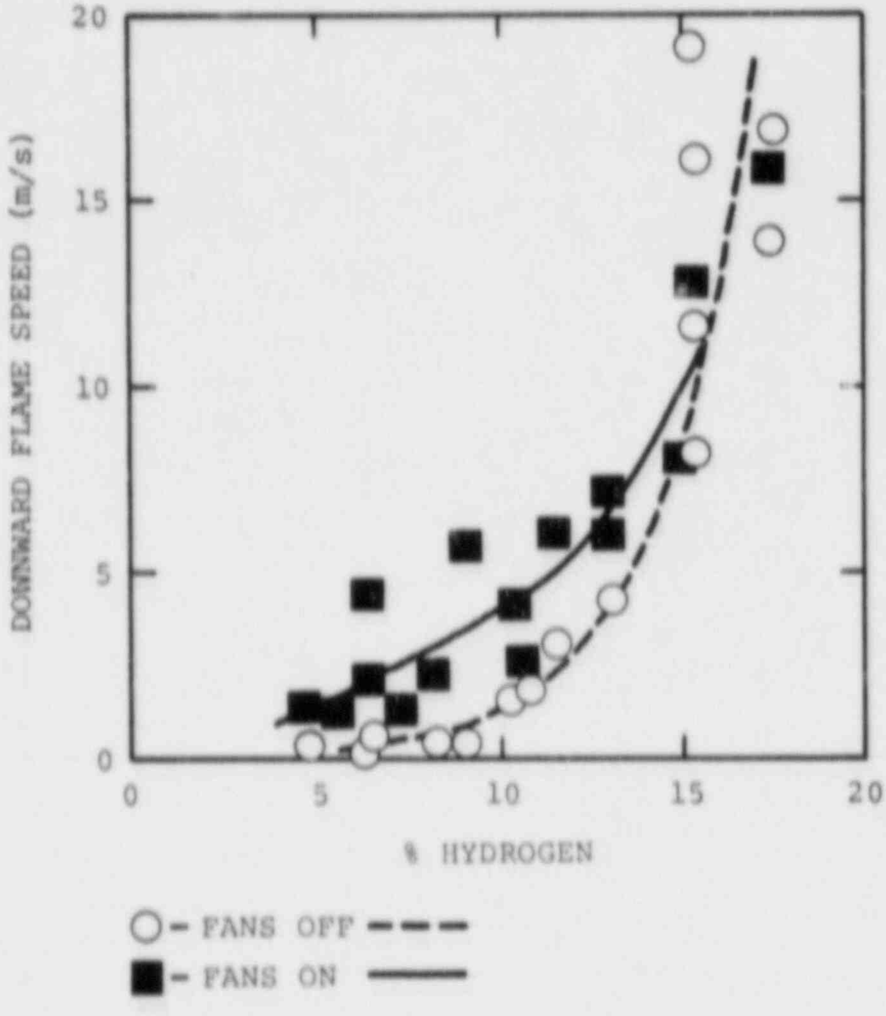

Figure 30. Downward Flame Speed (V_{down}), Fans Off and Fans On

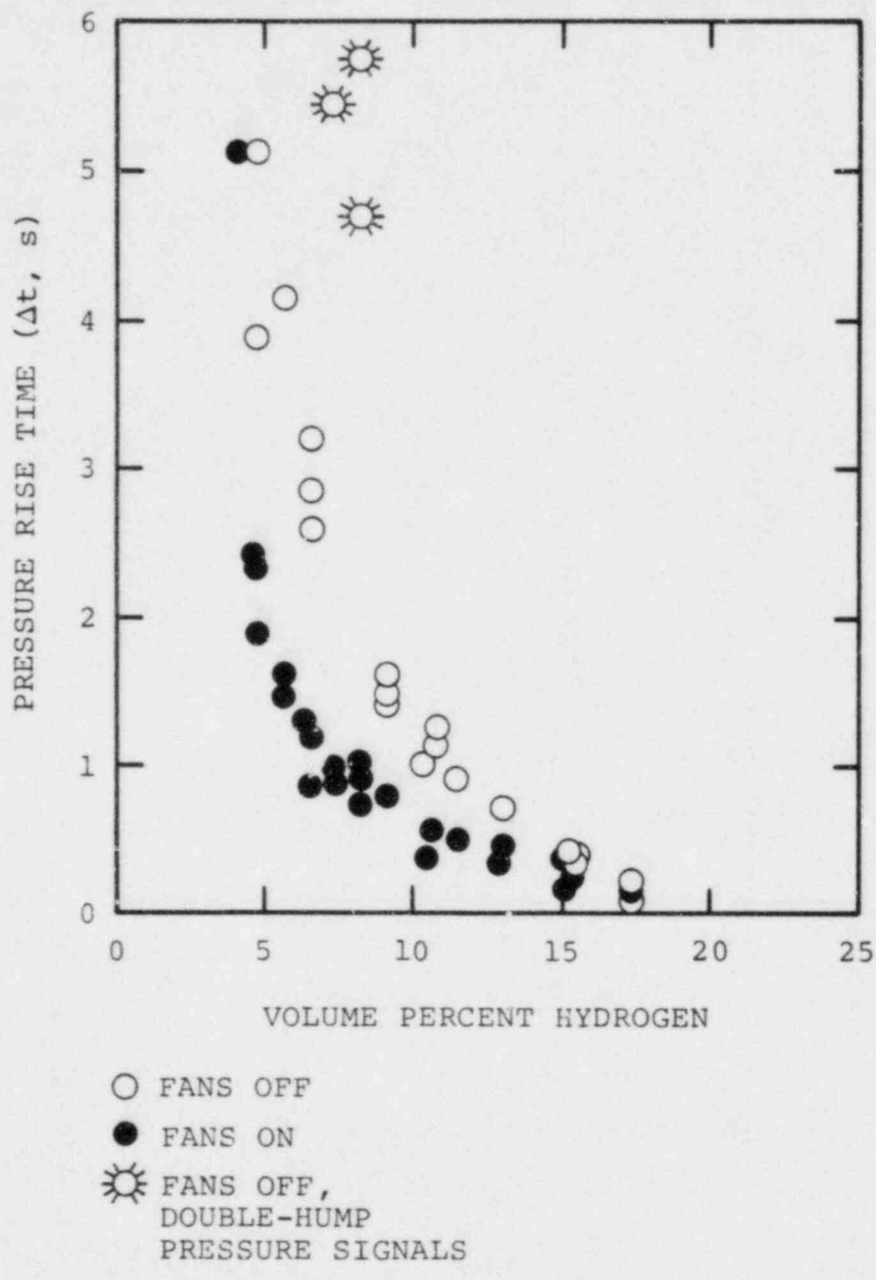

Figure 31. Pressure Rise Time (Δt) as a Function of H_2 Concentration

the "fans on" burns. In addition, the differences in the "fans on" and "fans off" pressure rise times decrease with increasing H_2 concentration.

The calculated mean pressure derivative ($\Delta P/\Delta t$) for all the VGES testing of ambient air and H_2 is shown in Figure 32 as a function of H_2 concentration. This figure indicates that the mean pressure derivative increases with increasing H_2 concentration and is larger for the "fans on" burns. In addition, for the "fans off" burns, $\Delta P/\Delta t$ does not exhibit a significant increase until the H_2 concentration is above ~8%. For the "fans on" burns, $\Delta P/\Delta t$ exhibits an increase above ~6% H_2 concentration. These observations tend to indicate that the chemical energy release rate does not significantly increase in quiescent mixtures until H_2 concentrations are above ~8%. For the "fans on" burns, the chemical energy release rates tend to increase for H_2 concentrations above ~6%.*

*It is important to keep in mind that the "fans on" burn data are very specific to the VGES tank and its fans. No extrapolations of "fans on" data can be made without analytical justification and additional tests in other size tanks using comparable fans.

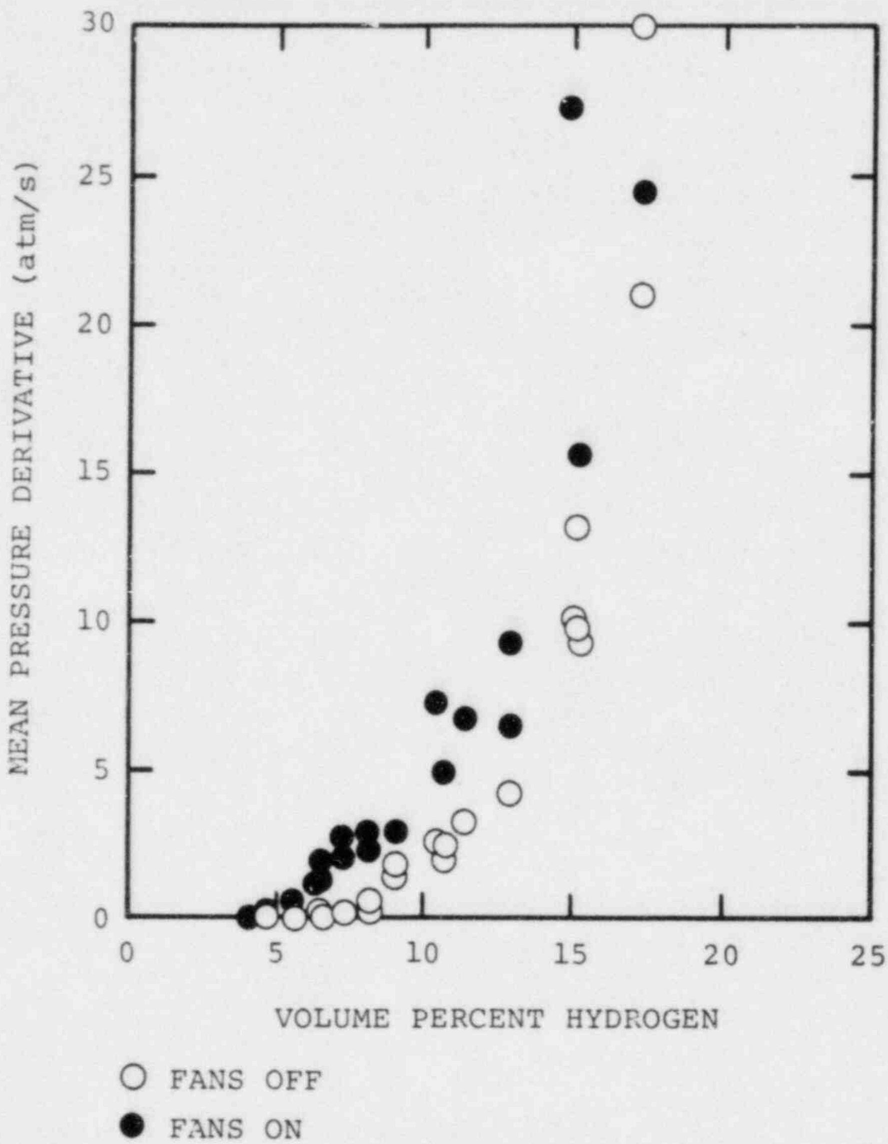

Figure 32. Mean Pressure Derivative as a Function of H_2 Concentration, Fans On and Fans Off

VII. Conclusions

The results of the VGES testing to date provide data covering a wide range of hydrogen combustion and mitigation phenomena. General observations noted during these studies are summarized below.

Hydrogen burns in the VGES tank were sometimes spatially asymmetric, accelerating as the burn moved up the tank and produced significant pressure rises at H_2 concentrations above 4.75%. Iso-arrival-time contour maps of the flame front suggest the presence of flame globules for burns in quiescent mixtures containing less than 8% to 9% hydrogen.

Measured flame propagation velocities increased rapidly as the initial H_2 concentration was increased. Upward flame velocities are larger than downward flame velocities. The difference was largest for low H_2 concentration burns and decreased as the H_2 concentration increased.

Pressure signals exhibiting double-humped behavior for H_2 concentrations in the range of 7% to 9% indicate that the upper and lower portions of the tank complete the combustion process at different times. This result occurs close to the downward flame propagation limit and does not occur during similar tests with the fans on.

The results obtained from combustion of H_2 with reduced air quantities indicate that as the total amount of air decreases, there is a slight decrease in the pressure rise, normalized peak pressure, and the mean pressure derivative for the same H_2 concentrations. The pressure rise time increases somewhat with a decrease in air quantity.

Testing with additional nitrogen added to hydrogen:air mixtures containing up to ~17% H_2 indicated no significant differences in the burn characteristics when compared to tests performed with similar total hydrogen concentration. The addition of nitrogen, however, diluted the initial H_2 concentration and produced burns indicative of the actual preburn H_2 concentration.

All three igniters used during the VGES testing were reliable in producing an ignition for the H_2 concentrations tested. Ignition occurred almost immediately upon initiation for the spark and 70-V glowplug igniters while the 14-V glowplug igniter required ~20 s to heat up to the ignition temperature of the mixtures tested.

The operation of fans during the testing had significant effect on the burn characteristics. Tests performed with the fans on showed increases in the burn velocity, pressure rise, peak pressure, and the mean pressure derivative and a decrease in the pressure rise time. The largest increase in the burn parameters (decrease with respect to the pressure rise time) occurs around 8% H_2 concentration. Below the ~8% H_2 concentration level, the primary effect of testing with the fans on was to increase the completeness of combustion. Above ~8% H_2 concentration, the primary effect of fan operation was to increase the chemical energy release rate.

The effects of CO_2 addition on hydrogen:air combustion is to reduce the peak pressure, pressure rise, and burn velocity, and to increase the time to peak pressure. While we performed a limited number of tests with CO_2, the results tend to indicate that ~54% CO_2 will inert a hydrogen:air mixture. Comparisons between tests with similar total H_2 concentrations but with and without CO_2 addition indicate that the peak pressure and pressure rise are reduced with increased CO_2.

The degree to which CO_2 simulates steam in a "cold" test environment could not be absolutely determined from the VGES testing. Comparisons of combustion with "cold" hydrogen:air:CO_2 mixtures and similar "hot" hydrogen:air:steam mixtures tend to indicate that CO_2 and steam have comparable combustion mitigation effects. However, more testing with hydrogen:air:CO_2 and hydrogen:air:steam mixtures should be performed to determine the combustion behavior of these systems at H_2-in-air concentrations below 10%.

For hydrogen:air mixtures with less than about 15% hydrogen, filling the tank with 620:1-expansion aqueous foam produced a reduction in the peak pressure and temperature. However, for mixtures greater than 15% H_2, the observed damage that resulted from an accelerated flame precludes the use of foam as a mitigation scheme.

In summary, the VGES testing has provided data on the combustion of hydrogen:air mixtures under various conditions. These data can be used to make preliminary assessments of the effects of hydrogen:air combustion on large systems. In addition, analytical models developed from these tests should provide a first-order predictive capability.

REFERENCES

1. D. Renfro et al., "Development and Testing of Hydrogen Ignition Devices," Proceedings of the Second International Conference on the Impact of Hydrogen on Water Reactor Safety, Albuquerque, New Mexico, October 1982, NUREG/CR-0038, EPRI RP 1932-35, SAND82-2456.

2. W. H. McCulloch et al., "Hydrogen Burn Survival: Preliminary Thermal Model and Test Results," NUREG/CR-2730, SAND82-1150, (August 1982).

3. J. H. S. Lee, "Flame Acceleration Mechanisms in Closed Vessels," presented at the Workshop on the Impact of Hydrogen on Water Reactor Safety, Albuquerque, New Mexico (January 25-28, 1981).

4. A. L. Furno, E. B. Cook, J. M. Kuchta, and D. S. Burgess, "Some Observations on Near-Limit Flames," 13th Symposium on Combustion, Pittsburg Comb. Inst., 593-599, (1971).

5. H. Tamm et al., "A Review of Recent Experiments at WNRE on Hydrogen Combustion," Proceedings of the Second International Conferece on the Impact of Hydrogen on Water Reactor Safety, Albuquerque, NM, October 1982, NUREG/CR-0038, EPRI RP 1932-35, SAND82-2456.

6. W. E. Lowry et al., "Final Results of the Hydrogen Igniter Experimental Program," NUREG/CR-2486, UCRL-53036 (February 1982).

7. S. F. Roller et al., "Medium-Scale Tests of H_2:Air:Steam Systems," preliminary draft, Proceedings of the Second International Conference on the Impact of Hydrogen on Water Reactor Safety, Albuquerque, NM, October 1982, NUREG/CR-0038, EPRI RP 1932-35, SAND82-2456.

8. M. Hertzberg, <u>Flammability Limits and Pressure Development in H_2-Air Mixtures</u>, Bu Mines PRC Report No. 4305 (1981).

9. W. Lowry, "Results of Thermal Igniter Tests in H_2:Air: Steam Environments," presented at the Workshop on the Impact of Hydrogen on Water Reactor Safety, Albuquerque, NM (January 25-28, 1981).

10. N. Liparulo and J. Olhoeft, "Glowplug H_2 Igniter Tests," presented at the Workshop on the Impact of Hydrogen on Water Reactor Safety, Albuquerque, NM (January 25-28, 1981).

APPENDIX A

The temperatures and pressures for two tests from each of the 11 TS are given in Figures A1 through A22. The pressures and iso-arrival-time contour plots from all the tests for which contour plots were developed are shown in Figures A23 through A64. Written on each contour plot is the ignition time after test initiation, the time difference between contours, and the time of the last contour (which is approximately equal to the time combustion was complete). The pressure records from the remaining tests are given in Figures A65 through A67. Tables 1 and 2 in the text should be referred to for initial conditions and gas chromatograph results pertinent for these tests. Tables 3 through 16 in the text provide summarized results obtained from these experiments.

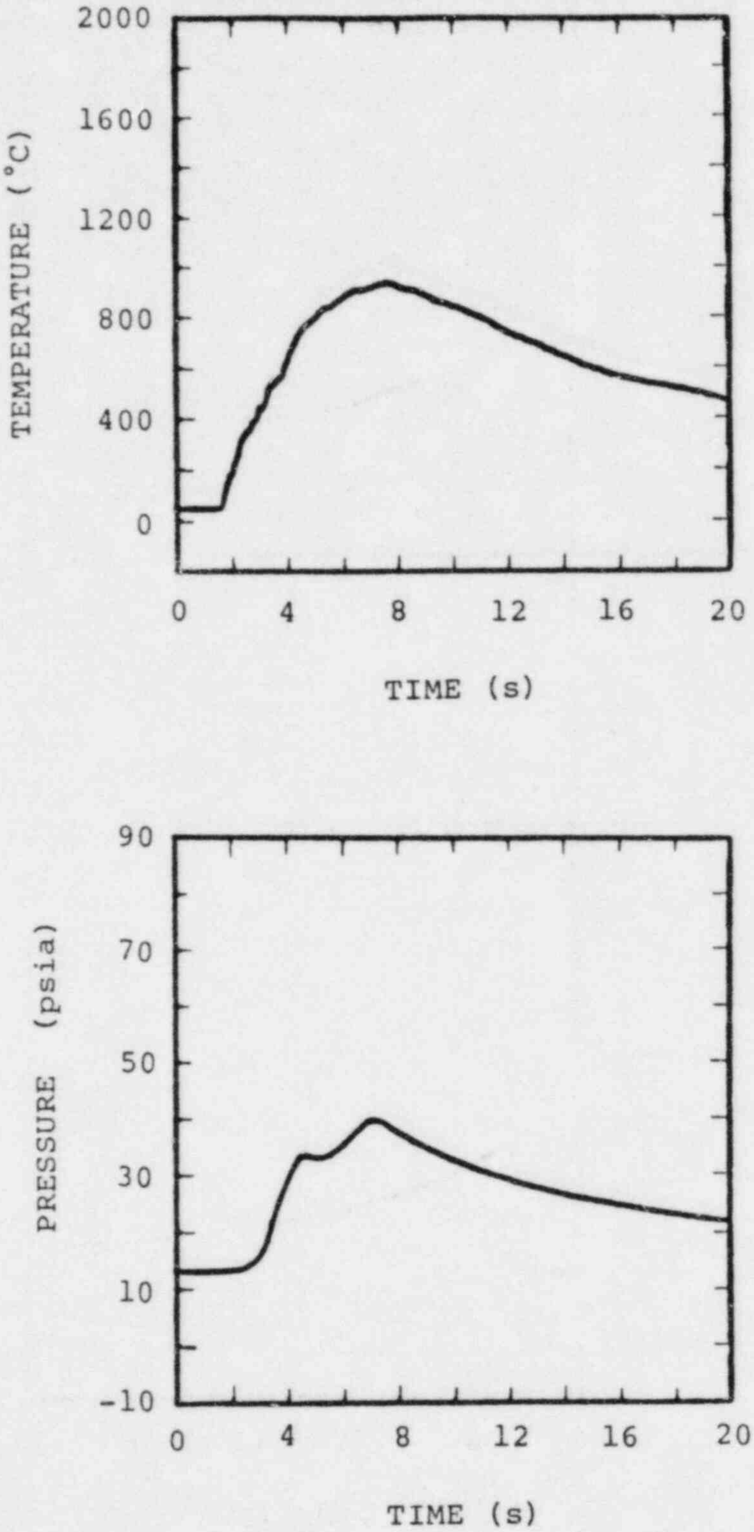

Figure A1. Temperature and Pressure for Test B8H9, 8.26% H_2, Fans Off

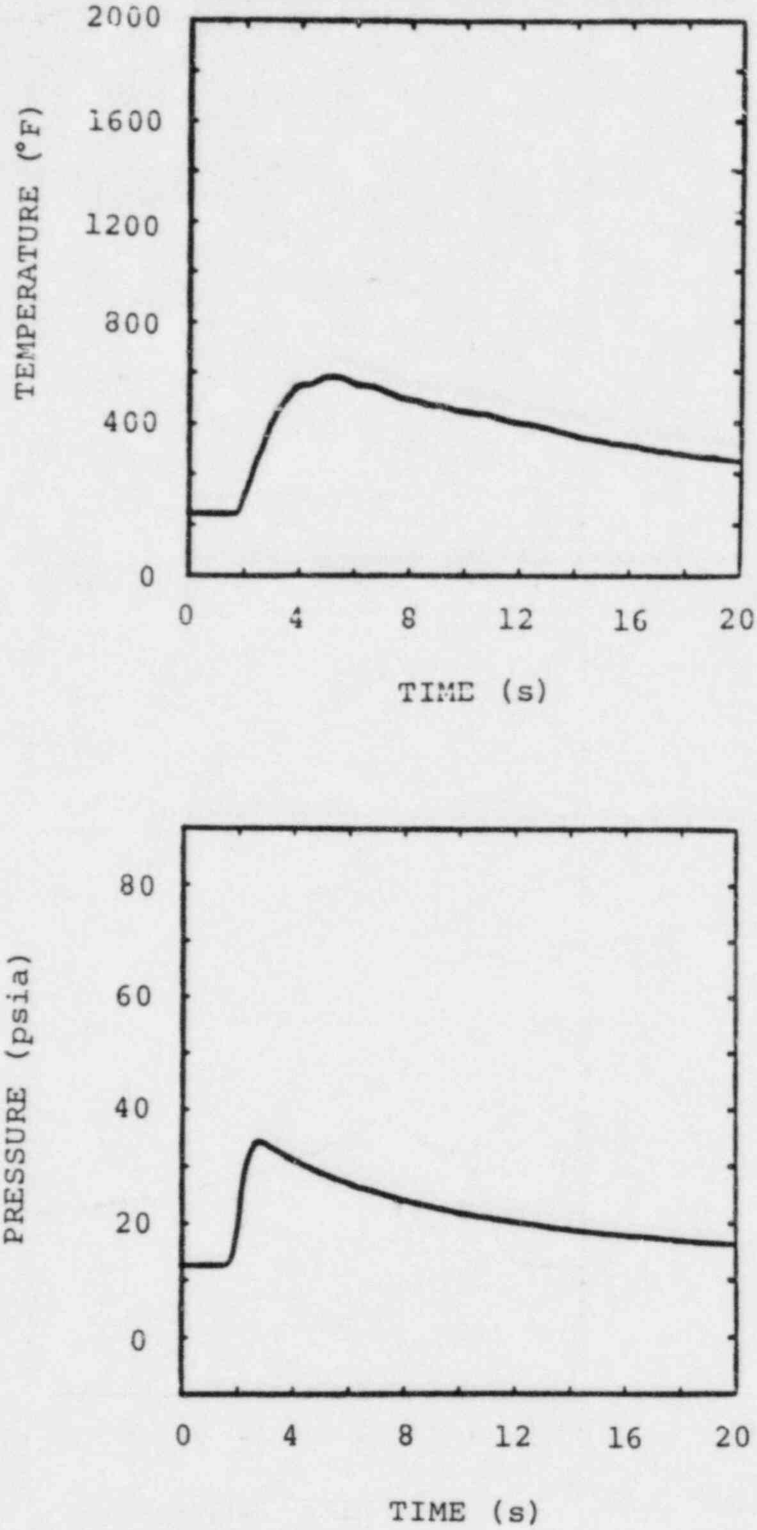

Figure A2. Temperature and Pressure for Test B13H7, 6.47% H_2, Fans On

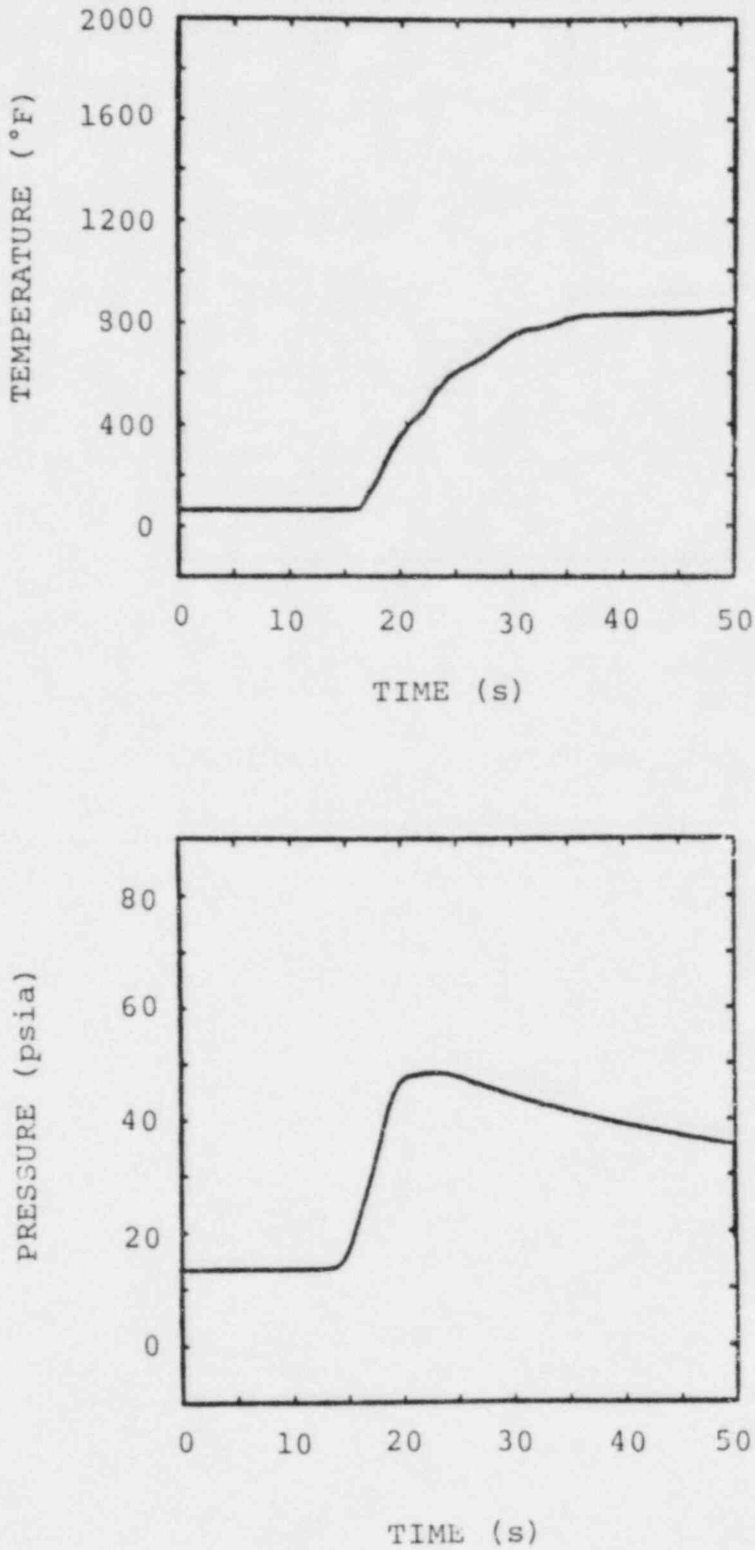

Figure A3. Temperature and Pressure for Test B21H9, 8.27% H_2, Raised 68 volt Glowplug, Fans On

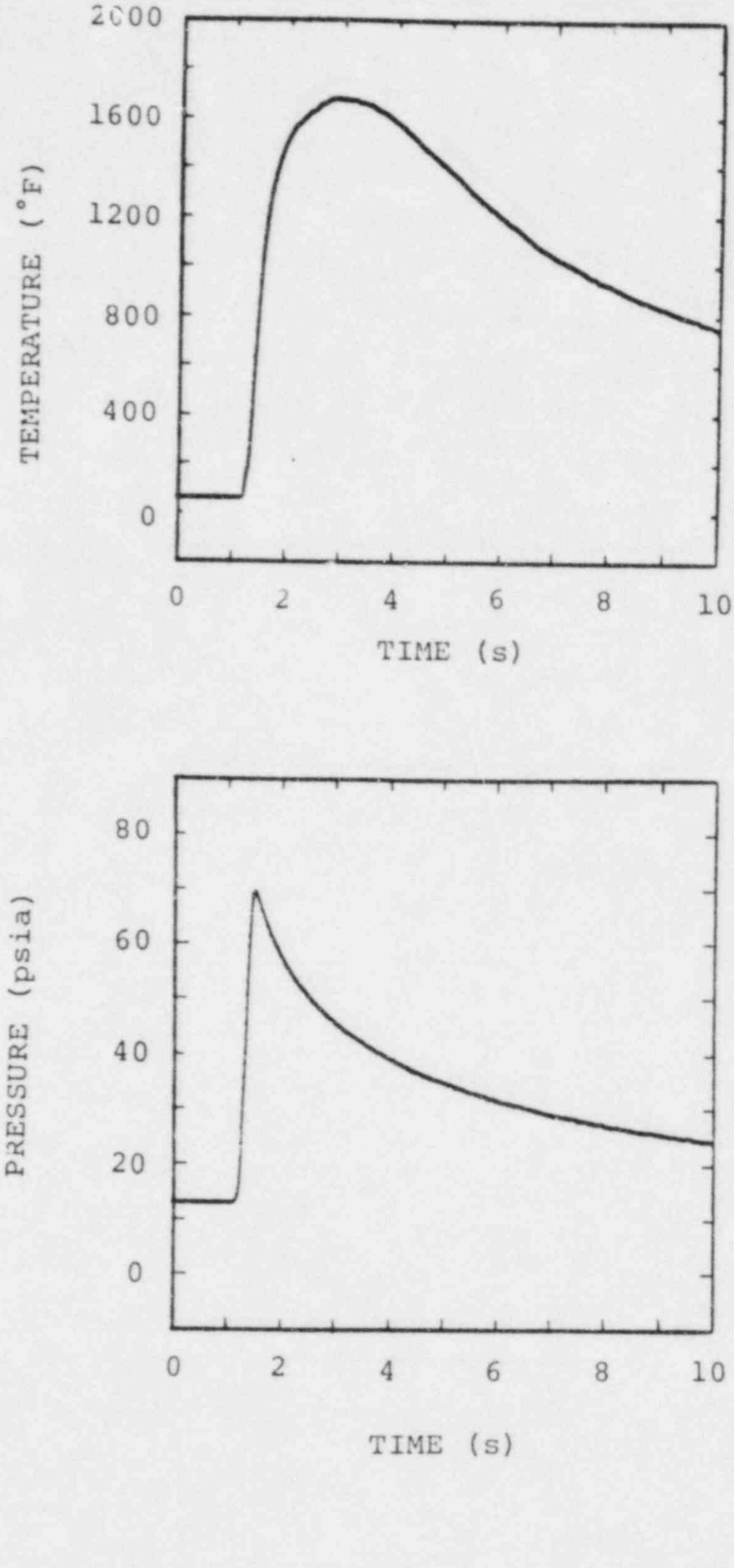

Figure A4. Temperature and Pressure for Test B25H18, 15.25% H_2, Raised 70 volt Glowplug, Fans Off

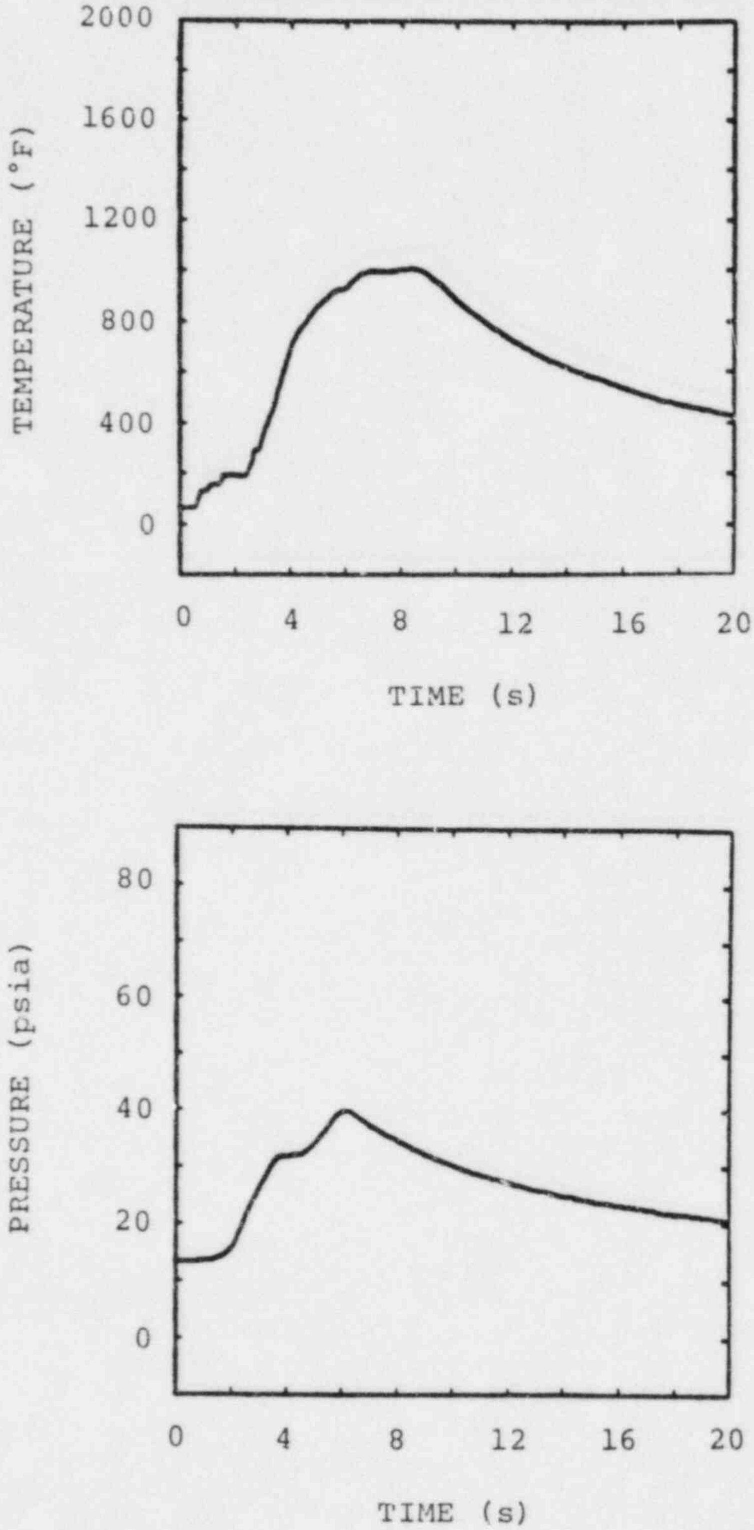

Figure A5. Temperature and Pressure for Test B29H9, 8.25% H_2, Spark Igniter, Fans Off

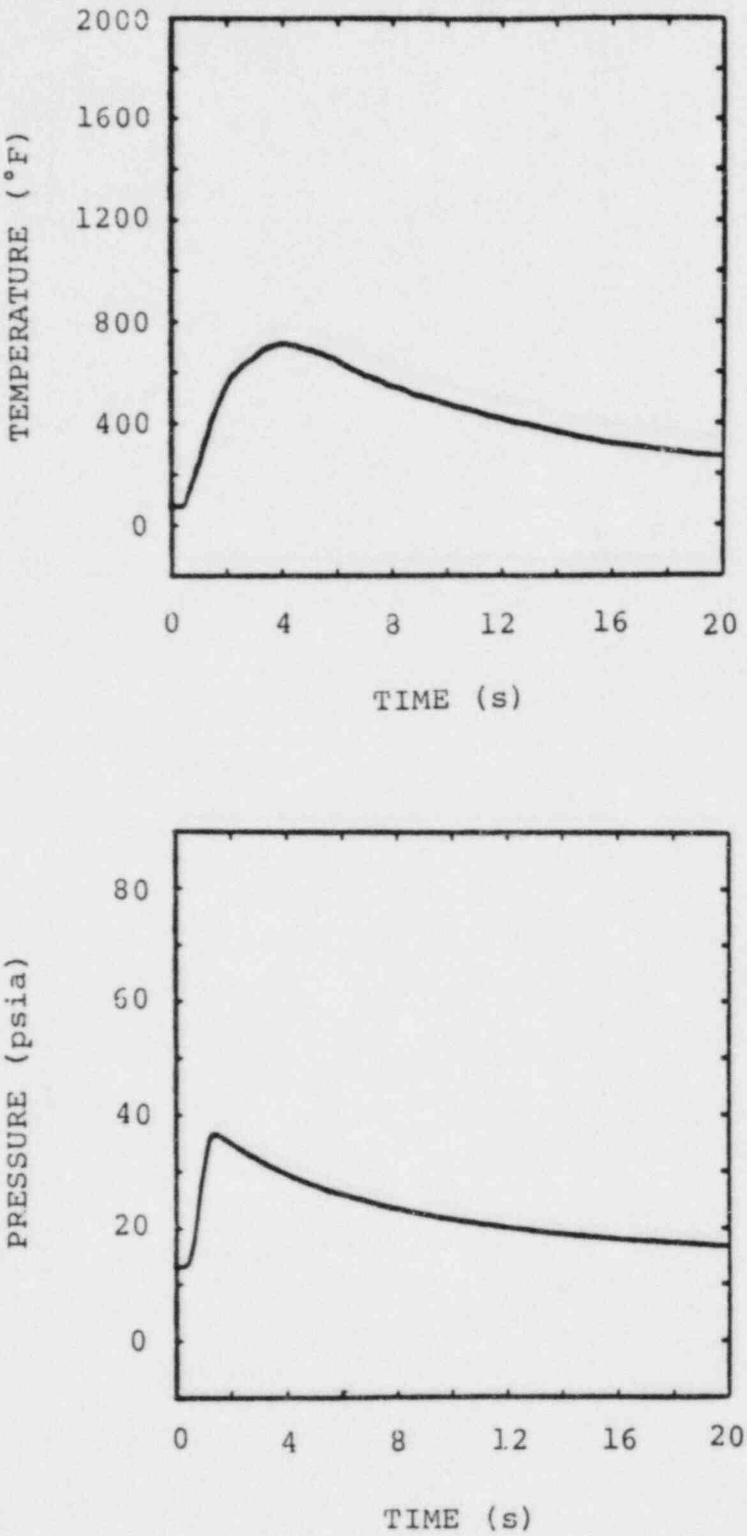

Figure A6. Temperature and Pressure for Test B32H7, 6.54% H_2, Spark Igniter, Fans On

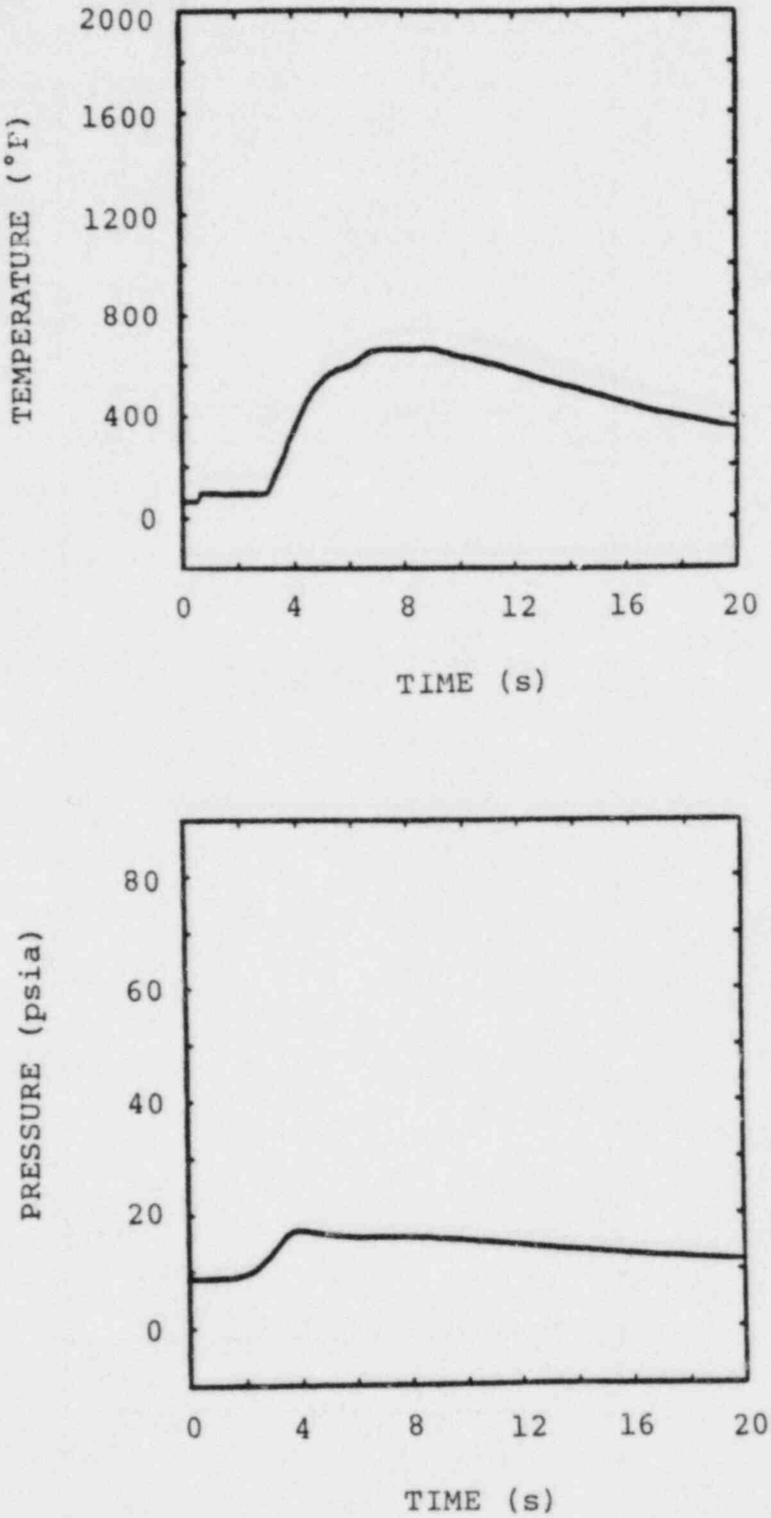

Figure A7. Temperature and Pressure for Test B39H8, 7.41% H_2, 400-Torr Air, Fans Off

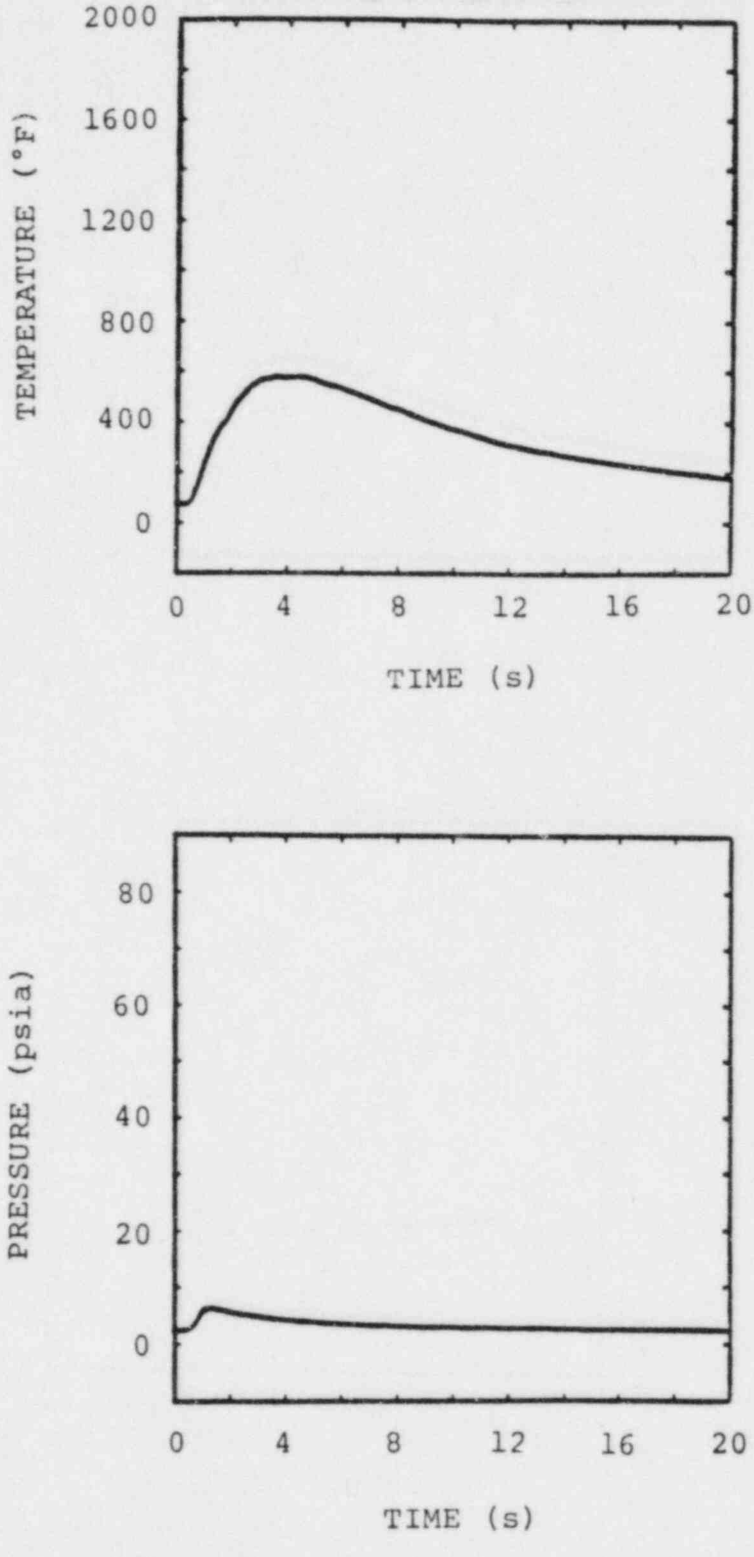

Figure A8. Temperature and Pressure for Test B44H8, 7.41% H_2, 100-Torr Air, Fans On

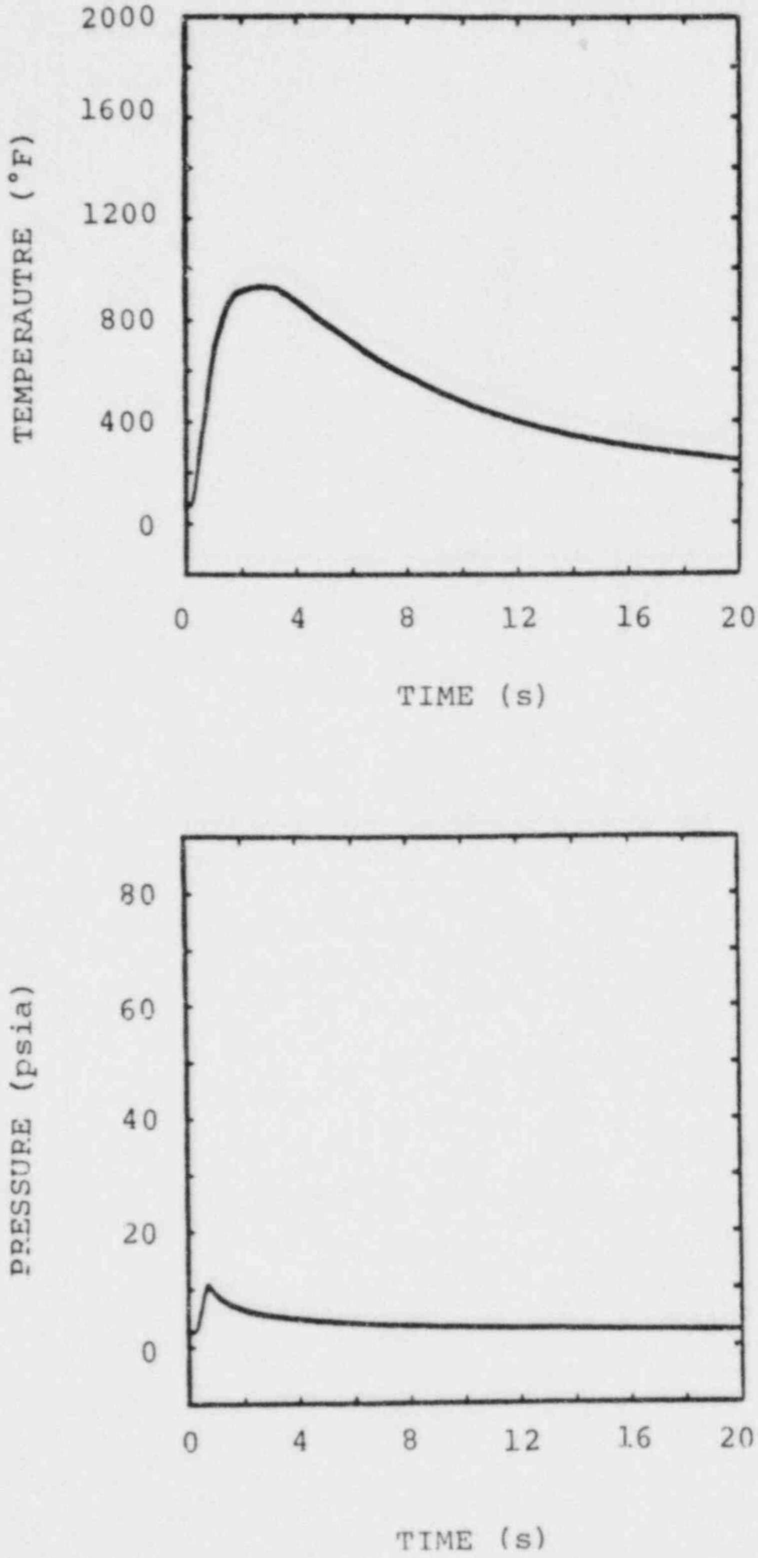

Figure A9. Temperature and Pressure for Test B45H18, 15.25% H_2, 100-Torr Air, Fans Off

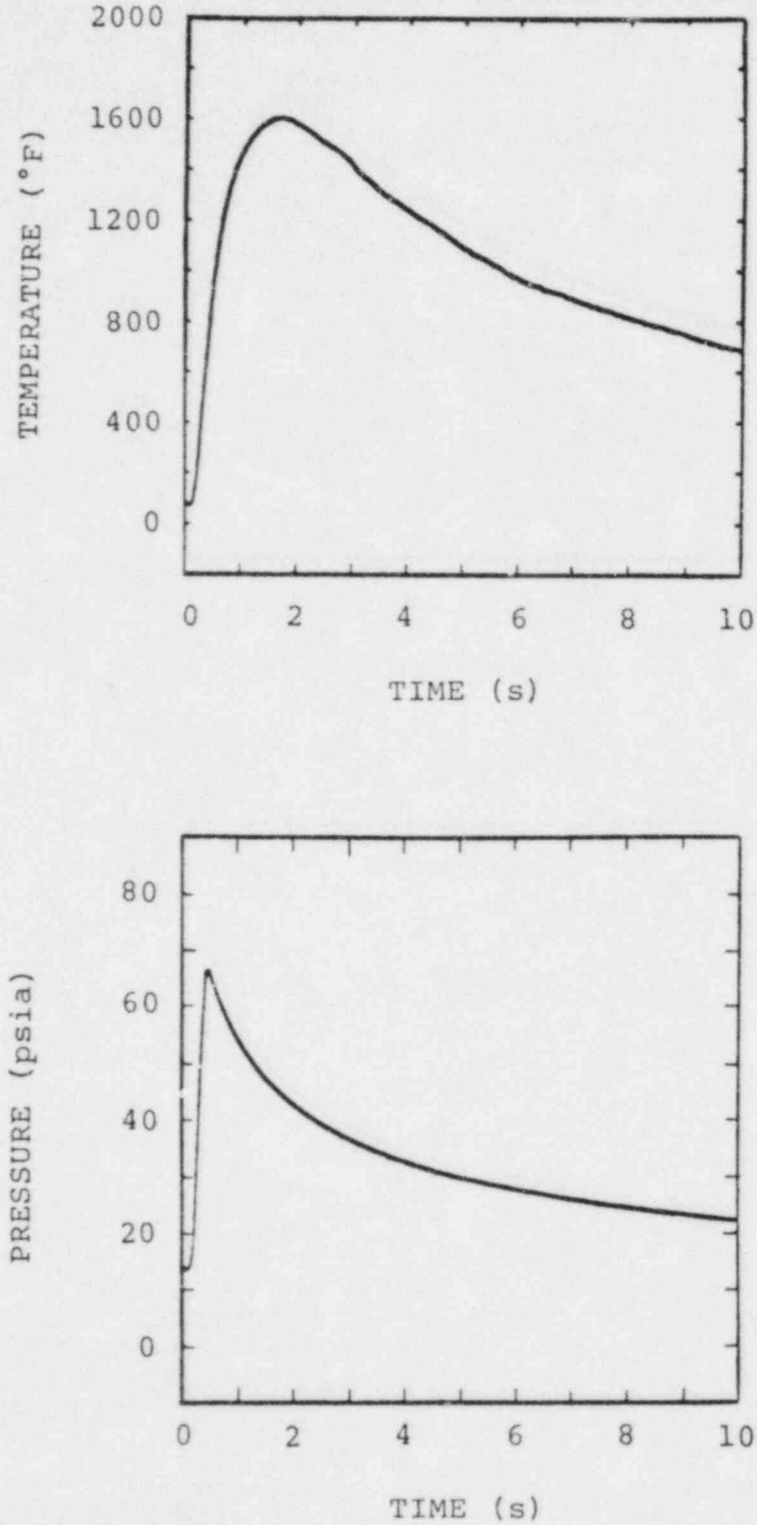

Figure A10. Temperature and Pressure for Test B50H18, 15.25% H_2, 28.25% added N_2 (200-Torr), Fans Off

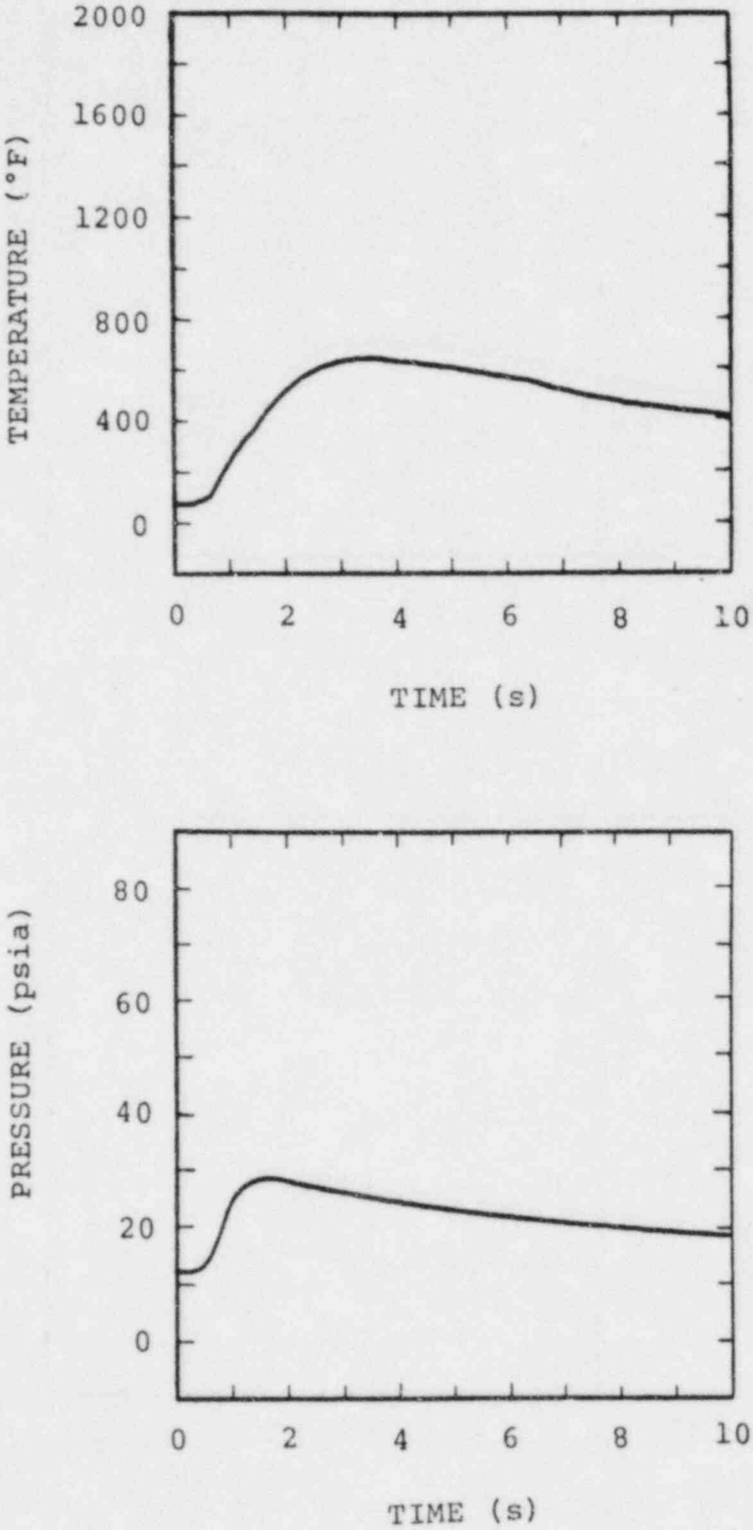

Figure A11. Temperature and Pressure for Test B52H10, 6.25% H_2, 31.25% added N_2 (200-Torr), Fans On

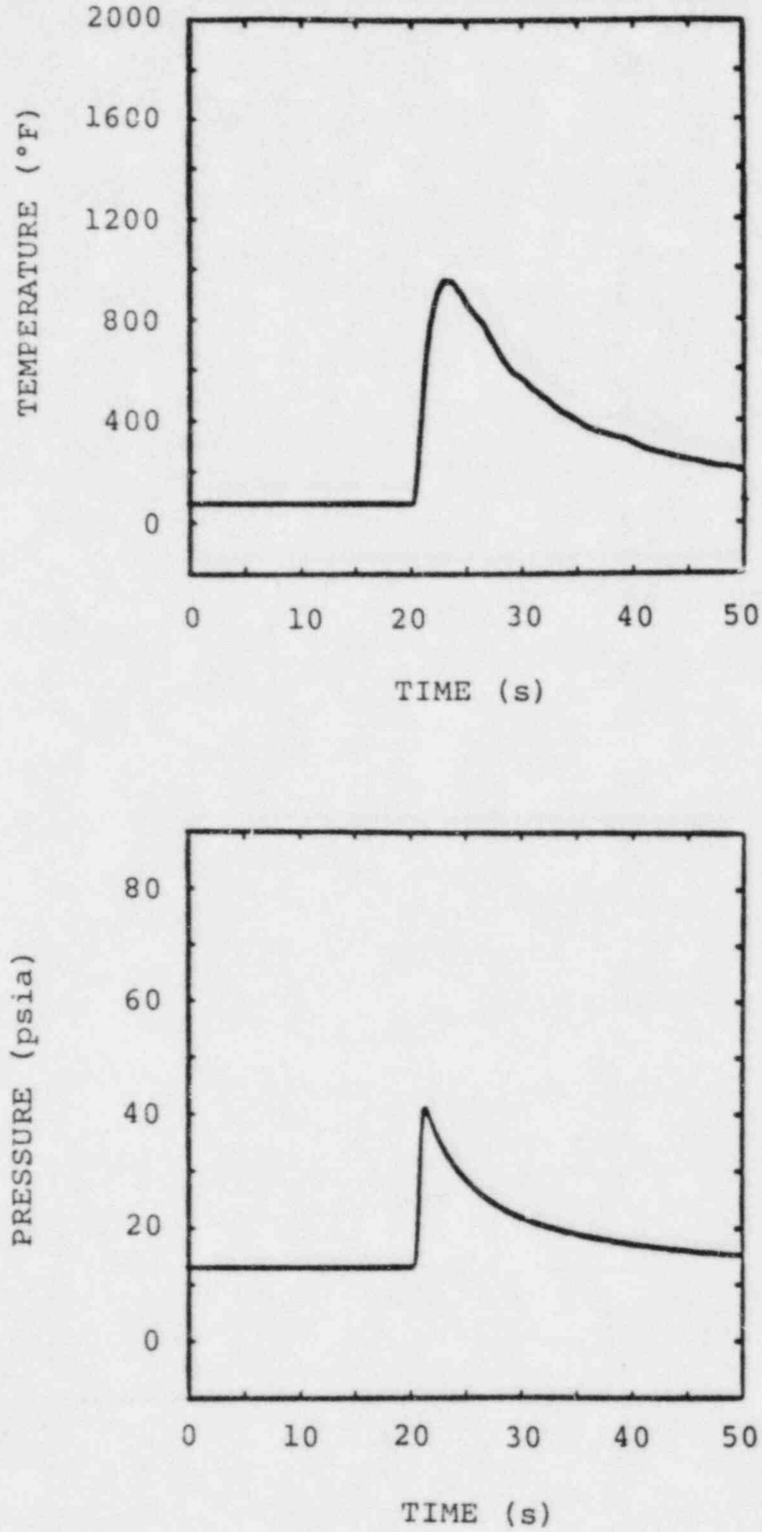

Figure A12. Temperature and Pressure for Test B55H8, 7.40% H_2, 14 volt Glowplug, Fans On

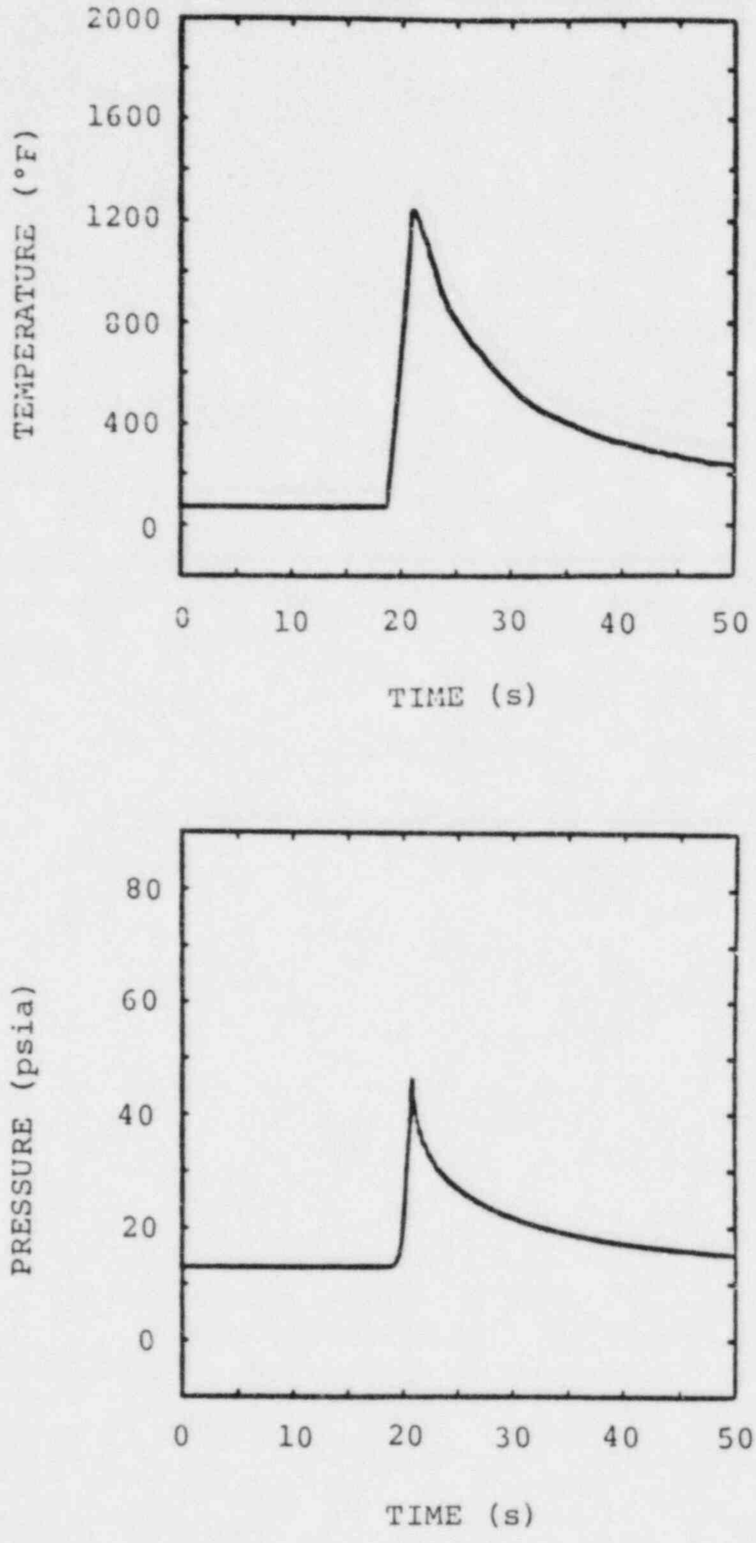

Figure A13. Temperature and Pressure for Test B56H10, 9.08% H_2, 14 volt Glowplug, Fans Off

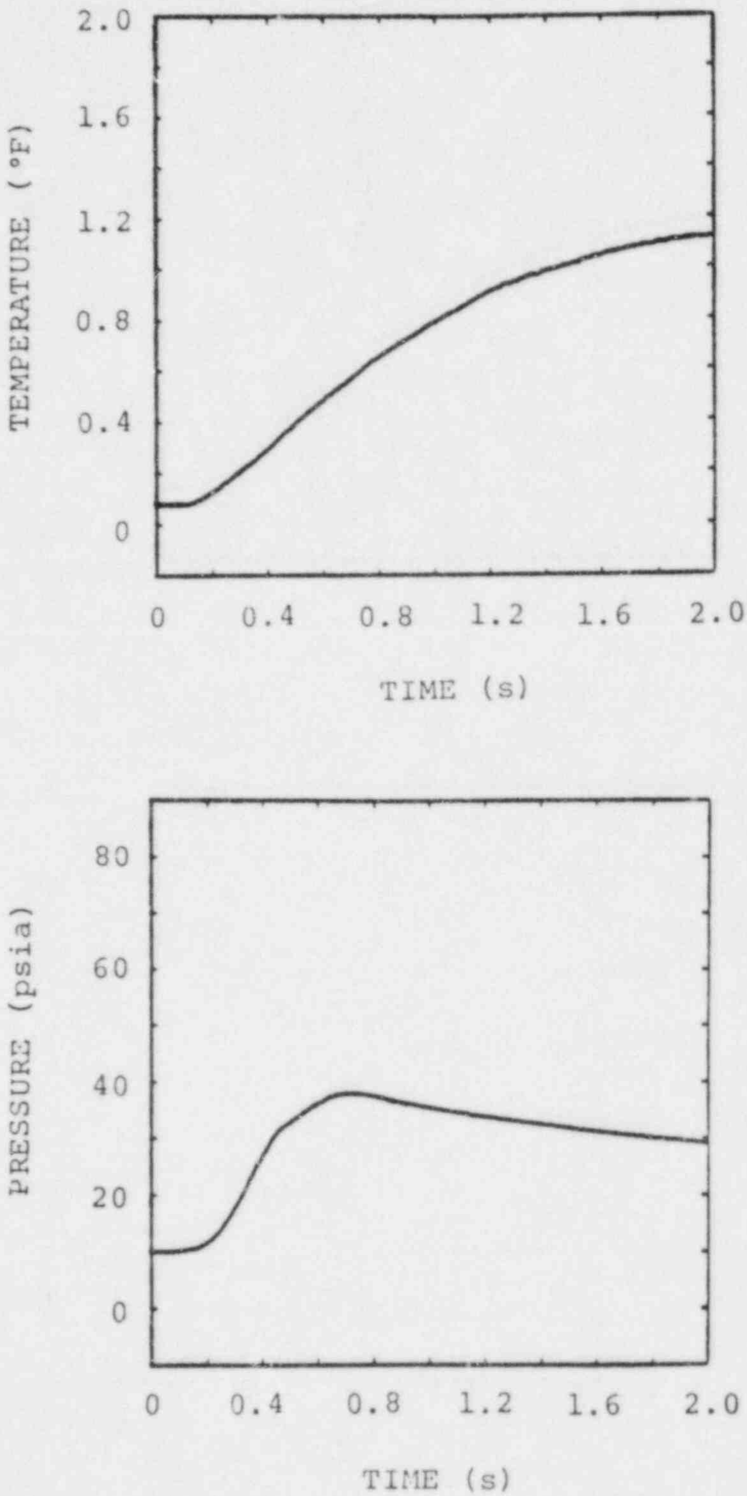

Figure A14. Temperature and Pressure for Test B61H12, 10.7% H_2, 400-Torr Air, Fans On

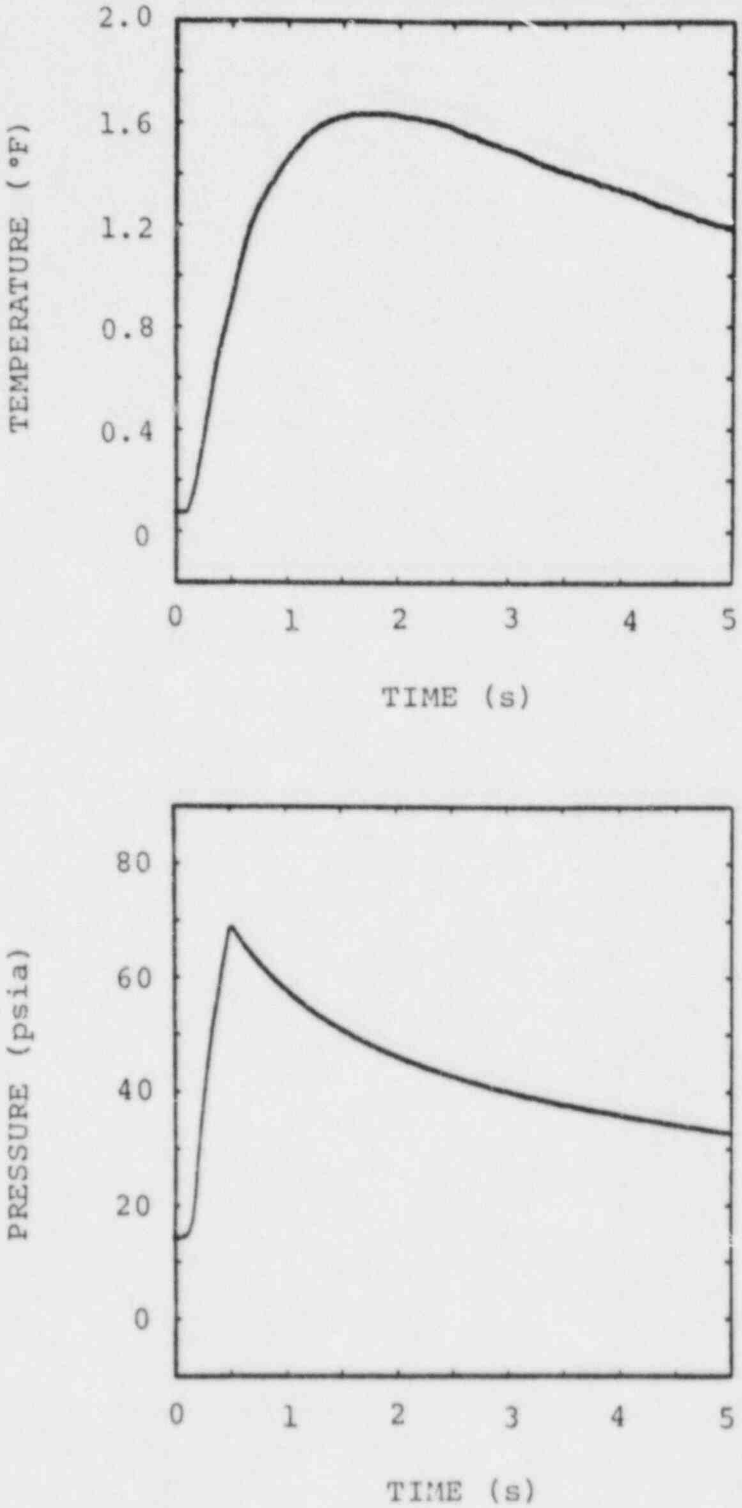

Figure A15. Temperature and Pressure for Test B71H18, 15.3% H_2, Fans Off

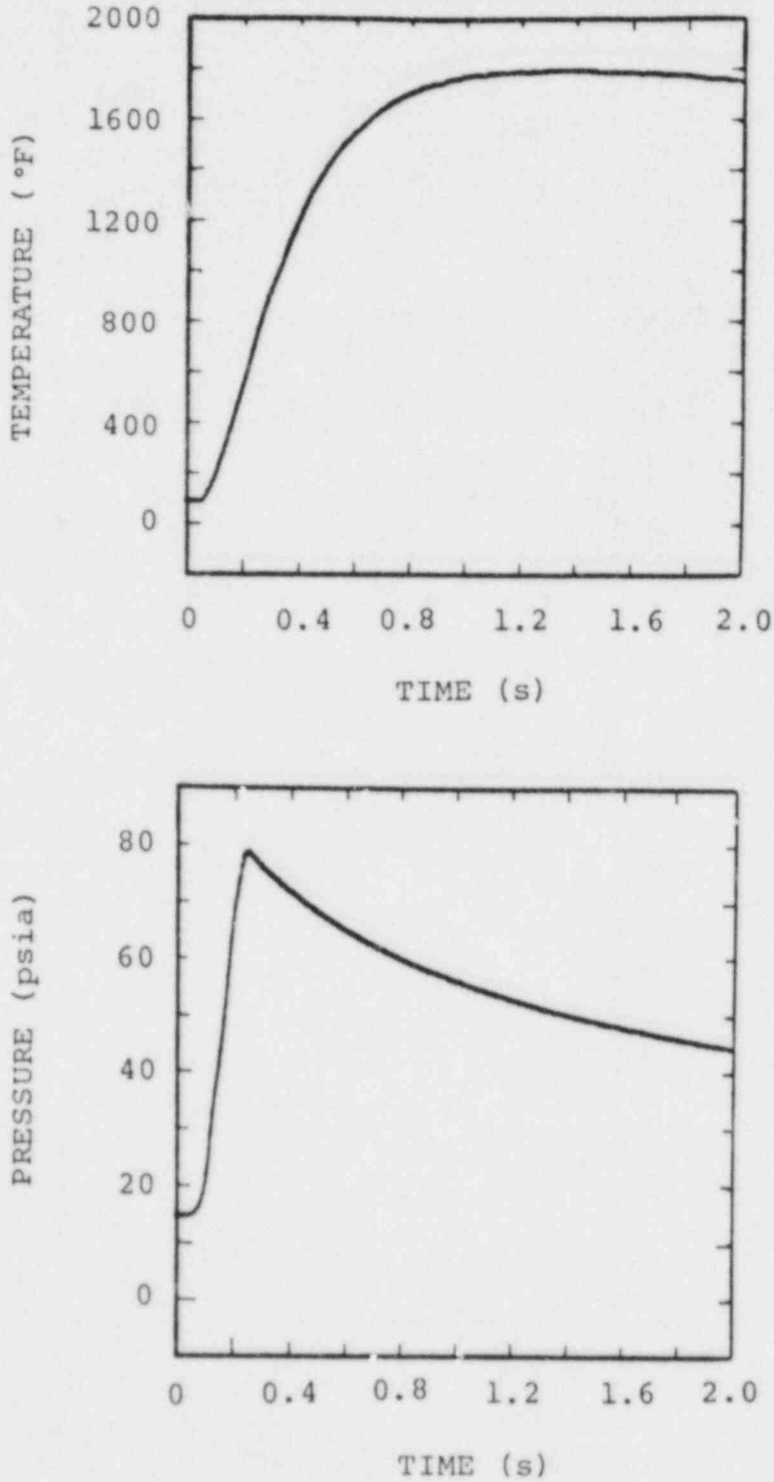

Figure A16. Temperature and Pressure for Test B74H21, 17.4% H_2, Fans On

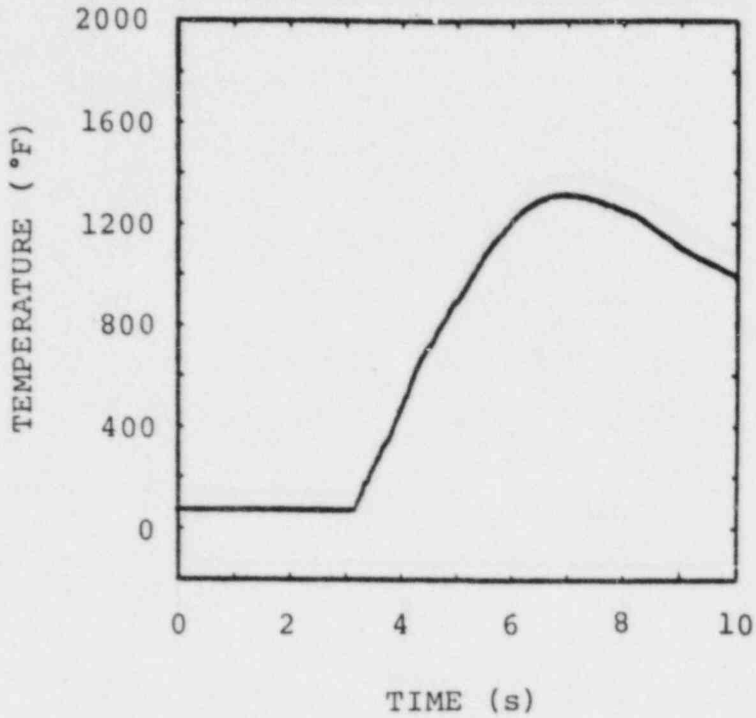

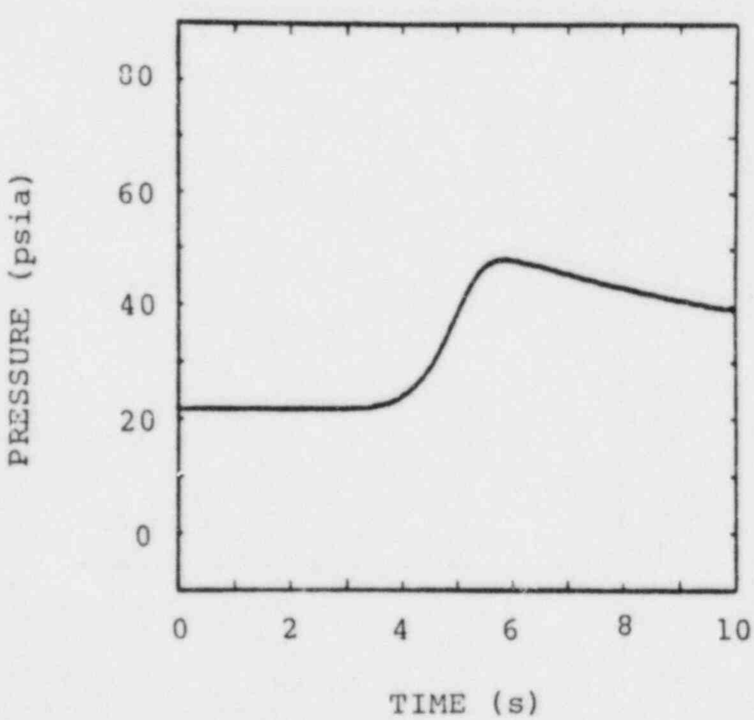

Figure A17. Temperature and Pressure for Test B79H37, 13.06% H_2, 52.17% CO_2, Fans Off

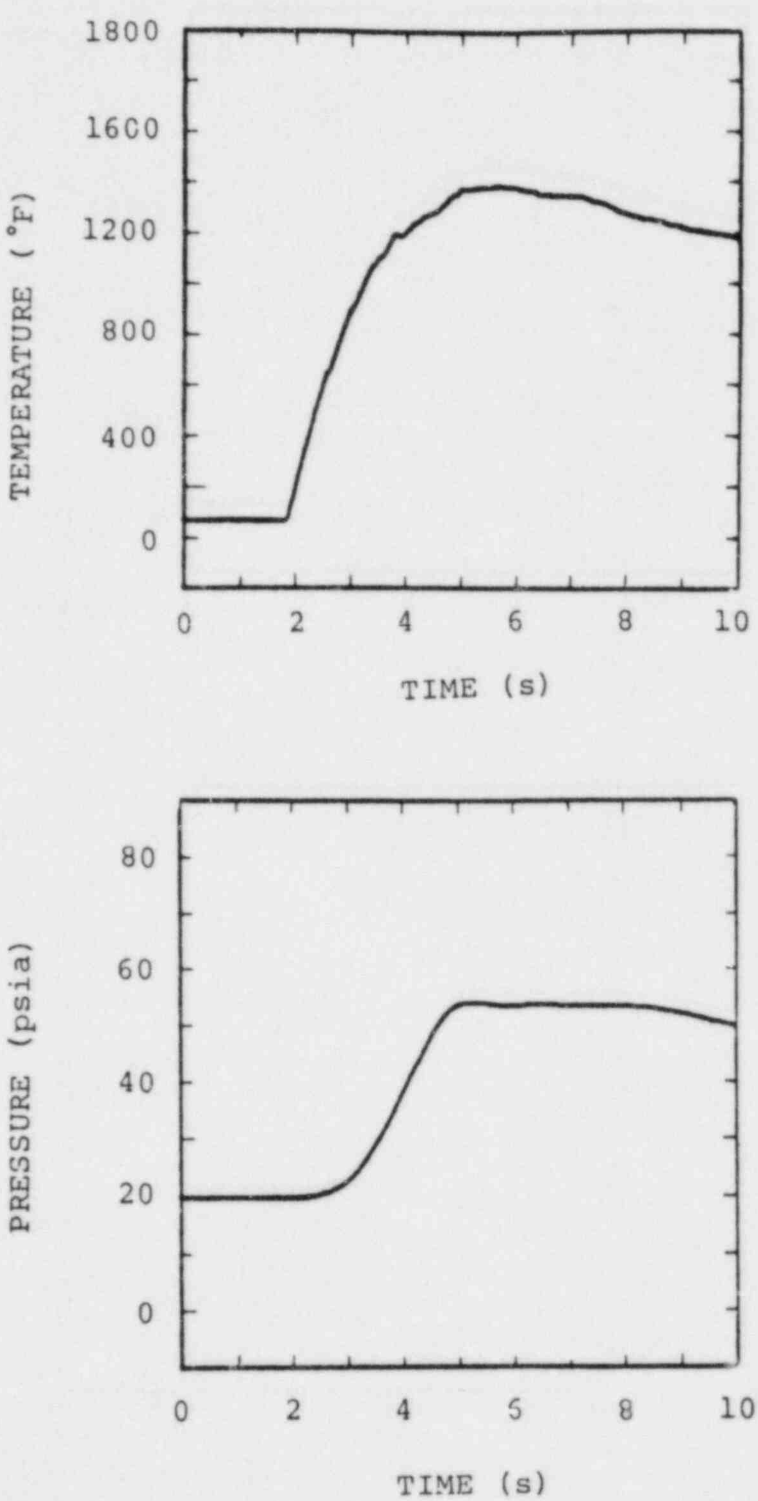

Figure A18. Temperature and Pressure for Test B82H37, 14.29% H_2, 47.62% CO_2, Fans Off

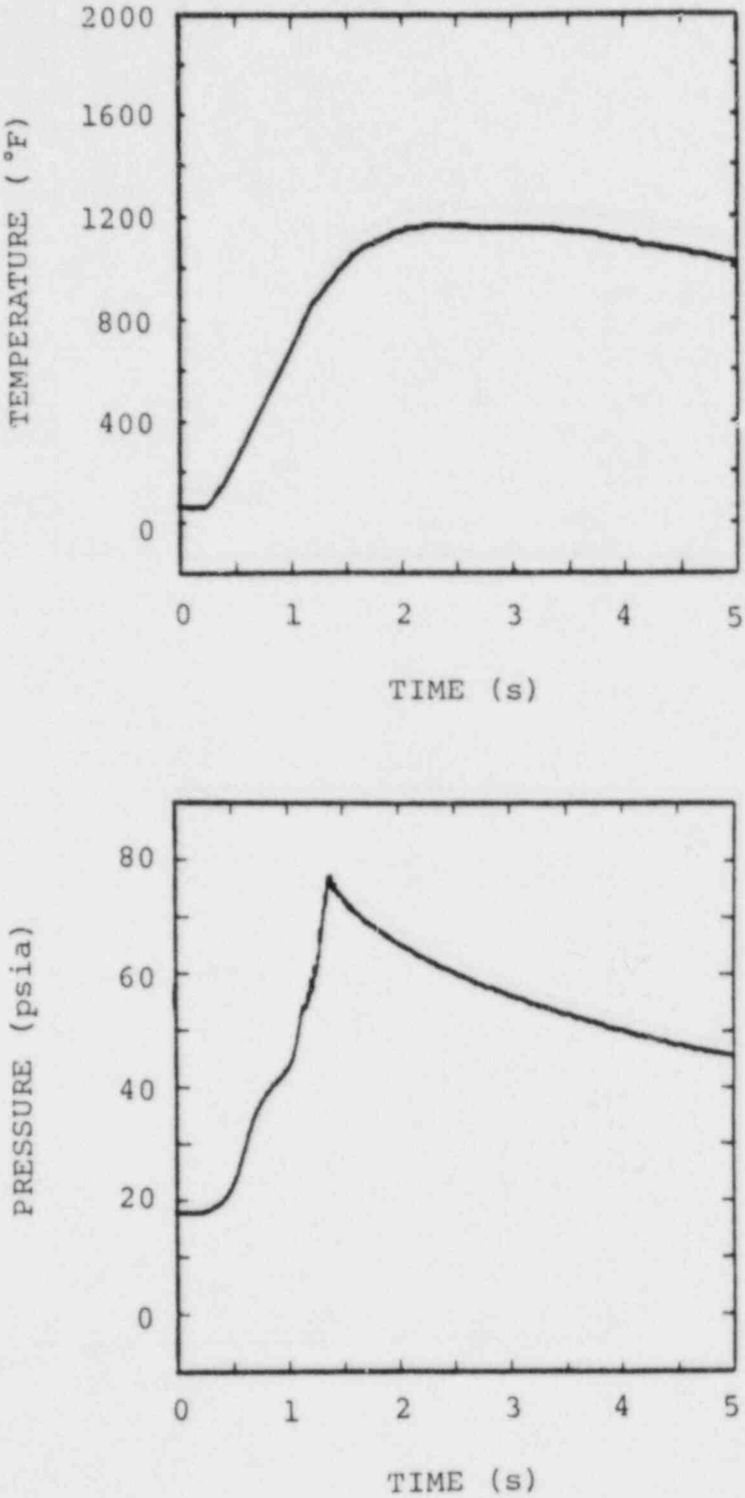

Figure A19. Temperature and Pressure for Test B88H11, 10.29% H_2, Fans Off

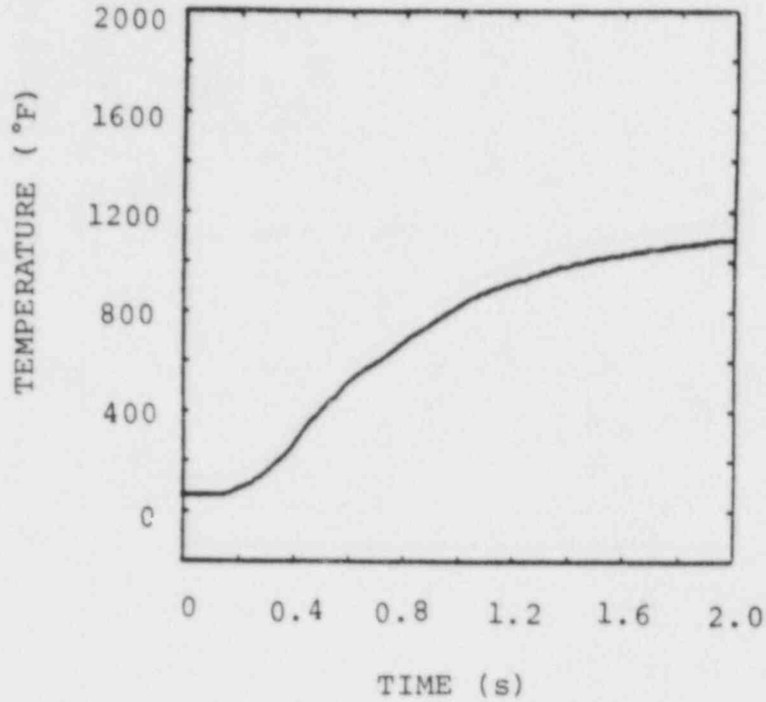

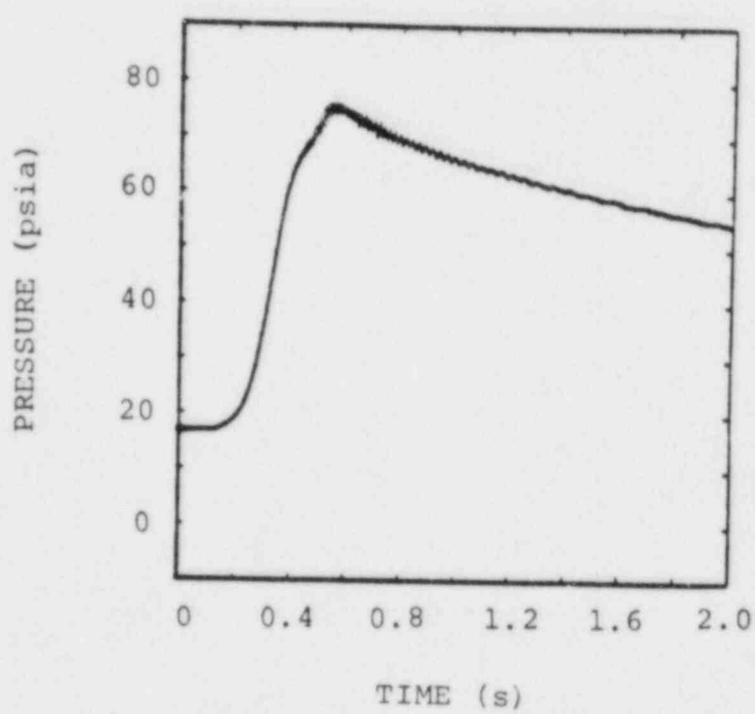

Figure A20. Temperature and Pressure for Test B89H11, 10.47% H_2, Fans On

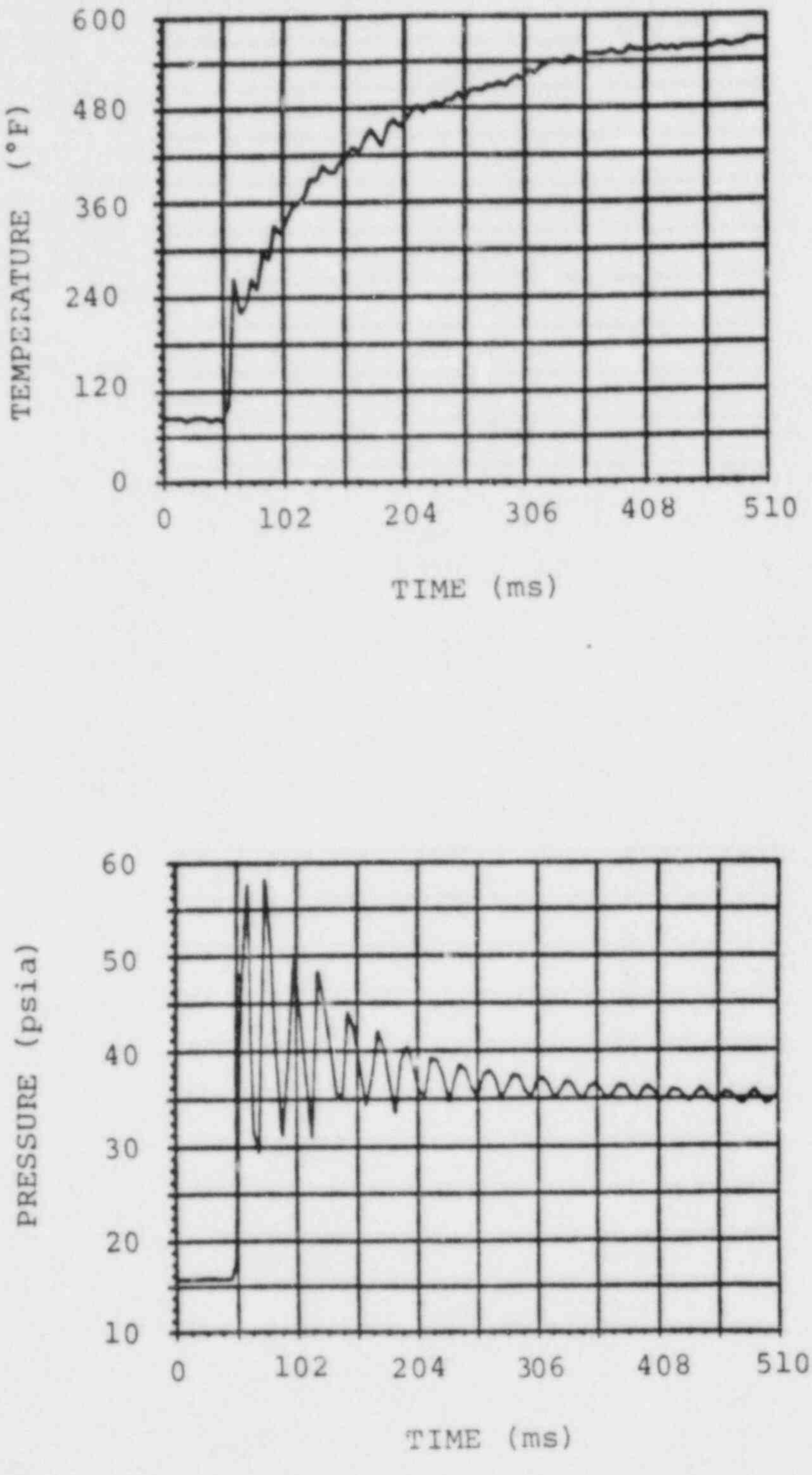

Figure A21. Temperature and Pressure for Test B96F25, 20% H_2, 620:1 Aqueous Foam

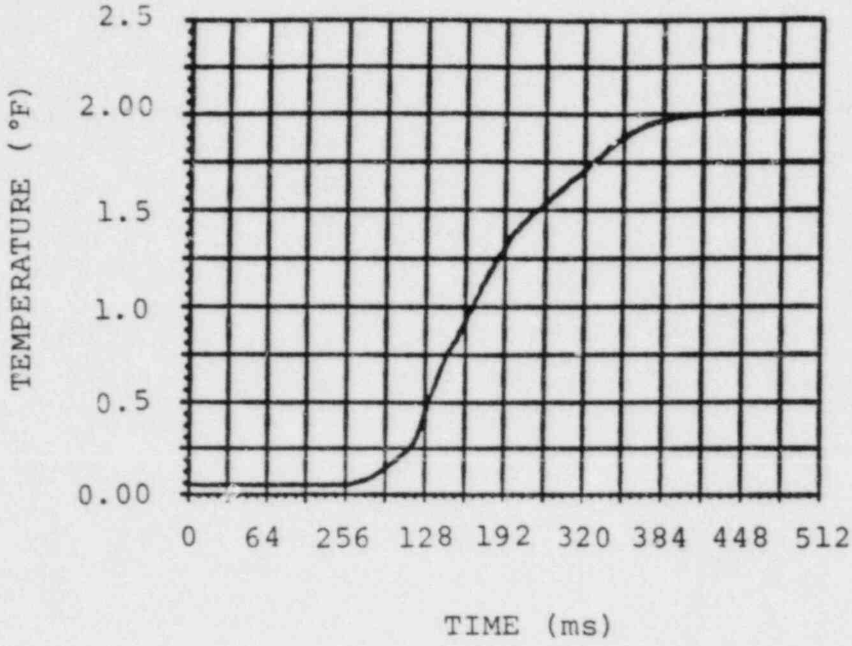

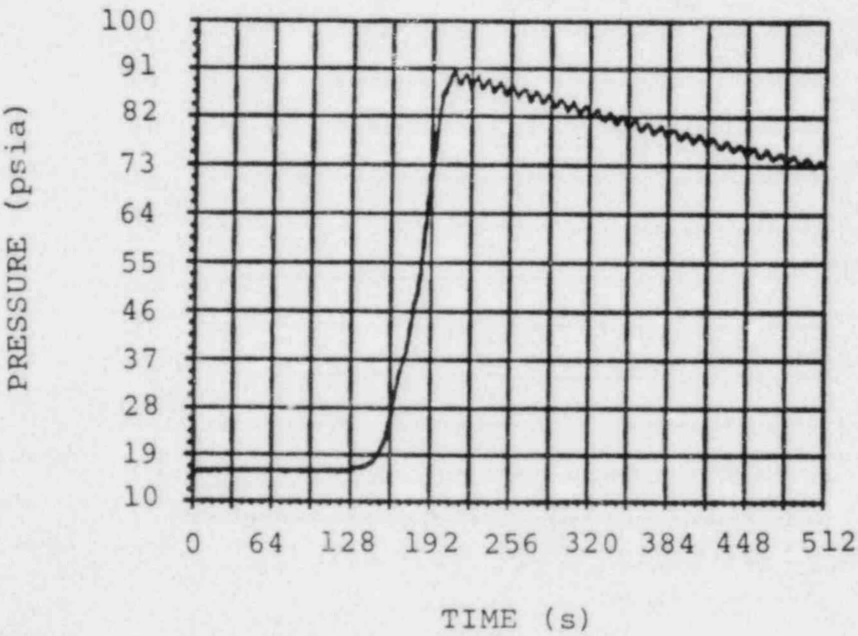

Figure A22. Temperature and Pressure for Test B03H25, 20% H_2, Fans Off

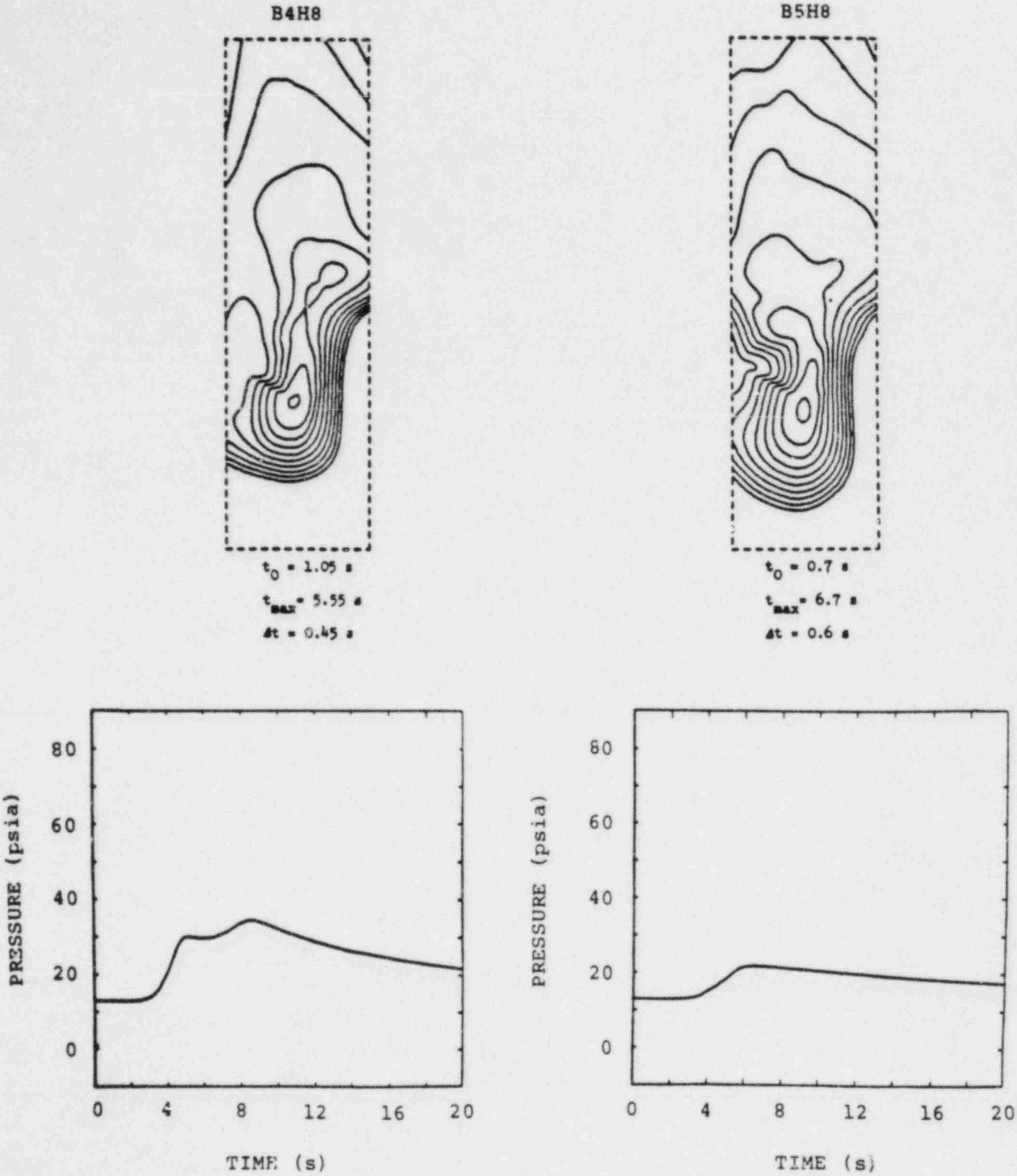
B4H8
t_0 = 1.05 s
t_{max} = 5.55 s
Δt = 0.45 s
B5H8
t_0 = 0.7 s
t_{max} = 6.7 s
Δt = 0.6 s
PRESSURE (psia)
TIME (s)
PRESSURE (psia)
TIME (s)

Figure A23

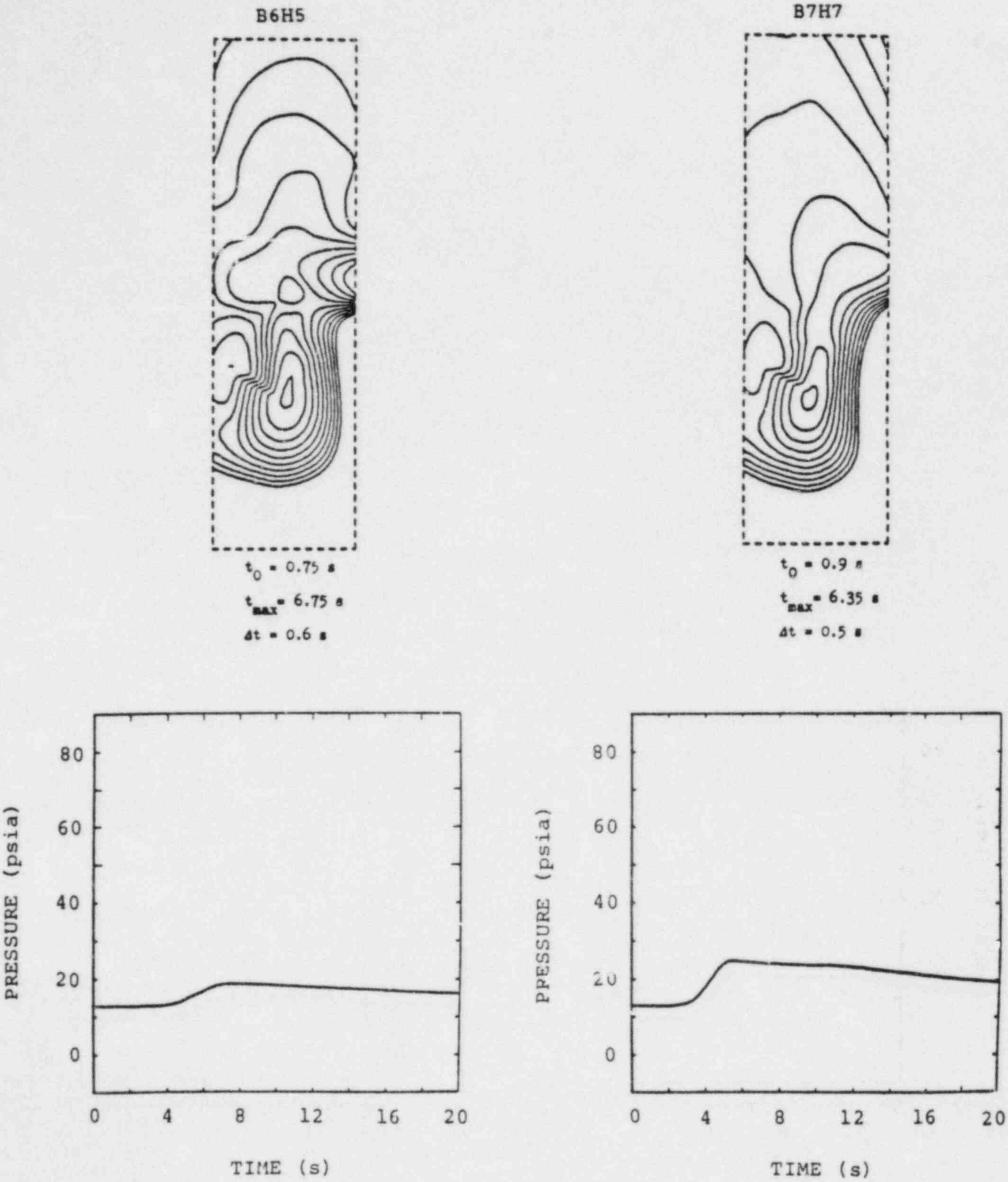
B6H5
B7H7
t0 = 0.75 s
tmax = 6.75 s
Δt = 0.6 s
t0 = 0.9 s
tmax = 6.35 s
Δt = 0.5 s
PRESSURE (psia)
80
60
40
20
0
0
4
8
12
16
20
TIME (s)
PRESSURE (psia)
80
60
40
20
0
0
4
8
12
16
20
TIME (s)

Figure A24

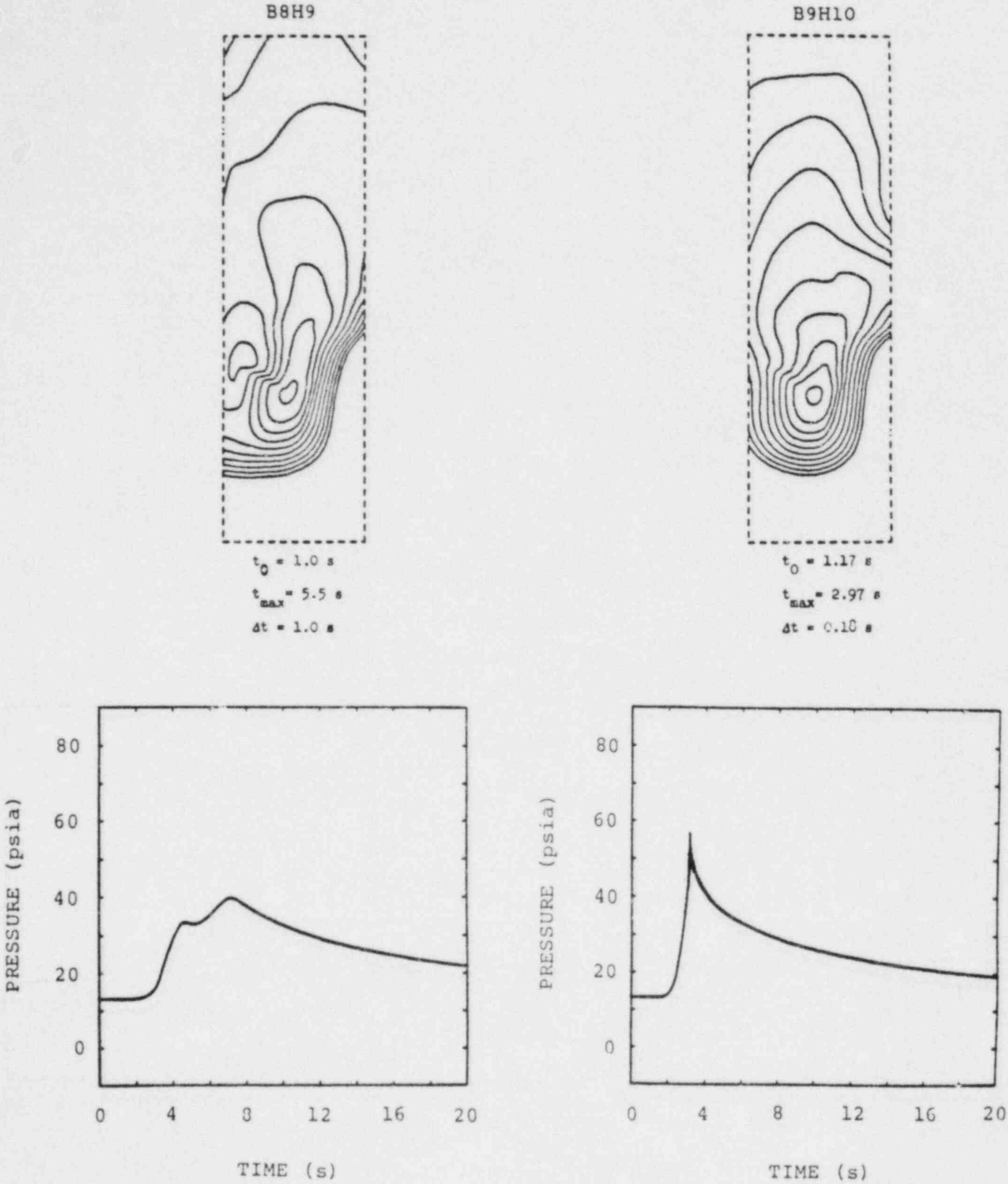
B8H9
B9H10
t_0 = 1.0 s
t_{max} = 5.5 s
Δt = 1.0 s
t_0 = 1.17 s
t_{max} = 2.97 s
Δt = 0.10 s
PRESSURE (psia)
TIME (s)
0
20
40
60
80
4
8
12
16

Figure A25

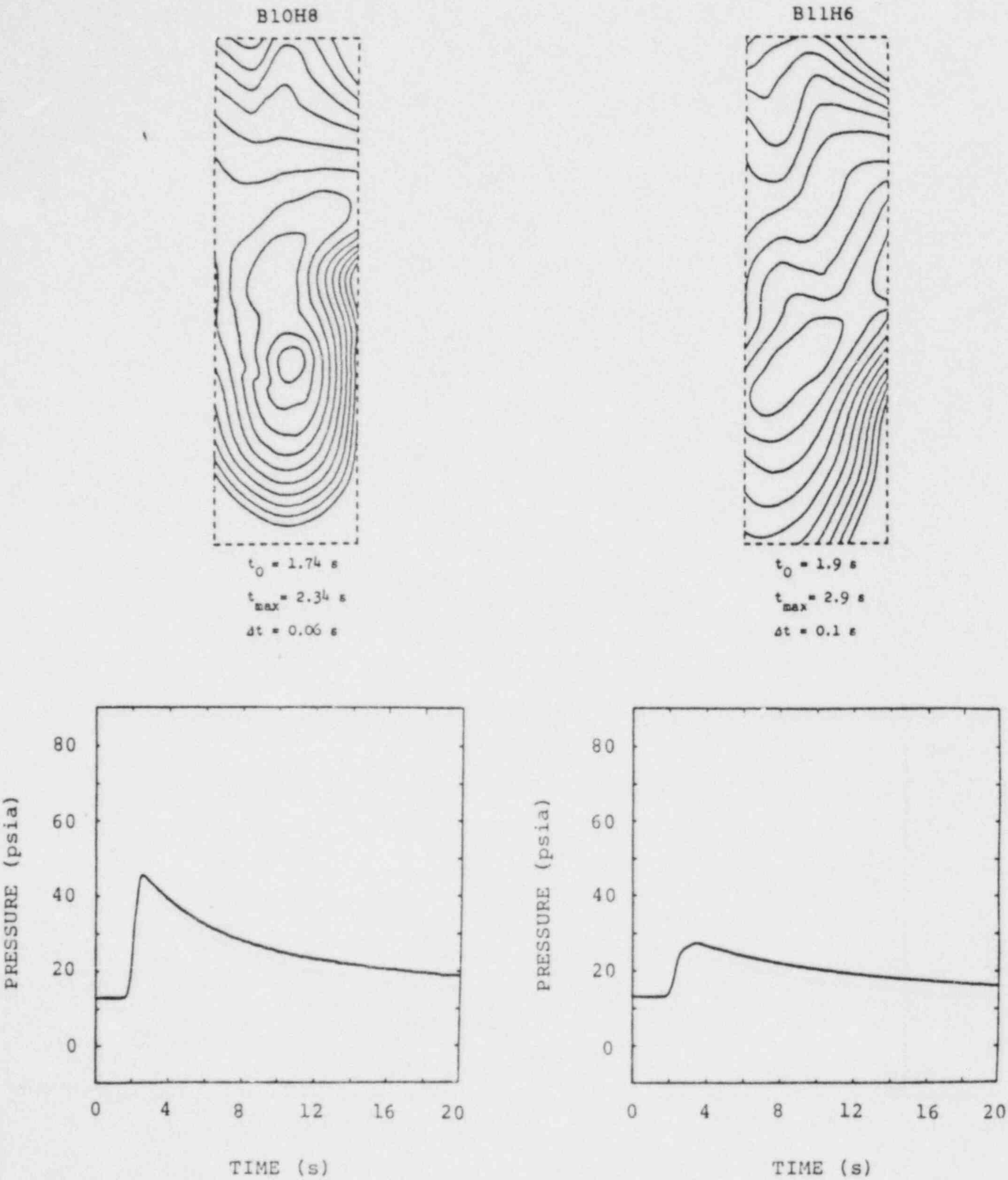
B10H8
t_0 = 1.74 s
t_{max}= 2.34 s
Δt = 0.06 s
B11H6
t_0 = 1.9 s
t_{max}= 2.9 s
Δt = 0.1 s
PRESSURE (psia)
80
60
40
20
0
0 4 8 12 16 20
TIME (s)
PRESSURE (psia)
80
60
40
20
0
0 4 8 12 16 20
TIME (s)

Figure A26

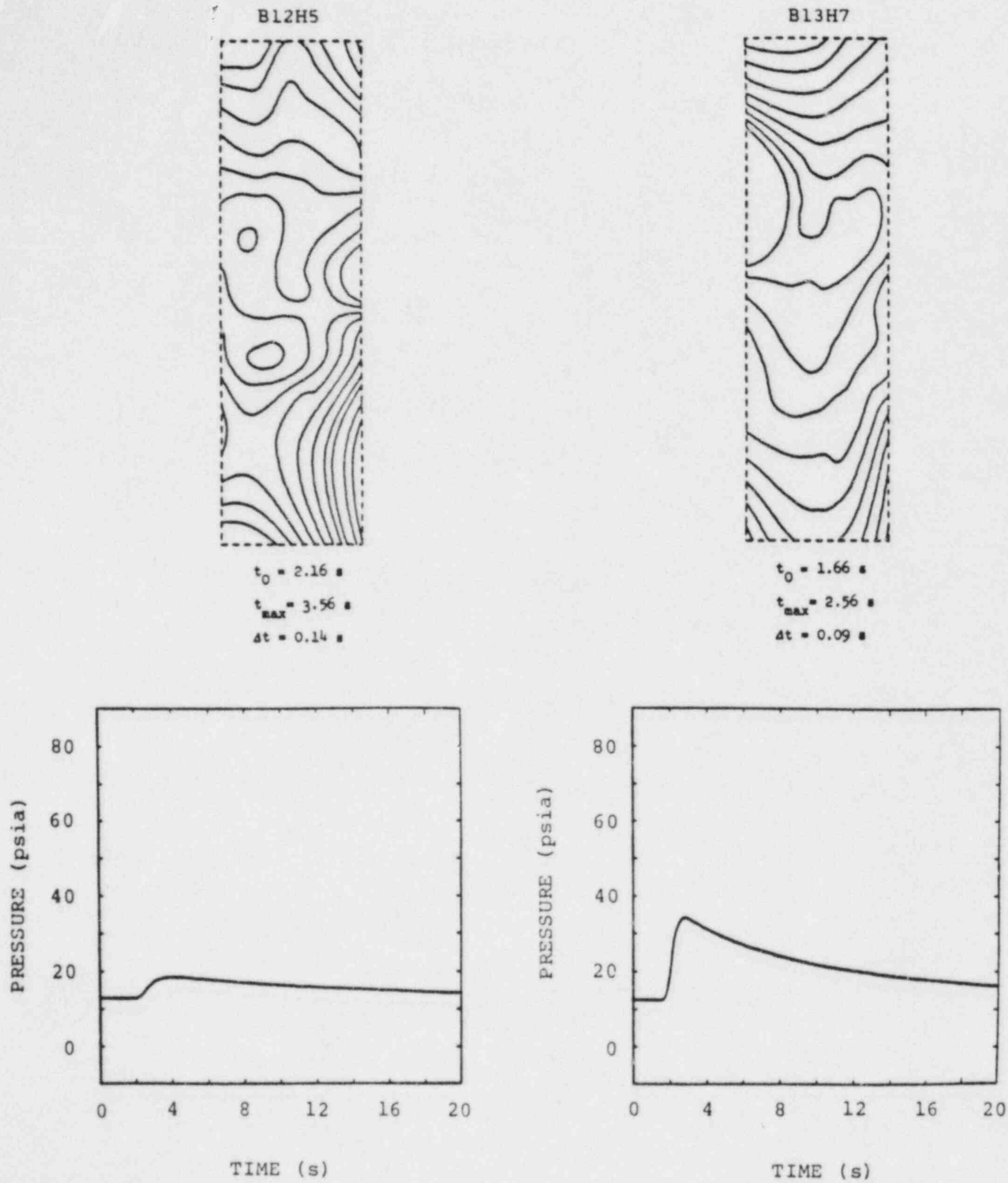
B12H5
B13H7
t0 = 2.16 s
tmax = 3.56 s
Δt = 0.14 s
t0 = 1.66 s
tmax = 2.56 s
Δt = 0.09 s
PRESSURE (psia)
0
20
40
60
80
0
4
8
12
16
20
TIME (s)
PRESSURE (psia)
TIME (s)

Figure A27

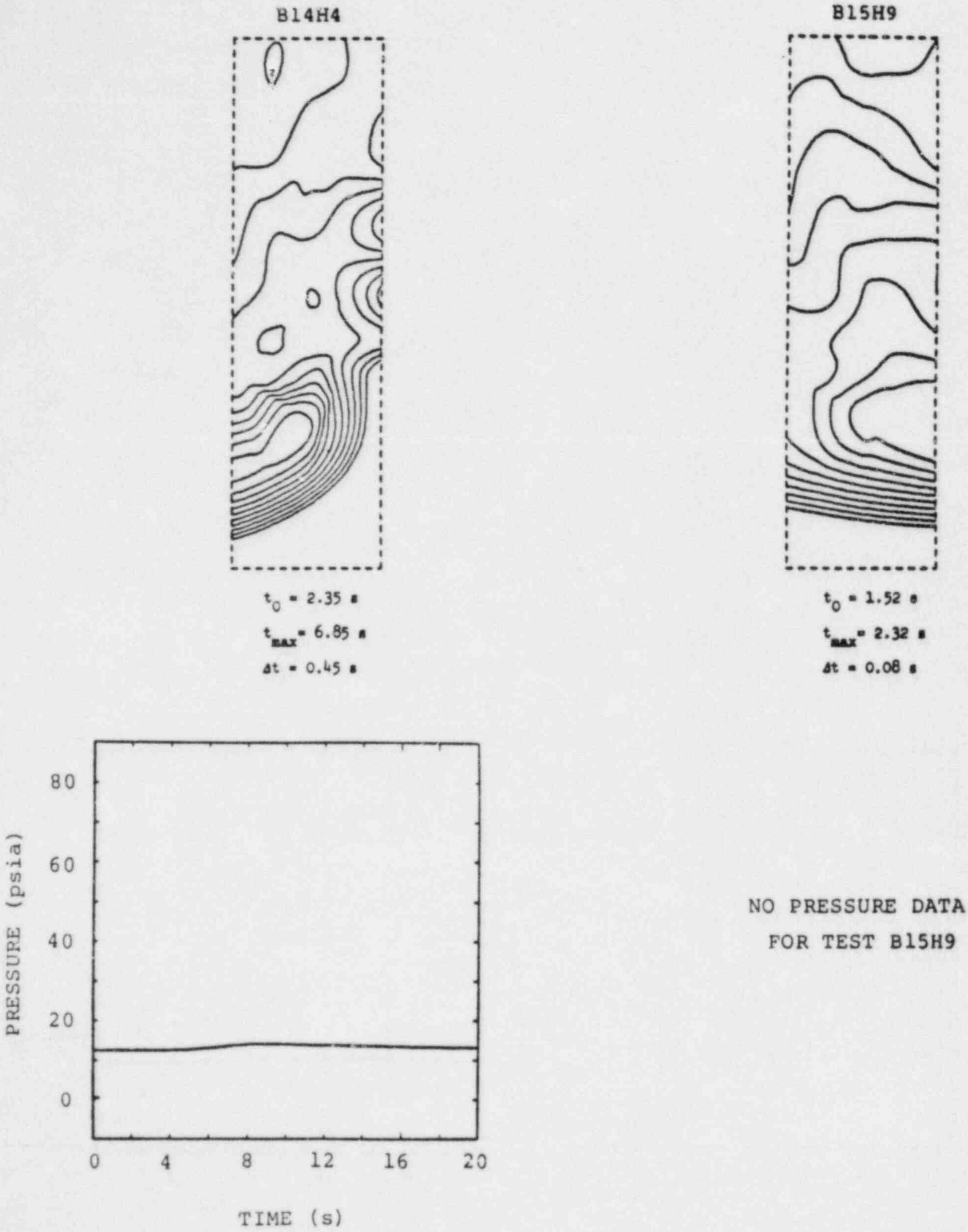
B14H4
t_0 = 2.35 s
t_{max} = 6.85 s
Δt = 0.45 s
B15H9
t_0 = 1.52 s
t_{max} = 2.32 s
Δt = 0.08 s
PRESSURE (psia)
80
60
40
20
0
0
4
8
12
16
20
TIME (s)
NO PRESSURE DATA
FOR TEST B15H9

Figure A28

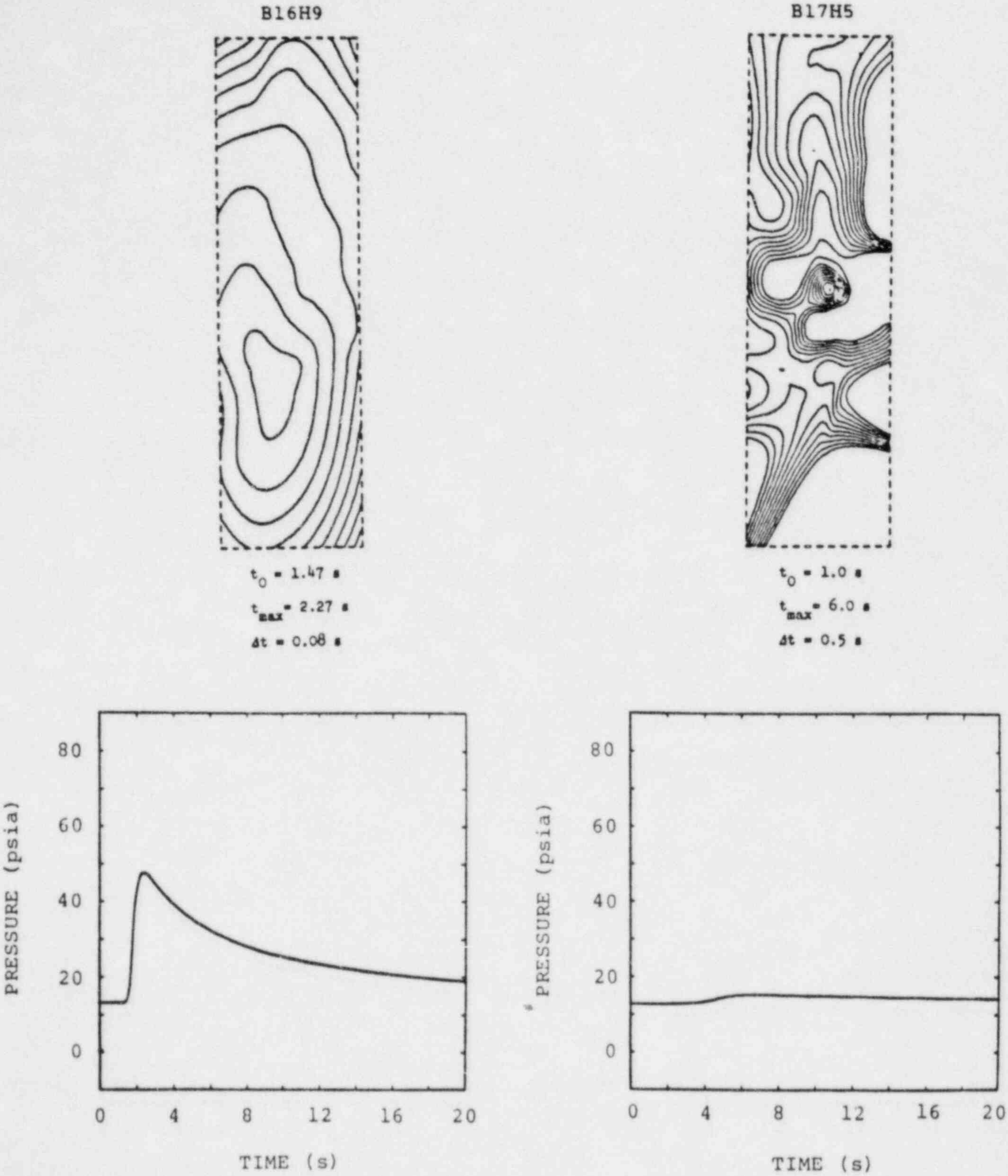
B16H9
t_0 = 1.47 s
t_{max} = 2.27 s
Δt = 0.08 s
B17H5
t_0 = 1.0 s
t_{max} = 6.0 s
Δt = 0.5 s
PRESSURE (psia)
80
60
40
20
0
0
4
8
12
16
20
TIME (s)
PRESSURE (psia)
80
60
40
20
0
0
4
8
12
16
20
TIME (s)

Figure A29

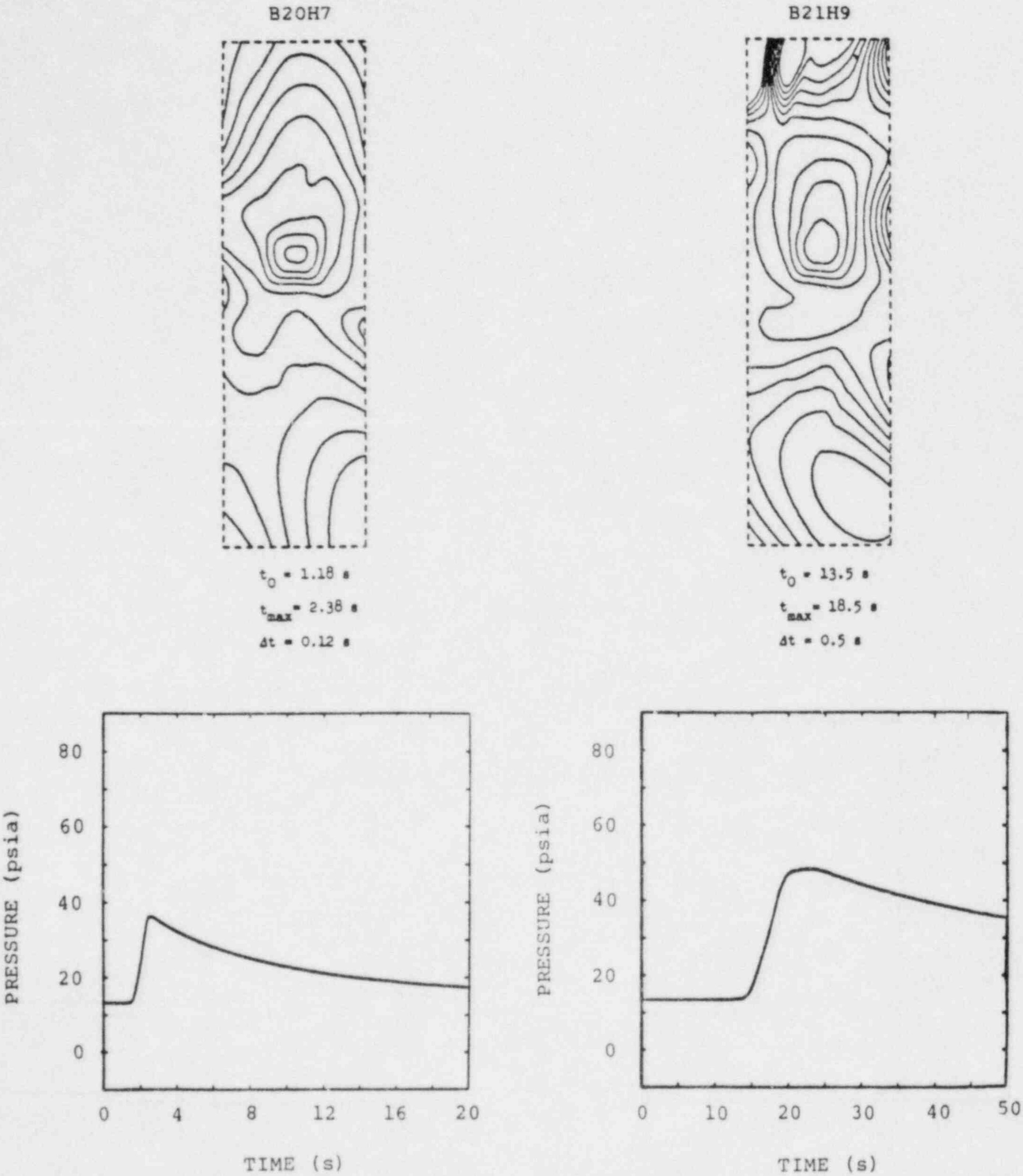
B20H7
t_0 = 1.18 s
t_{max} = 2.38 s
Δt = 0.12 s
B21H9
t_0 = 13.5 s
t_{max} = 18.5 s
Δt = 0.5 s
PRESSURE (psia)
0
20
40
60
80
TIME (s)
0
4
8
12
16
20
PRESSURE (psia)
0
20
40
60
80
TIME (s)
0
10
20
30
40
50

Figure A30

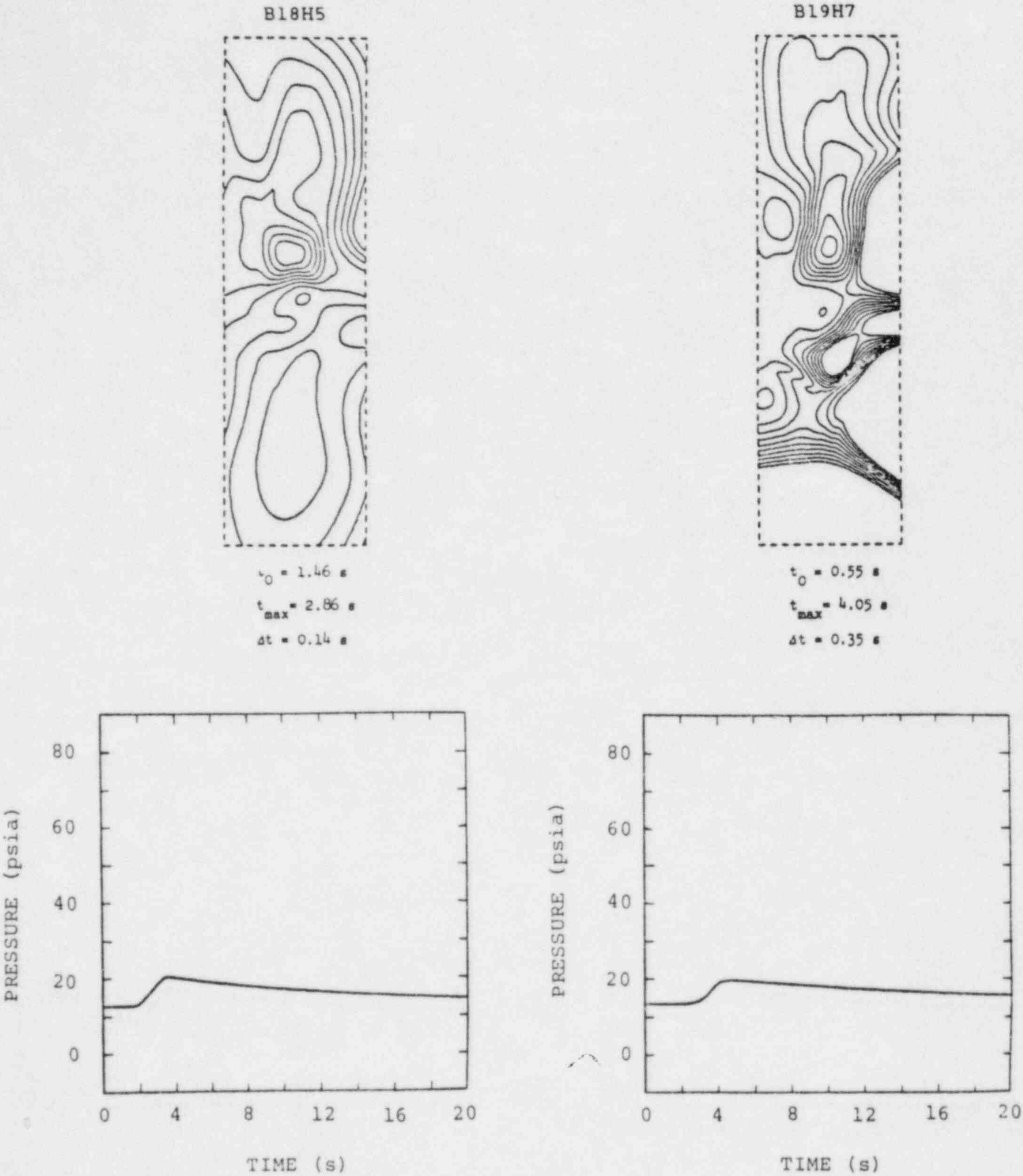
B18H5
t_0 = 1.46 s
t_{max}= 2.86 s
Δt = 0.14 s
B19H7
t_0 = 0.55 s
t_{max}= 4.05 s
Δt = 0.35 s
PRESSURE (psia)
80
60
40
20
0
0
4
8
12
16
20
TIME (s)
PRESSURE (psia)
80
60
40
20
0
0
4
8
12
16
20
TIME (s)

Figure A31

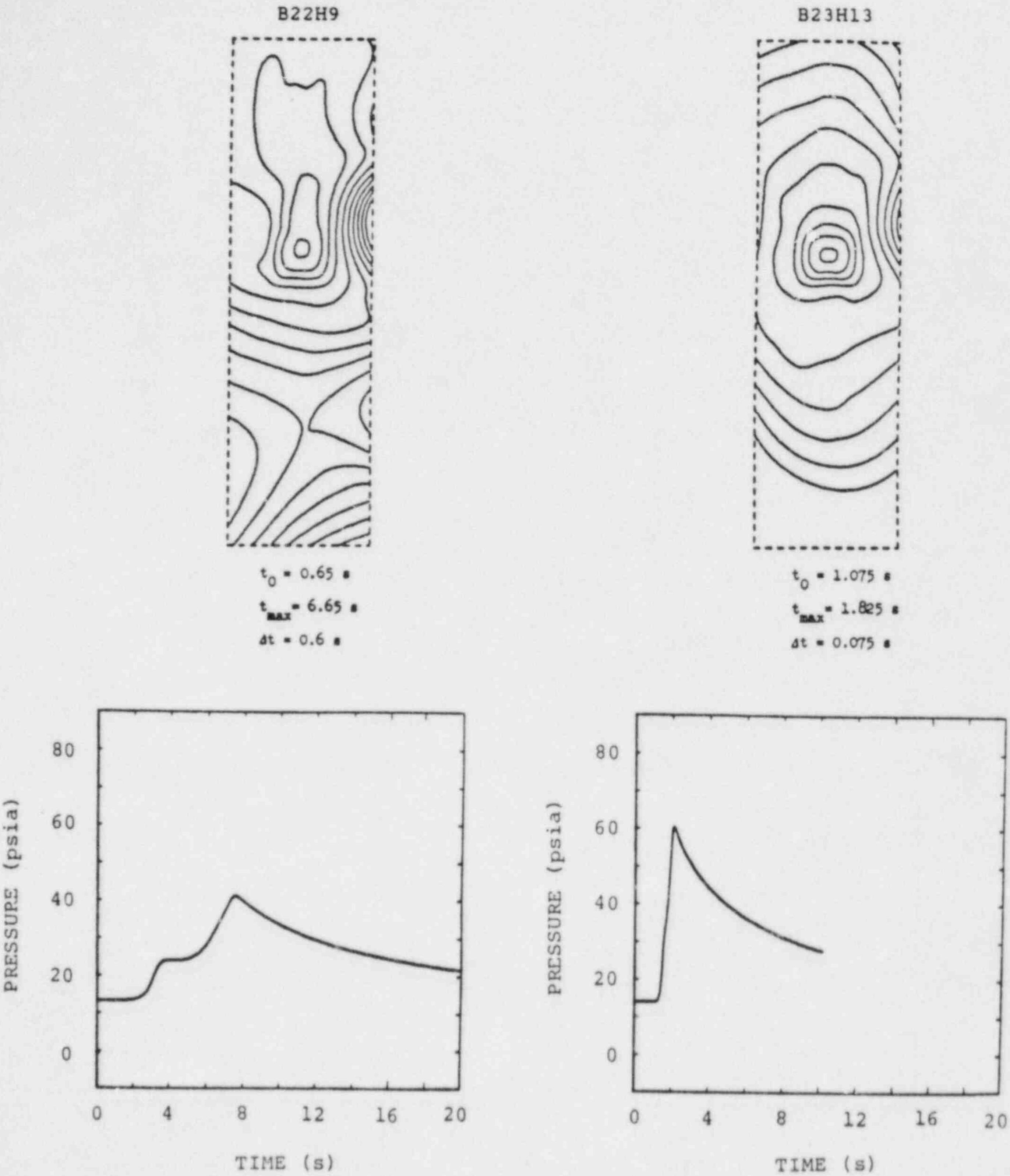
B22H9
B23H13
t_0 = 0.65 s
t_{max} = 6.65 s
Δt = 0.6 s
t_0 = 1.075 s
t_{max} = 1.825 s
Δt = 0.075 s
PRESSURE (psia)
TIME (s)
0
20
40
60
80
0
4
8
12
16
20

Figure A32

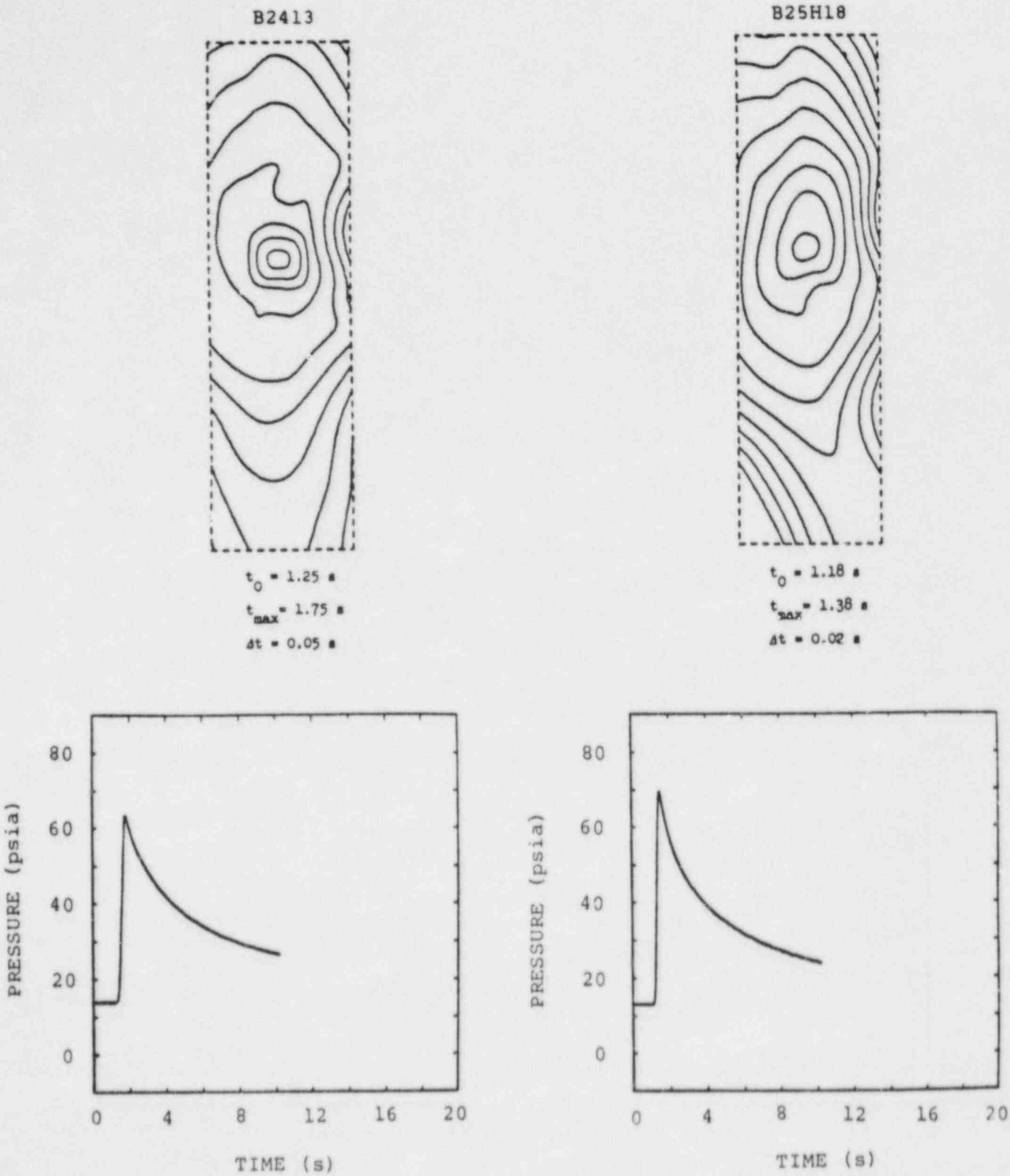
B2413
B25H18
t_0 = 1.25 s
t_{max} = 1.75 s
Δt = 0.05 s
t_0 = 1.18 s
t_{max} = 1.38 s
Δt = 0.02 s
PRESSURE (psia)
TIME (s)
0
4
8
12
16
20
20
40
60
80

Figure A33

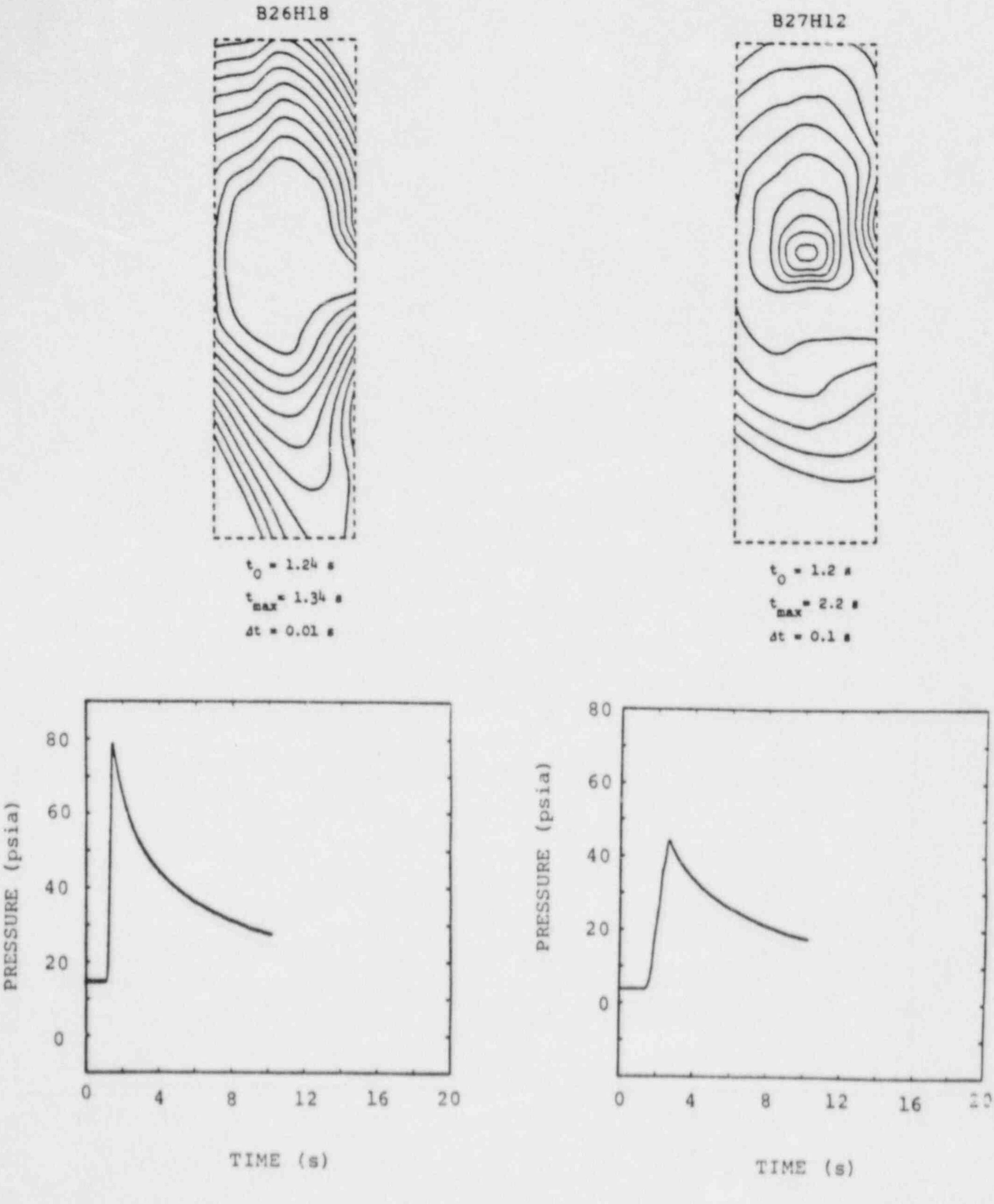
B26H18
t_0 = 1.24 s
t_{max} = 1.34 s
Δt = 0.01 s
B27H12
t_0 = 1.2 s
t_{max} = 2.2 s
Δt = 0.1 s
PRESSURE (psia)
80
60
40
20
0
0
4
8
12
16
20
TIME (s)
PRESSURE (psia)
80
60
40
20
0
0
4
8
12
16
TIME (s)

Figure A34

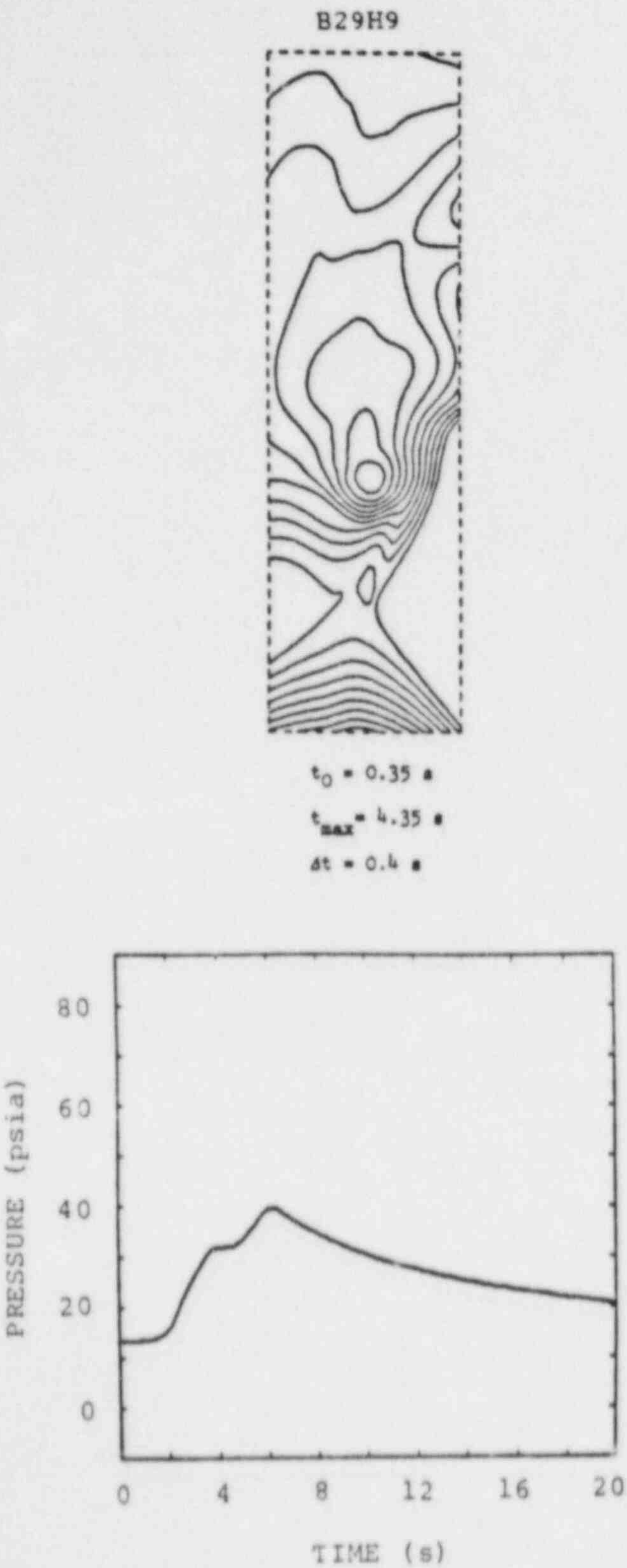
B29H9
t_0 = 0.35 s
t_{max} = 4.35 s
Δt = 0.4 s
PRESSURE (psia)
80
60
40
20
0
0 4 8 12 16 20
TIME (s)

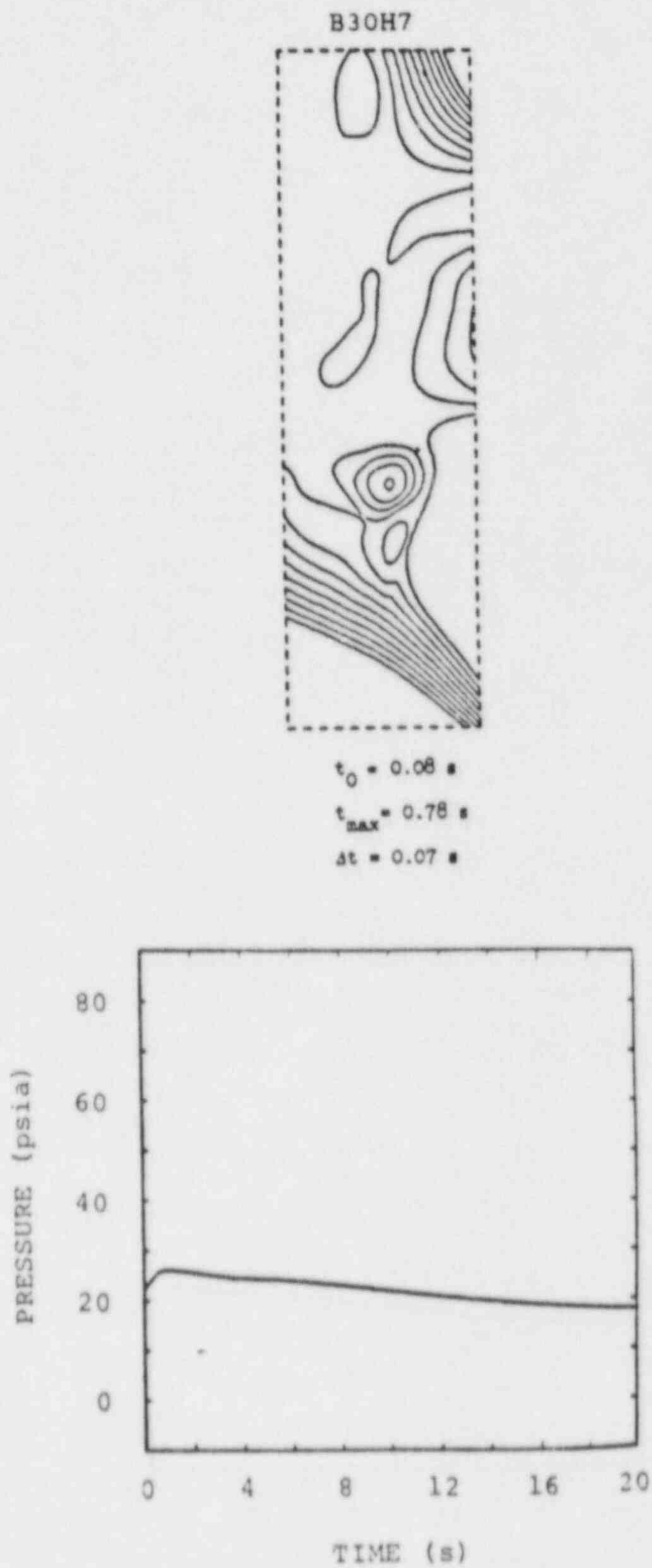
B30H7
t_0 = 0.08 s
t_{max} = 0.78 s
Δt = 0.07 s
PRESSURE (psia)
80
60
40
20
0
0 4 8 12 16 20
TIME (s)

Figure A35

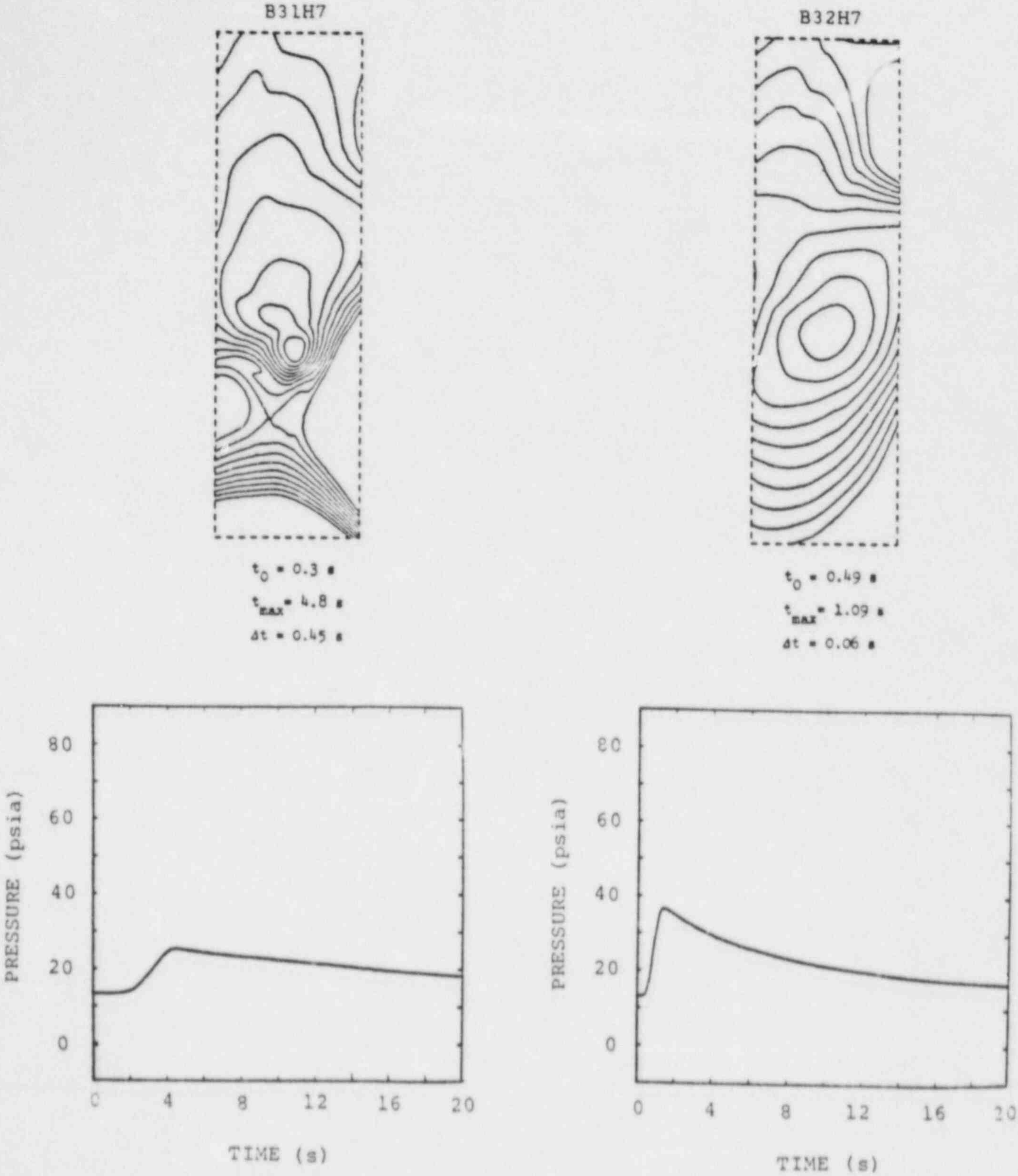

B31H7
t0 = 0.3 s
tmax = 4.8 s
Δt = 0.45 s
B32H7
t0 = 0.49 s
tmax = 1.09 s
Δt = 0.06 s
PRESSURE (psia)
80
60
40
20
0
TIME (s)
0
4
8
12
16
20
PRESSURE (psia)
80
60
40
20
0
TIME (s)
0
4
8
12
16
20

Figure A36

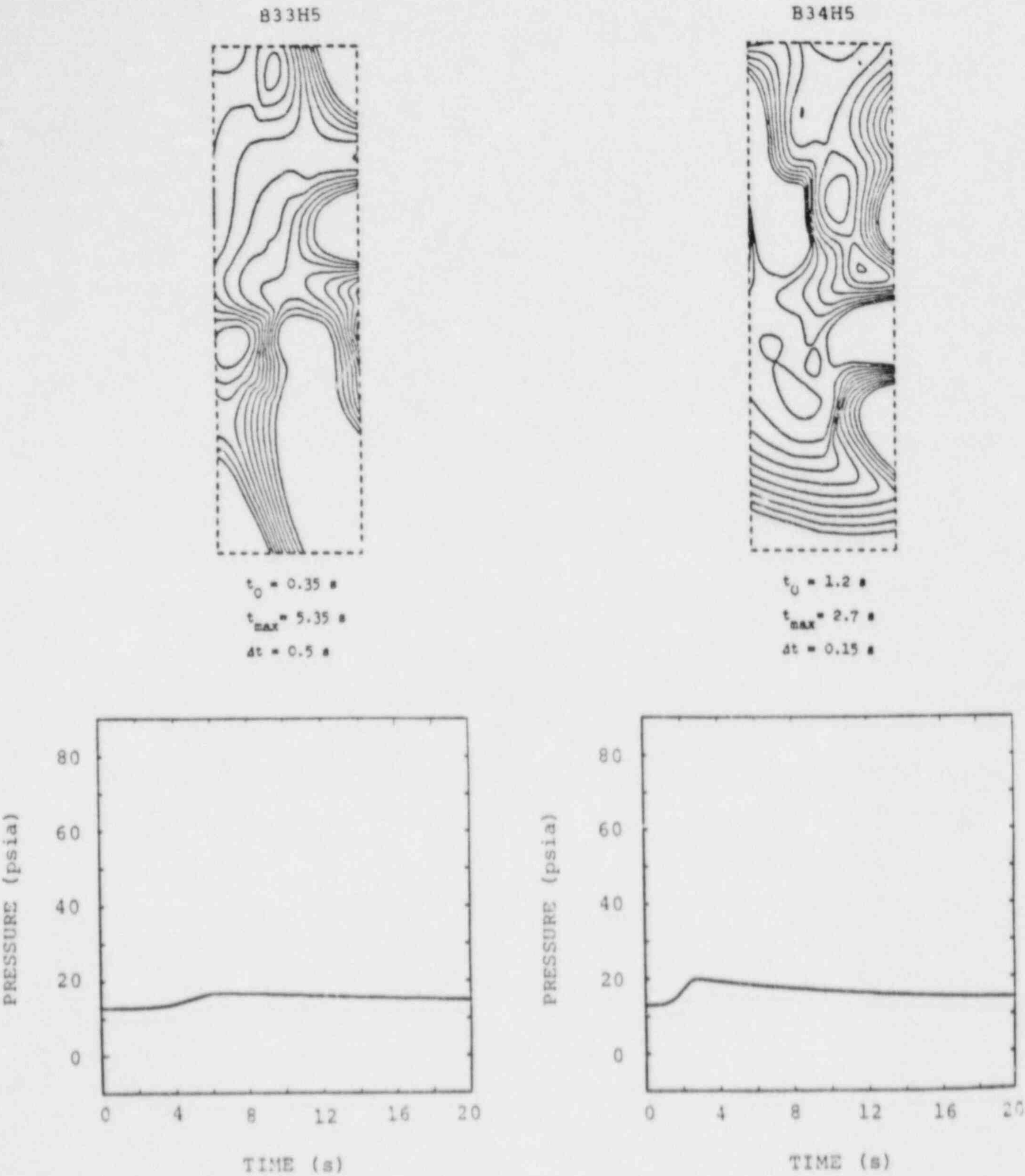
B33H5
B34H5
t_0 = 0.35 s
t_{max} = 5.35 s
Δt = 0.5 s
t_0 = 1.2 s
t_{max} = 2.7 s
Δt = 0.15 s
PRESSURE (psia)
80
60
40
20
0
0 4 8 12 16 20
TIME (s)
PRESSURE (psia)
80
60
40
20
0
0 4 8 12 16 20
TIME (s)

Figure A37

B35H9

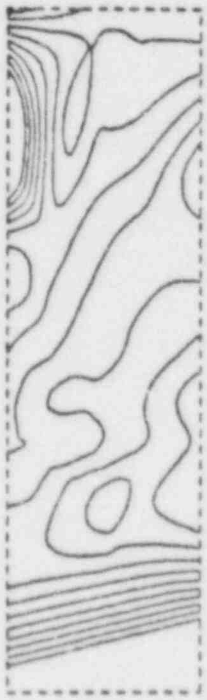

t_0 = 0.28 s

t_{max} = 0.98 s

Δt = 0.07 s

B36H8

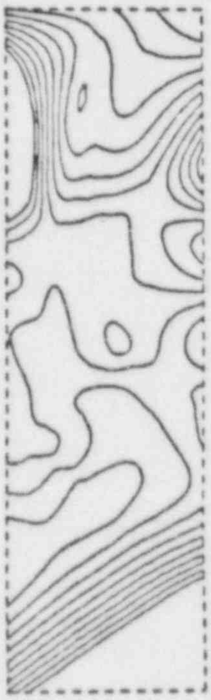

t_0 = 0.67 s

t_{max} = 1.47 s

Δt = 0.08 s

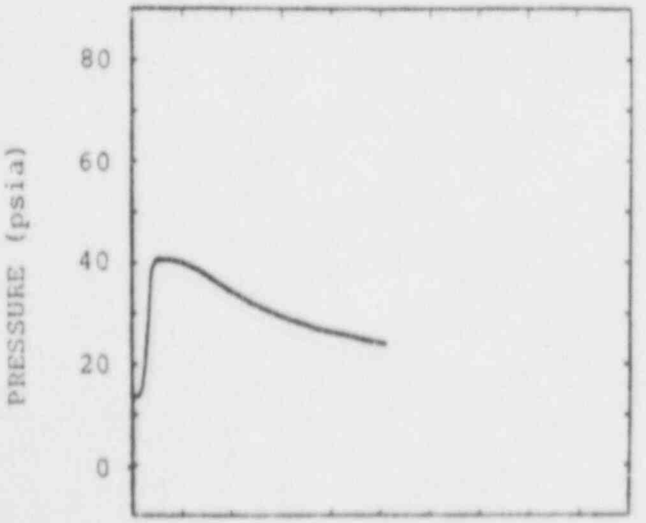

NO PRESSURE DATA
FOR TEST B3[illegible]

Figure A38

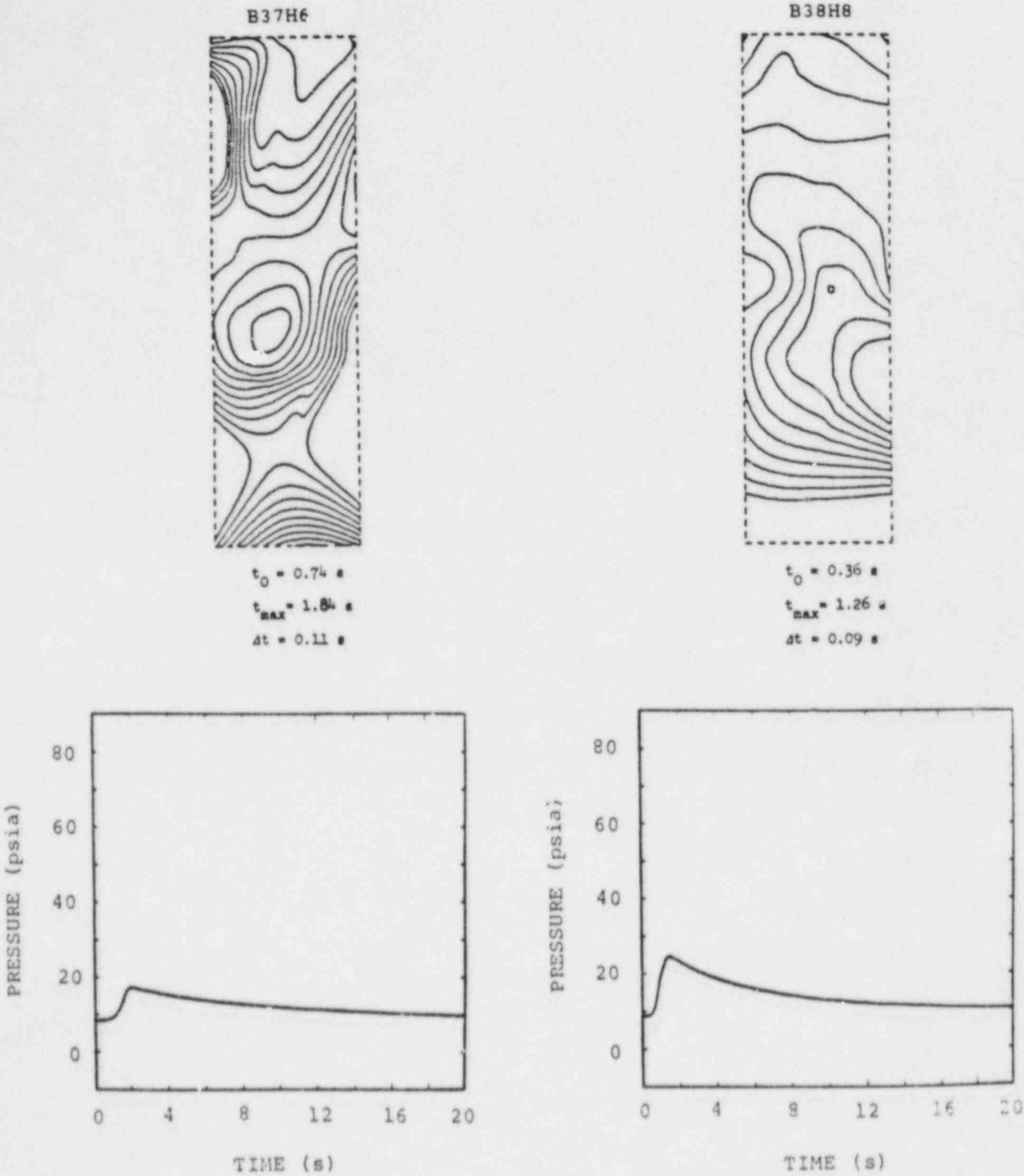
B37H6
B38H8
t_0 = 0.74 s
t_{max} = 1.84 s
Δt = 0.11 s
t_0 = 0.36 s
t_{max} = 1.26 s
Δt = 0.09 s
PRESSURE (psia)
TIME (s)
0
20
40
60
80
4
8
12
16

Figure A39

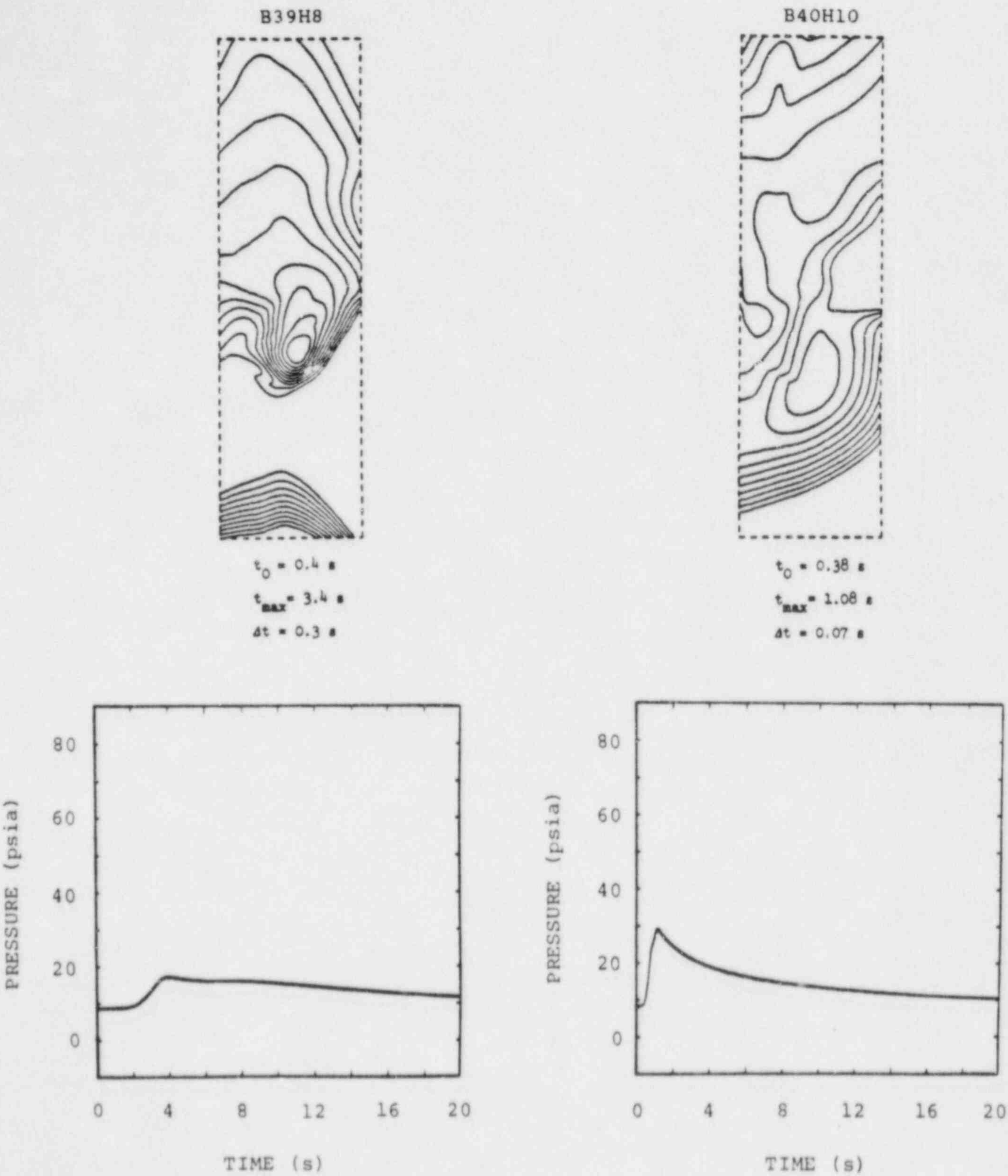

B39H8
B40H10
t_0 = 0.4 s
t_{max} = 3.4 s
Δt = 0.3 s
t_0 = 0.38 s
t_{max} = 1.08 s
Δt = 0.07 s
PRESSURE (psia)
0
20
40
60
80
0
4
8
12
16
20
TIME (s)
PRESSURE (psia)
0
20
40
60
80
0
4
8
12
16
20
TIME (s)

Figure A40

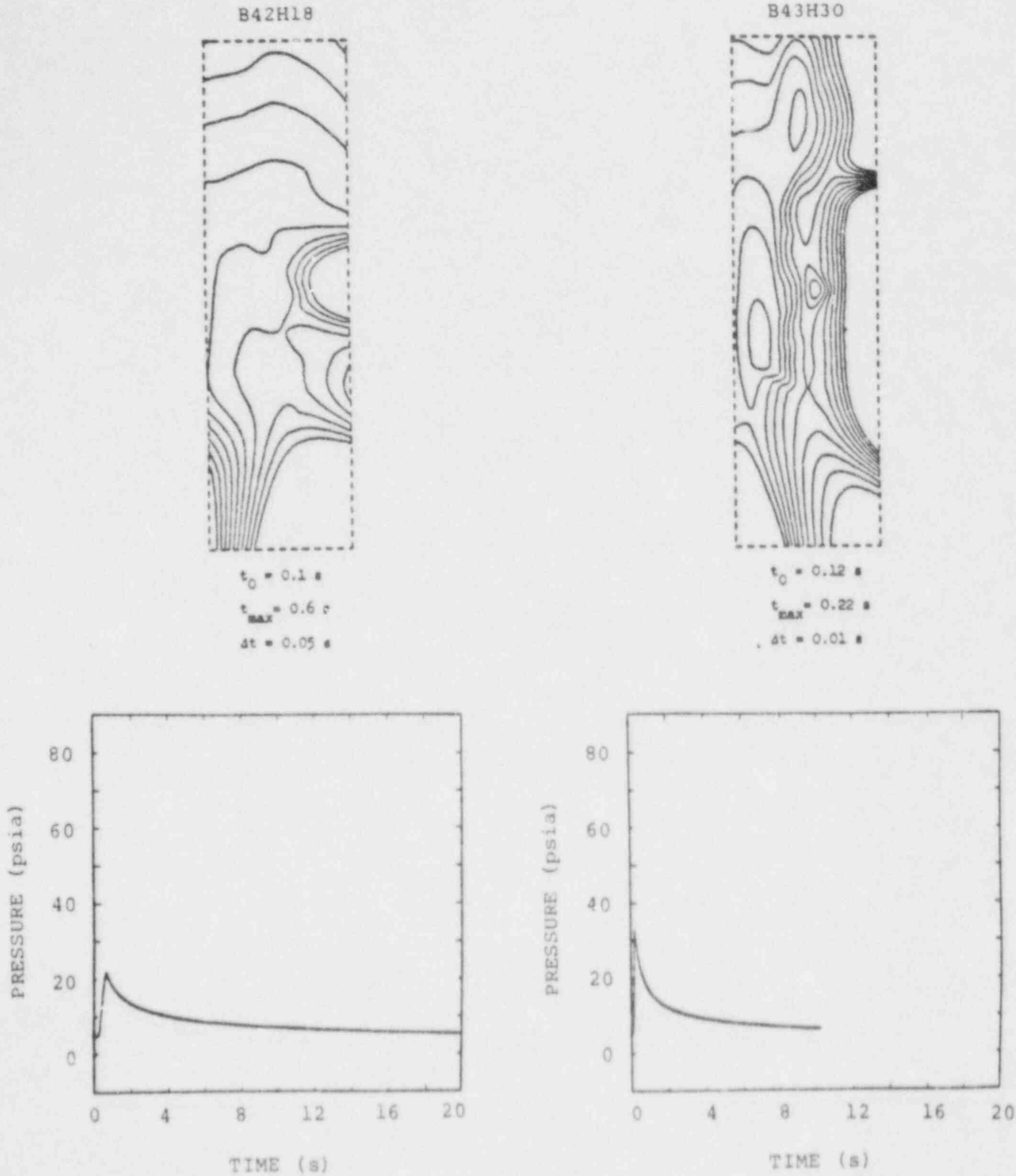
B42H18
B43H30
t0 = 0.1 s
tmax = 0.6 r
dt = 0.05 s
t0 = 0.12 s
tmax = 0.22 s
dt = 0.01 s
PRESSURE (psia)
TIME (s)
80
60
40
20
0
0
4
8
12
16
20
PRESSURE (psia)
TIME (s)
80
60
40
20
0
0
4
8
12
16
20

Figure A41


B44H8
t_0 = 0.38 s
t_{max} = 1.58 s
Δt = 0.12 s

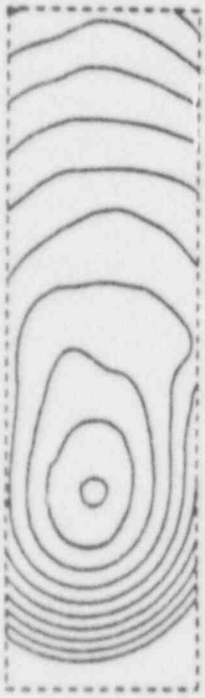
B45H18
t_0 = 0.21 s
t_{max} = 0.61 s
Δt = 0.04 s

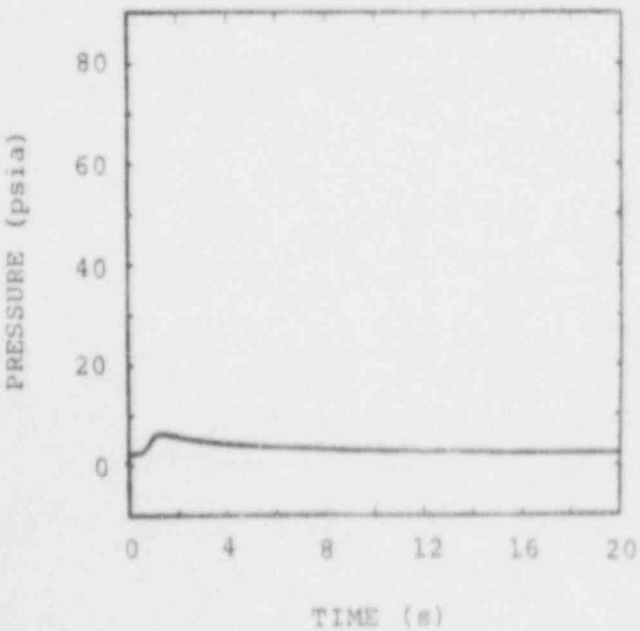
80
60
40
20
0
PRESSURE (psia)
0
4
8
12
16
20
TIME (s)

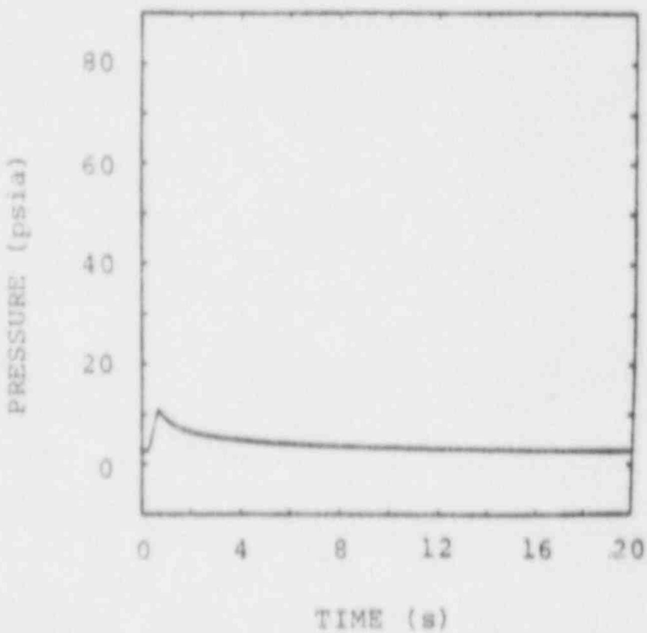
80
60
40
20
0
PRESSURE (psia)
0
4
8
12
16
20
TIME (s)

Figure A42

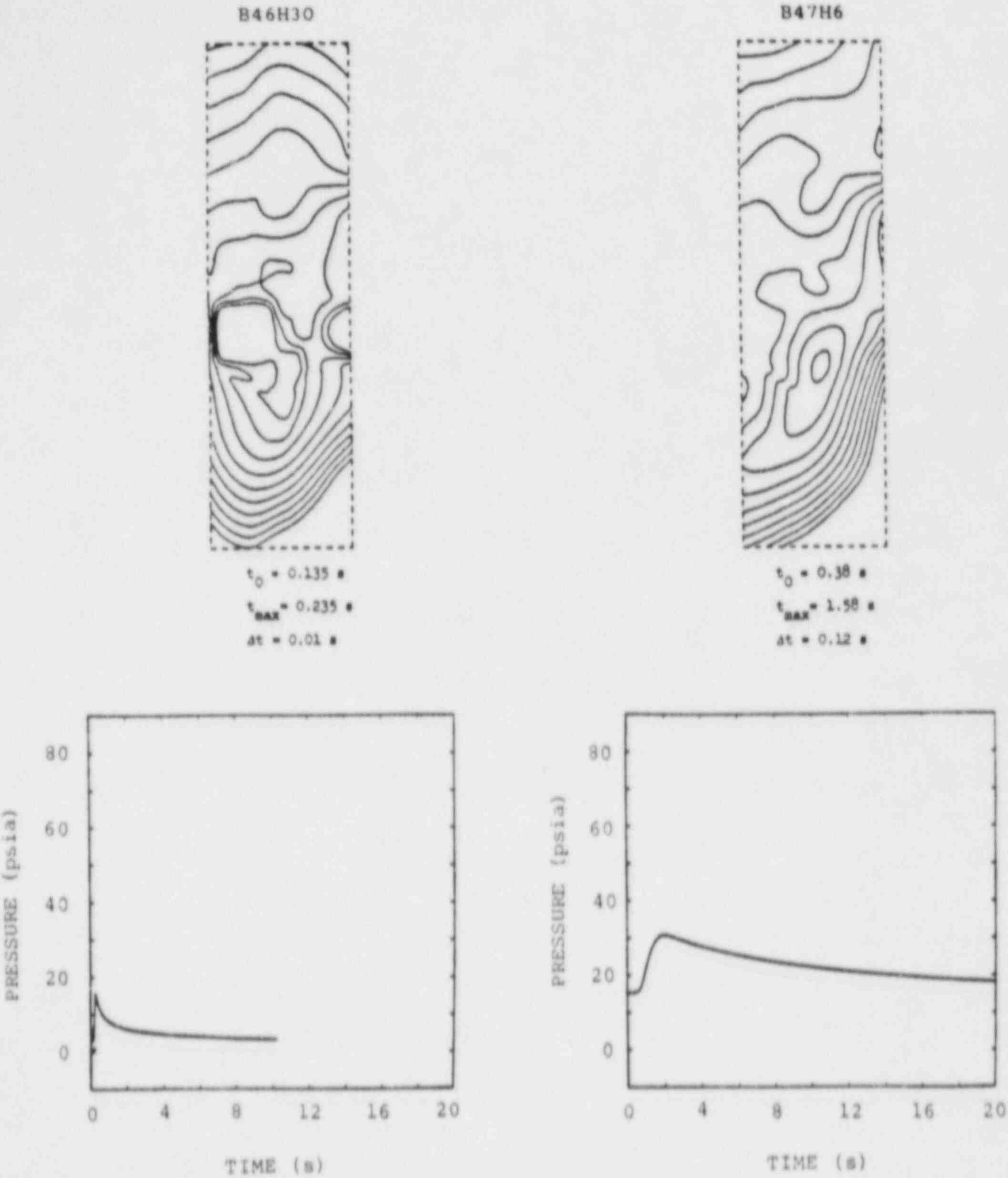
B46H30
B47H6
t0 = 0.135 s
tmax = 0.235 s
Δt = 0.01 s
t0 = 0.38 s
tmax = 1.58 s
Δt = 0.12 s
PRESSURE (psia)
80
60
40
20
0
0
4
8
12
16
20
TIME (s)
PRESSURE (psia)
80
60
40
20
0
0
4
8
12
16
20
TIME (s)

Figure A43

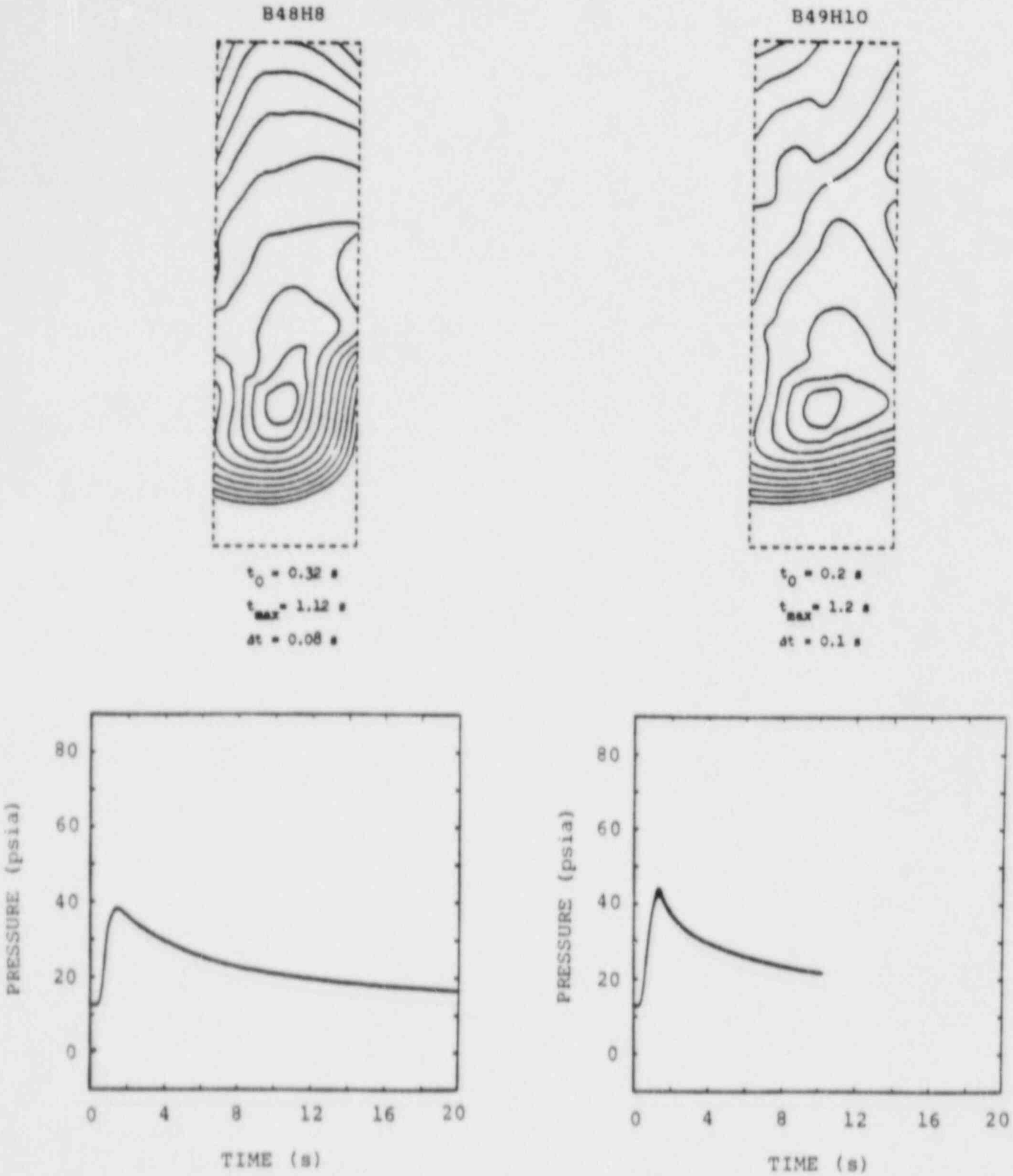
B48H8
B49H10
t_0 = 0.32 s
t_{max} = 1.12 s
dt = 0.08 s
t_0 = 0.2 s
t_{max} = 1.2 s
dt = 0.1 s
PRESSURE (psia)
80
60
40
20
0
0
4
8
12
16
20
TIME (s)

Figure A44

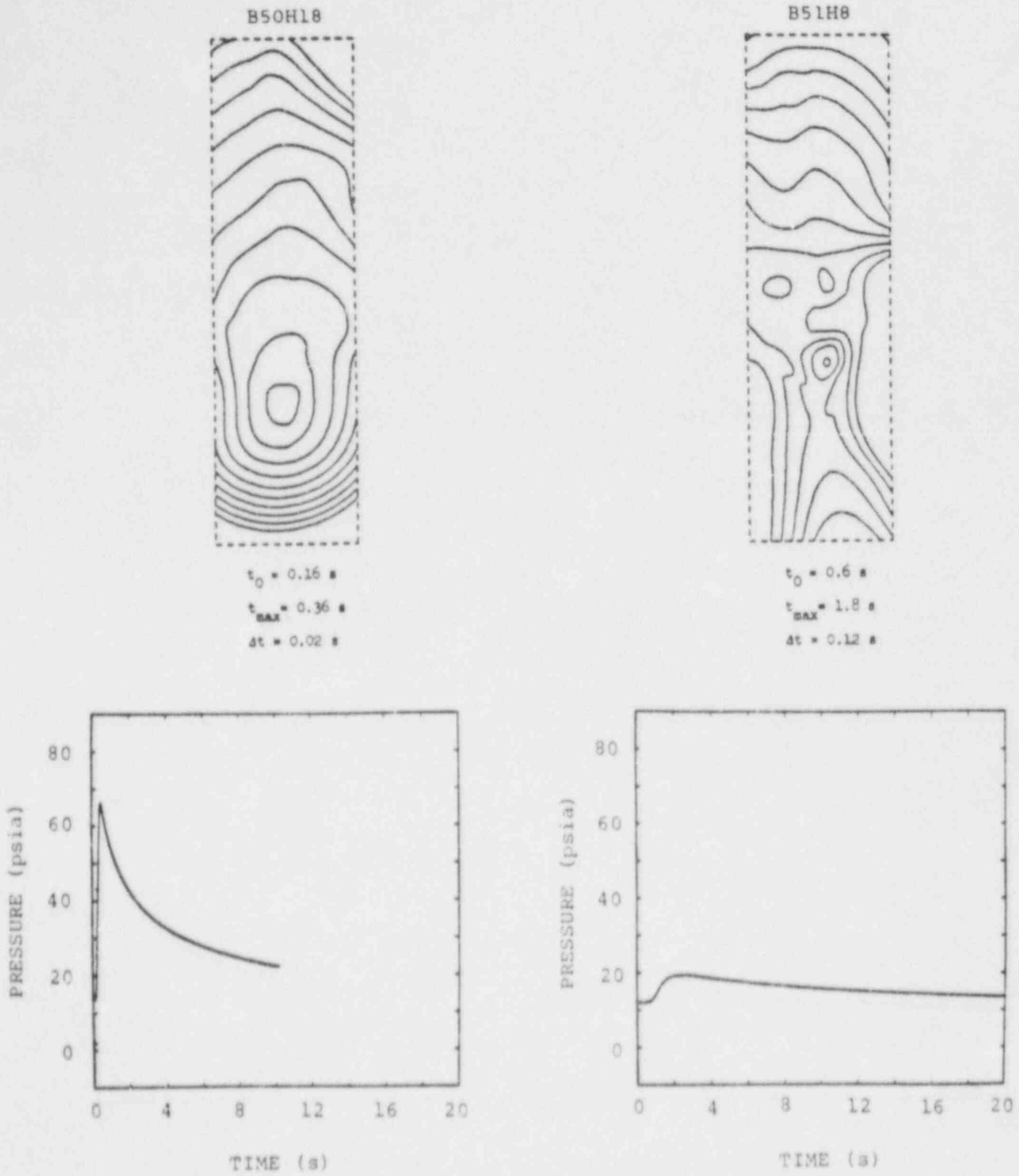

B50H18
t_0 = 0.16 s
t_{max} = 0.36 s
Δt = 0.02 s
B51H8
t_0 = 0.6 s
t_{max} = 1.8 s
Δt = 0.12 s
PRESSURE (psia)
TIME (s)
0
20
40
60
80
0
4
8
12
16
20

Figure A45

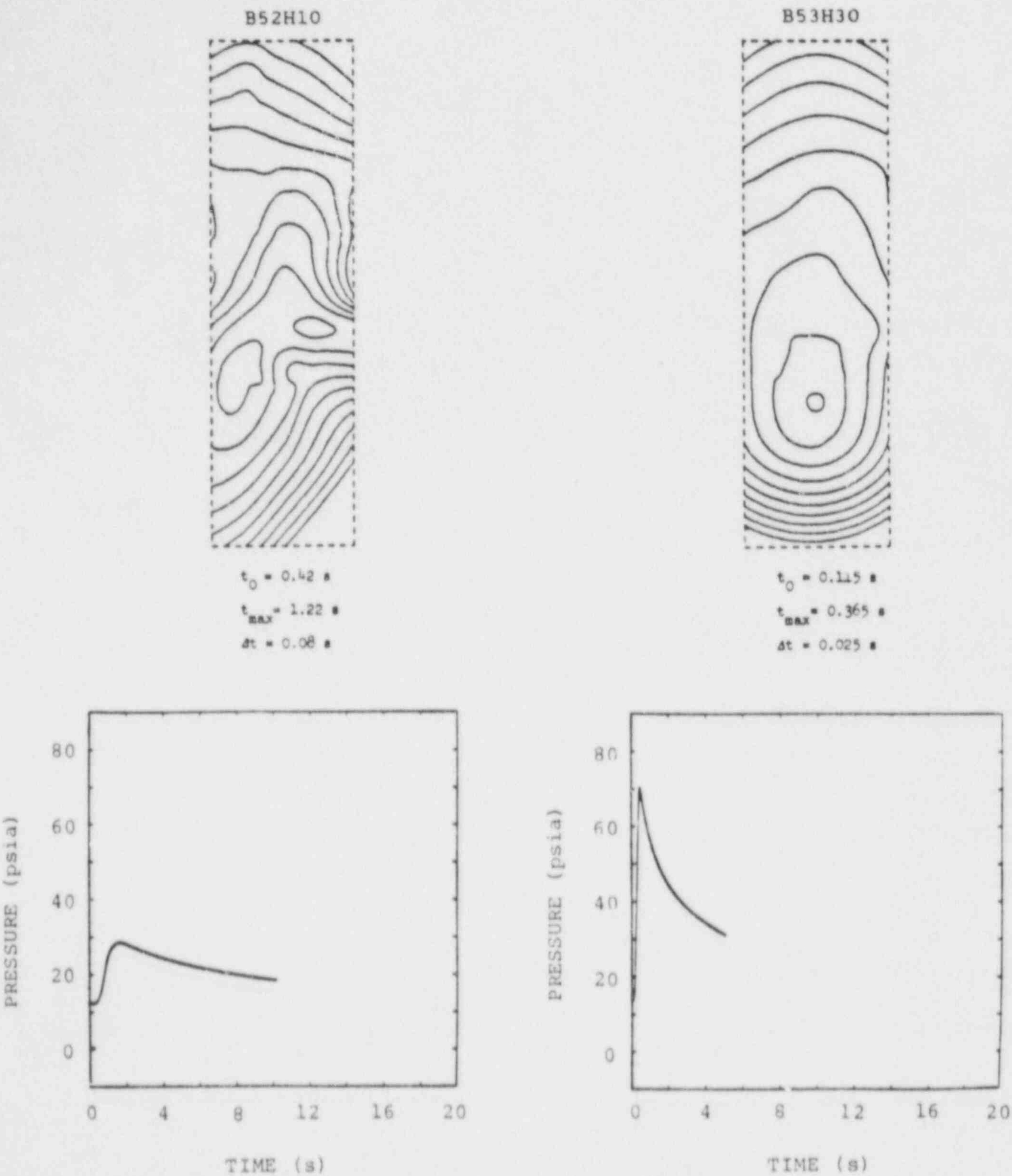
B52H10
B53H30
t0 = 0.42 s
tmax = 1.22 s
Δt = 0.08 s
t0 = 0.115 s
tmax = 0.365 s
Δt = 0.025 s
PRESSURE (psia)
80
60
40
20
0
0
4
8
12
16
20
TIME (s)
PRESSURE (psia)
80
60
40
20
0
0
4
8
12
16
20
TIME (s)

Figure A46

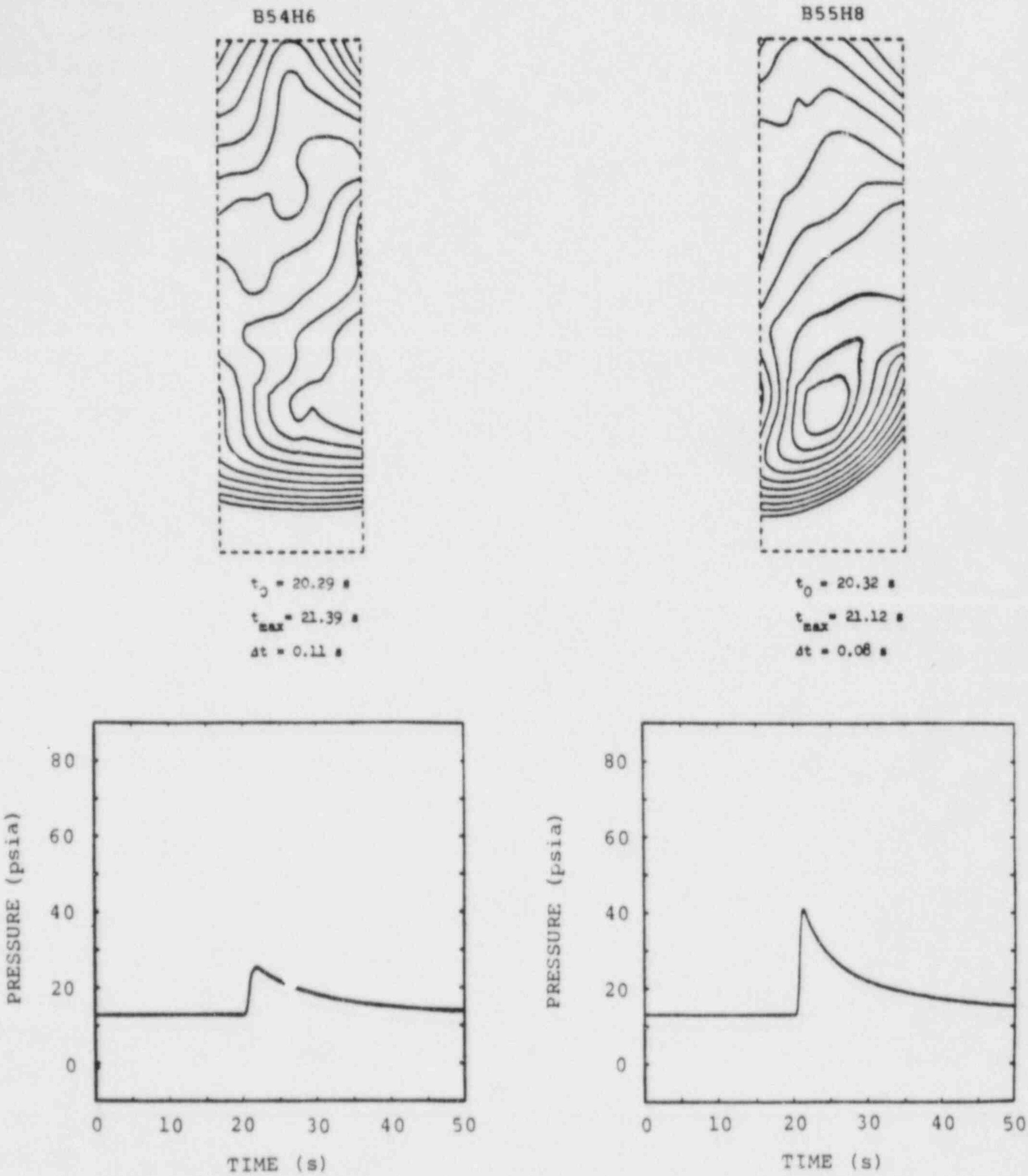
B54H6
B55H8
t_0 = 20.29 s
t_{max} = 21.39 s
Δt = 0.11 s
t_0 = 20.32 s
t_{max} = 21.12 s
Δt = 0.08 s
PRESSURE (psia)
TIME (s)
0
20
40
60
80
10
30
50
PRESSURE (psia)
TIME (s)

Figure A47

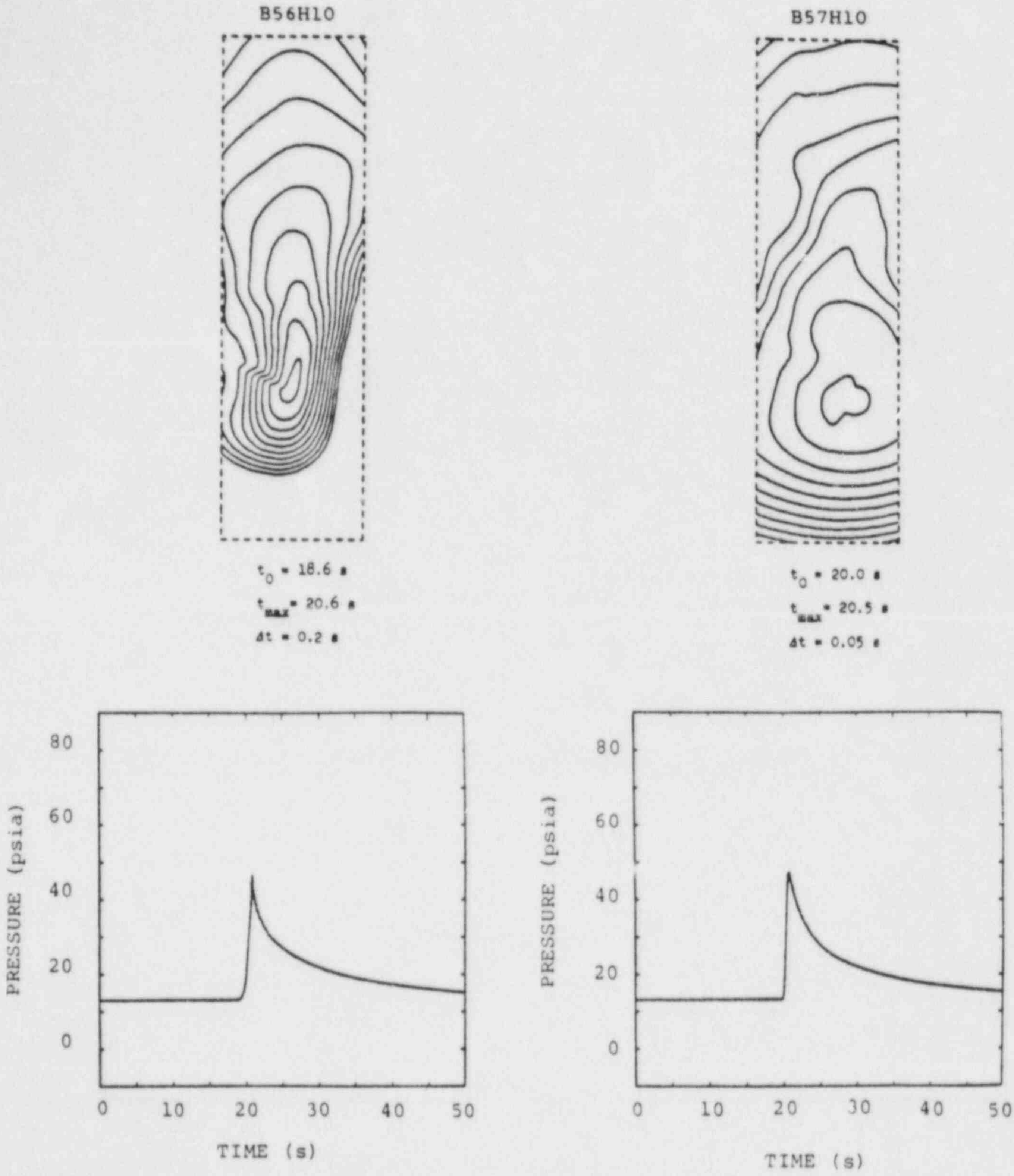
B56H10
t_0 = 18.6 s
t_{max} = 20.6 s
Δt = 0.2 s
B57H10
t_0 = 20.0 s
t_{max} = 20.5 s
Δt = 0.05 s
PRESSURE (psia)
80
60
40
20
0
TIME (s)
0
10
20
30
40
50

Figure A48

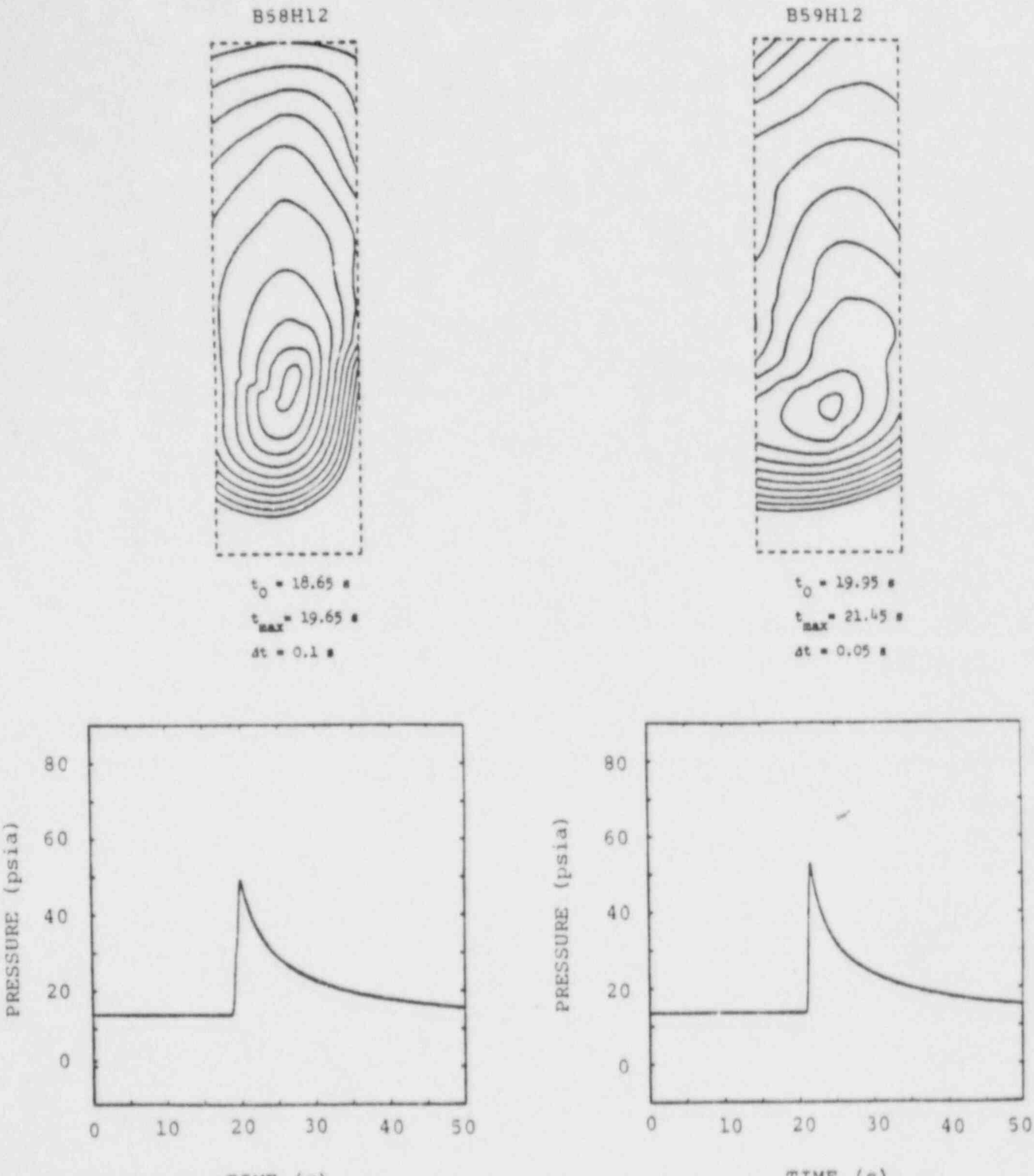
B58H12
t_0 = 18.65 s
t_{max} = 19.65 s
Δt = 0.1 s
B59H12
t_0 = 19.95 s
t_{max} = 21.45 s
Δt = 0.05 s
PRESSURE (psia)
0
20
40
60
80
TIME (s)
0
10
20
30
40
50

Figure A49

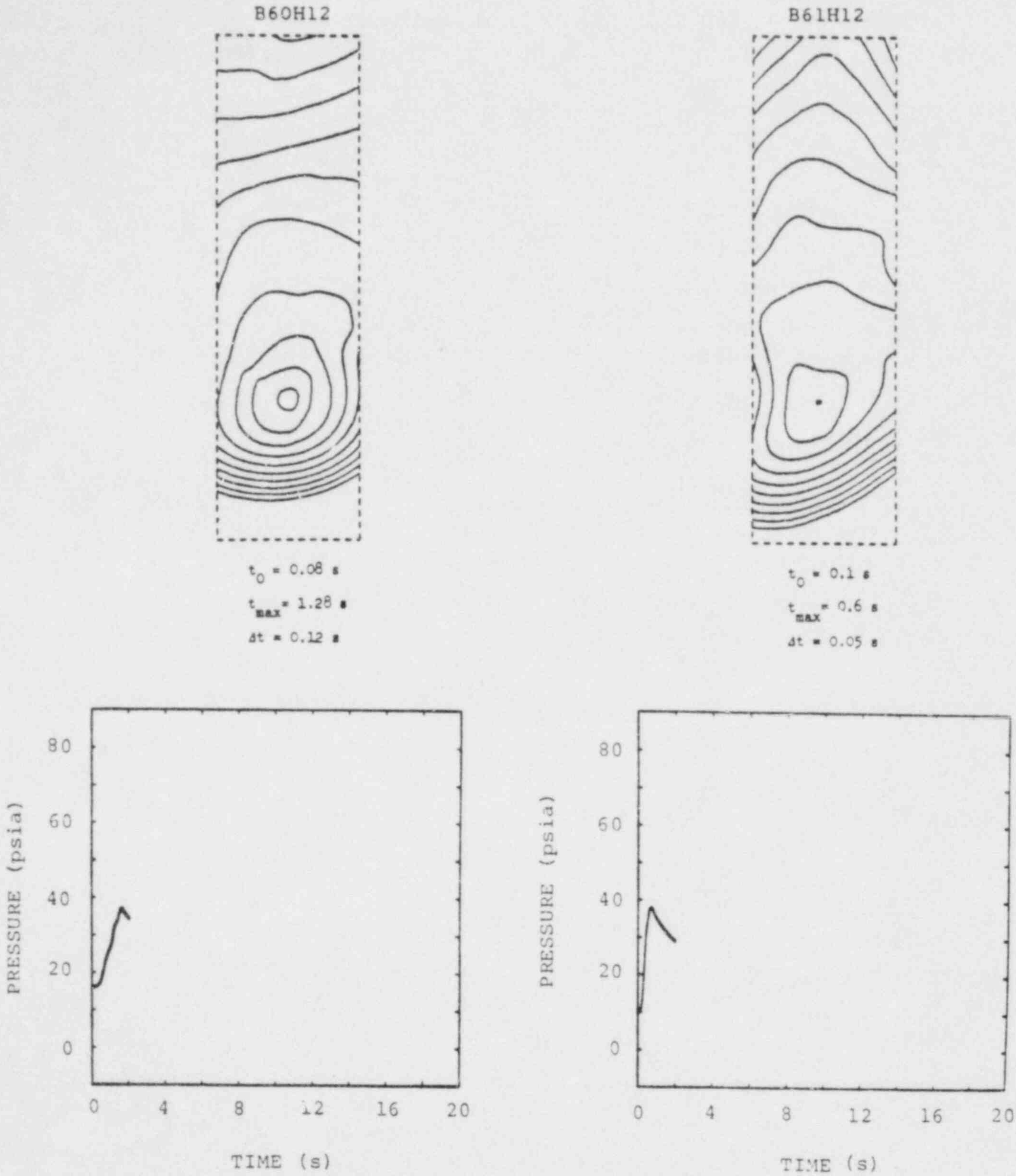
B60H12
t0 = 0.08 s
tmax = 1.28 s
Δt = 0.12 s
B61H12
t0 = 0.1 s
tmax = 0.6 s
Δt = 0.05 s
PRESSURE (psia)
0
20
40
60
80
TIME (s)
0
4
8
12
16
20
PRESSURE (psia)
0
20
40
60
80
TIME (s)
0
4
8
12
16
20

Figure A50

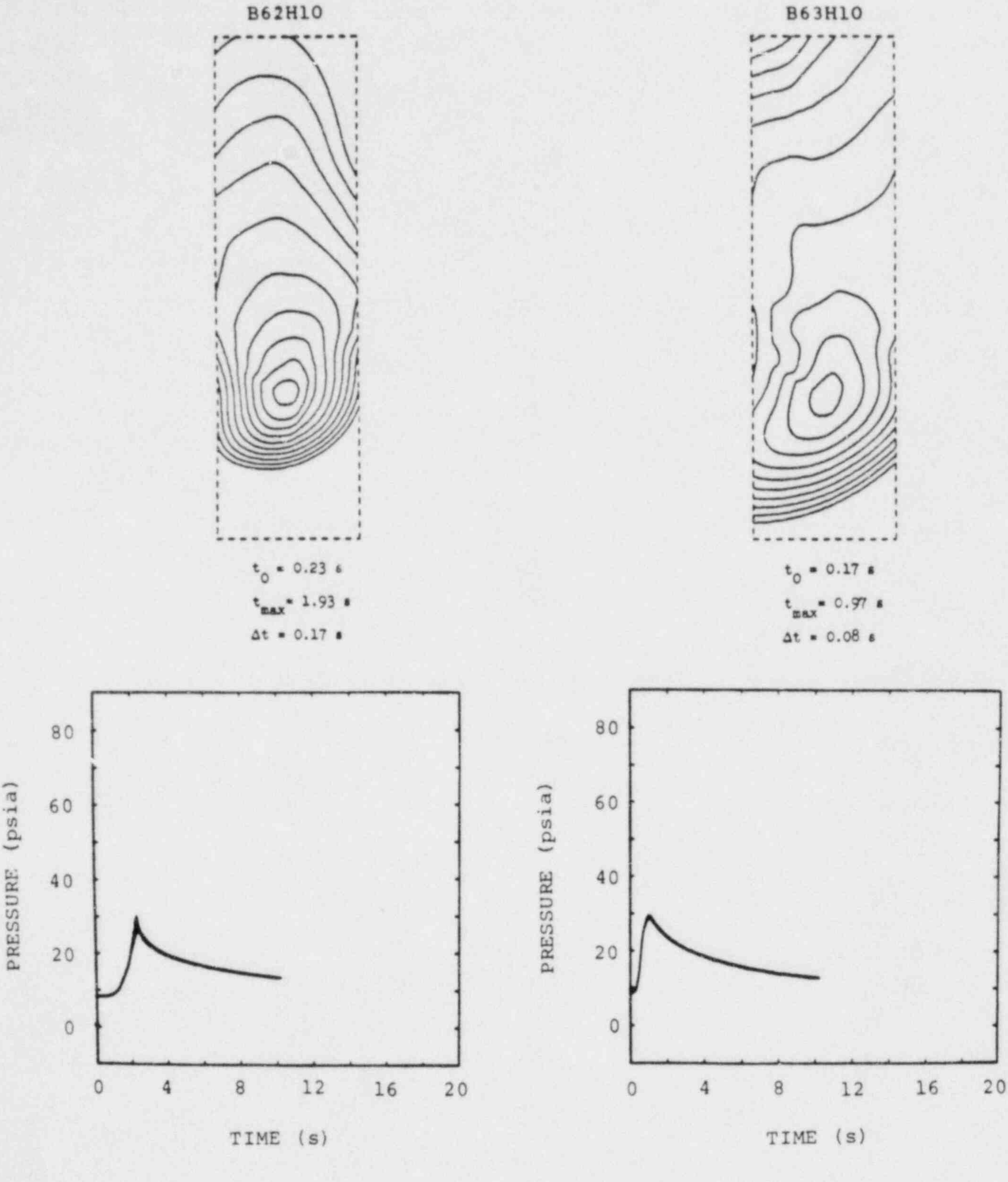
B62H10
t_0 = 0.23 s
t_{max} = 1.93 s
Δt = 0.17 s
B63H10
t_0 = 0.17 s
t_{max} = 0.97 s
Δt = 0.08 s
PRESSURE (psia)
0
20
40
60
80
TIME (s)
0
4
8
12
16
20
PRESSURE (psia)
0
20
40
60
80
TIME (s)
0
4
8
12
16
20

Figure A51

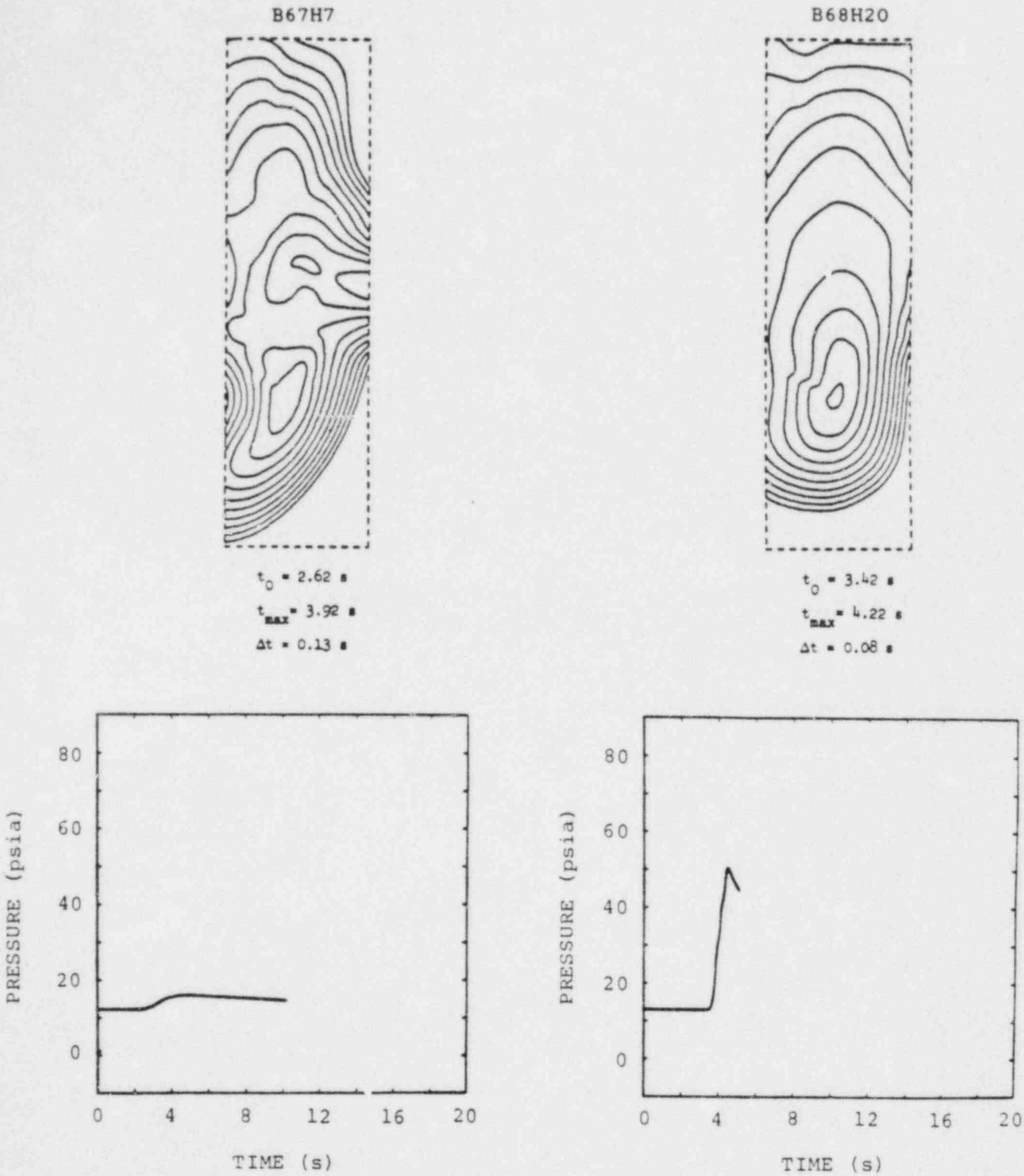
B67H7
B68H20
t_0 = 2.62 s
t_{max} = 3.92 s
Δt = 0.13 s
t_0 = 3.42 s
t_{max} = 4.22 s
Δt = 0.08 s
PRESSURE (psia)
TIME (s)
0
4
8
12
16
20
20
40
60
80

Figure A52

B69H15

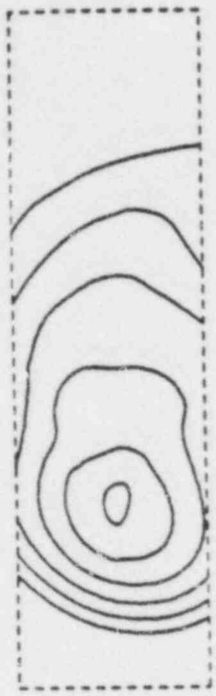

$t_0 = 0.136$ s

$t_{max} = 0.476$ s

$\Delta t = 0.034$ s

B70H15

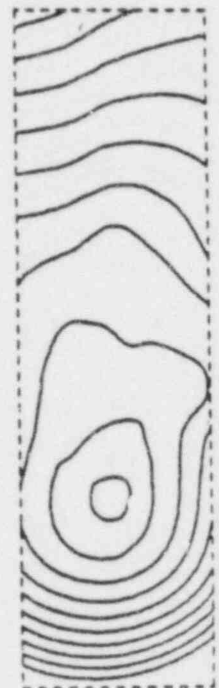

$t_0 = 0.135$ s

$t_{max} = 0.685$ s

$\Delta t = 0.055$ s

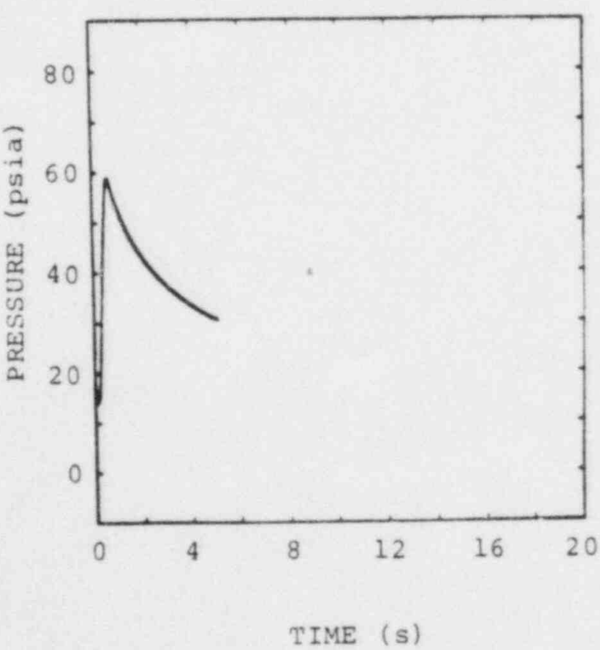

NO PRESSURE DATA
FOR TEST
B70H15

Figure A53

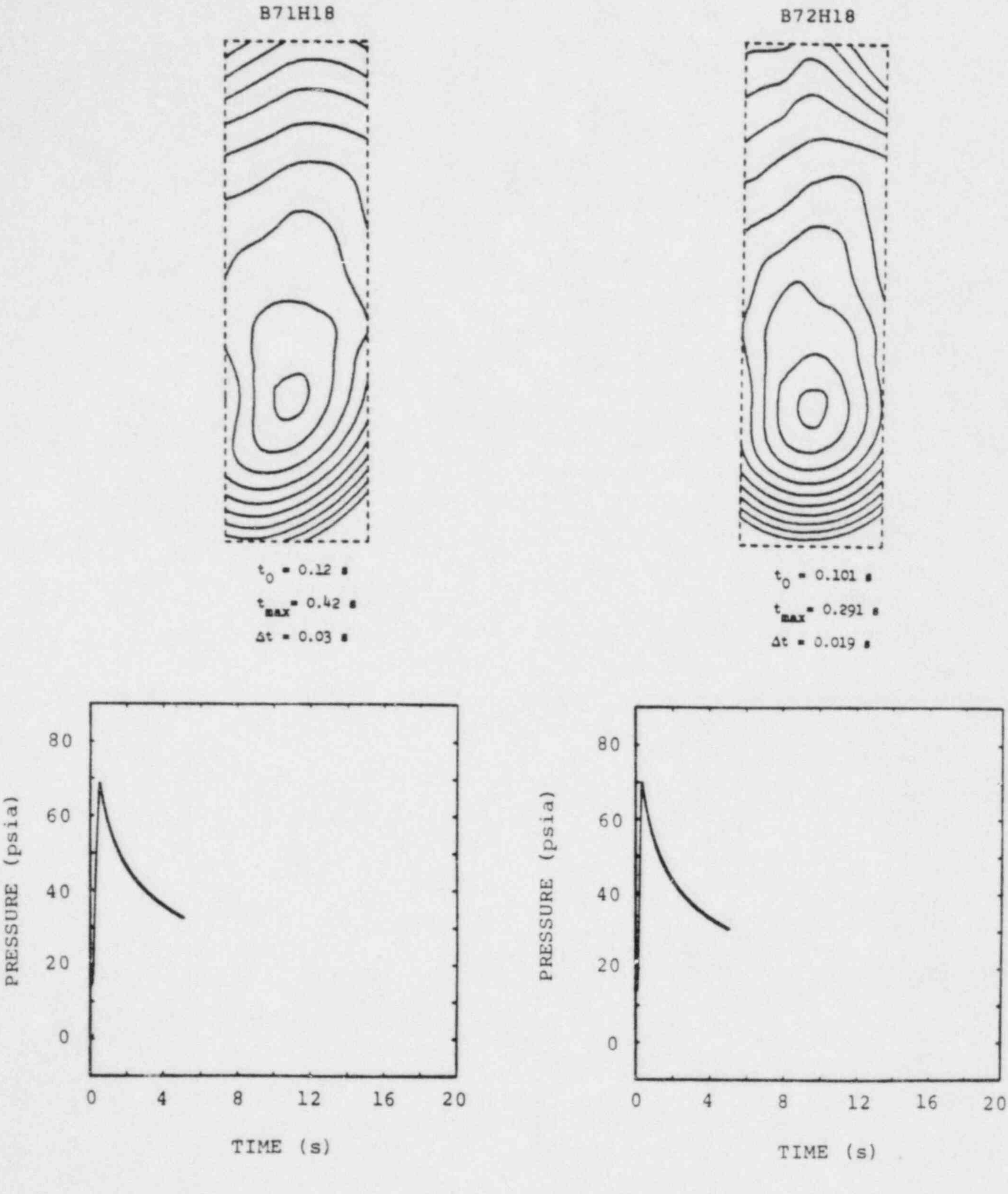
B71H18
B72H18
t_0 = 0.12 s
t_{max} = 0.42 s
Δt = 0.03 s
t_0 = 0.101 s
t_{max} = 0.291 s
Δt = 0.019 s
PRESSURE (psia)
TIME (s)
PRESSURE (psia)
TIME (s)

Figure A54

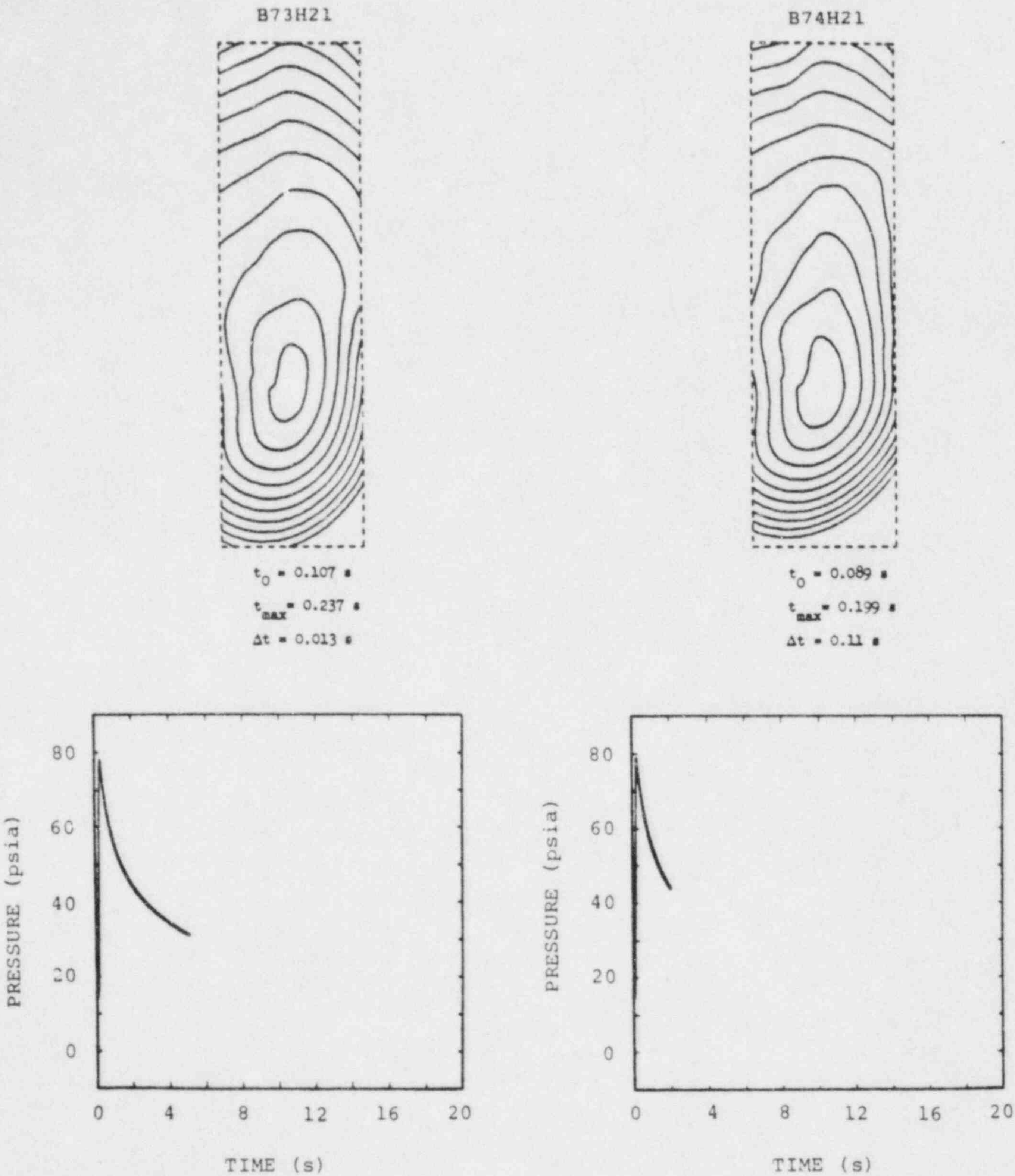
B73H21
B74H21
t_0 = 0.107 s
t_{max} = 0.237 s
Δt = 0.013 s
t_0 = 0.089 s
t_{max} = 0.199 s
Δt = 0.11 s
PRESSURE (psia)
TIME (s)
0
20
40
60
80
0
4
8
12
16
20

Figure A55

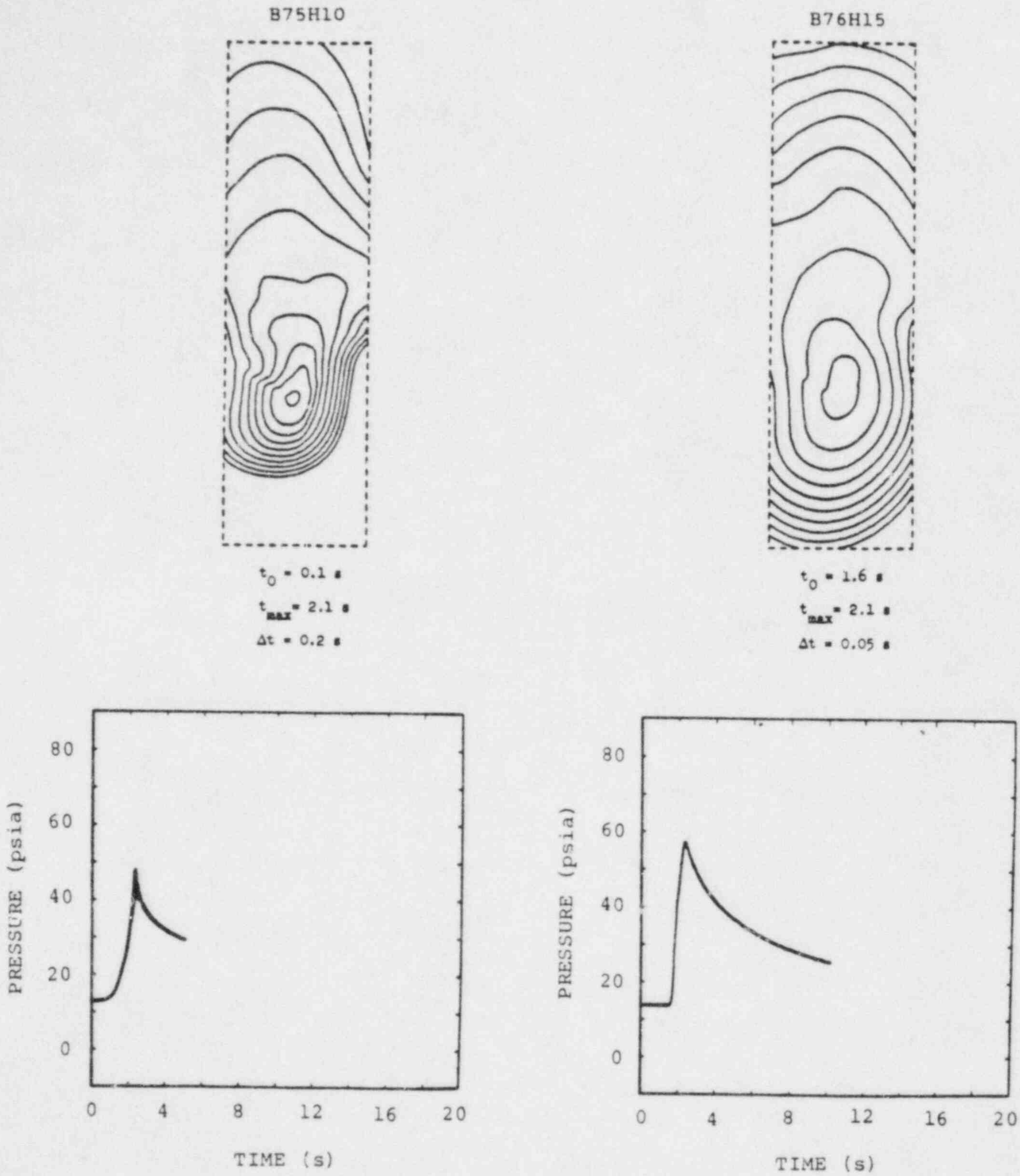
B75H10
B76H15
t0 = 0.1 s
tmax = 2.1 s
Δt = 0.2 s
t0 = 1.6 s
tmax = 2.1 s
Δt = 0.05 s
PRESSURE (psia)
80
60
40
20
0
0
4
8
12
16
20
TIME (s)
PRESSURE (psia)
80
60
40
20
0
0
4
8
12
16
20
TIME (s)

Figure A56

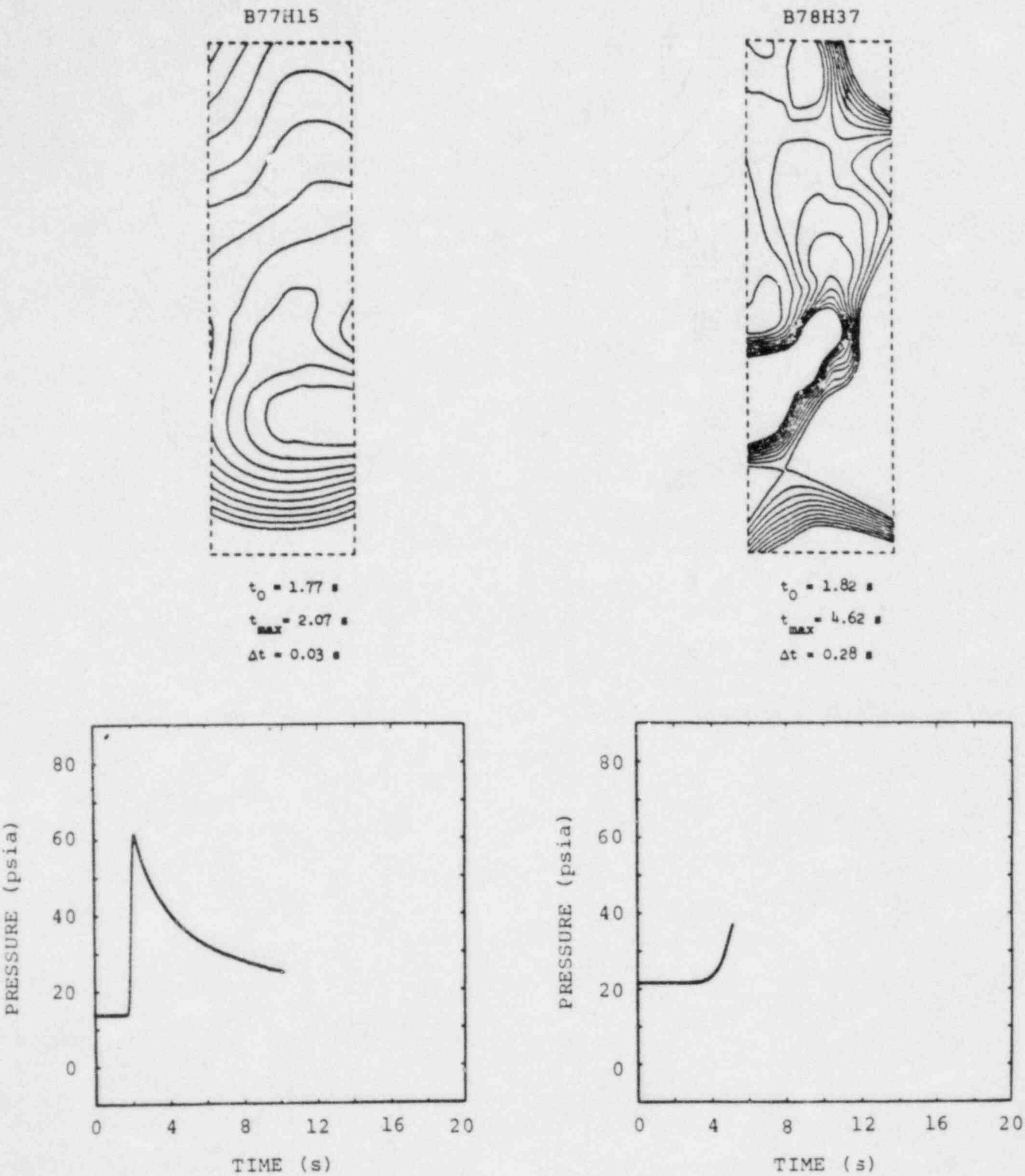
B77H15
B78H37
t0 = 1.77 s
tmax = 2.07 s
Δt = 0.03 s
t0 = 1.82 s
tmax = 4.62 s
Δt = 0.28 s
PRESSURE (psia)
80
60
40
20
0
0
4
8
12
16
20
TIME (s)
PRESSURE (psia)
80
60
40
20
0
0
4
8
12
16
20
TIME (s)

Figure A57

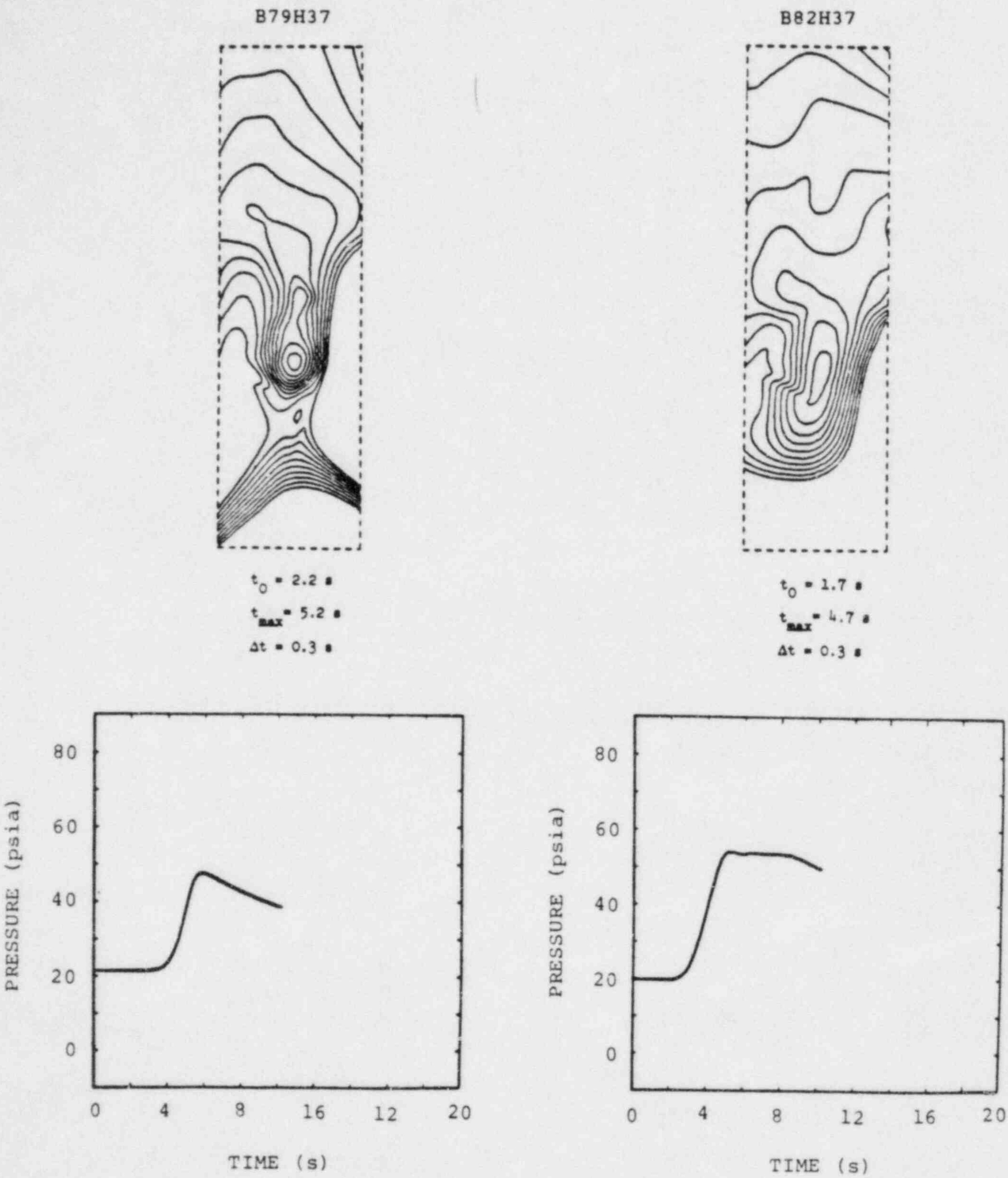

B79H37
t_0 = 2.2 s
t_{max} = 5.2 s
Δt = 0.3 s
B82H37
t_0 = 1.7 s
t_{max} = 4.7 s
Δt = 0.3 s
PRESSURE (psia)
80
60
40
20
0
0
4
8
16
12
20
TIME (s)
PRESSURE (psia)
80
60
40
20
0
0
4
8
12
16
20
TIME (s)

Figure A58

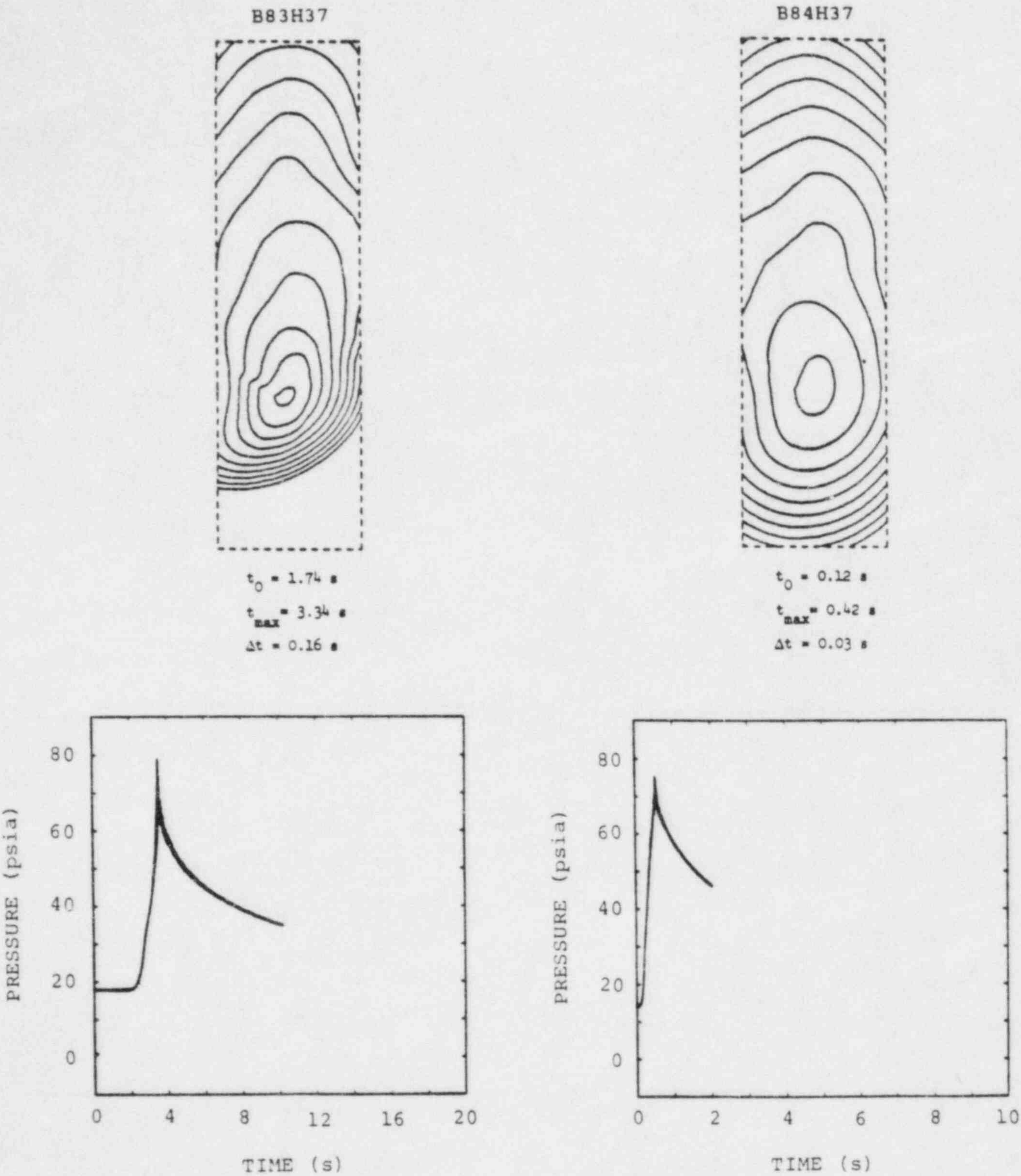

B83H37
t_0 = 1.74 s
t_{max} = 3.34 s
Δt = 0.16 s
B84H37
t_0 = 0.12 s
t_{max} = 0.42 s
Δt = 0.03 s
PRESSURE (psia)
0
20
40
60
80
TIME (s)
0
4
8
12
16
20
PRESSURE (psia)
0
20
40
60
80
TIME (s)
0
2
4
6
8
10

Figure A59

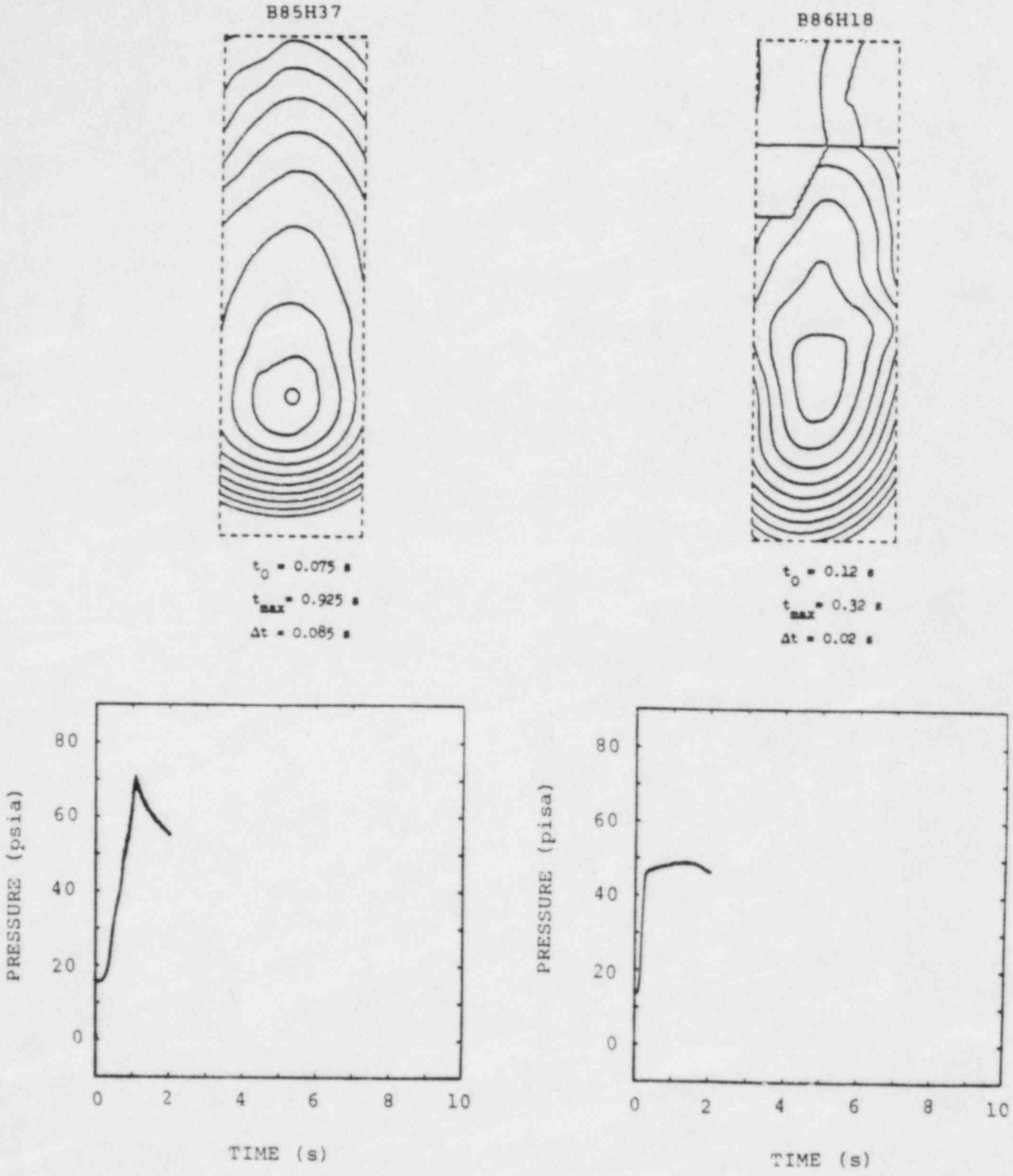
B85H37
t_0 = 0.075 s
t_{max} = 0.925 s
Δt = 0.085 s
B86H18
t_0 = 0.12 s
t_{max} = 0.32 s
Δt = 0.02 s
80
60
40
20
0
PRESSURE (psia)
0
2
4
6
8
10
TIME (s)
80
60
40
20
0
PRESSURE (pisa)
0
2
4
6
8
10
TIME (s)

Figure A60

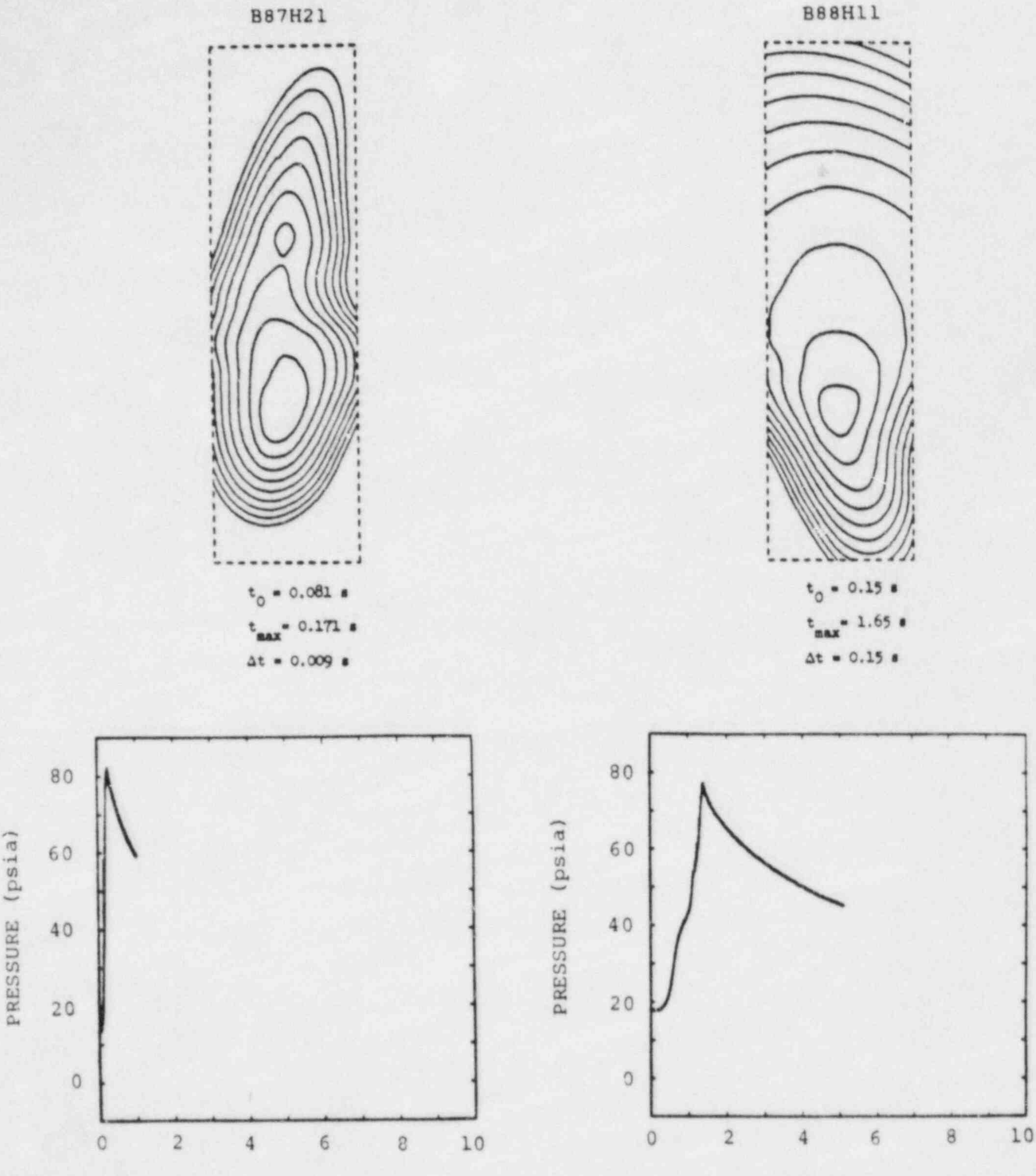
B87H21
B88H11
t_0 = 0.081 s
t_{max} = 0.171 s
Δt = 0.009 s
t_0 = 0.15 s
t_{max} = 1.65 s
Δt = 0.15 s
PRESSURE (psia)
TIME (s)
0
20
40
60
80
0
2
4
6
8
10
PRESSURE (psia)
TIME (s)

Figure A61

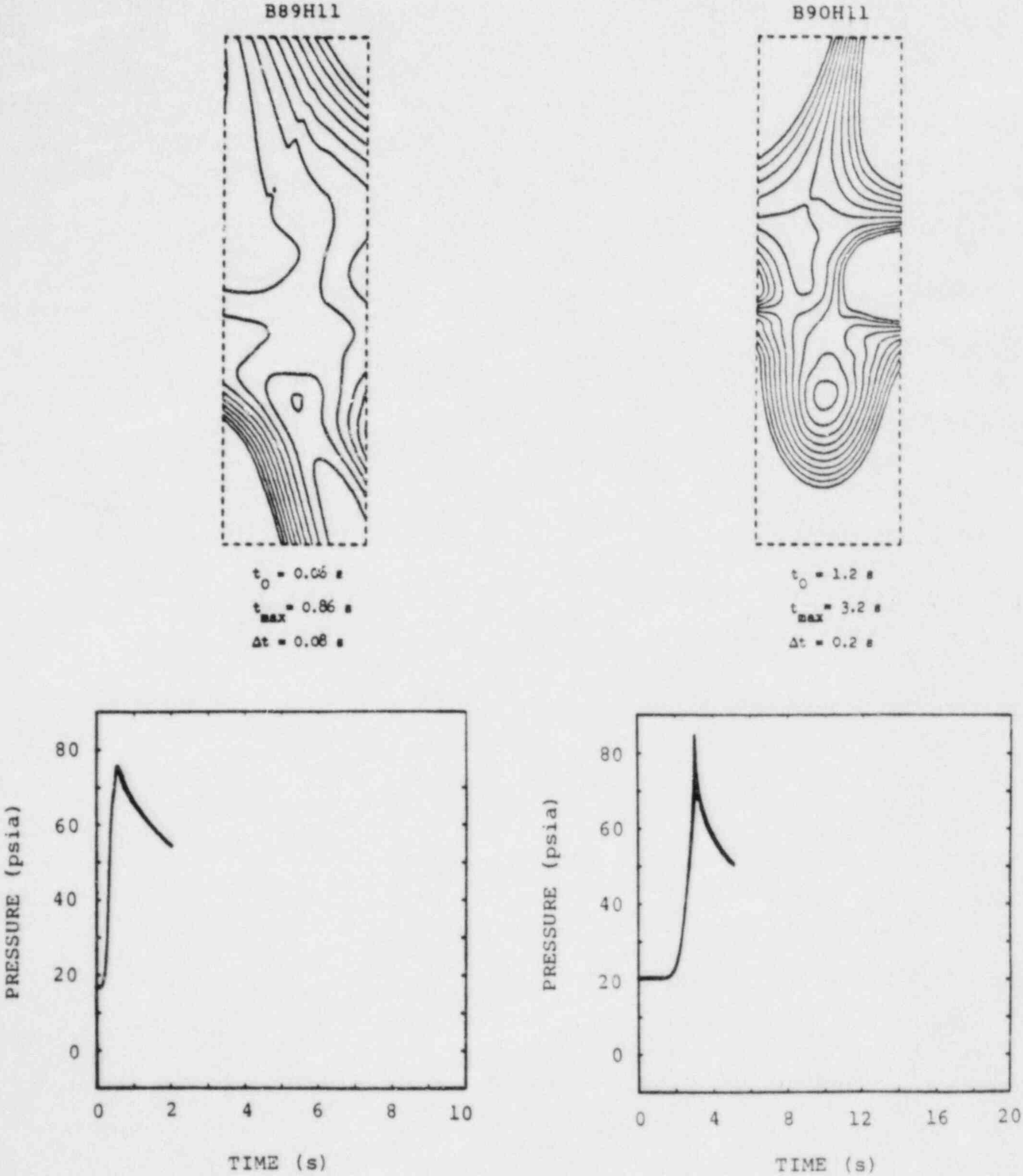
B89H11
t_0 = 0.06 s
t_{max} = 0.86 s
Δt = 0.08 s
B90H11
t_0 = 1.2 s
t_{max} = 3.2 s
Δt = 0.2 s
PRESSURE (psia)
TIME (s)
PRESSURE (psia)
TIME (s)

Figure A62

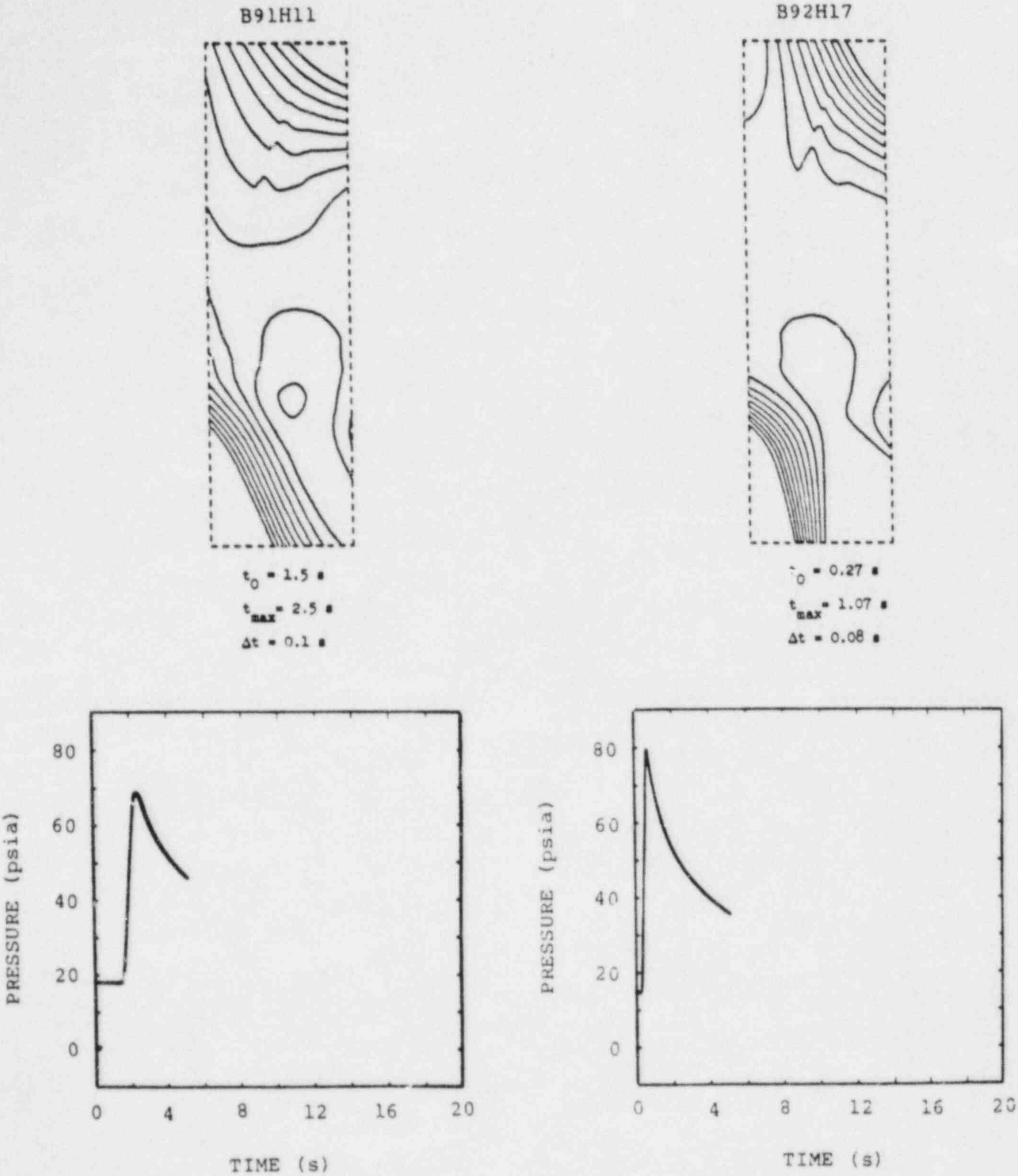
B91H11
t_0 = 1.5 s
t_{max} = 2.5 s
Δt = 0.1 s
B92H17
t_0 = 0.27 s
t_{max} = 1.07 s
Δt = 0.08 s
PRESSURE (psia)
0
20
40
60
80
TIME (s)
0
4
8
12
16
20
PRESSURE (psia)
0
20
40
60
80
TIME (s)
0
4
8
12
16
20

Figure A63

B93H17

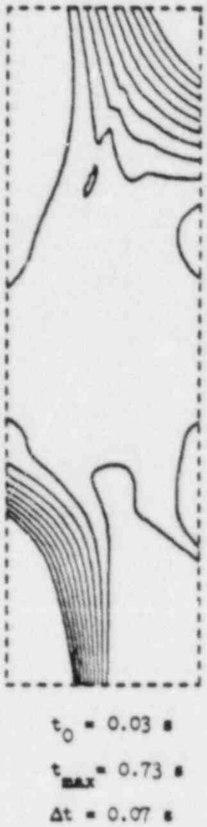

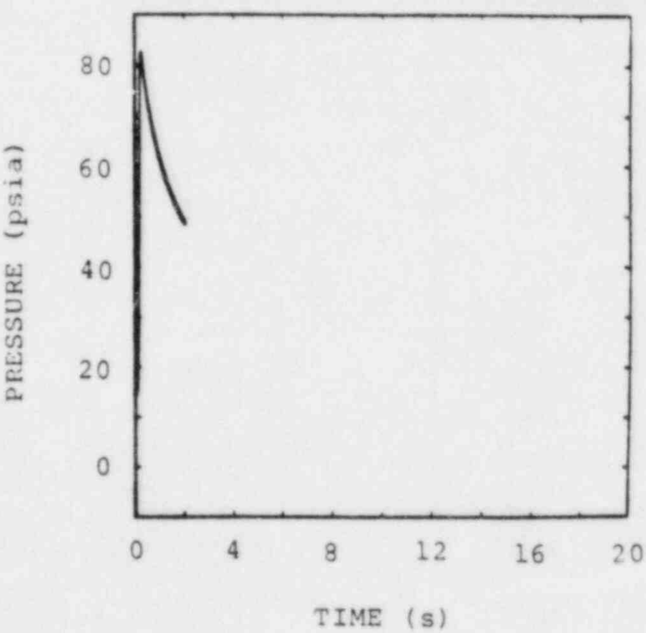

Figure A64

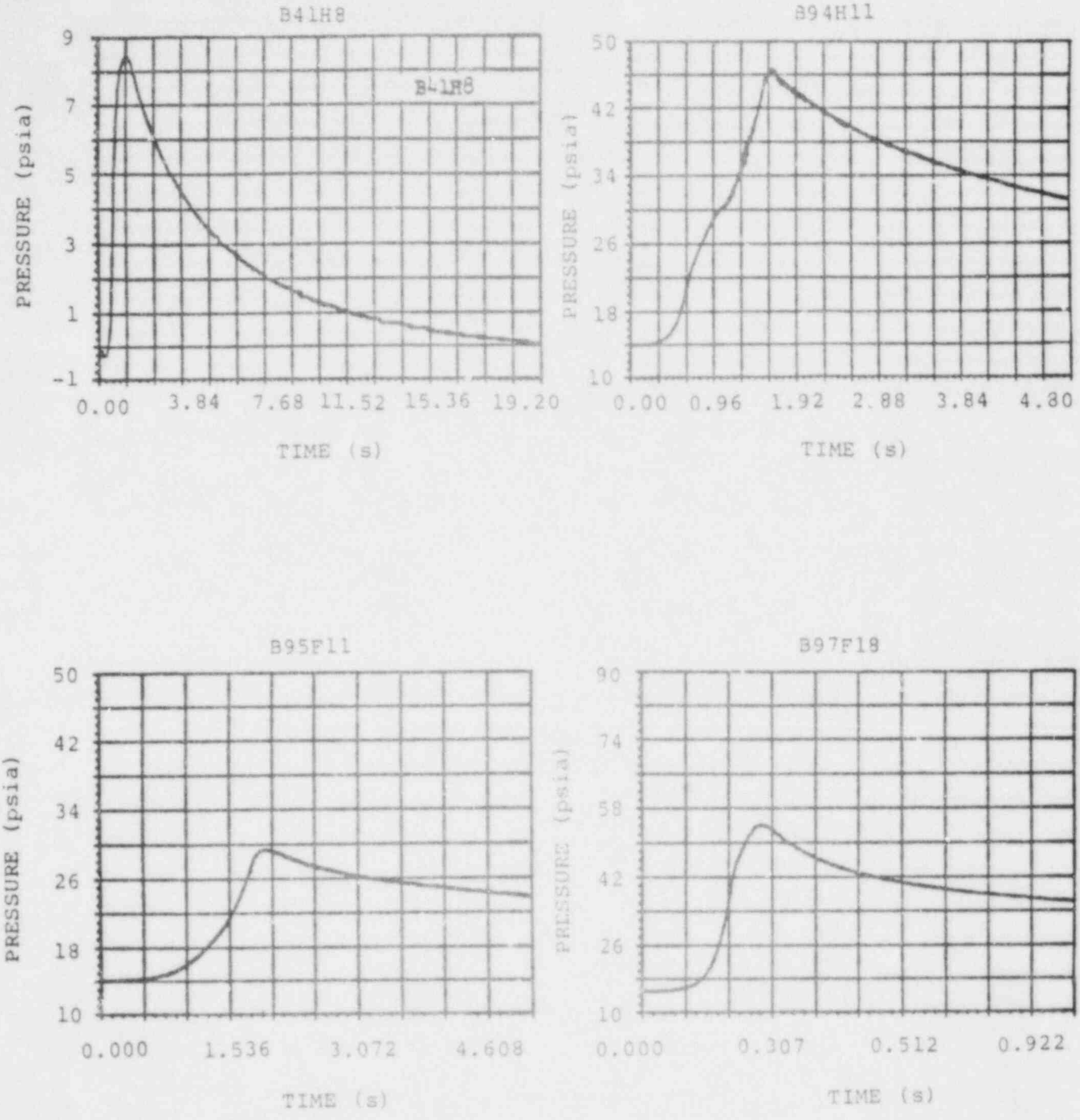

B41H8
PRESSURE (psia)
9
7
5
3
1
-1
0.00
3.84
7.68
11.52
15.36
19.20
TIME (s)
B94H11
PRESSURE (psia)
50
42
34
26
18
10
0.00
0.96
1.92
2.88
3.84
4.80
TIME (s)
B95F11
PRESSURE (psia)
50
42
34
26
18
10
0.000
1.536
3.072
4.608
TIME (s)
B97F18
PRESSURE (psia)
90
74
58
42
26
10
0.000
0.307
0.512
0.922
TIME (s)

Figure A65

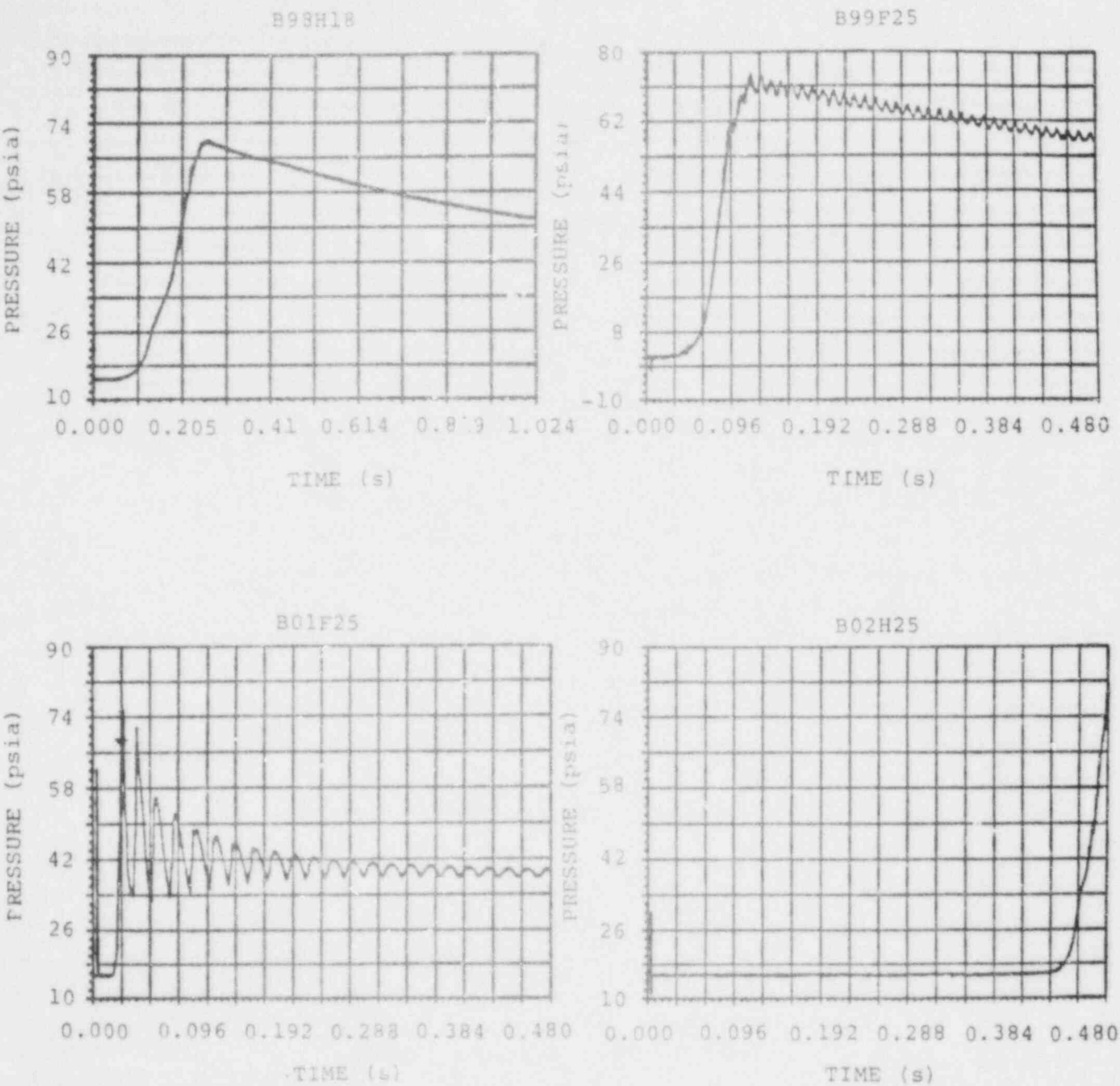
B98H18
PRESSURE (psia)
90
74
58
42
26
10
0.000 0.205 0.41 0.614 1.024
TIME (s)
B99F25
PRESSURE (psia)
80
62
44
26
8
-10
0.000 0.096 0.192 0.288 0.384 0.480
TIME (s)
B01F25
PRESSURE (psia)
90
74
58
42
26
10
0.000 0.096 0.192 0.288 0.384 0.480
B02H25
PRESSURE (psia)
90
74
58
42
26
10
0.000 0.096 0.192 0.288 0.384 0.480
TIME (s)

Figure A66

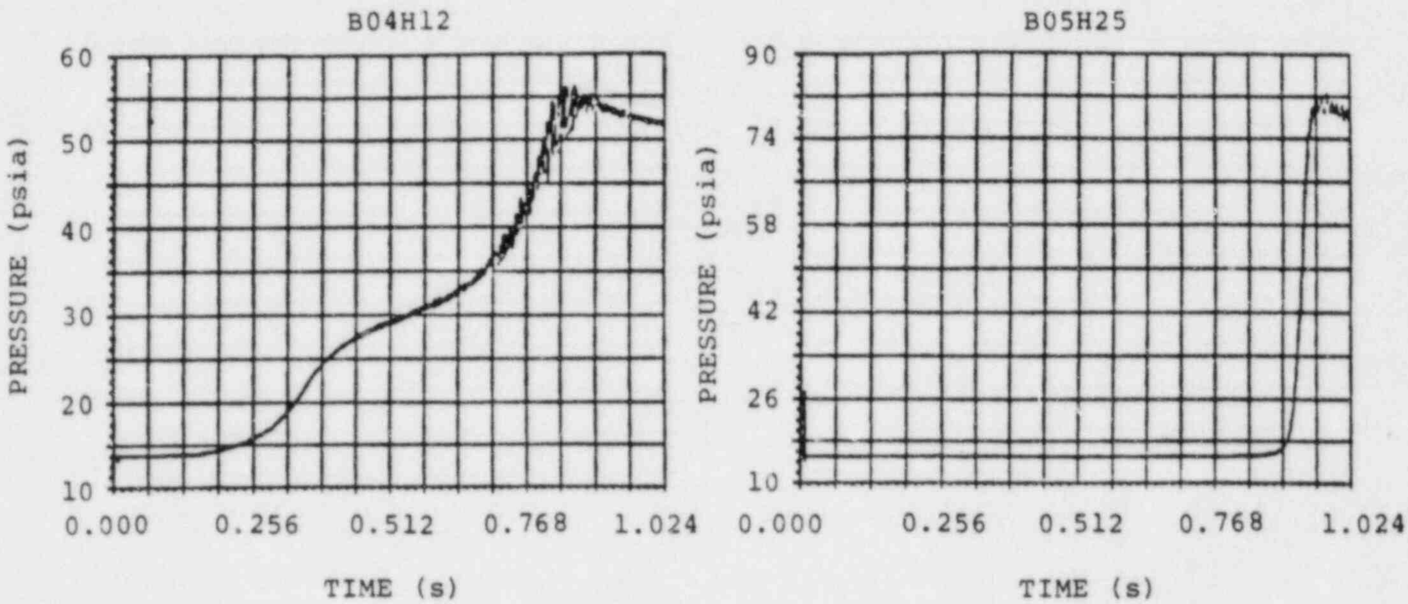
B04H12
PRESSURE (psia)
60
50
40
30
20
10
0.000
0.256
0.512
0.768
1.024
TIME (s)
B05H25
PRESSURE (psia)
90
74
58
42
26
10
0.000
0.256
0.512
0.768
1.024
TIME (s)

Figure A67

U. S. NRC Distribution Contractor (CDSI)
7300 Pearl Street
Bethesda, MD 20014
275 copies for R3

U. S. Bureau of Mines
Pittsburgh Research Center
P. O. Box 18070
Pittsburgh, PA 15236
Attn: M. Hertzberg

U. S. Nuclear Regulatory Commission (6)
Office of Nuclear Regulatory Research
Washington, DC 20555
Attn: G. A. Arlotto
R. T. Curtis
J. T. Larkins
L. C. Shao
K. G. Steyer
P. Worthington

U. S. Nuclear Regulatory Commission (5)
Office of Nuclear Regulatory Research
Washington, DC 20555
Attn: B. S. Burson
M. Silberberg
J. L. Telford
T. J. Walker
R. W. Wright

U. S. Nuclear Regulatory Commission (6)
Office of Nuclear Reactor Regulation
Washington, DC 20555
Attn: J. K. Long
J. F. Meyer
R. Palla
K. I. Parczewski
G. Quittschreiber
D. D. Yue

U. S. Nuclear Regulatory Commission (4)
Office of Nuclear Reactor Regulation
Washington, DC 20555
Attn: V. Benaroya
W. R. Butler
G. W. Knighton
T. M. Su
Z. Rosztoczy
C. G. Tinkler

U. S. Department of Energy
Operational Safety Division
Albuquerque Operations Office
P.O. Box 5400
Albuquerque, NM 87185
Attn: J. R. Roeder, Director

Swedish State Power Board
El-Och Vaermeteknik
Sweden
Attn: Eric Ahlstroem

Berkeley Nuclear Laboratory
Berkeley GL 139PB
Gloucestershire
United Kingdom
Attn: J. E. Antill

Gesellschaft fur Reakforsicherheit (GRS)
Postfach 101650
Glockengasse 2
5000 Koeln 1
Federal Republic of Germany
Attn: Dr. M. V. Banaschik

Battelle Institut E. V.
Am Roemerhof 35
6000 Frankfurt am Main 90
Federal Republic of Germany
Attn: Dr. Werner Baukal

UKAEA Safety & Reliability Directorate
Wigshaw Lane, Culcheth
Warrington WA34NE
Cheshire
United Kingdom
Attn: J. G. Collier (2)
S. F. Hall

British Nuclear Fuels, Ltd.
Building 396
Springfield Works
Salwick, Preston
Lancs
United Kingdom
Attn: W. G. Cunliffe

AERE Harwell
Didcot
Oxfordshire OX11 ORA
United Kingdom
Attn: J. Gittus, AETB (2)
J. R. Matthews, TPD

Kernforschungszentrum Karlsruhe
Postfach 3640
75 Karlsruhe
Federal Republic of Germany
Attn: Dr. S. Hagen (3)
Dr. J. P. Hosemann
Dr. M. Reimann

Simon Engineering Laboratory
University of Manchester
M139PL,
United Kingdom
Attn: Prof. W. B. Hall

Kraftwerk Union
Hammerbacher strasse 12 & 14
Postfach 3220
D-8520 Erlangen 2
Federal Republic of Germany
Attn: Dr. K. Hassman (2)
Dr. M. Peehs

Gesellschaft fur Reaktorsickerheit (GRS mbH)
8046 Garching
Federal Republic of Germany
Attn: E. F. Hicken (2)
H. L. Jahn

Technische Universitaet Muenchen
D-8046 Garching
Federal Republic of Germany
Attn: Dr. H. Karwat

McGill University
315 Querbes
Outremont, Quebec
Canada H2V 3W1
Attn: John H. S. Lee (3)

AEC, Ltd.
Whiteshell Nuclear Research Establishment
Pinawa, Manitoba, Canada
Attn: D. Liu (2)
H. Tamm

National Nuclear Corp. Ltd.
Cambridge Road
Whetestone, Leicester, LE83LH
United Kingdom
Attn: R. May

CNEN NUCLIT
Rome, Italy
Attn: A. Morici

Director of Research, Science & Education
CEC
Rue De La Loi 200
1049 Brussels
Belgium
Attn: B. Tolley

Bechtel Power Corporation
15740 Shady Grove Road
Gaithersburg, MD 20877
Attn: D. Ashton

Northwestern University
Chemical Engineering Department
Evanston, IL 60201
Attn: S. G. Bankoff

Brookhaven National Laboratory
Upton, NY 11973
Attn: R. A. Bari (2)
T. Pratt

Westinghouse Hanford Company
P. O. Box 1970
Richland, WA 99352
Attn: G. R. Bloom (3)
L. Muhlstein
R. D. Peak

UCLA
Nuclear Energy Laboratory
405 Hilgard Avenue
Los Angeles, CA 90024
Attn: I. Catton

Argonne National Laboratory
9700 South Cass Avenue
Argonne, IL 60439
Attn: H. M. Chung

Sandia National Laboratories
Directorate 6400
P. O. Box 5800
Albuquerque, NM 87185
Attn: R. Cochrell (20)

University of Wisconsin
Nuclear Engineering Department
1500 Johnson Drive
Madison, WI 53706
Attn: M. L. Corradini

Los Alamos National Laboratory
P. O. Box 1663
Los Alamos, NM 87545
Attn: H. S. Cullingford (4)
R. Gido
J. Carson Mark
G. Schott

Battelle Columbus Laboratory
505 King Avenue
Columbus, OH 43201
Attn: P. Cybulskis (2)
R. Denning

Power Authority State of NY
10 Columbus Circle
New York, NY 10019
Attn: R. E. Deem (2)
S. S. Iyer

Offshore Power System
8000 Arlington Expressway
Box 8000
Jacksonville, FL 32211
Attn: G. M. Fuls
D. H. Walker

Electric Power Research Institute
3412 Hillview Avenue
Palo Alto, CA 94303
Attn: J. J. Haugh (4)
K. A. Nilsson
G. Thomas
L. B. Thompson

Fauske & Associates
627 Executive Drive
Willowbrook, IL 60521
Attn: R. Henry

Mississippi Power & Light
P. O. Box 1640
Jackson, MS 39205
Attn: S. H. Hobbs

General Electric Co.
175 Curtner Avenue
Mail Code N 1C157
San Jose, CA 95125
Attn: K. W. Holtzclaw

NUS Corporation
4 Research Place
Rockville, MD 20850
Attn: R. Sherry

Duke Power Co.
P. O. Box 33189
Charlotte, NC 28242
Attn: F. G. Hudson (2)
A. L. Sudduth

Westinghouse Corporation
P. O. Box 355
Pittsburgh, PA 15230
Attn: N. Liparulo (3)
J. Olhoeft
V. Srinivas

General Physics Corporation
1000 Century Plaza
Columbia, MD 21044
Attn: Chester Kupiec

TVA
400 Commerce
W9C157-CD
Knoxville, TN 37902
Attn: Wang Lau

EG&G Idaho
Willow Creek Building, W-3
P. O. Box 1625
Idaho Falls, ID 83415
Attn: Server Sadik

Department of Aerospace Engineering
University of Michigan
Ann Arbor, MI 47109
Attn: Martin Sichel

Attn: Roger Strehlow
505 South Pine Street
Champaign, IL 61820

Applied Sciences Association, Inc.
P. O. Box 2687
Palos Verdes Pen., CA 90274
Attn: D. Swanson

Purdue University
School of Nuclear Engineering
West Lafayette, IN 47907
Attn: T. G. Theofanous

Acurex Corporation
485 Clyde Avenue
Mountain View, CA 94042

Astron
2028 Old Middlefield Way
Mountainview, CA 94043
Attn: Ray Torok

Bechtel Power Corporation
P. O. Box 3965
San Francisco, CA 94119
Attn: R. Tosetti

Thompson Associates
639 Massachusetts Avenue
Third Floor
Cambridge, MA 02139
Attn: Timothy Woolf

Factory Mutual Research Corporation
P. O. Box 688
Norwood, MA 02062
Attn: R. Zalosh

Lawrence Livermore Laboratories
L140
Box 808
Livermore, CA 94550
Attn: P. Prassinos

Sandia Distribution:
1131 B. Morosin
1131 W. B. Benedick (4)
1510 J. W. Nanziato
1512 J. C. Cummings (2)
1512 J. E. Shepherd
1513 D. W. Larson
1520 D. J. McCloskey
1530 L. W. Davison
1540 W. C. Luth
6400 A. W. Snyder
6410 J. W. Hickman
6411 V. L. Behr
6411 A. L. Camp
6411 S. E. Dingman
6411 F. E. Haskin
6420 J. V. Walker
6422 D. A. Powers
6427 M. Berman (15)
6427 L. S. Nelson
6427 E. W. Shepherd
6427 C. C. Wong
6440 D. A. Dahlgren
6442 W. A. von Riesemann
6444 S. L. Thompson
6445 B. E. Bader
3141 C. M. Ostrander (5)
3151 W. L. Garner
8424 M. A. Pound

NRC FORM 335 (2-84) NRCM 1102, 3201, 3202

U.S. NUCLEAR REGULATORY COMMISSION

BIBLIOGRAPHIC DATA SHEET

SEE INSTRUCTIONS ON THE REVERSE

1. REPORT NUMBER (Assigned by TIDC, add Vol. No., if any)
NUREG/CR-3273
SAND83-1022

2. TITLE AND SUBTITLE
COMBUSTION OF HYDROGEN:AIR MIXTURES IN THE VGES CYLINDRICAL TANK

3. LEAVE BLANK

4. DATE REPORT COMPLETED
MONTH | YEAR

5. AUTHOR(S)
W. B. Benedick, J. C. Cummings, P. G. Prassinos

6. DATE REPORT ISSUED
MONTH: May
YEAR: 1984

7. PERFORMING ORGANIZATION NAME AND MAILING ADDRESS (Include Zip Code)
Sandia National Laboratories
Albuquerque, NM 87185

8. PROJECT/TASK/WORK UNIT NUMBER

9. FIN OR GRANT NUMBER
A1246, A1336

10. SPONSORING ORGANIZATION NAME AND MAILING ADDRESS (Include Zip Code)
Office of Nuclear Regulatory Research
U.S. Nuclear Regulatory Commission
Washington, DC 20555

11a. TYPE OF REPORT
Technical

b. PERIOD COVERED (Inclusive dates)

12. SUPPLEMENTARY NOTES

13. ABSTRACT (200 words or less)

Sandia National Laboratories is currently involved in a number of experimental projects to provide data that will help quantify the threat of hydrogen combustion during nuclear plant accidents. Several experimental facilities are part of the Variable Geometry Experimental System (VGES). The purpose of this report is to document the experimental results from the first round of combustion tests performed at one of these facilities: a 5-m^3 cylindrical tank. The data provided by tests at this facility can be used to guide further testing and for the development and assessment of analytical models to predict hydrogen combustion behavior.

14. DOCUMENT ANALYSIS - a. KEYWORDS/DESCRIPTORS

b. IDENTIFIERS/OPEN-ENDED TERMS

15. AVAILABILITY STATEMENT
Unlimited

16. SECURITY CLASSIFICATION
(This page) Unclassified
(This report) Unclassified

17. NUMBER OF PAGES
165

18. PRICE

☆ U.S. GOVERNMENT PRINTING OFFICE: 1984—776-027 / 4312

ORG.	BLDG.	NAME	REC'D BY*	ORG.	BLDG.	NAME	REC'D BY*

120555078877 1 1AN1R3
US NRC
ADM-DIV OF TIDC
POLICY & PUB MGT BR-PDR NUREG
W-501
WASHINGTON DC 20555

Sandia National Laboratories